

A Thesis Submitted for the Degree of PhD at the University of Warwick

Permanent WRAP URL:

<http://wrap.warwick.ac.uk/109299>

Copyright and reuse:

This thesis is made available online and is protected by original copyright.

Please scroll down to view the document itself.

Please refer to the repository record for this item for information to help you to cite it.

Our policy information is available from the repository home page.

For more information, please contact the WRAP Team at: wrap@warwick.ac.uk

THE BRITISH LIBRARY
BRITISH THESIS SERVICE

TITLE ELECTROCHEMICAL STUDIES OF MODIFIED REDOX ENZYMES

AUTHOR VERONICA QING BRADFORD

DEGREE

AWARDING BODY

DATE University of Warwick OCTOBER 1991

THESIS

NUMBER

THIS THESIS HAS BEEN MICROFILMED EXACTLY AS RECEIVED

The quality of this reproduction is dependent upon the quality of the original thesis submitted for microfilming. Every effort has been made to ensure the highest quality of reproduction.

Some pages may have indistinct print, especially if the original papers were poorly produced or if the awarding body sent an inferior copy.

If pages are missing, please contact the awarding body which granted the degree.

Previously copyrighted materials (journal articles, published texts, etc.) are not filmed.

This copy of the thesis has been supplied on condition that anyone who consults it is understood to recognise that its copyright rests with its author and that no information derived from it may be published without the author's prior written consent.

Reproduction of this thesis, other than as permitted under the United Kingdom Copyright Designs and Patents Act 1988, or under specific agreement with the copyright holder, is prohibited.

1	2	3	4	5	6	REDUCTION X	12
cms						CAMERA	3
						No. of pages	

ELECTROCHEMICAL STUDIES OF MODIFIED REDOX ENZYMES

by

VERONICA QING BRADFORD

A thesis submitted for the degree of Doctor of Philosophy of the University
of Warwick

Department of Chemistry
University of Warwick
Coventry CV4 7AL
United Kingdom

October 1991

To my husband

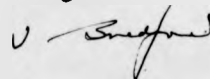
PAGE
NUMBERING
AS BOUND

DECLARATION

The work presented in this thesis was carried out in the Department of Chemistry, University of Warwick between November 1988 and April 1991 (with three months at MediSense) under the supervision of Professor P.N. Bartlett.

The work was conducted solely by the author. Where the work of other authors has been concerned this is clearly indicated.

Signed

A handwritten signature in dark ink, appearing to be 'S. Bartlett', written over a horizontal line.

CONTENTS

	Page
List of Figures	iv
List of Tables	xvi
Abbreviations	xx
Acknowledgements	xviii
Summary	xix
Chapter I Introduction	1
1.1 The Characteristics of Redox Enzymes	1
1.2 The Effect of Distance on the Rate of Electron Transfer	4
1.3 Direct Electrochemistry of Redox Enzymes	6
1.4 Mediated Electron Transfer	9
1.4.1 Homogeneous Mediation	11
1.4.2 Mediation in Heterogeneous Systems	13
1.5 Conducting Organic Salts	14
1.6 Modified Redox Enzymes	16
1.6.1 The Covalent Modification of Enzymes	17
1.7 Summary of Work Presented in this Thesis	18
Chapter II Experimental Techniques and Instrumentation	20
2.1 Introduction	20
2.2 Electrochemistry System	20
2.2.1 Electrochemical Instrumentation	20
2.2.2 Electrochemical cells and Electrodes	20
2.2.3 Deoxygenation of Solutions	26
2.3 Chemicals and Solutions	26
2.4 Spectroscopic Determination of Enzymic Activity and Protein Concentrations	28
2.4.1 Enzymic Activity	28
2.4.2 Protein Concentrations	31
2.5 Enzyme Modification	31
2.5.1 Covalent Modification	33
2.5.2 Non-Covalent Modification	34
2.5.3 Protein Purification	34
2.6 Determination of Mediator Incorporation for the Covalently and Non-Covalently Modified GOx Samples	37
2.6.1 Determination of Iron Content	37
2.6.2 Fluorescent Spectroscopy of the TTF Modified GOx Samples	37
2.7 Enzyme Membrane Electrodes	39
2.7.1 Construction of the Glassy Carbon Electrodes	39
2.7.2 Construction of Enzyme Membrane Electrodes	42
2.8 Isoelectric Points (pIs) of FAA Modified GOx	42
2.8.1 Isoelectric Focusing Gel Electrophoresis	42
2.8.2 Chromafocusing Chromatography	45
2.9 Hydrophobic Incorporation of TTF in BSA	47
2.9.1 The Extinction Coefficient of TTF in BSA at 320 nm	47
2.9.2 Saturated TTF Concentrations in BSA	51

	Page
Chapter III Studies of FAA Modified Glucose Oxidase	52
3.1 Introduction	52
3.1.1 Methods for the Covalent Modification of Glucose Oxidase	53
3.1.2 Properties of Covalently Modified Glucose Oxidase	59
3.2 Estimation of the Diffusion Coefficient and the Number of Electrons Transferred for FAA Modified Glucose Oxidase	67
3.2.1 Introduction	67
3.2.2 Rotating Disc Electrode Studies	70
3.2.3 Voltammetric Studies for FAA Modified GOx	84
3.2.4 Estimation of n and D for FAA Modified GOx	87
3.3 Catalytic Activity of FAA Modified GOx	90
3.3.1 Theory	90
3.3.2 Electrochemistry of FAA Modified GOx	98
3.3.3 Analysis for the Results of FAA Modified GOx	103
3.4 The Enzymic Substrate Specificity of FAA Modified GOx	105
3.5 GOx Modified with Different FAA Groups	112
3.5.1 Catalytic Activity and Iron Content	114
3.5.2 Kinetic Analysis	117
3.6 Determination of pIs for FAA Modified GOx Samples	119
3.7 Studies of FAA Modified GOx Purified by Chromatofocusing Chromatography	124
3.8 Conclusions	129
Chapter IV Operational Stabilities of Covalently Modified Glucose Oxidase	131
4.1 Introduction	131
4.1.1 Characteristics of Amperometric Enzyme Electrodes	131
4.1.2 Storage Stabilities of Covalently Modified GOx	133
4.1.3 Operational Stability	135
4.2 Theory	137
4.3 Membrane Enzyme Electrodes Based on Native Glucose Oxidase	144
4.4 Membrane Enzyme Electrodes Based on FMCA Modified GOx	148
4.4.1 Electrochemical Responses	150
4.4.2 Operational Stabilities of the Membrane Enzyme Electrodes Based on FMCA Modified GOx	160
4.5 Membrane Enzyme Electrode Based on FAA Modified GOx	166
4.5.1 Electrochemical Responses	166
4.5.2 The Selectivity of the FAA Modified GOx	175
4.6 Stabilities of Some Ferrocene Derivatives	177
4.6.1 Ferrocene Derivatives as Mediator-Titrants	177
4.6.2 Stability of Some Ferrocene Derivatives	182
4.7 Conclusions	183
Chapter V Non-Covalent Modification of Glucose Oxidase	188
5.1 Introduction	188
5.1.1 Conducting Organic Salts and Conducting Organic Salt Electrodes	188

	Page
5.1.2 Enzyme Electrocatalysis at Conducting Organic Salt Electrodes	193
5.1.3 Hydrophobic Interaction between Neutral Components of Organic Salts and Glucose Oxidase	196
5.2 Electrochemistry of TTF Modified GOx	197
5.3 Electrochemistry of TTF Modified GOx Samples Prepared at Different pH Values	201
5.4 Determination of TTF Quantities for the Modified GOx	206
5.4.1 Fluorescence Spectroscopic Studies	206
5.4.2 UV-Visible Spectroscopic Studies	210
5.4.3 Attempted Determination of the Amount of TTF using a Conventional Chemical Method	210
5.5 Stability Studies of TTF Modified GOx	212
5.6 Non-Covalent Modification of GOx with Iron(II)phthalocyanine and Some Ferrocene Derivatives	214
5.6.1 Electrochemistry of FePc	214
5.6.2 Catalytic Activity of FePc Modified GOx	217
5.6.3 Non-Covalent Modification of GOx with Water-Insoluble Ferrocenes	220
5.6.4 A Comparison of the Catalytic Activities for GOx Modified with Different Mediators	220
5.7 Conclusions	224
Chapter VI Electrochemical Studies of TTF Oxidation in Aqueous/BSA Media	226
6.1 Introduction	226
6.2 Theory	228
6.2.1 Relationships between the Micelle Solubilization Equilibrium Constant, the Formal Potential ($E^{0'}$) and the Observed Reversible Half-Wave Potential ($E_{1/2}^r$)	229
6.2.2 Reaction Scheme for the One-Electron Transfer Process	231
6.3 Determination of TTF Concentrations in BSA	233
6.3.1 The Extinction Coefficient of TTF in BSA at 320 nm	233
6.3.2 Saturated TTF Concentrations in BSA	233
6.4 Half-Wave Potentials and Electron Transfer Processes	234
6.4.1 Half-Wave Potentials	234
6.4.2 Electron Transfer Processes	239
6.5 Determination of the Diffusion Coefficients	241
6.6 RDE Kinetics of TTF Oxidation to Its Monocation, TTF^+ , in BSA	245
6.7 Conclusions	248
Chapter VII Conclusions and Future Directions	251
7.1 Conclusions	251
7.2 Future Directions	251
References	253
Appendix I A Mathematical Treatment of the Kinetic Model for Modified Enzymes	265
Appendix II Previous Publications	269

LIST OF FIGURES

Figure 1.1	The structures of flavins and their redox reactions (Reproduced from reference (16))	3
Figure 1.2	A schematic representation for the homogeneous mediation of flavoenzyme electrochemistry	12
Plate 2.1	Configuration of the electrochemical system	21
Figure 2.2	Schematic representations of electrochemical cells.	23
Figure 2.3	Diagram of the home-made saturated calomel reference electrode (0.82 actual size)	25
Figure 2.4	Typical result of an enzymic activity assay $\lambda = 520 \text{ nm}$ $l = 1 \text{ cm}$ GOx dilution: 1: 160,000 Initial absorbance: 0.1162 Final absorbance: 0.2782 Total time: 1 minute Rate of absorption: 0.164 per minute	30
Figure 2.5	UV spectra of (a) FAD in buffer and (b) FAD in glucose oxidase Reference: deionised H_2O [FAD] of (a): $1.20 \times 10^{-4} \text{ mol dm}^{-3}$ [GOx]: $1.64 \times 10^{-5} \text{ mol dm}^{-3}$ Cell path: 1 cm	32
Figure 2.6	The chemical structure of (a) Sephadex and (b) Sephacryl	36
Figure 2.7	A typical calibration curve for atomic adsorption spectroscopy of iron $\lambda = 248.5 \text{ nm}$	38
Figure 2.8	Emission spectra of tryptophan residues in glucose oxidase for (1) native and (2) TTF modified glucose oxidase [GOx] native = $2.8 \times 10^{-6} \text{ mol dm}^{-3}$ [GOx] modified = $3.2 \times 10^{-6} \text{ mol dm}^{-3}$ Excitation wavelength: 280 nm Emission wavelength: 340 nm	40

	page
Figure 2.9	41
Emission spectra of FAD in glucose oxidase for (1) native and (2) TTF modified glucose oxidase $\lambda_{EX} = 450 \text{ nm}$ $\lambda_{EM} = 520 \text{ nm}$ $[GOx] \text{ (native)} = 2.8 \times 10^{-6} \text{ mol dm}^{-3}$ $[GOx] \text{ (modified)} = 3.2 \times 10^{-6} \text{ mol dm}^{-3}$ Excitation wavelength: 450 nm Emission wavelength: 540 nm	
Figure 2.10	43
A glassy carbon enzyme membrane electrode (2.5 actual size)	
Figure 2.11	46
IEF gel electrophoresis pH gradient 4-6.5 1 & 8 - standard proteins, 4mg cm ⁻³ 2 - 6.25% FAA modified GOx, 4mg cm ⁻³ 3 - 12.5% FAA modified GOx, 4mg cm ⁻³ 4 - 25% FAA modified GOx, 4 mg cm ⁻³ 5 - 50% FAA modified GOx, 4 mg cm ⁻³ 6 - 100% FAA modified GOx, 4 mg cm ⁻³ 7 - Native GOx.	
Figure 2.12	48
Elution chart of chromatofocusing chromatography for 100% FAA modified GOx x - axis, elution volume, at 0.2 cm cm ⁻³ y - axis, OD ₂₈₀ , full scale 2.0	
Figure 2.13	49
UV - Visible spectra of saturated TTF in BSA a. saturated TTF in BSA, [BSA] = 1.9 mg cm ⁻³ b. BSA in buffer (85 mmol dm ⁻³ sodium phosphate, pH 7.0) [BSA] = 1.9 mg cm ⁻³ Reference: deionised H ₂ O Cell path: 1 cm	
Figure 2.14	50
Plot of absorbance of TTF in BSA at 320 nm vs TTF concentrations. [BSA] = 19.8 mg cm ⁻³ . [TTF] varies from 1.0×10^{-3} - $4.0 \times 10^{-3} \text{ mol dm}^{-3}$ Reference: solution of 19.0 mg cm ⁻³ BSA in buffer (0.85 mol dm ⁻³ sodium phosphate, pH 7.0). Cell path: 1 cm	
Figure 3.1	54
Schematic representations of the electron transfer mechanism for native and ferrocene modified glucose oxidase	
Figure 3.2	57
Reaction scheme of the covalent modification of glucose oxidase with ferrocenemonocarboxylic acid	

	page
Figure 3.3 pH optimum studies of FAA modified GOx filled symbols -- native GOx open symbols -- FAA modified GOx diamonds -- assay carried out in phosphate buffer (85 mmol dm ⁻³) circles -- assay carried out in citrate buffer (100 mmol dm ⁻³) (Reproduced from project report by D. Caruana, University of Warwick, 1990, p49)	61
Figure 3.4 Current-voltage curves for FAA modified GOx recorded using gold, platinum and glassy carbon electrodes. [GOx] = 8.6 x 10 ⁻⁶ mol dm ⁻³ electrode areas are identical for the electrodes: 0.384 cm ²	72
Figure 3.5 Levich plots for the reduction of FAA modified GOx at gold, platinum and glassy carbon electrodes. GOx concentrations are identical, [GOx] = 8.6 x 10 ⁻⁶ mol dm ⁻³ electrode areas are identical: 0.384 cm ² E vs SCE	74
Figure 3.6 Levich plots for the oxidation currents of FAA modified GOx at gold, platinum and glassy carbon electrodes. [GOx] = 8.6 x 10 ⁻⁶ mol dm ⁻³ , electrode areas are: 0.384 cm ²	75
Figure 3.7 Computer generated least squares best-fit for current-voltage curve of FAA modified GOx recorded using platinum electrode. electrode area: 0.384 cm ² rotation speed: 36 Hz [GOx] = 8.6 x 10 ⁻⁶ mol dm ⁻³	79
Figure 3.8 Computer generated least squares best-fit for current-voltage curve of FAA modified GOx recorded using glassy carbon electrode. electrode area: 0.384 cm ² rotation speed: 49 Hz [GOx] = 8.6 x 10 ⁻⁶ mol dm ⁻³	80
Figure 3.9 Plot of κ , from computer best-fit data, versus square root of rotation speed for current-voltage curves recorded using platinum and glassy carbon electrodes $\kappa = k'_D/k'_O$ where k'_O is the standard heterogeneous electrochemical rate constant, $k'_D = 1.554 D^{1/2} \omega^{1/2} \nu^{-1/4}$	82

	page
Figure 3.10 Cyclic voltammograms of FAA modified GOx recorded at three different sweep rates. [GOx] = 2.1×10^{-5} mol dm $^{-3}$ electrode: glassy carbon (0.384 cm 2)	85
Figure 3.11 Plot of cathodic peak currents versus square root of sweep rates for FAA modified GOx. [GOx] = 2.1×10^{-5} mol dm $^{-3}$ electrode: glassy carbon (0.384 cm 2)	86
Figure 3.12 Levich plot of the limiting currents of oxidation for FAA modified GOx. [GOx] = 2.1×10^{-5} mol dm $^{-3}$ electrode: glassy carbon (0.384 cm 2)	88
Figure 3.13 Dependence of the rate of enzyme reaction on the concentrations of substrate, $v = k_{cat} s / (K_M + s)$ k_{cat} is the maximum rate under specified experimental conditions, K_M is the Michaelis constant of the enzyme.	91
Figure 3.14 Computer calculated substrate titration curves for FAA modified GOx. k_{cat} is 1500 s $^{-1}$ k_i values are: □-- 10,000 s $^{-1}$, x -- 2000 s $^{-1}$, + -- 1000 s $^{-1}$, ◇-- 200 s $^{-1}$, Δ-- 50 s $^{-1}$	97
Figure 3.15 Theoretical plots of $e^2 D / j^2$ vs K_M / s for FAA modified GOx. $k_{cat} = 1500$ s $^{-1}$ k_i values are the same as those in figure 3.14	99
Figure 3.16 DC cyclic voltammograms of (a). FAA (1.0×10^{-5} mol dm $^{-3}$) in phosphate buffer (85 mmol dm $^{-3}$, pH 7.0), and (b), enzyme-bound FAA in phosphate buffer (85 mmol dm $^{-3}$, sodium phosphate, pH 7.0)	100
Figure 3.17 Cyclic voltammograms of FAA modified GOx (4.0×10^{-5} mol dm $^{-3}$) a. in the absence of glucose, and b. in the presence of glucose (50 mmol dm $^{-3}$),	101
Figure 3.18 Substrate titration curve for FAA modified GOx [GOx] = 4.0×10^{-5} mol dm $^{-3}$ electrode: platinum (0.384 cm 2) sweep rate: 5 mV s $^{-1}$	102

	page
Figure 3.19 Plot of $1/i^2$ versus $1/s$ for FAA modified GOx using equation (3.38). [GOx] = 4.0×10^{-5} mol dm $^{-3}$ electrode: platinum (0.384 cm 2) slope = 2.2×10^{-3} μA^{-2} mmol dm $^{-3}$ intercept = 1.5×10^{-4} μA^{-2}	104
Figure 3.20 Enzyme titration for FAA modified GOx E = 0.4 V vs SCE [glucose] = 100 mmol dm $^{-3}$ electrode: glassy carbon (0.384 cm 2)	106
Figure 3.21 Substrate titration curves for: a. native GOx with FMCA (1.0×10^{-3} mol dm $^{-3}$) as homogeneous mediator [GOx] = 1.8×10^{-5} mol dm $^{-3}$ b. FAA modified GOx [GOx] = 2.1×10^{-5} mol dm $^{-3}$ electrode: platinum (0.384 cm 2) E vs SCE	108
Figure 3.22 Plot of $1/i^2$ versus $1/s$ for the titration curve of 2-deoxy-glucose with native GOx using FMCA (1.0×10^{-3} mol dm $^{-3}$) as electron transfer mediators slope = 11.8×10^{-4} μA^{-2} mmol dm $^{-3}$ intercept = 0.42×10^{-4} μA^{-2} $I = nFA(2D_m e \Sigma k_E c_{E_0})^{1/2}$, where $D_m = 3.9 \times 10^{-6}$ cm 2 s $^{-1}$ $e \Sigma = 1.2 \times 10^{-6}$ mol dm $^{-3}$ $k_E = k_{cat} s/(s+K_M)$ $n = 2$, $F = 96480$ C mol $^{-1}$, $A = 0.384$ cm 2	110
Figure 3.23 Plot of $1/i^2$ versus $1/s$ for substrate titrations of FAA modified GOx with five different sugar substrates $D = 5.0 \times 10^{-7}$ cm 2 s $^{-1}$ $e \Sigma = 2.1 \times 10^{-5}$ mol dm $^{-3}$	111
Figure 3.24 Substrates titration curves of GOx modified with different number of FAA groups electrode: gold (0.125 cm 2) sample preparations as described in section 2.5.1 (Note: no catalytic activity was observed for 6.25% FAA modified GOx)	115
Figure 3.25 Plot of the ratio of the amount of FAA to GOx used for enzyme modification versus the average number of FAA groups per enzyme molecule in the resulting modified enzyme	116
Figure 3.26 Plot of $1/i^2$ versus $1/s$ for GOx modified with different number of FAA groups electrode: gold (0.125 cm 2) E vs SCE	118

	page
Figure 3.27 Standard calibration curve for IEF gel electrophoresis. pH gradient 4-6.5 enzyme sample concentrations: 4 mg cm ⁻³ potential between the electrodes: 2000 volts pH standards as listed in table 2.4	121
Figure 3.28 Elution charts of chromatofocusing: a. native GOx; b. 100% FAA modified GOx. x - axis: elution volume (5 cm ³ per cm) y-axis: OD at 280 nm (0-2.0)	126
Figure 3.29 Substrate titration curves for different enzyme components of 100% FAA modified GOx isolated using chromatofocusing. [GOx] ₁ = 1.9 x 10 ⁻⁵ mol dm ⁻³ [GOx] ₂ = 4.0 x 10 ⁻⁶ mol dm ⁻³ [GOx] ₃ = 2.9 x 10 ⁻⁶ mol dm ⁻³ [GOx] ₄ = 5.4 x 10 ⁻⁶ mol dm ⁻³ electrode: gold (0.125 cm ²)	128
Figure 4.1a The effect at different storage conditions on the activity of the FMCA modified GOx. (Reproduced from PhD thesis, R.G. Whitaker, 1989, University of Warwick)	134
Figure 4.1b Comparison of the storage stability of: a) FAA modified GOx, b) FMCA modified GOx, at 4°C, pH 7.0 under N ₂ . (Reproduced from PhD thesis, R.G. Whitaker, 1989, University of Warwick)	134
Figure 4.2 Stability of A) FAA modified GOx, and B) FMCA modified GOx to continuous potential cycling (5mV s ⁻¹ , 20°C) (Reproduced from PhD thesis, R.G. Whitaker, 1989, University of Warwick)	136
Figure 4.3 Reaction mechanism for an enzyme electorode	139
Figure 4.4 Substrate titration curve for the membrane enzyme electrode based on native GOx (0.12 mg) with 1 mmol dm ⁻³ FMCA present in the bulk solution. E 0.508 Volts vs SCE A 0.125 cm ²	145

	page
Figure 4.5 Plot of s_{∞}/i ($\text{mmol dm}^{-3}/\mu\text{A}$) vs s_{∞} (mmol dm^{-3}) for the membrane enzyme electrode based on native GOx (0.12 mg) A 0.125 cm E 0.508 volts vs SCE	146
Figure 4.6 Plot of y ($\text{mmol}^{-1} \text{ dm}^3$) vs p for the membrane enzyme electrode based on native GOx (0.12 mg).	147
Figure 4.7 Plot of the current, corrected for background (0.16 μA), as a function of the concentration of ferrocenemonocarboxylic acid added to the bulk solution for a membrane enzyme electrode based on native GOx (0.15 mg) placed in 0.11 mol dm^{-3} glucose.	149
Figure 4.8 Substrate titration curves for Batch I of the FMCA modified GOx membrane enzyme electrodes. E 0.50 Volts vs SCE Enzyme loadings and electrode surface areas are given in table 4.3 Background currents for the electrodes: $i_{b_1} = 1.25 \times 10^{-3} \mu\text{A}$, $i_{b_2} = 0.02 \mu\text{A}$, $i_{b_3} = 0.035 \mu\text{A}$, $i_{b_4} = 0.085 \mu\text{A}$.	152
Figure 4.9 Substrate titration curves for Batch II of the FMCA modified GOx membrane enzyme electrodes. E 0.50 volts vs SCE, Enzyme loadings and electrode surface areas are given in table 4.3 Background currents for the electrodes: $i_{b_1} = 7.25 \times 10^{-3} \mu\text{A}$, $i_{b_2} = 0.0225 \mu\text{A}$, $i_{b_3} = 0.085 \mu\text{A}$, $i_{b_4} = 0.015 \mu\text{A}$.	153
Figure 4.10 s_{∞}/i vs s_{∞} plots for Batch I of the FMCA modified GOx membrane enzyme electrodes. Enzyme loadings and electrode surface areas are listed in table 4.3	154
Figure 4.11 s_{∞}/i vs s_{∞} plots for Batch II of the FMCA modified GOx membrane enzyme electrodes. Enzyme loadings and electrode surface areas are listed in table 4.3	155
Figure 4.12 Plots of y ($\text{mmol}^{-1} \text{ dm}^3$) vs p for Batch I of the FMCA modified membrane enzyme electrodes	157
Figure 4.13 Plots of y ($\text{mmol}^{-1} \text{ dm}^3$) vs p for Batch II of the FMCA modified membrane enzyme electrodes	158

	page
Figure 4.14A Calibration curves of membrane enzyme electrode based on FMCA modified GOx (0.08 mg). Curve a -- freshly prepared, Curve b -- 20 minutes after the initial measurements. E: 0.50 Volts vs SCE	162
Figure 4.14B Calibration curves of membrane enzyme electrode based on FMCA modified GOx (0.08 mg). Curve a -- freshly prepared, curve c -- the same electrode but with 1 mmol dm ⁻³ FMCA present in the bulk. E: 0.50 Volts vs SCE	162
Figure 4.15 Calibration curves for Batch III of the membrane enzyme electrodes based on FMCA modified GOx Group plots A -- in the absence of 1 mmol dm ⁻³ FMCA, Group plots B -- in the presence of 1 mmol dm ⁻³ FMCA E: 0.50 Volts vs SCE Enzyme loadings: E--1, 0.04 mg; E--2, 0.06 mg; E--3, 0.08 mg; E--5, 0.10 mg; E--6, 0.12 mg.	163
Figure 4.16 Decrease of catalytic current as a function of time for a membrane enzyme electrode based on FMCA modified GOx (0.06 mg) in 90.9 mmol dm ⁻³ glucose. Electrode surface area: 0.125 cm ² E: 0.50 Volts vs SCE Background current: 0.19 μA.	165
Figure 4.17 Substrate titration curves for a batch of freshly prepared membrane enzyme electrodes based on FAA modified GOx. E: 0.40 Volts vs SCE Enzyme loadings: E--1, 0.14 mg; E--E, 0.21 mg; E--5, 0.28 mg; E--6, 0.42 mg. Background currents for electrodes: i _{b1} = 0.28 μA, i _{b2} = 0.12 μA, i _{b3} = 0.55 μA, i _{b4} = 0.18 μA	168
Figure 4.18 Substrate titration curves for a batch of freshly prepared membrane enzyme electrodes based on FAA modified GOx with identical loadings (0.21 mg). E: 0.40 Volts vs SCE Background currents for electrodes: i _{b1} = 0.275 μA, i _{b2} = 0.325 μA, i _{b3} = 0.30 μA, i _{b4} = 0.4 μA	169

		page
Figure 4.19	s_{∞}/i vs s_{∞} plots for the membrane enzyme electrodes based on FAA modified GOx with different enzyme loadings. Enzyme loadings: E--1, 0.14 mg; E--3, 0.21 mg; E--5, 0.28 mg; E--6, 0.42 mg	170
Figure 4.20	s_{∞}/i vs s_{∞} plots for the membrane enzyme electrodes based on FAA modified GOx with identical loadings (0.21 mg).	171
Figure 4.21	Substrate titration curves for the batch of membrane enzyme electrodes based on FAA modified GOx with different enzyme loadings, after being stored in buffer (0.15 mol dm ⁻³ sodium phosphate containing 0.20 mol dm ⁻³ NaCl, pH 7.0) for 20 hrs at room temperature. E: 0.40 Volts vs SCE.	173
Figure 4.22	s_{∞}/i for the batch of membrane enzyme electrodes based on FAA modified GOx with different enzyme loadings, after being stored in buffer (0.15 mol dm ⁻³ sodium phosphate containing 0.20 mol dm ⁻³ NaCl, pH 7.0) for 20 hrs at room temperature.	174
Figure 4.23	Responses of a membrane enzyme electrode based on FAA modified GOx to five different sugar substrates. Enzyme loading: 0.21 mg E: 0.40 Volts vs SCE	176
Figure 4.24	Change in optical absorbance vs charge plots for the generation and removal of 1,1'-bis(hydroxymethyl) ferricinium ion. Concentration of 1,1'-bis(hydroxymethyl) ferrocene: 1.03 mmol dm ⁻³ and 1.22 mmol dm ⁻³ benzylviologen chloride in phosphate buffer, pH 7.0; Wavelength: 595 nm, Optical cell path: 1.25 cm.	179
Figure 4.25	Plots of absorbance vs time for FMCA ⁺ = o; FAA ⁺ = ϕ ; and BHMf = \bullet . Concentrations are 1-2 mmol cm ⁻³ in phosphate buffer at pH 7.0 (Reproduced from reference (115))	181
Figure 4.26	A typical plot of the decrease of absorbance as a function of time for ferrocenemono-carboxylic acid. Concentration of FMCA: 1.02 mmol dm ⁻³ in sodium phosphate buffer, 0.15 mol dm ⁻³ containing 0.20 mol dm ⁻³ NaCl, pH 7.0. Optical wave length: 630 nm Cell path: 1 cm	184

	page
Figure 4.27 A typical plot of $\ln(c_0/c_t)$ vs t for the ferricinium ions of ferrocenemonocarboxylic acid ($1.02 \text{ mmol dm}^{-3}$ in 0.15 mol dm^{-3} sodium phosphate buffer containing 0.20 mol dm^{-3} NaCl, pH 7.0 at room temperature)	185
Figure 5.1 The structures of some common donor and acceptor moecules	190
Figure 5.2 Structure of the oxidised and reduced forms of TTF and TCNQ respectively. (Reproduced from ref. (160))	191
Figure 5.3 Calibration curves of TTF modified glucose oxidase. Curves a, b and c correspond to the responses of the three different kinds of samples (first, second and third) described in section 5.2. Electrode material, Pt (0.384 cm^2). Recorded at a fixed potential of 0.35 V vs SCE.	199
Figure 5.4 Cyclic voltammograms of TTF modified glucose oxidase: (a) in the absence of glucose; (b) in the presence of glucose (90 mmol dm^{-3}). Sweep rate: 5 mV s^{-1} , $[\text{GOx}] = 1.02 \times 10^{-4} \text{ mol dm}^{-3}$. Electrode: GC (0.384 cm^2). Buffer: 85 mmol dm^{-3} phosphate, pH 7.0	200
Figure 5.5 Substrate titration curves for the samples of GOx modified with TTF at pH values 4.0, 5.0, 6.0 and 7.0 in the absence and presence of surfactant (Titron X-100). E: 0.35 V vs SCE. Electrode: Au (0.125 cm^2)	203
Figure 5.6 Calibration curve for TTF modified GOx prepared at pH 7.0, in the presence of surfactant (Titron X-100) for 1 hour and in the absence of surfactant for 1 hour or 3 hours. E: 0.35 V vs SCE. Electrode: Au (0.125 cm^2)	204
Figure 5.7 Emission spectra of FAD: (a), in H_2O , $[\text{FAD}] = 1.3 \times 10^{-4} \text{ mol dm}^{-3}$; (b), in native GOx, $[\text{GOx}] = 7.8 \times 10^{-4} \text{ mol dm}^{-3}$. $\lambda_{\text{EX}} = 280 \text{ nm}$. Cell path: 1 cm	208
Figure 5.8 UV - Visible spectra of TTF: 1. in purified sample of TTF modified GOx, $A_{450} = 0.17$, 2. in native GOx, $A_{450} = 0.18$; 3. in EtOH , $[\text{TTF}] = 7 \times 10^{-4} \text{ mol dm}^{-3}$; 4. saturated in buffer (0.15 mol dm^{-3} sodium phosphate containing 0.2 mol dm^{-3} NaCl, pH 7.0). Cell path: 1 mm	211

	page
Figure 5.9 Electrochemistry of iron(II)phthalocyanine at different electrode surfaces: a. edge plane graphite (GP/E), b. basal plane graphite (GP/B), c. glassy carbon (GC/k), d. platinum (PLT/KT), E. gold electrode (Au/T). Solvent: DMSO Electrolyte: 0.1 mol dm ⁻³ LiCl Sweep rate: 100 mV s ⁻¹	216
Figure 5.10 UV-visible spectra of GOx: 1. native, [GOx] = 5.3 x 10 ⁻⁵ mol dm ⁻³ , 2. modified with FePc, [GOx] = 5.3 x 10 ⁻⁵ mol dm ⁻³ . peak a: characteristic absorption for the FePc modified GOx. Cell path: 1 cm Buffer: 85 mmol dm ⁻³ phosphate, pH 7.0	218
Figure 5.11 Substrate titration curve of FePc modified GOx E: 0.35 V vs SCE Electrode: Au (0.125 cm ²)	219
Figure 5.12 The structures of some ferrocene derivatives used for enzyme modification. a. ferrocene (parent), b. 1,1'dimethyl ferrocene. The other ferrocene derivatives listed are nominated as FD(1), FD(2), FD(3), FD(4) and FD(5) respectively.	221
Figure 5.13 Cyclic voltammograms of GOx modified with a ferrocene derivative, FD(1): a. in the absence of glucose, b. in the presence of glucose (8 mmol dm ⁻³). [GOx] = 4.0 x 10 ⁻⁵ mol dm ⁻³ Electrode: platinum (0.35 cm ²) sweep rate: 5mV s ⁻¹	222
Figure 5.14 Glucose calibration curves for the samples of GOx modified with a ferrocene derivative, FD(1): a. solution of saturated FD(1) in buffer (85 mmol dm ⁻³ phosphate, pH 7.0), with a known concentration of enzyme, [GOx] = 1.0 x 10 ⁻⁴ mol dm ⁻³ ; b. FD (1) modified GOx, purified by gel filtration, [GOx] = 4.02 x 10 ⁻⁴ mol dm ⁻³	223
Figure 6.1 A plot of TTF concentrations versus the corresponding BSA concentrations. The molar extinction coefficient used is 5.9 x 10 ³ dm ³ mol ⁻¹ cm ⁻¹	235
Figure 6.2 Cyclic voltammograms of (1) TTF saturated in buffer (0.15 mol dm sodium phosphate containing 0.2 mol dm ⁻³ NaCl, pH 7.0) and (2) TTF saturated in a BSA solution ([BSA] = 19.8 mg cm ⁻³) at (a),platinum and(b), glassy carbon electrodes. Sweep rates: 5 mV s ⁻¹ Electrode areas: A _{pl} = A _{GC} = 0.384 cm ²	236

	page
Figure 6.3 Polarograms of TTF saturated in a BSA solution ($[BSA] = 94 \text{ mg cm}^{-3}$) recorded at a platinum electrode (0.384 cm^2). Sweep rate: 5 mV s^{-1}	238
Figure 6.4 Corrected Tafel plots for the first and second oxidation steps of TTF saturated in a BSA solution ($[BSA] = 94 \text{ mg cm}^{-3}$)	240
Figure 6.5 Koutecky-Levich plots for the first and second oxidation steps of TTF saturated in a BSA solution ($[BSA] = 94 \text{ mg cm}^{-3}$) at $E_1 = 300 \text{ mV}$ and $E_2 = 500 \text{ mV}$.	242
Figure 6.6 Plots of cathodic peak currents versus the square root of sweep rates for both the first and second oxidation steps of TTF saturated in a BSA solution ($[BSA] = 19 \text{ mg cm}^{-3}$). Potential range: $0\text{-}500 \text{ mV}$ vs SCE. Electrode: platinum (0.384 cm^2)	243
Figure 6.7 Koutecky-Levich plots for the first oxidation step of TTF saturated in a BSA solution ($[BSA] = 98.0 \text{ mg cm}^{-3}$) Electrode: platinum (0.384 cm^2) Potential range : $0\text{-}350 \text{ mV}$ vs SCE	246
Figure 6.8 A plot of the reciprocal of the Koutecky-Levich limiting intercept versus the concentrations of BSA (Data from Table 6.2)	249

LIST OF TABLES

Table 1.1	The properties of an ideal redox mediator	10
Table 2.1	Details of working electrodes	24
Table 2.2	Quantities of FAA and their percentage nomination	34
Table 2.3	Details of enzyme membrane electrodes	42
Table 2.4	Contents of pI calibration kit	44
Table 3.1	Properties of covalently modified glucose oxidase	66
Table 3.2	Enzymatic activities of covalently modified glucose oxidase (5-6, 120)	66
Table 3.3	Relationships for the number of electrons transferred and the diffusion coefficient of an electroactive species using different electrochemical techniques	69
Table 3.4	Limiting current values for oxidation and reduction of FAA modified GOx	73
Table 3.5	Computer mathematical curve-fit programme for the polarograms of FAA modified GOx	81
Table 3.6	Computer best-fit data for polarograms recorded using platinum and glassy carbon electrodes	83
Table 3.7	Specificity of native and FAA modified GOx	112
Table 3.8	Iron contents for the samples of FAA modified GOx	117
Table 3.9	Values of $e\sum/i_L$ and k_1 for GOx samples modified with different number of FAA groups	119
Table 3.10	pI values of native and FAA modified GOx samples	121
Table 3.11	AAS results for enzyme fractions of 100% FAA, 50% FAA and 25% FAA modified GOx	127
Table 4.1	Stability data for ferrocenes modified GOx (at 4°C, pH 7.0 under N_2)	135
Table 4.2	Summary of the analysis of data for membrane enzyme electrodes	143
Table 4.3	Values of enzyme loadings for FMCA modified GOx membrane enzyme electrodes	150
Table 4.4	Values of $[s_{\infty}/i]_0$ and k'_{ME} for the FMCA modified GOx membrane enzyme electrodes	151

Table 4.5	Values of K_{ME} , K_M and k_{cat} for two batches of membrane enzyme electrodes using FMCA modified GOx	page 160
Table 4.6	Results of batch III of the FMCA modified GOx membrane enzyme electrodes in the presence and absence of 1 mmol dm^{-3} FMCA	164
Table 4.7	Kinetic analysis of the results for the membrane enzyme electrodes based on FAA modified GOx	167
Table 4.8	Analysis of the results for the substrate specificity studies using FAA modified GOx membrane enzyme electrodes	175
Table 4.9	Electrochemical and optical properties of ferrocene derivatives	182
Table 4.10	Value of E^0 and the half lives of some ferrocene derivatives	183
Table 5.1	Activities of GOx samples modified with TTF at different pH values	205
Table 5.2	The values of limiting currents for GOx modified with different mediators	224
Table 6.1	Summary of the half-wave potentials (vs SCE) for TTF oxidation in BSA, CTAC and acetonitrile	237
Table 6.2	Analysis of the rate constant (k_R) for TTF solubilised in BSA solution	247

ACKNOWLEDGEMENTS

I would like to express my deepest gratitude to Professor P.N. Bartlett for his patient and helpful supervision of this work and for his many inspiring suggestions during the course of this project. I am also grateful to him for reading my manuscript and for his comments on the write-up.

I would also like to thank the following:

MediSense Inc. for their financial support.

Drs. S. Williams and G. Sanghera of MediSense for their help and dialogue during my placement at MediSense;

My colleagues of the electrochemistry group at Warwick for their comments and companionship, in particular Neil Blair for his selfless friendship and Vanessa Eastwick-Field for proof reading Chapters II and IV.

I am deeply indebted to my husband and both our families for their support throughout the past years and to whom, I express my greatest appreciation and love.

Finally, I would like to thank Mrs. H. Taylor for typing this thesis.

SUMMARY

In this thesis, methods for enzyme modification and electrochemical studies of modified redox enzymes are described. The modification methods are presented in terms of covalent and non-covalent processes.

Detailed studies are presented for covalently modified glucose oxidase with redox mediators based on ferrocenes. A good understanding is obtained for the kinetics of direct electron transfer between GOx modified with ferroceneacetic acid and a metallic electrode. An estimation for the number of electrons transferred and the diffusion coefficient of this modified enzyme was achieved using combined results from cyclic voltammetry and rotating disc voltammetry studied. The catalytic activity of this modified enzyme was investigated and the data were analysed using our theoretical model. The model includes the reactions between the modified enzyme and the substrate, the reoxidation of enzyme by the attached mediators and the regeneration of the mediators at the electrode. This model is fully explained in Chapter III.

The stabilities of glucose oxidase modified with ferrocenes were investigated by entrapping the modified enzyme behind a dialysis membrane. A direct correlation is established between the stabilities of the ferrocenes and the corresponding modified enzymes.

A novel enzyme modification method, non-covalent modification, is described. The catalytic activities of glucose oxidase modified with several hydrophobic mediators were studied and the determinations of the amount of mediators incorporated within the enzyme were also carried out.

A further investigation of the molecular interaction between mediators and proteins is demonstrated for the model system of TTF in aqueous/BSA media. The oxidation of TTF in a BSA solution was studied and the results were analysed.

Finally, the overall conclusions and possible future directions of this project are given.

ABBREVIATIONS

FAD	flavin adenine dinucleotide
FMN	flavin mononucleotide
GOx	glucose oxidase
SCE	saturated calomel electrode
NAD	nicotinamide adenine dinucleotide
TTF	tetrathiofulvalene
TCNQ	7,7,8,8 - tetracyanoquinodimethane
NMP	N-methyl phenazine
NMA	N-methyl acridine
FMCA	ferrocenemonocarboxylic acid
FAA	ferroceneacetic acid
FePc	iron(II)phthalocyanine
CoPc	cobalt(II)phthalocyanine
BSA	bovine serum albumin
CTAC	cetyl trimethylammonium chloride
Na-HEPES	N-2-hydroxyethylpiperazine-N ⁺ -2-ethanesulfonic acid, sodium salt
DAF	dimethylaminomethyl ferrocene
FBA	ferroceneboronic acid
FEA	ferrocene ethanol amine
4-AP	4-aminophenazone
DHSA	3,5-dichloro-2-hydroxy benzene sulphonic acid
pI	isoelectric point
IEF	isoelectric focusing
DEC	1-(3-dimethyl aminopropyl)-3-ethylcarbodiimide
AAS	atomic absorption spectroscopy
BHMF	1,1'-bis-(hydroxy methyl) ferrocene
TTN	tetrathionaphthacene

TMSA	tetramethoxyselenanthracene
TNAP	11,11,12,12-tetracyanonaphtho-2,6-quinodimethane
PVC	poly (vinyl chloride)
EPG	edge plane graphite
BPG	basal plane graphite
RDE	rotating disc electrode

CHAPTER I INTRODUCTION

The work presented in this thesis is concerned with the modifications of redox enzymes and studies of the modified enzymes using electrochemical and biochemical methods. Studies of the characteristics and properties of covalently modified enzymes are presented and the results are analysed using our theoretical model. A novel enzyme modification method, non-covalent modification, is described. This non-covalent modification of enzymes proceeds via the intermolecular attractive forces between the mediator molecules and enzymes. Originally aimed at providing an understanding for the mechanism of conducting organic salt electrodes (1-4), this non-covalent method for the modification of enzymes has proven advantages over the covalent modification method reported in the literature (5-6); it is easy to use, effective and can be used with many mediator materials.

Working/operational stabilities of modified enzymes, investigated by the construction of a membrane enzyme electrode are described and the analysis of the results using an established kinetic model (7) are discussed. Finally, further studies on the hydrophobic interaction between mediator molecules and proteins are reported.

In this introduction we begin by describing briefly the characteristics of redox enzymes and the electron transfer processes in biological systems. We then describe the various means of achieving direct electron transfer between redox enzymes and electrode surfaces.

1.1 The Characteristics of Redox Enzymes

Redox enzymes (8-9), in general, are large complex proteins which catalyse the specific oxidation or reduction of one or more substrates within a living cell. These enzymes contain redox centres or "active" sites deeply buried beneath the enzyme surface. Substrate molecules must diffuse into the

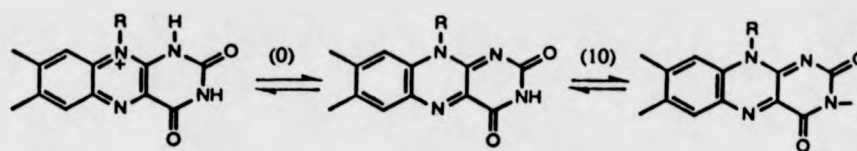
interior of the enzyme to exchange electrons with the active sites for a redox reaction to occur.

The redox enzymes can be divided into several groups based on the type of prosthetic group present. These are: flavin containing enzymes (10), quinone containing enzymes (11-12), dehydrogenases (13-15), haem containing enzymes (for example, cytochrome peroxidase (EC 1.11.1.7)) and copper containing enzymes (for example, galactose oxidase (EC 1.1.3.9)). A detailed review of the properties of these redox enzymes can be found in reference (16). In this section, we will concentrate on the characteristics of flavin containing enzymes since this type of enzyme is directly relevant to this work.

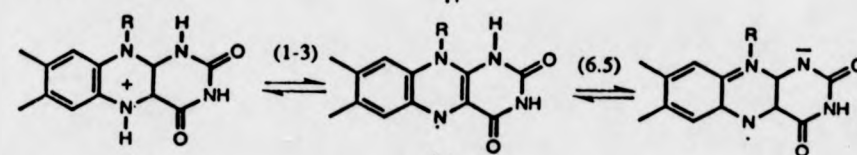
There are over 80 enzymes in this group, containing either flavin adenine dinucleotide (FAD) or flavin mononucleotide (FMN) at the active site.⁽¹⁷⁾ The majority of these 80 enzymes are FAD containing enzymes. The flavin group is strongly bound to the protein structure (18), and in some cases, bound covalently to an amino acid residue of the enzyme (for example, in succinate dehydrogenase (EC 1.3.99.1) (16). The structures of flavins and their redox reactions, which are described in detail by the authors of references (19-20), are shown in figure 1.1.

The classification of flavoenzymes has been discussed in the literature (16). There are two types of classification for flavoenzymes. First, the group of enzymes having a specific metal cofactor requirement (generally iron or molybdenum) are called metalloflavoenzymes, for example, glucose oxidase (EC 1.1.3.4) or xanthine oxidase (EC 1.2.3.2). The exact function of the metal in these flavoenzymes apparently remains unclear (21). Second, the flavoenzymes are classified in terms of being oxidases or dehydrogenases, depending on their behaviour towards molecular oxygen. In flavo-dehydrogenases, the reduced flavin groups show little tendency to be reoxidised by molecular oxygen (22). Flavo-oxidases, on the other hand, are

Quinone State (FAD or FMN)



Semiquinone State



Hydroquinone State (FADH₂ or FMNH₂)

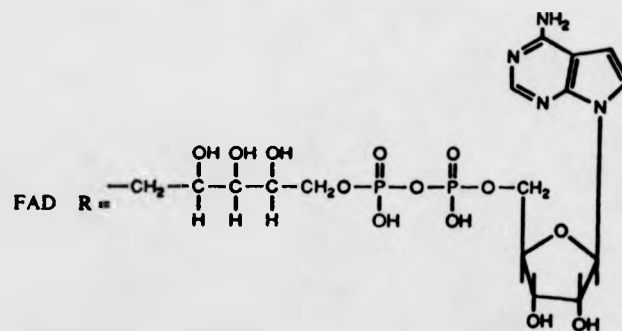
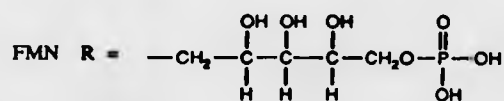
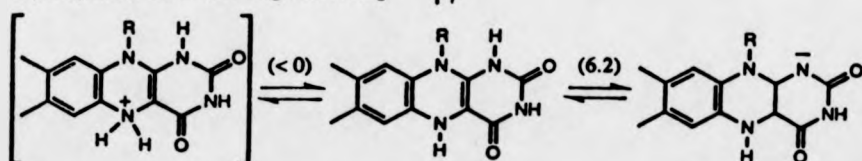


Figure 1.1 The structures of flavins and their redox reactions. Figures in brackets are pk_s of species. (Reproduced from reference (16)).

readily reoxidised by molecular oxygen producing hydrogen peroxide as a by-product of the enzyme reaction (23). A typical flavo-oxidase catalysed reaction is illustrated by the glucose oxidase (GOx) catalysed reaction of β -D-glucose with molecular oxygen:



These reactions may be monitored either through the formation of hydrogen peroxide or the consumption of oxygen (24-26).

It is apparent that these enzymes are large in size (for example glucose has a diameter of 86 Å (25)) with molecular weights greater than 1×10^4 Dalton (glucose oxidase has a molecular mass of 150,000 - 186,000 Dalton) (26). The location of the flavin prosthetic group or groups within the enzyme structure has important effects on efforts to achieve direct electron transfer at simple metallic electrodes. A major obstacle to rapid electron transfer between the prosthetic group and the electrode is the large distance (27). The theoretical aspects of the effects of distance on electron transfer rates will now be described.

1.2 The Effect of Distance on the Rate of Electron Transfer

If we consider the typical sizes of redox enzymes (for instance, glucose oxidase described above), it is clear that even in the absence of any complications such as protein fouling at the electrode, one of the major causes for slow electron transfer is distance, always assuming that the electron transfer is thermodynamically favourable. The effect of distance on electron transfer and in particular its effect on electron transfer in redox proteins and biological systems has been reviewed by several authors (28-29).

We will describe below briefly the existing theoretical aspects on this subject (29).

A general expression for the electrochemical rate constant can be written as (16):

$$k' = k_E' \nu k_{el}(r) \exp(-\Delta G^*/RT) \quad (1.3)$$

where k' is the heterogeneous rate constant,

k_E' describes the diffusion pre-equilibrium,

ν is the effective frequency for nuclear motion
along the reaction coordinate,

$k_{el}(r)$ is the electronic transfer coefficient
or averaged transition probability for electron
transfer at a fixed separation distance r of the
reactants, and

ΔG^* is the free energy of activation.

In the above equation, $k_{el}(r)$ is about unity (29) for adiabatic reaction (a reaction in which there is substantial electronic coupling between the reactants) and is usually assumed to vary with r at large separation distance between the reactants. For electron transfer reactions over large distances, this distance dependence is expressed as:

$$\nu k_{el}(r) = \nu_0 \exp(-\beta(r-r_0)) \quad (1.4)$$

where r_0 is the value of distance at which $\nu k_{el}(r)$ equals ν_0 .

The value of β in eqn. (1.4) is about 12 nm^{-1} for aromatic molecules in non-biological systems. The values of β are likely to vary somewhat from system to system, depending, for example, on the vertical ionization potential of the redox site and its determination for various model systems, for reactions of ground states, electronically excited states, anions, and cations, and its dependence on the intervening material present a central experimental problem in this field. A rough interpretation of β is in terms of electron tunnelling through a square potential barrier. Using a standard

quantum-mechanical tunnelling formula,

$$\beta = (4\pi/h) (2m V_0)^{1/2} \quad (1.5)$$

where m is the mass of the electron, V_0 is the height of the potential barrier. Values of β of 11 and 15 nm⁻¹ give V_0 of 1.1 and 2.1 eV respectively.

For biological redox couples, some additional factors must be considered in the calculations. First, the molecules are not spherically symmetric so that $(r-r_0)$ in equation (1.4) must be replaced by the actual separation. Second, the protein around the redox site is inhomogeneous, so that some paths may be more favourable than others for electron transfer.

Even so, it is clear that as the distance increases the probability of electron transfer decreases. A simple calculation shows that, for example, if the FAD in GOx is 30 Å below the protein surface then $k_{el}(r)$ will be reduced by a factor of 2×10^{-14} . In order to tackle the problem of achieving direct electron transfer between redox enzymes and simple electrodes, a number of strategies have been investigated. These strategies will be described in the following sections. First, we will describe the results for the unmodified, unmediated reaction at metallic electrodes.

1.3 Direct Electrochemistry of Redox enzymes

In this section we describe the electrochemical behaviour of enzymes containing redox active prosthetic groups (for example, FAD). The redox properties of the free prosthetic groups in solution in the absence of the protein have been studied extensively and in some cases, are reasonably understood (30-31). However, since the environment within the enzyme structure is very different from that in solution and varies from enzyme to enzyme, the redox potential of the prosthetic group bound to an enzyme may be shifted from that of the same group in solution. For example, flavoproteins (not necessarily enzymes) are known with redox potentials

ranging from -730 to -50 mV vs SCE (32), at pH 7.0.

We will consider a specific flavoenzyme, glucose oxidase, as an example. Glucose oxidase (E.C. 1.1.3.4), isolated from strains of *A. niger* (33), has attracted much attention from electrochemists because of its use in amperometric sensors (34-43) and the importance of glucose measurement (44-48). Although the full crystal structure of the enzyme has yet to be determined (preliminary results have been published on X-ray diffraction studies of the crystals of the deglycosylated enzyme (49)), it is known to consist of two identical subunits, each containing a FAD centre and has a hydrodynamic radius of 4.3 nm (50). The redox potential of the FAD prosthetic group of glucose oxidase has been reported to be of -305 mV vs SCE at pH 5.3 (51). This value for glucose oxidase may be compared with the value for the FAD/FADH₂ couple in solution of -568 mV vs SCE at pH 7.0 (52). This clearly demonstrates that the environment at the active site of the enzyme can have a profound effect on the redox reaction of the FAD centres.

Much of the earlier work on achieving direct electron transfer between the prosthetic groups of enzymes and electrodes was carried out using mercury electrodes (53-54). It is known that a number of proteins adsorb irreversibly on mercury electrodes (55-58). It is suggested that in such systems the existence of mercury-disulphide interactions between the electrodes and the disulphide groups in the protein cause the flavoenzyme to become flattened at the electrode surface (59). As a consequence of this distortion to the enzyme structure the flavin groups could then get close enough to the electrode for electron transfer to occur. However, this distortion in the protein structure will mean that the currents observed will be several fold larger than those observed for the enzyme in its native globular state (16). The distortion may also result in the loss of enzymatic activity and specificity such that direct electron transfer is of little use for practical applications.

A recent report by Bockris and co-workers also showed evidence for electron transfer to strongly adsorbed glucose oxidase at graphite and gold electrodes. At graphite electrodes, they found evidence for some extensive and slow unfolding leading to the adsorption of FAD directly onto the electrode surface (60). These processes were found to be dependent on enzyme concentration. At low enzyme concentrations ($< 20 \mu\text{mol dm}^{-3}$), direct electron transfer was observed from the undistorted enzyme molecules. At gold electrodes, they observed similar processes (71). They conclude that the adsorption of enzyme on gold proceeds in three stages: the enzyme is adsorbed initially with its long axis perpendicular to the electrode surface, this adsorbed enzyme then undergoes a transition to become adsorbed with its long axis parallel to the electrode surface, it is in this configuration that slow unfolding of the enzyme occurs with significant loss of tertiary structure. According to their calculations of the electrostriction pressure, the authors estimate that the pressure experienced by the enzyme at the electrode surface can be as high as 1000 atm. This pressure arises from the high electric field in the double layer and it is likely to be the cause for the enzyme unfolding.

In order to overcome the problems of protein distortion and electrode fouling, a number of authors have investigated the possibility of direct electron transfer between immobilised enzymes and modified electrodes (61-63). These approaches are aimed at immobilising the enzyme in a specific conformation by using covalent coupling or cross linking so that protein distortion can be prevented. Nevertheless, the results from such experiments appear to be irreproducible and sensitive to the immobilisation techniques used. For instance an apparent direct electron transfer was observed when L-amino acid oxidase (EC 1.4.3.2) or xanthine oxidase was immobilised onto cyanuric chloride modified graphite electrode (61,64), but when glucose oxidase was covalently linked to a glassy carbon electrode (65)

using carbodiimide coupling no direct electrochemistry was recorded.

In many cases, the difficulty in understanding direct electrochemical behaviour of flavoenzymes is due to the possibility that either the direct electrochemistry results from the presence of free flavin acting as a mediator, or because there exists some impurity in the enzyme solution. There is no easy way to distinguish between the electrochemical response due to electron transfer from enzyme bound flavin or free flavin.

Generally, direct electron transfer between flavoenzymes and modified electrodes is largely dependent on the immobilisation procedure and for adsorbed flavoenzymes, the electrochemical response is likely to result from the free flavin groups. An alternative method for studying enzyme electrochemistry is to use indirect techniques to facilitate the electron transfer between flavin centres and metallic electrodes. Many methods have been developed in this area. In the following sections, we will describe these methods.

1.4 Mediated Electron Transfer

This section describes the use of artificial electron acceptors or mediators (22) to shuttle electrons between the flavin centres of an enzyme and an electrode. This mediated electron transfer mechanism is often described in terms of homogeneous mediation or heterogeneous mediation (16). Literature reports on both of these mediated electron transfer systems are summarised.

Most oxidase enzymes can utilise artificial electron acceptors or mediators. These mediators are usually low molecular weight molecules, capable of diffusing into the interior of the enzyme and exchanging electrons with flavin groups. In this process, the mediator is cycled between its oxidised and reduced states. Traditionally organic dyes, such as phenazine methosulphate and 2,6-dichlorophenolindophenol (66) as well as inorganic

compounds such as ferricyanide (67) have been used as electron acceptors for flavins. However, these mediators have many unsuitable properties, in particular for use in enzyme electrodes or biosensors. For example, organic dyes can undergo rapid autoxidation, they are cytotoxic, unstable in the reduced form and have pH dependent redox potentials (69). The criteria for an ideal redox mediator have been described by several authors (16). They are given in table 1.1.

Table 1.1 The properties of an ideal redox mediator

-
1. reversible electrochemistry
 2. rapid reaction with the redox enzyme
 3. well defined n value (1 or 2 electrons)
 4. stable in both oxidised and reduced form
 5. pH independent redox potential
 6. not prone to autoxidation
 7. soluble in aqueous and organic media
 8. amenable to chemical substitution to provide a range of redox potentials (below 500 mV vs SCE in most cases)
-

The structures and properties of ferrocene (bis (η^5 - cyclopentadienyl) iron, $\text{Fc}p_2$) and its many derivatives have resulted in considerable number of studies (69-70) in recent years. Ferrocene and some of its derivatives exhibit reversible electrochemistry and fast enzyme kinetics with a number of flavoenzymes (68,72,81). They also fulfill the criteria listed in table 1.1. By appropriate substitution of the cyclopentadiene rings, their redox potentials can be tuned to match the required enzyme reaction. In general, ferrocene derivatives appear to be the ideal choice of mediators for indirect electrochemistry of flavoenzymes.

1.4.1 *Homogeneous Mediation*

In the homogeneous mediation regime, both the mediator and the enzyme diffuse freely in the solution. The mediator is generated at the electrode and diffuses into the bulk solution where it meets and reacts with the enzyme. The reaction cycle completes when the mediator molecules diffuse back to the electrode to become re-oxidised or re-reduced (16). A schematic representation is shown in figure 1.2.

Using cyclic voltammetry it is possible to assess the effectiveness of a particular mediator/enzyme combination using theory developed for the EC' catalytic case and to determine the second order rate constant for the reaction between the enzyme and the mediator (73-75). A summary of the literature on this can be found in reference (16).

In the efforts to search for new and better mediators, it is informative to consider whether or not there are any relationships between the physical and structural properties of mediator compounds for a particular enzyme and the kinetics of the reaction. The reaction of glucose oxidase with ferrocene derivatives has been studied (68). Ferrocene derivatives of varying charge and solubility with redox potentials ranging between 100 and 400 mV (vs SCE) have been shown to accept electrons from glucose oxidase. However, the published results reveal little direct correlation between the redox potentials of mediators and the second order rate constant for the enzyme/mediator reaction. This appears to imply that the rate limiting step in this system is not the electron transfer or that the redox potential of the mediator may have been shifted significantly when it is inside the enzyme. The exact mechanism of enzyme/mediator interaction is not well understood at present (16).

There are a number of other examples (76-78) of mediated reactions involving electrochemical regeneration of the redox mediator. From literature studies, it is apparent that until a better understanding of the mechanism of

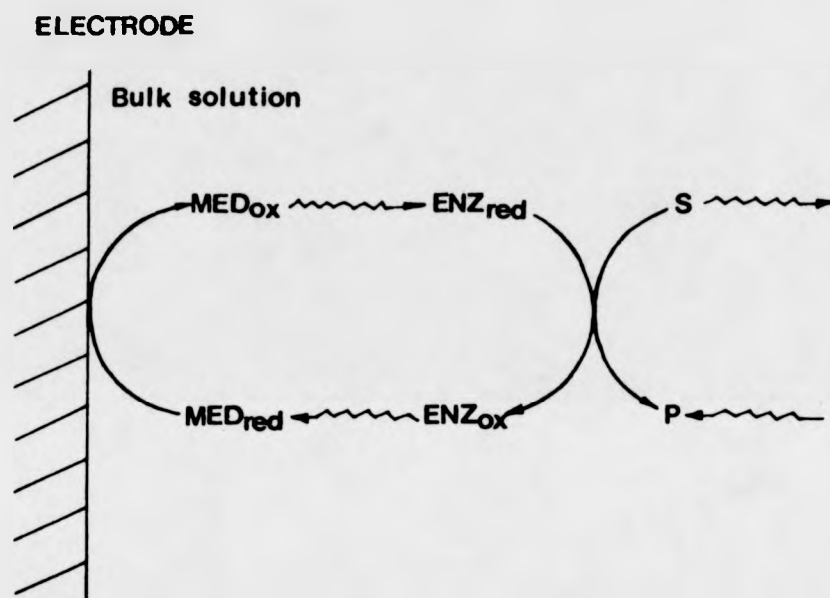


Figure 1.2 A Schematic representation for the homogeneous mediation of flavoenzyme electrochemistry.

MED_{ox} and MED_{red} are the oxidised and reduced forms of the mediator respectively; ENZ_{red} and ENZ_{ox} are the reduced and oxidised forms of the enzyme; S and P represent the substrate and the product.

enzyme and mediator electron transfer reaction is achieved, the choice of a mediator for an enzyme reaction still has to depend largely on experimental trial and error.

1.4.2 Mediation in Heterogeneous Systems

In the heterogeneous mediation regime, the mediator and/or the enzyme is immobilised at the electrode surface. Much of this work was carried out using an immobilised flavoenzyme/soluble mediator system. A large number of reports dealing with the heterogeneous electron transfer between the immobilised glucose oxidase and a mediator in solution have been published (79-82).

Studies of such heterogeneous systems include the mediated electron transfer between the enzyme entrapped in a porous or gelled layer and an electrode using the benzoquinone/hydroquinone couple (79), or the covalently immobilised glucose oxidase with 1,1'-dimethyl ferrocene localised at the electrode by the inclusion in a conducting paste (80-82). The latter configuration of electrode has been used with a variety of redox enzymes (83-86).

Another method for immobilising the enzyme at the surface of an electrode is to entrap it within an electropolymerised film. This technique has the advantages of allowing excellent control over deposition, of being simple to carry out and of allowing the deposition of one layer on top of another (16). Conducting polymers, such as poly(pyrrole) (86-89) and poly(N-methylpyrrole) (90) have been used to immobilise glucose oxidase. The enzyme appears to be incorporated in the growing film because the negatively charged enzyme can balance the positive charge on the oxidised polymer film. In addition to poly(pyrrole) and poly(N-methylpyrrole) electrochemically polymerised phenol (91), indole (92), aniline (91,93) and o-phenylenediamine (94) films have also been used to entrap glucose oxidase.

Pre-polymerised poly(pyrrole) films have also been used as a support for the immobilisation of glucose oxidase (95-96). In these immobilised enzyme systems, the enzyme reaction is catalyzed by the use of a mediator.

Several research groups have also investigated heterogeneous electron transfer systems where the mediators are either immobilised with the enzyme free in solution or coimmobilised with the enzyme. This approach is aimed at overcoming the problem of the mediator leaching out of the electrode and being lost to the bulk solution for the systems of immobilised enzymes described above. Reports have shown that covalently immobilised glucose oxidase can be used with strongly absorbed N-methyl phenazinium ion (97) to make a glucose sensitive electrode. The catalytic currents, in this case, may be due to the small amount of mediators desorbed from the electrode surface and these mediator molecules are responsible for shuttling electrons between the enzyme active site and the electrode.

In the next two sections, we will describe the approaches for studying direct enzyme electrochemistry by the use of conducting organic salt electrodes and by modifying the enzyme with electron transfer mediators or relays. Literature reports on these two methods are reviewed and the enzyme modification techniques used in the work presented in this thesis are outlined.

1.5 Conducting Organic Salts

Electrodes made from highly conducting organic salts have been used in bioelectrochemistry by a number of groups (1-4). The application of these materials has included the oxidation of NADH (107) and the redox reactions of redox enzymes (78). Details of the mechanism of conducting organic salt electrodes in biocatalysis are described in Chapter V.

Conducting organic salts are known to be easily prepared by combining suitable organic electron donors and electron acceptors (108). Examples of

some electron donor and acceptor compounds are given in Chapter V, figure 5.1. To achieve high conductivity it is essential that these electron donors and acceptors form separate stacks and there is partial charge transfer between the stacks (16). The most well studied organic salt is probably tetrathiofulvalinium tetracyanoquinodimethanide (TTF.TCNQ) complex. This complex is a black crystalline material with a conductivity comparable with graphite (109). High conductivity is found along the direction of the TTF and TCNQ stacks while much lower conductivity exists perpendicular to the stacks (16).

Conducting organic salts can be made into electrodes in a number of ways. The preparation procedures are detailed in Chapter V. The electrochemistry of TTF.TCNQ (110) and several other donor-TCNQ (111) electrodes in aqueous solution have been studied by Jaeger and Bard. Their study showed that the stable potential window for these materials was determined by the oxidation or reduction of the acceptor and donor. Within the stable range, these materials behave very much like ordinary electrode materials. For example, reversible electrochemistry of ferro/ferri cyanide redox couple has been observed at these electrodes.

Conducting organic salt electrodes were first used in enzyme catalysis by Kulys et al. (98-102). They used NMP.TCNQ (NMP⁺ is N-methyl phenazinium), NMP (TCNQ), and NMA.TCNQ (NMA⁺ is N-methyl acridinium) as electrode materials either in the form of pressed pellets or as a paste. They observed direct oxidation for glucose oxidase (*Penicillium vitale*, EC 1.1.1.4), lactate dehydrogenase (EC 1.1.2.3), peroxidase (EC 1.11.1.7) (98-101) and xanthine oxidase (EC 1.2.3.3) (102) at these electrodes. Based on their results, they concluded that the electron exchange with the lactate dehydrogenase and with peroxidase proceeded directly at the electrode. For the oxidation of glucose oxidase, they proposed a homogeneous mediated mechanism (112).

Albery et al. extended the use of organic conducting salts as electrode materials for flavoproteins (77). They studied a number of conducting salts as electrode materials for the oxidation of glucose oxidase (7). They found that TTF.TCNQ was the best electrode material amongst all of the salts studied because of its low background currents. They also reported oxidation of xanthine oxidase, D-amino acid oxidase (EC 1.4.3.3), L-amino acid oxidase (EC 1.4.3.2) and choline oxidase (EC 1.1.3.1.7) (78,103-106) at TTF.TCNQ electrodes. Based on their findings, they proposed a heterogeneous electron transfer mechanism (3) where one of the species is mobile on the electrode surface and is responsible for the interaction between the active site of the enzyme and the electrode. A fuller discussion of the controversy over the exact mechanism of enzyme catalysis at conducting organic salt electrodes can be found in Chapter V.

In conclusion, these conducting salts are particularly good materials to make electrodes for biocatalysis. The electrode reactions are fast and the organic salts are very stable (16). A recent study has shown that a TTF.TCNQ electrode for glucose was able to work up to 28 days when implanted in the brain of a freely moving rat (113).

1.6 Modified Redox Enzymes

The majority of the work presented in this thesis is concerned with the modified enzyme systems. In these systems, direct electrochemistry at bare metallic electrodes is achieved by attaching a number of mediator molecules to the polypeptide backbone of the enzyme. These mediators are responsible for the electron transfer between the active site of the enzyme and the electrodes. This approach for obtaining direct electrochemistry of redox enzymes has a distinct advantage over those already discussed above; the modified enzymes will not introduce toxicity into the system and hence they may be of use in *in vivo* sensor devices. The literature methods for enzyme

modification, the covalent modifications and a novel method for modifying enzymes, the non-covalent modification are briefly introduced below (further details of these methods are described in Chapters III and V respectively).

1.6.1 *The Covalent Modification of Enzymes*

A number of research groups have investigated the effect of covalently attaching the mediator to the amino acid residues of the enzyme. Hill first reported a method of utilising mixed anhydride to attach ferrocene centres to glucose oxidase (114). The modified GOx was observed to give a catalytic current in the presence of glucose. Recently, Degani and Heller (5-6) reported covalent modification of glucose oxidase with ferrocenemonocarboxylic acid (FMCA) and ferroceneacetic acid (FAA) as well as ruthenium pentaamine complexes. They have also carried out successful modifications of D-amino-acid oxidase with ferrocenes and ruthenium pentaamine mediators. The attached mediator molecules, or electron relays, are believed to act as "stepping stones" allowing the electrons to be transferred in several short steps, instead of one long step. When substrate was present, catalytic responses were obtained for all the modified enzyme samples.

In any practical applications of the covalently modified enzymes, the attached mediator molecules are cycled between their reduced and oxidised forms repeatedly, thus both forms should be stable. We have carried out studies for the working stabilities of the FMCA and FAA modified glucose oxidases (47) by entrapping the modified enzyme in a thin layer behind a dialysis membrane at the electrode surface. The details are presented in Chapter IV.

The modifications of enzymes (covalently or non-covalently) with electron transfer relays are an interesting means of obtaining direct electrochemistry for redox enzymes. This approach can provide a useful

probe into the nature of electron transfer between the prosthetic groups of redox enzymes and simple electrodes.

1.7 Summary of Work Presented in This Thesis

Chapter II of this thesis is concerned with all the experimental techniques and instrumentation employed during the course of this project. Details of the electrochemical and biochemical methods are described.

In Chapter III we present a detailed study for the properties and characteristics of the ferroceneacetic acid modified glucose oxidase. The electrochemical behaviour of this FAA modified GOx in the absence of glucose was studied using both cyclic voltammetry and rotating disc voltammetry. The catalytic properties of FAA modified GOx were investigated in the presence of glucose and several other sugar substrates. The results are analysed using our theoretical model.

In Chapter IV studies of the working stabilities of FMCA and FAA modified GOx are reported and an analysis of the results using the established theory (117) are presented.

In Chapter V the details of non-covalent modification of GOx with TTF, Fe(II)Pc and some ferrocene derivatives are described. The catalytic activities of these modified enzymes are assessed and a comparison is made of the efficiency of different modified enzymes.

Chapter VI describes further studies of the hydrophobic interaction between mediators and proteins for the model system of TTF, solubilised in BSA solution. Kinetic properties of this system are analysed following the theoretical model developed by Eddowes and Grätzel (198-199) for the system of TTF solubilised in aqueous/CTAC micelle media.

In the final chapter of this thesis, a general conclusion of this project is given in terms of achieving direct electron transfer between the prosthetic groups of redox enzymes and simple electrodes and an understanding of the

catalytic and kinetic properties of the modified enzymes. Suggestions for future research opportunities from this project are also given.

CHAPTER II EXPERIMENTAL TECHNIQUES AND INSTRUMENTATION

2.1 Introduction

This chapter contains details of all the experimental work described in this thesis. Details of the electrochemical measurements are presented and the biochemical techniques employed in this project (such as assay of enzyme activity, determination of protein isoelectric points using gel electrophoresis and chromatofocusing chromatography) are described. The use of atomic absorption spectroscopy and fluorescence spectroscopy as a means to determine the respective quantities of the covalently and non-covalently bound mediators in glucose oxidase are presented. The construction of enzyme membrane electrodes and the preparation of protein-mediator conjugates are also described.

2.2 Electrochemistry System

2.2.1 *Electrochemical Instrumentation*

All electrochemical measurements were made using a conventional three electrode system controlled by a potentiostat (Oxford Electrodes). The triangular-wave generator has a voltage output of -5.0 volts to +5.0 volts and the DC voltage source has an output of ± 5.0 volts. The voltage outputs were recorded either on a XY-t chart recorder (Bryans Instruments, Gould 60000 series) or an auto-ranging multimeter (Keithley 175). For rotating disc electrodes studies a rotator and controller (both made by Oxford Electrodes) were used. In all electrochemical experiments solutions were thermostatted at $25 \pm 0.10^\circ\text{C}$ using a Grant W38 circulating water bath. The general layout of the apparatus is shown in Plate 2.1.

2.2.2 *Electrochemical Cells and Electrodes*

2.2.2.1 Cells

The electrochemical cells were specially designed and made of Pyrex glass by the departmental glass-blower or obtained from Oxford University. Three different



Plate 2.1 Configuration of the electrochemical system



types of cells were used. The first was a jacketed, three-compartment macro-cell used to study sample volumes of 10-25 cm³. It was constructed to allow thermostatted water to be pumped through the jacket thereby maintaining the cell contents at a constant temperature. Built-in nitrogen inlet allows oxygen-free nitrogen to be bubbled through the solution prior to an experiment, and to be passed over the solution during the experiment. The counter electrode is separated from the bulk of the solution by a glass frit in order to prevent products of the counter electrode reaction mixing with the bulk solution.

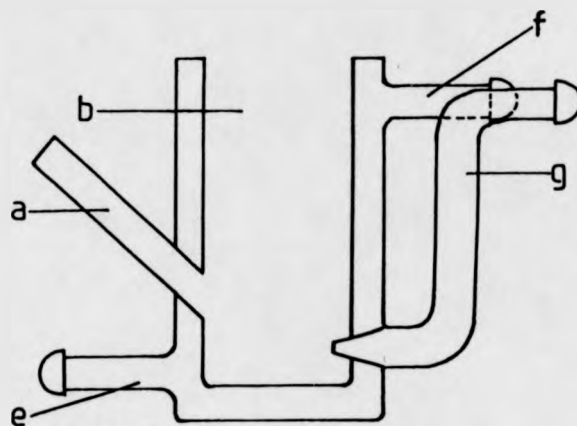
The second cell design was a semi-macro two compartment cell suitable to study samples of 2-5 cm³. In this cell, the main compartment for working and counter electrode was connected to the reference electrode section through a fine capillary.

The third was a micro-cell similar to the semi-macro cell already described. It was used to study samples of 0.5-1.0 cm³. The main section in this cell was connected to the reference section through a fine hole and the reference compartment was designed for use with commercial calomel electrode (Radiometer).

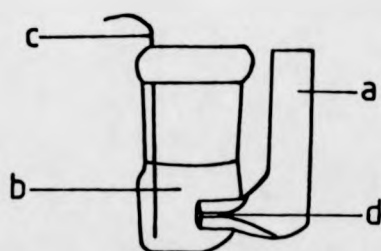
Schematic representations of these cells is shown in figure 2.2

2.2.2.2 Electrodes

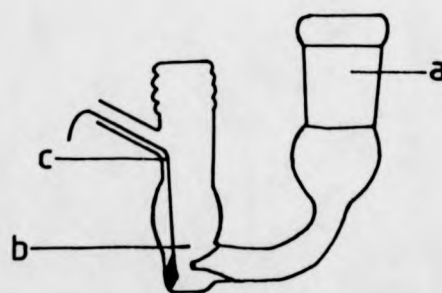
Rotating disc working electrodes were obtained from Oxford Electrodes. A small gold electrode and edge plane and basal plane graphite electrodes were kindly lent by MediSense Inc. Rotating disc working electrodes were made of gold, platinum or glassy carbon and the surrounding sheath materials were Teflon, Araldite or KelF. The electrode surface areas were measured using a travelling microscope by taking the mean value of ten randomly selected diameters for each electrode. Details of the electrodes used in this work are given in Table 2.1.



macro-cell (0.7 actual size)
 a--section for reference electrode
 b--section for working electrode
 e--water-inlet
 f--water-outlet, g--N₂ inlet



semi-macro cell (actual size)
 a--section for reference electrode
 b--section for working electrode
 c--Pt counter electrode
 d--capillary



micro-cell (actual size)
 a--section for reference electrode
 b--section for working electrode
 c--Pt counter electrode

Figure 2.2

Schematic representations of electrochemical cells.

Table 2.1 Details of Working Electrodes

Marking	Electrode	Sheath	Area/cm ²
PLT/KT	Platinum	KelF	0.384
PLT/E	Platinum	Araldite	0.385
GC/K	Glassy C [*]	KelF	0.385
AU/T	Gold	Teflon	0.386
Au/TI	Gold	Araldite	0.124
GP/E	EP ⁺ graphite	Araldite	0.165
GP/B	BP ^Δ graphite	Araldite	0.175

* - glassy carbon

+ - edge plane graphite

Δ - basal plane graphite

The working electrodes were cleaned prior to each experiment by polishing with both 1.0 μm and 0.3 μm alumina (Engis) followed by a thorough rinsing with deionised water. When there was mechanical damage or chemical contamination of the electrode surface, the electrodes were polished using various grades of diamond spray (Engis). 6 μm lapping spray (Engis) was first applied to a lapping pad (Engis) together with Hyprez lubrication fluid (Engis). Polishing was carried out using a purpose-built device in conjunction with the rotator. This was followed by polishing with 3 μm diamond spray (Engis) on a fresh polishing pad lubricated with Hyprez fluid (Engis). A mirror finish of the electrodes was finally achieved by hand polishing with 1.0 μm and 0.3 μm alumina slurry on absorbent cotton wool buds.

The saturated calomel electrode (SCE) was used as the reference electrode throughout. Reference electrodes were either home-made (shown in figure 2.3) or of a commercial type (Radiometer). In the case of the home-made electrodes the potentials were periodically checked against a commercial standard SCE to ensure consistency of the reference electrode potential. If deviation of greater than

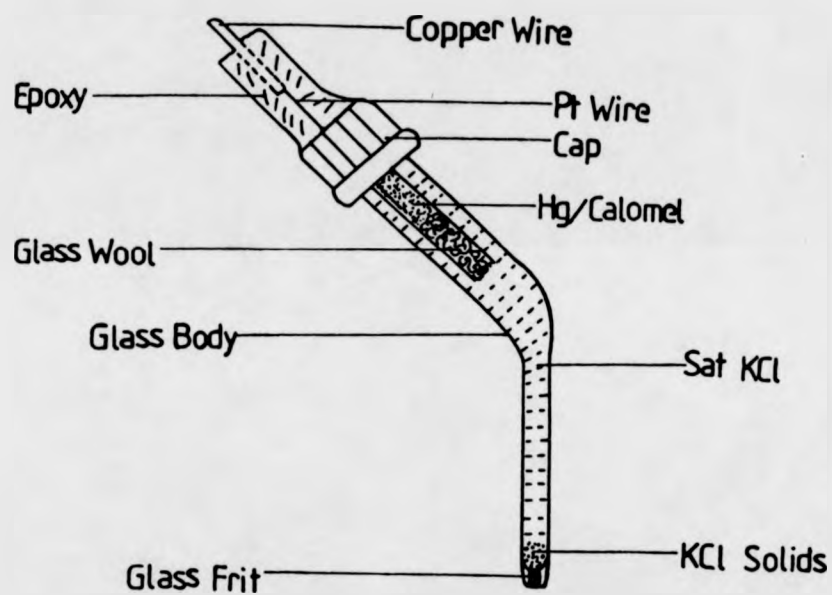


Figure 2.3

Diagram of the home-made saturated calomel reference electrode (0.82 actual size)

+/- 2 mV was found the electrode was repacked with calomel and retested before further use.

Counter electrodes were either made from a length of platinum wire or from a piece of platinum gauze, spot-welded to a suitable length of platinum wire. The counter electrodes were cleaned in flame when necessary.

2.2.3 *Deoxygenation of Solutions*

Deoxygenation of solutions was achieved by bubbling oxygen-free nitrogen through the solution for 15-20 minutes prior to the experiment. Two nitrogen sources were used: either a commercial nitrogen cylinder or a gas boiled off liquid nitrogen produced by the department. In the latter case the nitrogen was pretreated before use by passing it through a line of dreschel bottles containing a caustic solution of anthraquinone-2-sulphate in contact with zinc mercury amalgam. This deoxygenating solution was prepared in the following manner: Zinc metal (35 g) were washed with HCl (30 cm³, 2 mol dm⁻³) for 30 seconds and with 2% Hg₂Cl₂ (30 cm³) for further 30 seconds. The zinc mercury was then rinsed with deionised water and NaOH (12 g), anthraquinone sulphonate (0.6 g) were added together with deionised water (300 cm³). The mixture was stirred at room temperature for 30 minutes or until dark red. The solution turns straw yellow when exhausted.

2.3 Chemicals and Solutions

The majority of chemicals were purchased from commercial suppliers and used without further purification. Glucose oxidase (concentrated aqueous solution) and some ferrocene derivatives (as indicated) were generous gifts from MediSense Inc.

Disodium hydrogen orthophosphate (AnalaR) was purchased from Fisons. N-2-hydroxyethylpiperazine-N'-2-ethanesulfonic acid, sodium salt (Na-HEPES), AnalaR, was obtained from Sigma. Sodium chloride (AnalaR) was purchased from Fisons and lithium chloride (AnalaR) from BDH. The following mediator compounds were used:

Ferrocenemonocarboxylic Acid (FMCA), Aldrich, 98%;
Ferroceneacetic Acid (FAA), Aldrich, 98%;
Tetrathiafulvalene (TTF), Aldrich, 97%;
7,7,8,8-Tetracyanoquinone dimethane (TCNQ), Aldrich, 98%;
Iron(II)phthalocyanine (FePc), Strem Chemicals;
Cobalt(II)phthalocyanine (CoPc), Strem Chemicals;
Dimethylaminomethyl Ferrocene (DAF), Aldrich, 98+%;
Ferroceneboronic Acid (FBA), Aldrich, pure;
t-Butyl Ferrocene, Aldrich;
Ferrocenethanolamine (FEA), MediSense Inc.

β -D-glucose was the most common enzyme substrate. It was obtained from BDH, AnalaR grade. 2-deoxy-D-glucose (Sigma, Grade III), D-mannose (Sigma), D-xylose (BDH) and D-galactose (Sigma, 99.9%) were also employed as substrates to study the specificity of glucose oxidase. All buffered solutions of substrate isomers were allowed to equilibrate at room temperature for at least 24 hours before use.

The enzyme glucose oxidase (GOx, E.C. 1.1.3.4) from strains of *A. Niger* was obtained either from Sigma (Type VII, 176.9 units mg^{-1}) or was a gift from MediSense (concentrated aqueous solution, 150-210 mg cm^{-3} 180-250 units mg^{-1}). Each batch of stock glucose oxidase solution obtained from MediSense was filtered through a 0.22 μm sterile syringe membrane filter (Millipore MILLEX-GV) to avoid bacterial contamination. The filtered enzyme solution was then transferred into a number of 1 cm^3 sterile sample vials with secure caps (Sigma) using a Gilson P-1000 pipette with pipette tips sterilised by autoclave at 120 $^{\circ}\text{C}$. These vials containing the enzyme solution were stored at 4 $^{\circ}\text{C}$ until required.

Peroxidase from horse radish (E.C.1.11.1.7) was purchased from Sigma, type II, 150-200 units mg^{-1} . Bovine Serum Albumin (BSA, fraction V) was also obtained from Sigma.

All solutions were prepared with deionised water obtained either from Millipore Milli Q water purification system or from a Whatman R050 water purification system.

Glassware was cleaned by soaking in 2-5% Decon 90 detergent solution overnight and rinsed thoroughly with deionised water. In case of severe contamination, the glassware was treated by sonicating in an ultrasonic bath containing 2-5% Decon 90 solution. pH measurements were made using a Coming 145 pH meter and combination electrode (BDH or Whatman).

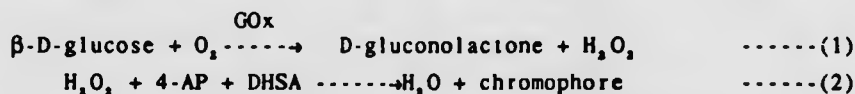
2.4 Spectroscopic Determination of Enzymic Activities and Protein Concentrations

In this section, details of the determination of the enzymic activity and concentrations of glucose oxidase by UV-Visible spectroscopy are presented. The activity of stock enzyme was assayed immediately upon receipt from MediSense and the assay was repeated regularly to ensure the storage stability of the enzyme. Enzyme concentrations were always recorded before each experiment.

2.4.1 *Enzymic Activity*

The enzymic activity of a protein is usually expressed in units per cm³ or units per mg of protein. A unit of glucose oxidase activity is defined as the amount of enzyme required to oxidize 1.0 μmol of β-D-glucose to D-gluconolactone per minute at pH 7.0 and 30°C. This is the definition used throughout this thesis.

The assay was carried out using a dye-based colorimetric method, first described by Barham and Trinder (118-119). The following reactions take place during the assay:



4-AP ----- 4-Aminophenazone, is a reagent for
glucose in the presence of phenol and
peroxidase;

DHSA ----- 3,5 -dichloro-2-hydroxy benzene sulphonic
acid, is used in oxidative enzyme systems for
the determination of uric acid and cholesterol.

The H_2O_2 produced in the first reaction forms a colour complex, the chromophore on reacting with 4-AP in the presence of DHSA and peroxidase (POD). This chromophore has an absorption maximum at 520 nm. The rate of H_2O_2 production, which corresponds to the glucose oxidase activity, is monitored by following the absorbance change per minute at 520 nm.

The assay reagents and procedures are described below.

Sodium phosphate buffer solution ($0.133 \text{ mol dm}^{-3}$), pH7.0; DHSA solution (20 mmol dm^{-3}) containing 0.03% w/v peroxidase; β -D-glucose solution (1 mol dm^{-3}) and 4-AP solution (8 mmol dm^{-3}) were prepared and stored at 4°C . A composite solution containing 0.2 cm^3 of glucose (1 mol dm^{-3}), 0.2 cm^3 of the DHSA/POD solution and 1.55 cm^3 of the sodium phosphate buffer was freshly prepared for each assay. Stock enzyme solutions were diluted to a suitable concentration so that OD_{520} (optical density at 520 nm) would change by 0.1 min^{-1} on average. The composite solution was equilibrated at 30°C for 15 minutes before each assay. $50 \mu\text{l}$ of the diluted GOx sample was added to the cuvette containing the composite solution and well-stirred. $50 \mu\text{l}$ of the 4-AP solution was then added and $OD_{520 \text{ nm}}$ was recorded using either a Phillips PUB8700 spectrophotometer or a Hewlett Packard 8415A diode array spectrophotometer. Figure 2.4 shows typical results of an enzyme activity assay.

The activity of glucose oxidase can be calculated as follows:

$$\text{units cm}^{-3} = A \cdot x \cdot B/y$$

A - $OD_{520 \text{ nm}}$ per minute (sample-blank)

x - conversion factor to give $OD_{520 \text{ nm}}$ for a 1 cm^3 of GOx sample,

hence for $50 \mu\text{l}$ sample $x = 20$.

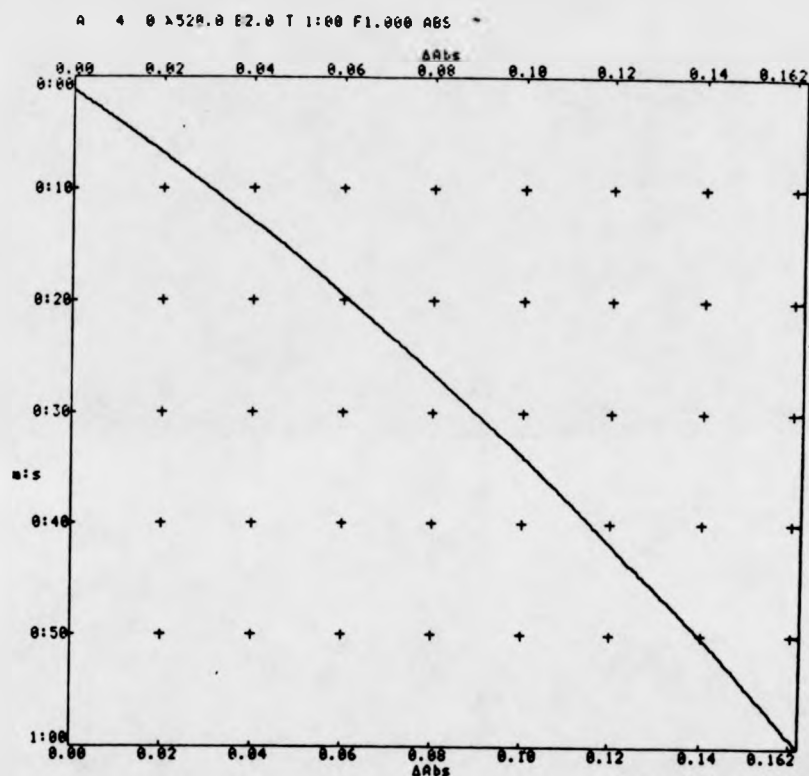


Figure 2.4

Typical result of an enzymic activity assay
 $\lambda = 520 \text{ nm}$
 $l = 1 \text{ cm}$
 GOx dilution: 1: 160,000
 Initial absorbance: 0.1162
 Final absorbance: 0.2782
 Total time: 1 minute
 Rate of absorption: 0.164 per minute

B - enzyme dilution factor

y - unit conversion factor for OD_{450nm} produced in presence of hydrogen peroxide (1×10^{-6} mol dm⁻³) by peroxidase.

It has a value of 12 for this assay system.

Enzyme activities expressed in units per mg can be obtained by dividing the value above with the value of enzyme concentration in mg cm⁻³.

2.4.2 Protein Concentrations

Glucose Oxidase is known to contain two flavin adenine dinucleotide (FAD) co-factors per molecule. In the oxidised form the FAD imparts a very distinctive yellow colour to the enzyme and has an absorption maximum at 450 nm (figure 2.5). The concentration of glucose oxidase in solution can then be determined using this absorption maximum at 450 nm using an extinction coefficient at 450 nm of 14.1×10^3 mol⁻¹ dm³ cm⁻¹ (25).

Since there are two FAD per enzyme molecule,

$$c = A_{450}/2\epsilon l, \text{ in mol dm}^{-3}$$

The concentration of enzyme samples are sometimes expressed in mg cm⁻³. This can be obtained by multiplying the molar concentration with the molecular weight, throughout this thesis the molecular weight of GOx is taken to be 186,000 Daltons (25).

Concentration of all glucose oxidase samples used in this thesis were determined using the method above.

2.5 Enzyme Modification

Direct electrochemistry of glucose oxidase at bare metallic electrode surfaces was achieved by modifying the enzyme with mediator molecules. The mediators were either covalently or non-covalently bound within the enzyme. The modifications of the GOx samples are presented below together with details of their purification.

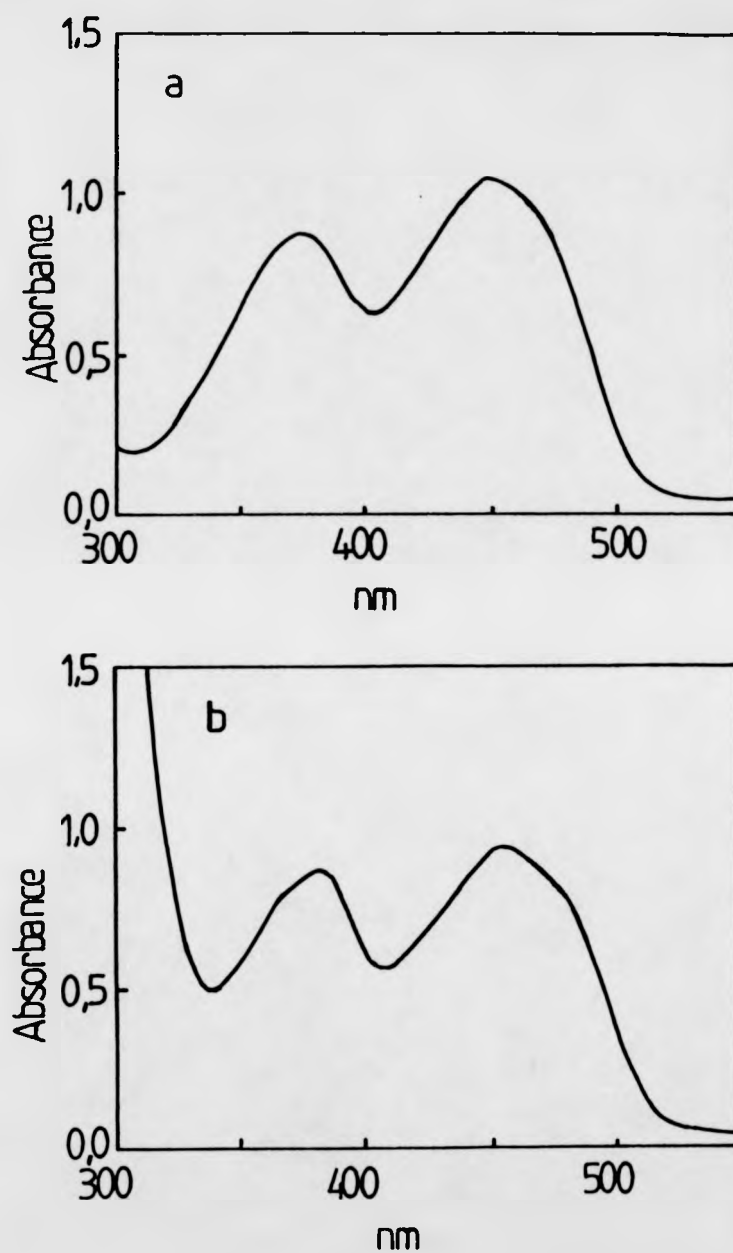


Figure 2.5

UV spectra of (a) FAD in buffer and (b)
 FAD in glucose oxidase.
 Reference: deionised H_2O
 $[FAD]$ of a: $1.20 \times 10^{-4} \text{ mol dm}^{-3}$
 $[GOx]$: $1.64 \times 10^{-5} \text{ mol dm}^{-3}$
 Cell path: 1 cm

2.5.1 Covalent Modification

GOx was modified with ferrocenemonocarboxylic acid (FMCA) and ferroceneacetic acid (FAA) using the method described by Degani and Heller (5-6). Their method involves the formation of peptide linkages between the carboxyl groups of FMCA or FAA and the lysine residues of the enzyme using a water-soluble coupling reagent. The lysine residues were exposed to the mediator molecules by partially denaturing the enzyme with urea (3 mol dm⁻³).

The reactions were carried out in an ice bath (4°C). Na-HEPES (200 mg), FMCA or FAA (60 mg) and urea (480 mg) were dissolved in deionised water (4 cm³) with stirring. The pH was adjusted to between 7.0 and 7.2 by dropwise addition of HCl (2.0 mol dm⁻³). GOx (100 mg) (Sigma or MediSense) and DEC (50 mg, 1-(3-dimethylaminopropyl)-3-ethyl carbodiimide hydrochloride) was then added. The pH was again adjusted to 7.0. The reaction mixture contained in a vial was stirred in the ice bath for a further 20 minutes and was then sealed with parafilm and placed in the ice bath in the refrigerator for 16 hours (overnight). The next morning, the vial was taken out of the refrigerator and the undissolved solid removed with a cotton wool plug. The resulting clear solution was further purified on a gel filtration column. Details of the gel filtration chromatography are presented in section 2.5.3.

Additional samples were also prepared using the standard method but with reduced amounts of FAA and carbodiimide. The literature quantity of FAA, i.e. 60 mg, was nominated as 100% FAA, half of the literature quantity of FAA was nominated as 50%, and so on. The relationship between the FAA quantity used in the modification step and the percentage nomination is shown in table 2.2.

Table 2.2 Quantities of FAA and their percentage nomination

FAA quantity/mg	Percentage nomination (%)
60	100
30	50
15	25
7.5	12.5
3.75	6.25

2.5.2 Non-Covalent Modification

Glucose oxidase was also modified non-covalently with water-insoluble materials such as TTF, TCNQ and iron(II)phthalocyanine. The modification reaction was carried out using hydrophobic incorporation.

Typically urea (3 mol dm^{-3}) was again employed to reversibly denature the enzyme molecules. Urea (360 mg) was dissolved in 2 cm^3 of buffer (85 mmol dm^{-3} sodium phosphate, pH 7.0) followed by $150\text{--}200 \mu\text{l}$ of stock glucose oxidase (MediSense, 156 mg cm^{-3} and $182 \text{ units mg}^{-1}$). The mixture was stirred constantly during the modification process. Excess TTF or iron(II)phthalocyanine solids were then added together with $4 \mu\text{l}$ of surfactant Triton X-100 (BDH). The mixture was stirred at room temperature for 2 hours.

The undissolved mediator solids were then filtered off through a cotton wool plug and the filtrate was further purified using gel filtration.

Additional TTF modified enzyme samples were also prepared at pH values 3.0, 4.0, 5.0, 6.0 in the presence and absence of surfactant (Triton X-100). These modified enzyme samples were prepared in McIlvaine buffer solutions (0.1 mol dm^{-3} citric acid and 0.2 mol dm^{-3} sodium phosphate), adjusted to the required pH by addition of citric acid (1.0 mol dm^{-3}).

2.5.3 Protein Purification

The modified glucose oxidase samples were separated from other starting materials using gel filtration chromatography. Gel filtration chromatography elutes

molecules according to their molecular sizes (molecular mass). As a solute passes down a chromatographic bed its movement depends upon the bulk flow of the mobile phase and upon the Brownian motion of the solute molecules which causes their diffusion both into and out of the stationary phase. Thus very large molecules which cannot enter the gel pores will elute fastest down the column and small molecules which are able to enter the gel pores and establish a partition between the mobile phase and stationary phase will be eluted later. In case of modified glucose oxidase samples, the enzyme (MW 186,000 Dalton) can be effectively separated from other reactants (MW < 500). Separation of the native and the modified glucose oxidase (with molecular mass difference in the order of a few hundred Dalton) may be achieved by choosing the appropriate gel media such as Sephadex G-100 or Sephacryl S-400. However, removal of the excess native GOx from the modified enzyme does not affect the results for the modified enzyme therefore selection of gel media for protein purification in this thesis is made so that a reasonable flow rate can be obtained.

Sephadex G-15 or Sephacryl S-100 (Pharmacia) were chosen as the gel media. The chemical structures of sephadex and sephacryl are shown in figure 2.6. Sephadex G-15 was purchased as dry beads and it was swollen at room temperature in phosphate buffer (85 mmol dm⁻³, pH 7.0) for 3 hours before use. A XK 16 x 70 cm jacketed glass column (Pharmacia) was employed and the gel media was packed by pouring the evenly shaken slurry into the column and allowing the gel to settle under gravity. The gel bed was equilibrated by running 2-3 bed volumes of the eluent buffer (85 mmol dm⁻³ sodium phosphate, pH 7.0) through the column. The eluent buffer was filtered through a 0.22 µm membrane filter using a Millipore ultrafiltration unit to ensure that it was particle free.

Enzyme samples were applied to the column using a SA-5 sample applicator (Pharmacia). For Sephadex G-15, elution was performed using a peristaltic pump (P-1, Pharmacia) at 2 cm³ min⁻¹ and sample fractions were collected using a FRAC-200 fraction collector. For Sephacryl S-100, elution was performed using a

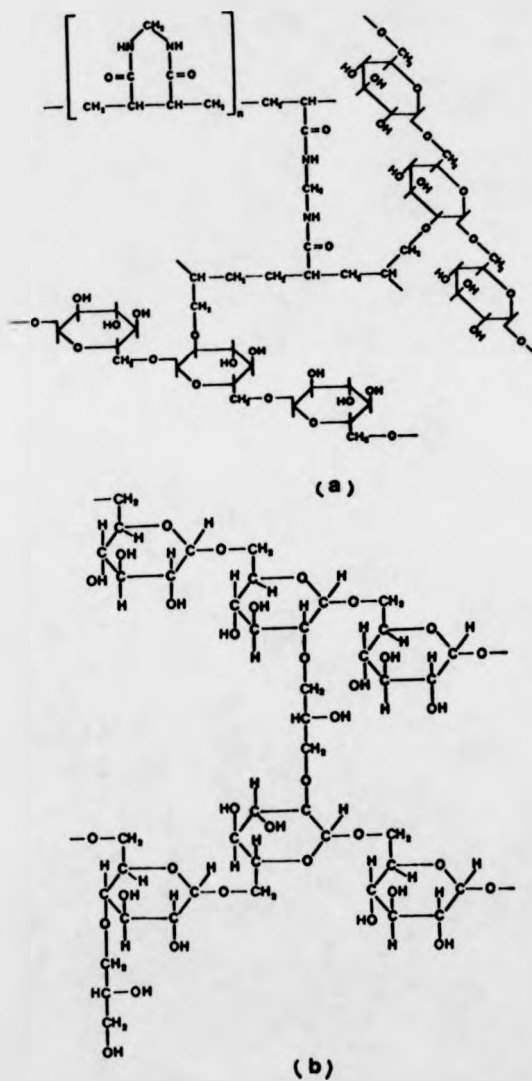


Figure 2.6 The chemical structure of (a) Sephadex and (b) Sephacryl

FPLC system (Pharmacia). This comprises a gradient programmer (GP-250 plus), two high precision pumps (P-500), a monitor (UV-1), a fraction collector (FRAC-100), an injector valve (P-7) and a chart recorder (REC-102). Elution was achieved at $0.5 \text{ cm}^3 \text{ min}^{-1}$ and sample fractions were 3 cm^3 .

2.6 Determination of Mediator Incorporation for the Covalently and Non-Covalently Modified GOx Samples

The average number of mediator molecules incorporated into each glucose oxidase molecule was determined using atomic absorption spectroscopy for the mediators containing iron. For the GOx samples modified with TTF through hydrophobic incorporation, the number TTF molecules per enzyme was estimated using fluorescence spectroscopy. The details are described below.

2.6.1 *Determination of Iron Content*

A series of ferric chloride solutions were prepared with concentrations ranging from $1 \mu\text{g cm}^{-3}$ to $50 \mu\text{g cm}^{-3}$. Their absorption at 248.5 nm due to iron was recorded using an atomic absorption spectrophotometer (Varian Techtron AA6). A calibration curve (figure 2.7) was then constructed by plotting the absorbance against the iron concentration for these ferric chloride calibrated solutions. The absorbance of the native and modified enzyme solutions were measured and their iron contents were then estimated from the calibration curve.

2.6.2 *Fluorescence Spectroscopy of the TTF Modified GOx Samples*

Attempts were made to detect the incorporated of TTF molecules by fluorescence spectroscopy. The possible quenching of the fluorescence of FAD or tryptophan residues in the presence of TTF were investigated.

Experiments were carried out using a Perkin Elmer L-50 automated fluorimeter with compatible data processing software. Native GOx solution were diluted with buffer (0.15 mol dm^{-3} sodium phosphate and 0.2 mol dm^{-3} sodium chloride, pH

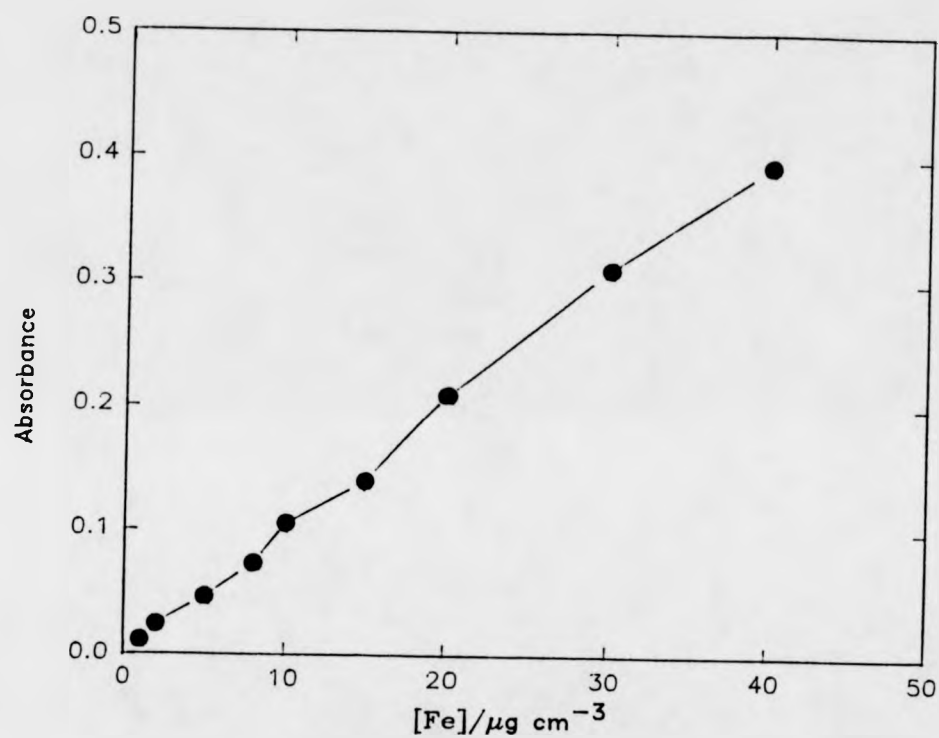


Figure 2.7 A typical calibration curve for atomic absorption spectroscopy of iron
 $\lambda = 248.5 \text{ nm}$

7.0) and purified using gel filtration before use to eliminate interference from free FAD in solution. Native and TTF modified glucose oxidase samples were diluted with the same buffer as above to the order of 10^{-7} mol dm $^{-3}$. Quartz cuvettes of 1 cm cell path were used and the excitation and emission slit width were set to 5.0 and 3.5 respectively. FAD emission spectra (excitation 450 nm) were recorded for native and TTF modified glucose oxidase samples (figure 2.9). Tryptophan emission spectra (excitation 280 nm) were also recorded for native and TTF modified GOx samples (figure 2.8).

2.7 Enzyme Membrane Electrodes

Enzyme membrane electrodes were constructed both with native and ferrocene modified glucose oxidase samples using home-made glassy carbon electrodes. Details of preparations of these enzyme membrane electrodes are described below.

2.7.1 *Construction of the Glassy Carbon Electrodes*

The glassy carbon electrode was prepared in-house by press fitting a piece of glassy carbon rod (2-3 mm, from David Feckenham, diameter 0.4cm) into a Teflon sheath at liquid nitrogen temperature. Electrical contact was achieved by placing a piece of tinned-copper wire of suitable length in some mercury which is in contact with the glassy carbon rod. The wire was then sealed into the Teflon with the electrode using Aradite.

The coarse electrode surface was polished using the method described in section 2.2 until a mirror finish was achieved. Six of these electrodes were made and their surface areas were measured using a travelling microscope, by taking the mean value of ten random diameters, details are given in table 2.3.

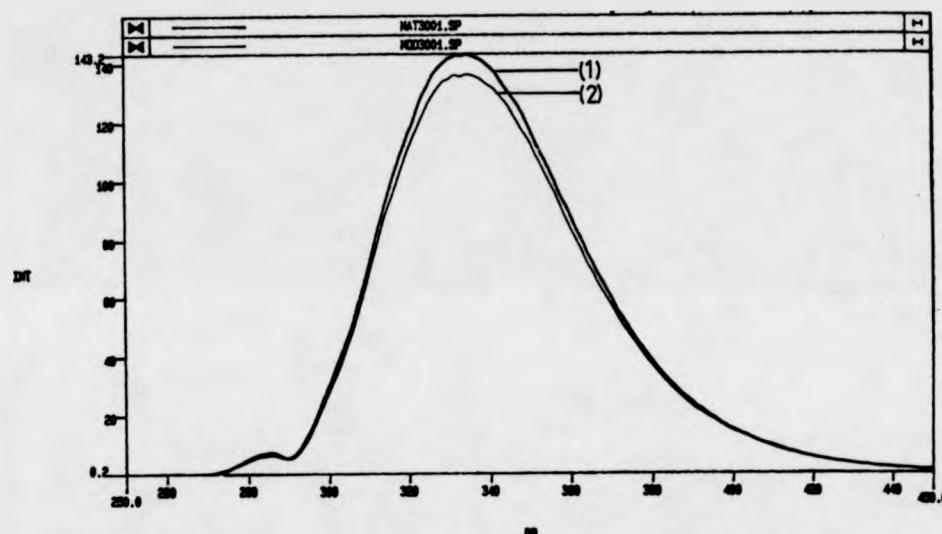


Figure 2.8

Emission spectra of tryptophan residues in glucose oxidase for (1) native and (2) TTF modified glucose oxidase
 $[GOx]_{\text{native}} = 2.8 \times 10^{-6} \text{ mol dm}^{-3}$
 $[GOx]_{\text{modified}} = 3.2 \times 10^{-6} \text{ mol dm}^{-3}$
 Excitation wavelength: 280 nm
 Emission wavelength: 340 nm

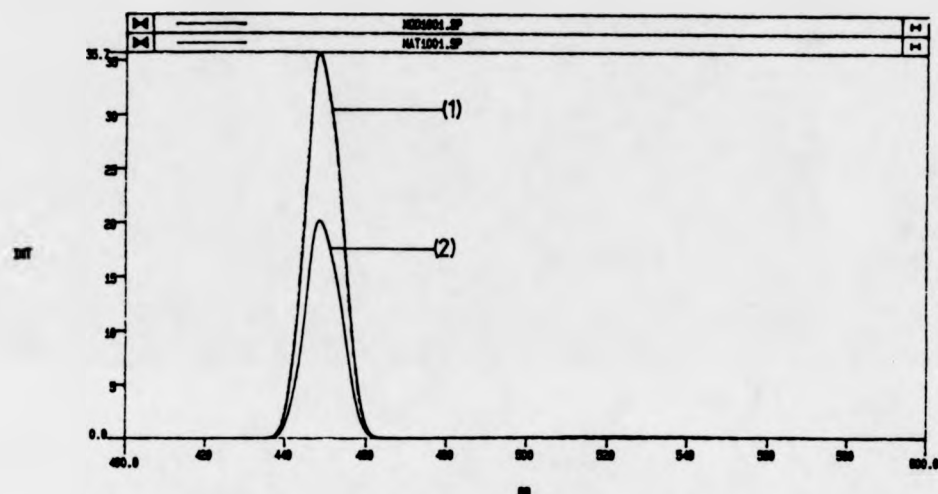


Figure 2.9

Emission spectra of FAD in glucose oxidase for
 (1) native and (2) TTF modified glucose oxidase
 $[\text{GOx}] \text{ (native)} = 2.8 \times 10^{-6} \text{ mol dm}^{-3}$
 $[\text{GOx}] \text{ (modified)} = 3.2 \times 10^{-6} \text{ mol dm}^{-3}$
 Excitation wavelength: 450 nm
 Emission wavelength: 540 nm

Table 2.3 Details of Enzyme Membrane Electrodes

Electrode	Surface Area/cm ²
E--1	0.125
E--2	0.124
E--3	0.122
E--4	0.126
E--5	0.127
E--6	0.125

2.7.2 Construction of Enzyme Membrane Electrodes

Native and modified enzyme samples were prepared and purified as described in earlier sections. A measured volume of the enzyme solution (typically 5-30 μ l) was placed onto the electrode surface using a Gilson pipette. Care was taken to ensure that the droplet was sited in the centre of the glassy carbon disc. The enzyme droplet was allowed to evaporate at room temperature until viscous and a piece of dialysis membrane (Medicell, pre-treated as specified by the manufacturer) was placed over the electrode surface and held in place by two silicon rubber "O" rings, figure 2.10.

2.8 Isoelectric Points (pIs) of FAA Modified GOx

The determination of the isoelectric points of the native and FAA modified glucose oxidase samples using isoelectric focusing gel electrophoresis is described in this section. The use of chromatofocusing chromatography to separate enzyme samples of different pIs is also presented.

2.8.1 *Isoelectric Focusing Gel Electrophoresis*

IEF experiments were carried out using a Phastsystem (Pharmacia) with precast gels. These precast gels comprise a cellulose base with polyacrylamide gel media set at a suitable pH gradient. Samples were applied using a 8-well sample

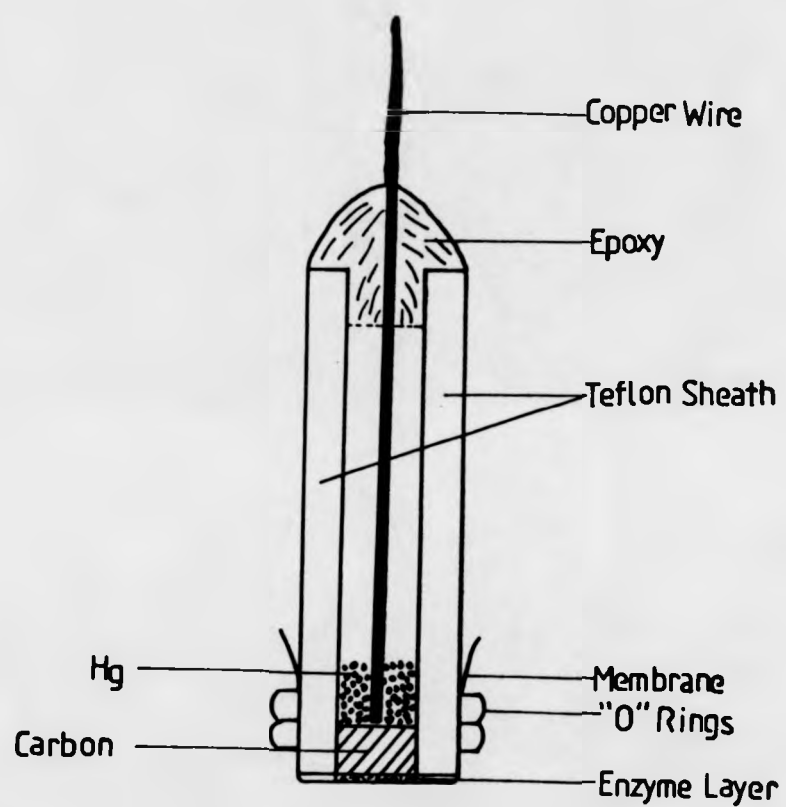


Figure 2.10 A glassy carbon enzyme membrane electrode (2.5 actual size)

applicator. Standard proteins of known pI values were also purchased from Pharmacia in pI calibration kits. The contents of the calibration kits are listed in table 2.4.

Table 2.4 Contents of pI calibration kit

Broad pI calibration kit (pH 3-10) (24+/-1.5°C)	
Protein standards:	pH
amyloglucosidase	3.50
methyl red (dye)	3.75
soybean trypsin inhibitor	4.55
β -lactoglobulin A	5.20
bovine carbonic anhydrase B	5.85
human carbonic anhydrase B	6.55
horse myoglobin-acidic band	7.35
lentil lectin-acidic band	8.15
lentil lectin-middle band	8.45
lentil lectin-basic band	8.65
trypsinogen	9.30
Low pI calibration kit (pH 4-6.5) (24+/-1.5°C)	
Protein standards:	pH
pepsinogen	2.80
amyloglucosidase	3.50
methyl red (dye)	3.75
glucose oxidase	4.15
soybean trypsin inhibitor	4.55
β -lactoglobulin A	5.20
bovine carbonic anhydrase B	5.85
human carbonic andydrase B	6.55

Native and modified glucose oxidase samples were diluted to 4 mg cm^{-3} with buffer solution (20 mmol dm^{-3} sodium phosphate and 50 mmol dm^{-3} sodium chloride, pH 7.0). $1 \mu\text{l}$ of each enzyme sample as well as the pI standards were applied to the IEF gel. A broad pH gradient gel (3-10) was used for initial experiments and further accurate measurements were carried out using IEF pH 4-6.5 gels. All protein samples were allowed to migrate in a potential range of 2000 volts between the anode and cathode for a suitable period of time. The phastGel IEF was developed using the Coomassie staining technique, in which the triphenylmethane anionic dye Coomassie preferentially forms dye complexes with proteins in the gel matrix. The rate of complex formation is limited essentially by the rate of diffusion of the dye into the gel. Once the proteins are sufficiently stained, excess Coomassie was washed from the gel matrix leaving the dark blue bands against a clear background. After development, the gel was dried at room temperature. A typical IEF gel (pH 4-6.5) for the FAA modified glucose oxidase samples is shown in figure 2.11. The distance of each protein sample had migrated towards the cathode was measured and a calibration curve was constructed by plotting this distance against the pI of the appropriate standard protein sample. The pI of the unknown protein can then be estimated.

2.8.2 *Chromatofocusing Chromatography*

Experiments were carried out on a pre-packed Mono P column (HR 5x20 cm, Pharmacia) with Polybuffer Exchanger (PBE94, Pharmacia). A pH interval of 5-4 was chosen as determined by IEF electrophoresis. The start buffer, piperazine ($0.025 \text{ mol dm}^{-3}$) was adjusted to pH 5.5 by dropwise addition of HCl (2 mol dm^{-3}). Polybuffer 74 (Pharmacia) was used as eluent buffer. The Polybuffer was used as 1:10 dilution and its pH was adjusted to pH 4.0. The purified FAA modified GOx samples were concentrated to the value of 20 mg cm^{-3} using an Amicon enzyme concentration unit (8MQ, 10,000 membrane filter) prior to the experiment.

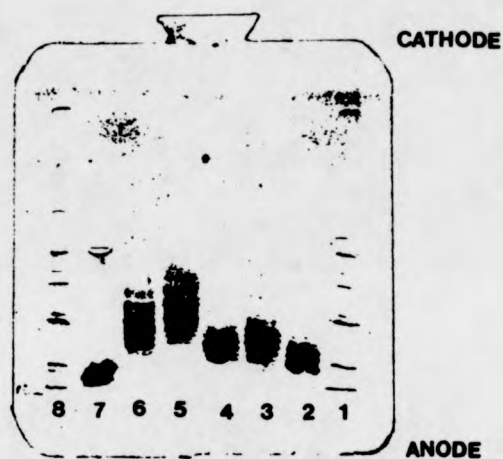


Figure 2.11 IEF gel electrophoresis for native and FAA modified glucose oxidases at pH gradient 4-6.5
 1, 8 - standard proteins 4mg cm⁻³
 2 - 6.25% FAA modified GOx 4mg cm⁻³
 3 - 12.5% FAA modified GOx 4mg cm⁻³
 4 - 25% FAA modified GOx 4 mg cm⁻³
 5 - 50% FAA modified GOx 4 mg cm⁻³
 6 - 100% FAA modified GOx 4 mg cm⁻³
 7 - Native GOx

The column was first equilibrated with 2-3 bed volumes of the start buffer. 500 μ l of the enzyme sample was then applied to the column through the sample loop of a P-7 valve. Elution was performed using a FPLC system, as described above, at 0.5 $\text{cm}^3 \text{min}^{-1}$. Sample fractions were collected and elution peaks were recorded using a REC-102 chart recorder (figure 2.12).

2.9 Hydrophobic Incorporation of TTF in BSA

In this section, further studies of hydrophobic incorporation between protein and mediators are discussed. The study was carried out for the model system of TTF, solubilised in BSA solution through hydrophobic interaction. Experimental procedures are described below.

The desired quantity of bovine serum albumin (BSA) (15.6 - 156 mg) was dissolved in 8 cm^3 of buffer solution (150 mmol dm^{-3} sodium phosphate containing 200 mmol dm^{-3} sodium chloride, pH 7.0) at room temperature with mechanical stirring. Excess TTF solids were then added and the mixture stirred for a further 2 hours. The undissolved TTF solids were then filtered off using a cotton wool plug and the clear solution purified using a small column packed with pre-swollen Sephadex G-15. This column was made from a 10 cm^3 glass syringe. Some glass wool was placed in the syringe needle holder and this was covered with a piece of filter paper.

2.9.1 *The Extinction Coefficient of TTF in BSA at 320 nm*

The extinction coefficient of TTF in BSA solution was determined by measuring the absorbance of TTF at 320 nm. (figure 2.13). Five vials contains solutions of BSA (195 mg cm^{-3}) were prepared. TTF solids were dissolved in the BSA solutions to make up TTF concentrations of 1.0×10^{-3} - 4.0×10^{-3} mol dm^{-3} . A plot of the absorbance at 320 nm against the TTF concentrations was linear (figure 2.14). The extinction coefficient can then be obtained from the gradient of the plot using the Beer-Lambert law,

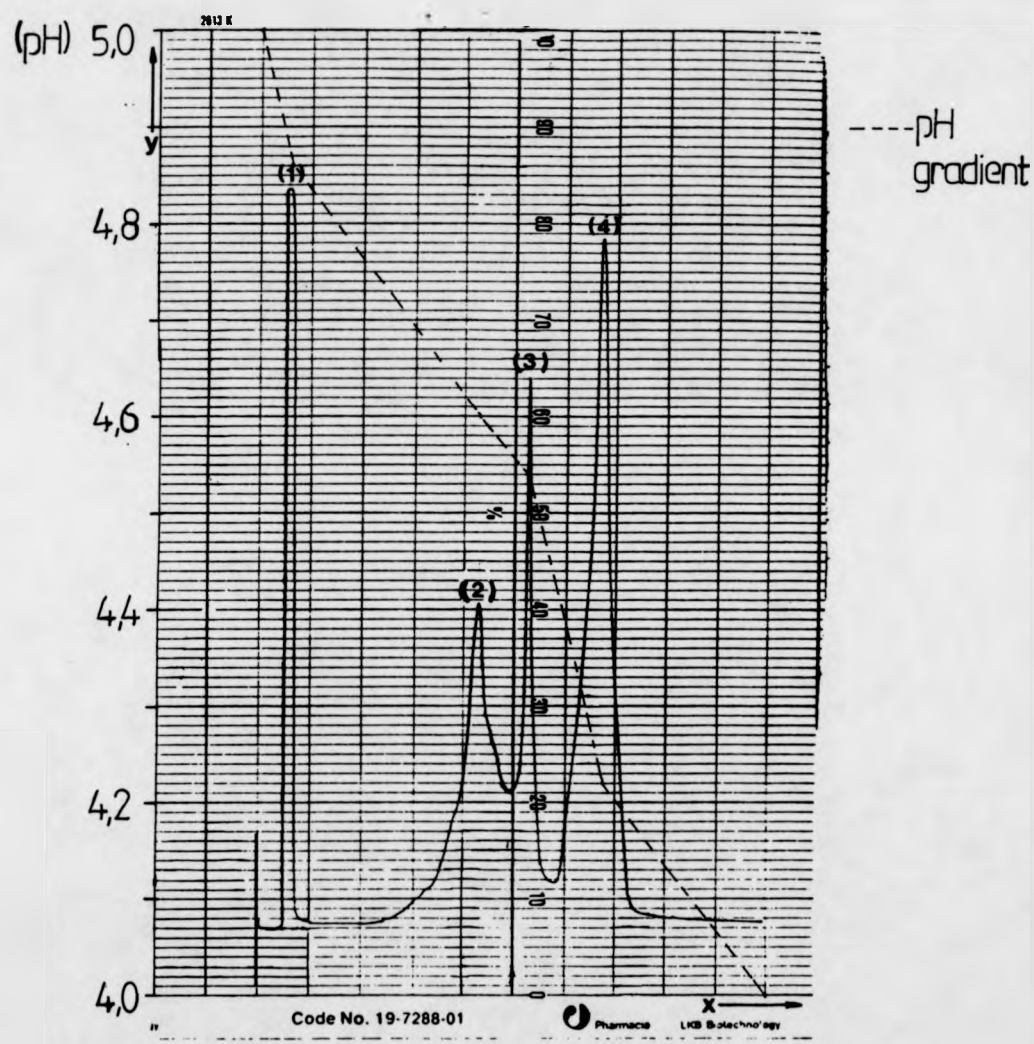


Figure 2.12

Elution chart of chromatofocusing chromatography for 100% FAA modified GO_x

x - axis, elution volume, at 0.2 cm cm^{-1}

y - axis, OD_{280} , full scale 2.0

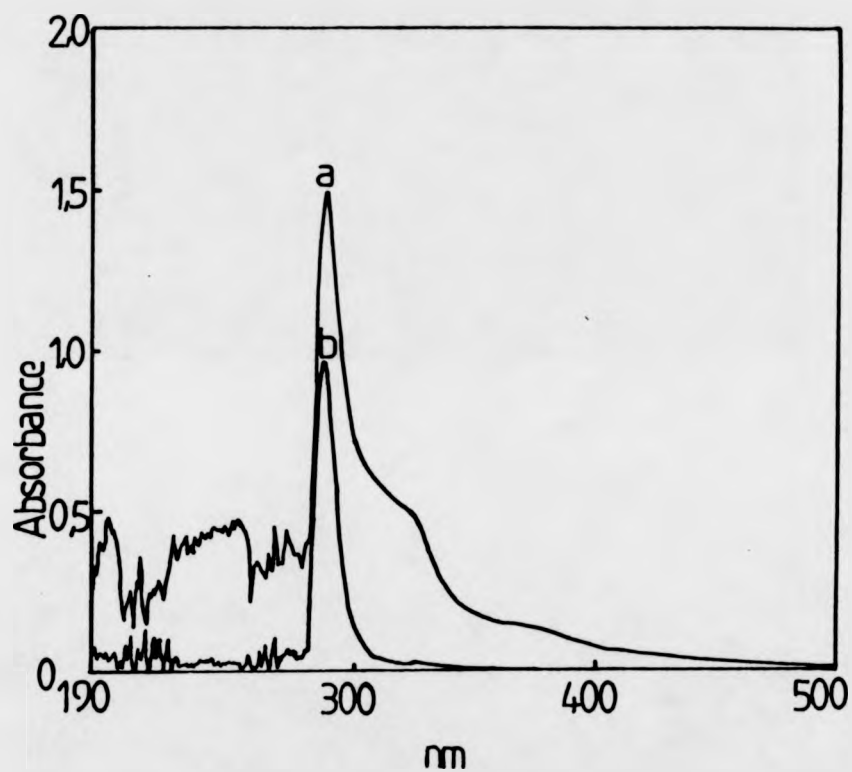


Figure 2.13

UV - visible spectra of saturated TTF in BSA

a. saturated TTF in BSA, $[BSA] = 1.9 \text{ mg cm}^{-3}$

b. BSA in buffer (85 mmol dm^{-3} sodium phosphate, pH 7.0)

$[BSA] = 1.9 \text{ mg cm}^{-3}$

Reference: deionised H_2O

Cell path: 1 cm

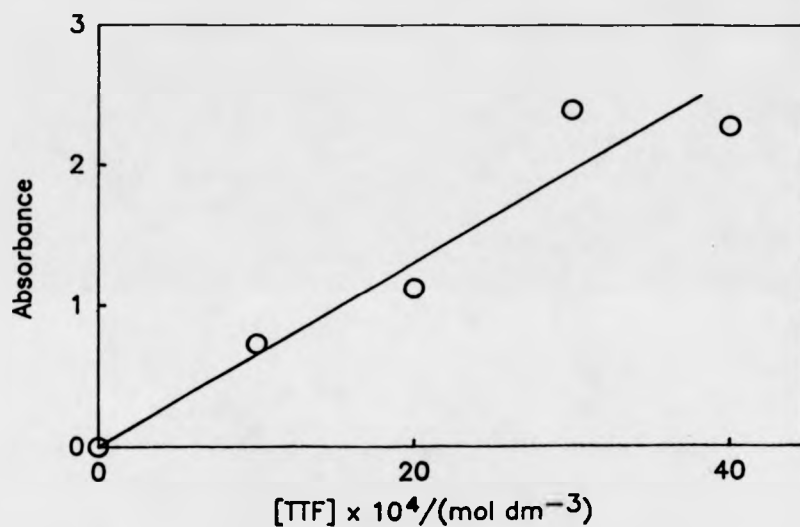


Figure 2.14

Plot of absorbance of TTF in BSA at 320 nm vs TTF concentrations. [BSA] = 19.8 mg cm⁻³.
 [TTF] varies from 1.0 x 10⁻⁵ - 4.0 x 10⁻⁵ mol dm⁻³
 Reference: solution of 19.0 mg cm⁻³ BSA in buffer
 (0.85 mol dm⁻³ sodium phosphate, pH 7.0).
 Cell path: 1 cm

$$\text{gradient} = A_{320}/[\text{TTF}]$$

$$A_{320} = \epsilon cl, \text{ and } l = 1 \text{ cm}$$

$$\text{so the } \epsilon = A_{320}/cl = \text{gradient}/l$$

2.9.2 Saturated TTF Concentrations in BSA

From the extinction coefficient determined above, the relative concentrations of saturated TTF in BSA can be estimated. To do this a series of BSA solutions ranging from 1.9 to 19.0 mg cm⁻³ were prepared. The solutions were then saturated with TTF and the absorption at 320 nm was recorded for each solution at room temperature.

CHAPTER III STUDIES OF FAA MODIFIED GLUCOSE OXIDASE

Following the success of the modification of glucose oxidase with ferroceneacetic acid, we have carried out detailed studies of the enzymatic and electrochemical properties of the modified enzyme. These studies are described in this chapter. The results of studies of the catalytic responses of the modified enzyme for glucose oxidation are presented together with the kinetic analysis based on our model. The results of rotating disc electrode studies and voltametric studies of the modified enzyme are analysed. The substrate specificity of the modified GOx is discussed. Modified GOx samples prepared using the literature method (5-6) but with reduced quantities of FAA were characterised and the isoelectric points for FAA modified GOx samples are also presented.

3.1 Introduction

In chapter I, the methods of achieving direct electrochemistry for glucose oxidase at simple metallic electrode surfaces were reviewed. The methods include: a). the use of a homogeneous redox mediator (66-67), b). immobilisation of the enzyme and/or the mediator at the electrode surface (45,71,82,85) c). the use of a conducting organic salt electrode (1-4), d). modifications of the enzyme itself with a redox mediator (5-6,114). The former three options have been explored extensively in the literature. Our interest has been concentrated on the last option. This option is the one best suited for the development of *in vivo* biosensors.

A critical requirement of direct electron transfer in biological systems appears to be the distance between active centre of the enzyme and the electrode surface (16). For most FAD containing enzymes, for example glucose oxidase and D-amino acid oxidase, the active sites are deeply "buried" inside the enzyme structure (27,121). Although partially denaturing

the enzyme with some reagents, such as urea, enables one to gain some form of access to the active site of the enzyme, the distance between the active site and the electrode surface is usually too great for the direct exchange of electrons with the electrode. Studies by Marcus and Sutin (29) have demonstrated clearly the effect of distance on the rate of electron transfer. They concluded that the rate of electron transfer decreases exponentially with the distance between the reactants (section 1.2). Thus the rationale for modifying an enzyme by attaching a number of redox mediators to the amino acid residues on the polypeptide backbone is that in this way we add some electron-transfer relays or "stepping stones" to allow the electron to transfer via several short steps instead of one long "jump" (figure 3.1). An excellent review of the criteria for covalent modification of glucose oxidase and D-amino acid oxidase can be found in the PhD thesis by R.G. Whitaker (120).

In the remaining parts of this section, work involving covalent modification methods for glucose oxidase will be reviewed and studies of the characteristics of the resulting modified enzymes will be discussed.

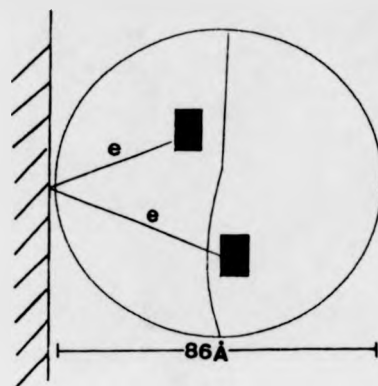
3.1.1 *Methods for the Covalent Modification of Glucose Oxidase.*

Covalent modification methods for glucose oxidase carried out by Hill (114), Degani and Heller (5-6) and Bartlett et al. (122) are described in this section.

(i) A covalent modification of glucose oxidase was carried out by Hill (114).

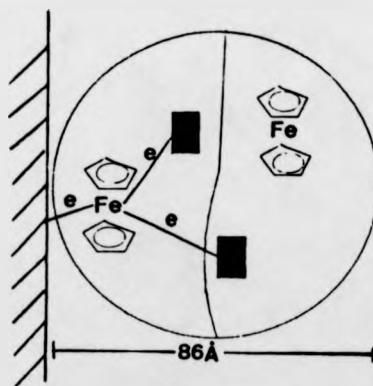
In this method, ferrocenemonocarboxylic acid (FMCA) was coupled to glucose oxidase using isobutylchloroformate. The terminal amine of the protein was involved in the reaction with a carbonic anhydride of ferrocene. The author demonstrated that in the absence of glucose the enzyme exists as its oxidised form, enzyme-FAD and no catalytic reaction was seen; however, on addition of D-glucose the enzyme exists

Electrode



Native glucose oxidase

Electrode



Modified glucose oxidase

Figure 3.1 Schematic representations of the electron transfer mechanism for native and ferrocene modified glucose oxidase. ■ -- FAD

as enzyme-FADH₂ and the catalytic reaction could take place between this reduced form of the enzyme and a ferricinium ion of the ferrocene at oxidising potentials.

The reaction was initially performed at -80°C. Isobutylchloroformate (0.13 cm³) and triethylamine (0.14 cm³) were added to a solution of ferrocenemonocarboxylic acid (1 mmol dm⁻³ in dry tetrahydrofuran) with constant stirring. Care must be taken to ensure that the reaction mixture is anhydrous to prevent the hydrolysis of the anhydride product. The mixture was stirred for 30 minutes at -80°C and then allowed to warm to room temperature and stirred for further 6 minutes. The resulting ferrocene carbonic anhydride was added dropwise to a cooled (2°C) solution of glucose oxidase (150 mg in 50 cm³ of 0.1 mol dm⁻³ NaHCO₃ solution) and pH of the solution was maintained at 8.0 with NaHCO₃ (0.1 mol dm⁻³). The reaction mixture was stirred at 4°C for 24 hours. Unreacted ferrocene and precipitated enzyme were removed by centrifugation and the resulting protein was dialysed against pH 8.5 borate buffer (0.2 mol dm⁻³ boric acid, 0.05 mol dm⁻³ borax).

Hill determined the iron content of the modified enzyme using atomic absorption spectroscopy and found a mean value of eight ferrocenes coupled to each molecule of glucose oxidase. Electrochemically, the responses of the modified enzyme to glucose were investigated using cyclic voltammetry in a conventional three-electrode cell. Kinetic studies carried out by the author show that the ferrocene monocarboxylic acid molecule which is linked to the enzyme through an amide bond, acts as a reversible, one electron mediator.

- (ii) Degani and Heller (5-6) subsequently reported methods for chemical modification of glucose oxidase. In their first report (5), the details of the covalent modification of glucose oxidase with ferrocenemono-

carboxylic acid were described. In this method, the ferrocene monocarboxylic acid was coupled, or attached, to the enzyme using a water soluble coupling reagent, a carbodiimide (DEC, 1-[3-(dimethylamino)propyl]-3-ethylcarbodiimide hydrochloride). The reaction scheme is shown in figure 3.2. Their results showed that using this method, an average value of 12 ferrocenes were coupled to each enzyme molecule for the resulting modified enzyme and that the modified enzyme gave a catalytic current in the presence of D-glucose.

The modification reaction was carried out in an ice bath (4°C). Ferrocenemonocarboxylic acid (80 mg) was dissolved in 4 cm³ solution of Na-HEPES (sodium 4-(2-hydroxyethyl)-1-piperazine ethane sulphonate, 0.15 mol dm⁻³) to give a turbid solution of pH 7.3 ± 0.1 . The pH was adjusted to this value by adding hydrochloric acid (0.10 mol dm⁻³) dropwise. DEC (100 mg) was then added, followed by urea (810 mg, 3.4 mol dm⁻³). The pH was again adjusted to 7.2-7.3 and glucose oxidase (60 mg) was added. The pH was finally checked and adjusted to 7.2-7.3. The solution was transferred to a glass vial and sealed with paraffin foil. The sealed vial was left immersed in an ice bath for around 15 hours (overnight). The unreacted solids or any precipitates of the solution were removed by centrifugation and the resulting supernatant was filtered through a 0.2 μm membrane filter. The modified enzyme was then purified on a gel filtration column (2 cm diameter, 22 cm length) of sephadex G-15 in sodium phosphate buffer (0.085 mol dm⁻³ pH 7.0).

The activity of the enzyme before and after the chemical modification was determined colorimetrically by measuring the rate of bleaching of 2,6-dichloro-indolephenol in the presence of glucose (50 mmol dm⁻³) under a N₂ atmosphere. The authors found that between 1/2 and 1/3 of the original activity was retained after chemical

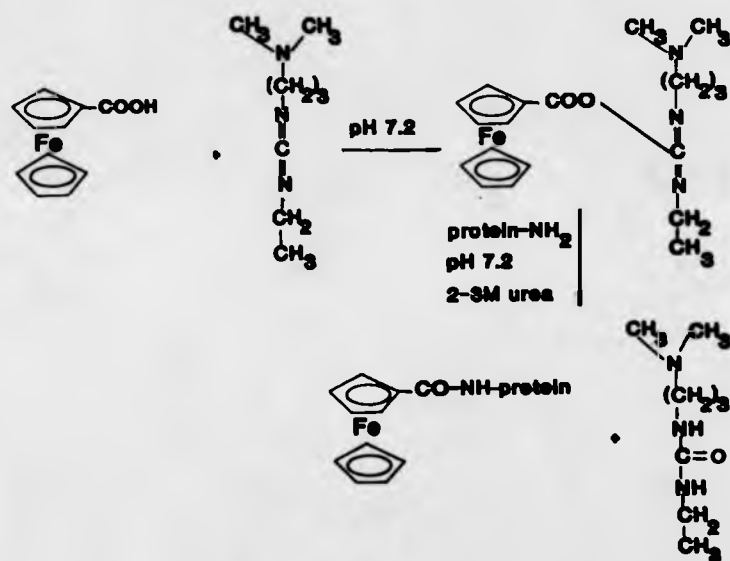


Figure 3.2 Reaction scheme of the covalent modification of glucose oxidase with ferrocenemonocarboxylic acid

modification. The electrochemical responses of the modified glucose oxidase was studied using d.c. cyclic voltammetry at gold, platinum and glassy carbon electrodes in oxygen-free environment. Degani and Heller observed that the modified enzyme responded to additions of glucose while the unmodified enzyme showed no response. This clearly demonstrates that the electrons from the enzyme active centre could be transferred to the electrode via ferrocene electron relays at a measurable rate.

To confirm that the electrochemical activation of the enzyme is caused by its chemical modification and not by the transport of soluble, unattached ferrocene species, the authors demonstrated that firstly, any ferrocene species originating from the non-covalently attached ferrocenes would dissociate and be removed by gel filtration. Secondly, they prepared a solution of the ferrocene modified glucose oxidase incubated with glucose (50 mmol dm^{-3}) at 25°C under N_2 for 24 hrs and again subjected to gel filtration. They found that only the coloured band for the modified enzyme was present on the column.

This work clearly confirms that the electrochemical activation of the enzyme is caused by the covalently attached ferrocenes and not by the freely diffusing ferrocene mediators.

In a consecutive publication (6), the authors showed that direct electrochemical communication between the FAD/FADH_2 centres of the enzyme and the metal or carbon electrodes could be established through bonding any of five different electron-transfer relays to the protein. They showed that the target amino acid residues for relay-bonding could be lysine, tyrosine, tryptophan or histidine and the electron-relays could be ferrocenemonocarboxylic, ferroceneacetic acid or ruthenium pentaamine. The amide bonds between the lysine residues of glucose oxidase or D-amino acid oxidase and the ferrocenes were formed by the

procedure described in their previous publication (5). As for the coupling of ruthenium pentaamine to glucose oxidase, the authors described two reaction routes. The first was the bonding between the ruthenium pentaamine complex of isonicotinic acid and glucose oxidase. The second was the pyridyl azo binding of ruthenium pentaamine to glucose oxidase.

- iii) Bartlett et al. (122) extended the enzyme covalent modification of Degani and Heller to ferrocene derivatives in which there is an alkyl chain between the cyclopentadienyl ring and the carboxylate. Their results show that the modification of the enzyme by these ferrocene derivatives provides a number of advantages over the original modification of Degani and Heller. In particular, the use of ferroceneacetic acid gives a modified enzyme which is more stable on storage, operates at less positive potentials and exhibits faster kinetics.

3.1.2 *Properties of Covalently Modified Glucose Oxidase*

This section describes the characterisation of chemically modified glucose oxidase carried out by Degani and Heller (5-6), and Bartlett et al. (122). The enzymatic activity, electrochemical activity, electron-relay density, diffusion coefficient, redox potentials and storage stability have been studied. A summary of their results is presented.

3.1.2.1 *Enzymatic Activities*

The chemical modification of glucose oxidase is usually carried out in the presence of 2-3 mol dm⁻³ urea. At these concentrations of urea, the protein structure unfolds reversibly (5-6) so that the interior of the enzyme is partially accessible. On removal of urea in the subsequent purification process (usually carried out by gel filtration chromatography on sephadex G-15) the protein returns to its usual structure. At higher (6-8 mol dm⁻³)

concentrations urea alters the enzyme structure drastically and often irreversibly (123). Degani and Heller found that the relay-modified enzymes retained over 60% of the residual activity of the native, unmodified enzyme (table 3.2) although chemical and structural changes occurred during the modification.

The effect of pH on the enzymatic activity for the ferroceneacetic acid modified GOx was investigated in our laboratory (124). The activity of FAA modified GOx was assayed using an oxygen electrode in the pH range of 3.0 to 8.0. An enzyme solution of pH 3.0-6.0 was prepared in citrate phosphate buffer (0.10 mol dm^{-3}) and an enzyme solution of pH 6.0-8.0 was prepared in phosphate buffer ($0.085 \text{ mol dm}^{-3}$). The studies show that for both native and the FAA modified glucose oxidase, the pH optimum was at pH 5.6. This clearly demonstrates that the chemical modification of GOx with FAA did not alter the pH optimum of the enzyme (figure 3.3). However, it is evident that the enzymatic activity of the FAA modified GOx is lower than that of the native GOx at all pH values studied. At pH 7.0, the activity of the FAA modified GOx is approximately 50% of the corresponding activity of the native GOx. This result of activity of FAA modified GOx assayed using oxygen electrode is in agreement with the studies by Degani and Heller in which they reported the loss of 40-50% of the residual activity for the chemically modified GOx using spectroscopic assay method (6).

3.1.2.2 Catalytic Activities and Redox Potentials

All the chemically modified GOx samples reported in the literature (5-6, 114,122) are able to undergo direct electrochemistry at platinum, gold, glassy carbon or graphite electrodes. At potentials equalling or exceeding the redox potentials of the electron relays, the modified enzymes respond to their enzyme's substrates and show faradaic currents which increase with substrate

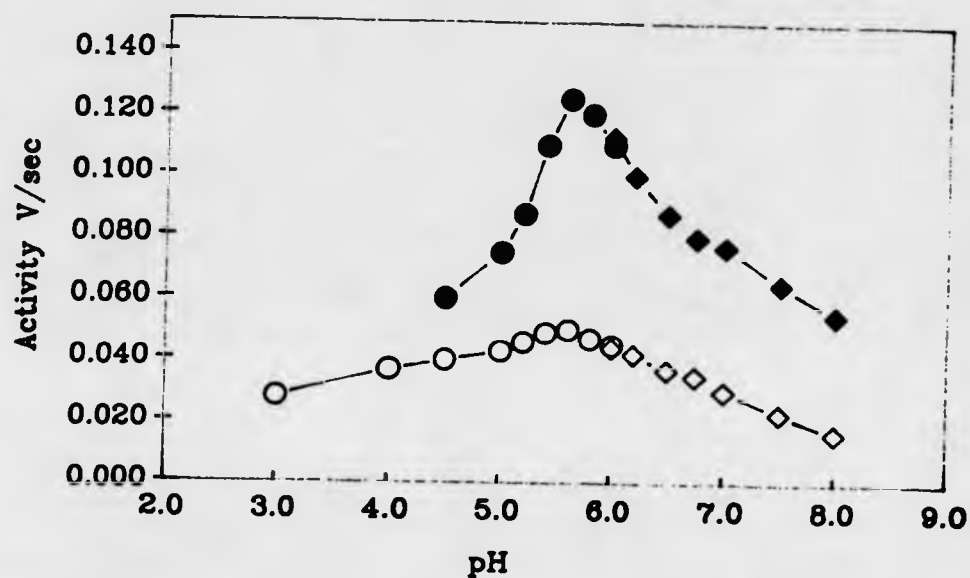


Figure 3.3 pH optimum studies of FAA modified GOx
 filled symbols -- native GOx
 open symbols -- FAA modified GOx
 diamonds -- assay carried out in phosphate buffer (85 mmol dm⁻³)
 circles -- assay carried out in citrate buffer (100 mmol dm⁻³)
 (Reproduced from project report by D. Caruana, University of Warwick, 1990, p49)

concentrations across a defined concentration range. In most cases, the limiting currents, i.e. the currents observed at sufficiently high oxidising potentials and at saturated substrate concentrations, increase with the number of relays per enzyme molecule (the exception is the modification of GOx by ferrocenebutanoic acid (122) in which the modified enzyme contains an average of 29 ferrocenes per enzyme but exhibits lower limiting currents than the FAA modified GOx which only has 22 FAA relays per enzyme).

Bartlett et al. studied the catalytic activity of three ferrocene relay modified GOxs; enzyme modified with ferrocenemonocarboxylic acid (FMCA), ferroceneacetic acid (FAA) and ferrocenebutanoic acid (FBA). They observed that the FAA modified GOx gave the largest limiting current amongst the three ferrocene modified GOxs. Their analysis for the catalytic responses of the modified enzymes show that the value of k_{cat} (the rate constant describing how fast the enzyme is turning over the substrate) for the FAA modified GOx is much greater than that of the other two ferrocene modified GOxs. This clearly demonstrates that the FAA modified GOx has faster kinetics compared to the FMCA and FBA modified GOxs.

The redox potentials of the enzyme-bound relays were estimated in the presence of substrates using cyclic voltammetry (6) or by analysis of the waveshapes (120). Analysis of the waveshape in the presence of glucose for the FMCA, FAA and FBA modified glucose oxidases were carried out by R.G. Whitaker (120). The thermodynamic E^0 of the modified enzymes were estimated using a corrected Tafel plot (a plot of $\ln(i_L/i - 1)$ versus the potential, E , where i_L is the limiting current value). The values of the redox potentials for relay modified enzymes are given in table 3.1.

Whitaker concluded that the E^0 of the modified enzymes reflects the E^0 of the ferrocene modifier employed and he observed that the E^0 values showed some dependence on the glucose concentrations. This dependence of E^0 value on the concentration of glucose implies that the modified enzymes

may be involved in a complex reaction. Thus an understanding of the electrode reactions for the relay modified enzymes may be achieved by exploring the direct electrochemistry of the modified enzymes in the absence of the substrate. We have carried out much more detailed studies of the direct electron exchange between the FAA modified GOx and the electrode in the absence of glucose. The results of these studies are presented in section 3.2.

3.1.2.3 Diffusion Coefficients and Electron-Relay Densities

Diffusion coefficients of the relay-bound enzymes were studied by Degani and Heller, using the dynamic light scattering technique (125). They found that some polymerisation of the dimeric enzyme occurred for the modifications involving carbodiimide. This polymerisation resulted in the decrease of the diffusion coefficient for the modified enzyme (table 3.1). Modifications not involving carbodiimide do not alter the diffusion coefficient significantly for the resulting modified enzyme (table 3.1).

The number of electron relays per enzyme molecule for ferrocenes and ruthenium pentaamine modified glucose oxidases were determined using atomic absorption spectroscopy, the results are also given in table 3.1.

In order to establish direct electron transfer between the enzyme and the metal electrode, an adequate density of electron relays is needed. This means that a sufficient number of relays need to be attached to the enzyme to shorten the electron tunnelling distances between the active centre of the enzyme and the electrode surface (section 1.2). From table 3.1, the average number of relays per enzyme molecule varies from 2 (for ruthenium pentaamine azo bonding of glucose oxidase) to 29 (for ferrocenebutanoic acid modified GOx). Several questions arise from this large variation in the number of relays per enzyme molecule for the modified enzyme: (1) What is the minimum number of relays per enzyme required for direct electron

exchange between the modified enzyme and the electrode to take place? (2) What are the necessary locations of these relays in order to fulfil the requirements of electron transfer distances? The latter question cannot be answered at the present time because the three-dimensional structure of glucose oxidase is still unknown. We have carried out studies concerning the former question for the system of FAA modified glucose oxidase by varying the FAA and correspondingly DEC quantities used in the initial modification reaction. These studies will be discussed in section 3.6.

3.1.2.4 Stabilities of the Modified Enzymes

This section describes the studies carried out by Degani and Heller for the initial working stabilities of the relay-modified enzymes in homogeneous solution.

The samples of native and relay modified glucose oxidases were incubated in glucose solution (30 mmol dm^{-3} , oxygen-free). Periodically retrieved samples were purified on gel filtration column to remove all low molecular weight species. The rate of decrease of the electrochemical activity for these modified enzymes was measured by d.c. cyclic voltammetry.

They found that apparently, the ruthenium pentaamine modified glucose oxidase with 14 relays per enzyme was the most stable when the enzyme-bound ruthenium is in its trivalent state. The modified enzyme shows stable electrochemistry for over a week. However, if the ruthenium is reduced to its divalent state, current falls by 10% in less than 5 minutes (table 3.2). It is apparent that generally, the ruthenium pentaamine modified glucose oxidase show much better working stability than the ferrocene modified GOxs and that the FMCA and FAA modified glucose oxidases have equivalent initial working stabilities (table 3.2).

The storage stabilities of the FMCA and FAA modified glucose oxidases investigated by Whitaker (120) will be discussed in the relevant sections of

Chapter IV.

In the remaining parts of this chapter, our studies for the properties of the FAA modified GOx will be presented.

Table 3.1 Properties of covalently modified glucose oxidase (5-6)

Relay/Enzyme	Number of relays per enzyme	E^0 (V vs SCE)	Diffusion coefficient (10^{-7} , $\text{cm}^2 \text{s}^{-1}$)
GOx	None	-0.291	4.1 ± 0.4
Fc-CO-NH-GOx	$12 \pm 1/13^*$	$0.26/(0.30-0.33)^*$	2.9 ± 0.3
Fc-CH ₂ -CO-NH-GOx	$13 \pm 1/22^*$	$0.11/0.13-0.18^*$	2.9 ± 0.3
(NH ₃) ₃ RuN <chem>c1ccccc1</chem> -CO-NH-GOx	6 ± 1	0.059	4.9 ± 0.5
(NH ₃) ₃ -RuN <chem>c1ccccc1</chem> -N=N-GOx	2 ± 0.3	0.159	4.3 ± 0.4
(NH ₃) ₃ Ru-GOx	14 ± 1	-0.221	-
Fc-(CH ₂) ₄ -CO-NH-GOx	29^*	$0.09-0.11^*$	-

Table 3.2 Enzymatic activities of covalently modified glucose oxidase (5-6, 120)

Relay/Enzyme	Activity upon chemical modification (% of the native GOx)	Activity left after 1 week storage (%)	Period to 10% loss in current
Fc-CO-NH-GOx	60 ± 5	45*	2 ± 0.5 hr
Fc-CH ₂ -CO-NH-GOx	60 ± 10	85*	2 ± 0.5 hr
(NH ₃) ₃ RuN <chem>c1ccccc1</chem> -CO-NH-GOx	75 ± 5		10 ± 2 hr
(NH ₃) ₃ RuN <chem>c1ccccc1</chem> -N=N-GOx	270 ± 30		10 ± 2 hr
(NH ₃) ₃ Ru-GOx	70 ± 5		as Ru ³⁺ > 1 week as Ru ³⁺ < 5 min**
Fc-(CH ₂) ₄ -CO-NH-GOx	--		< 10*+

* Data from reference (120)

*+ In oxygen-free buffer with saturating glucose

** Store at 4°C under N₂ at pH 7.0.

3.2 Estimation of the Diffusion Coefficient and the Number of Electrons Transferred for FAA Modified Glucose Oxidase

In this section, we describe our studies for the estimation of the diffusion coefficient and the number of electrons exchanged at the electrode for FAA modified GOx using electrochemical methods. The studies presented in this section were carried out in the absence of glucose. To the best of our knowledge, this kind of direct electrochemical study of the chemically modified enzyme has not been reported so far. Rotating disc electrode voltammetry for FAA modified GOx at platinum, gold and glassy carbon electrode surfaces are presented along with the results of kinetic analysis. Cyclic voltammetric studies for the modified enzyme are also detailed and the results are analysed.

3.2.1 *Introduction*

The diffusion coefficient for FAA modified GOx was determined by Degani and Heller using dynamic light scattering (125). They found that the value of the diffusion coefficient for the FAA modified GOx is slightly lower than that of the native GOx (table 3.1) and they proposed that this was due to some polymerisation of the dimeric enzyme in the presence of the coupling reagent, the carbodiimide. According to the Stokes-Einstein relation, (126) which connects the diffusion coefficient and the viscosity of liquids,

$$D = kT/6\pi\eta a \quad (3.1)$$

the diffusion coefficient of FAA modified glucose oxidase should be approximately equivalent to that of the native GOx because the viscosity of the liquid medium (η) and the radius of the enzyme molecule (a) would not have changed substantially before and after the enzyme modification. The diffusion coefficient of the FAA modified GOx is now estimated using electrochemical methods.

The number of electrons transferred during the oxidation of the modified

enzyme may also be estimated using a number of electrochemical methods provided that the value for D is known. This value of n represents the number of electrons transferred per enzyme molecule and it may relate to the number of accessible ferrocene groups on the enzyme.

Theoretically, the value of the diffusion coefficient and the number of electrons transferred may be estimated using the following electrochemical methods;

1. Rotating disc voltammetry using the Levich equation for the totally mass transport limited case:

$$i_L = 1.554 nFA D^{2/3} \nu^{-1/6} \omega^{1/2} C_o^* \quad (3.2) \quad (127)$$

where n is the number of electrons transferred during the oxidation and reduction reaction,

F is the Faraday, (96480 Cmol⁻¹)

A is the electrode area (cm²),

D is the diffusion coefficient (cm² s⁻¹),

ν is the kinematic viscosity (cm² s⁻¹),

ω is the rotation speed (Hz), and

C_o^* is the bulk concentration of the electroactive species (mol dm⁻³).

The slope of the Levich plot (i_L versus $\omega^{1/2}$) is $1.554 nFA D^{2/3} \nu^{-1/6} C_o^*$ which contains the parameters n and D .

2. Cyclic voltammetry where the relationship between the peak currents and the sweep rates can be used to estimate n and D . For a reversible system,

$$i_p = 0.4463 nFA C_o^* (nF/RT)^{1/2} \nu^{1/2} D^{1/2} \quad (3.3) \quad (128)$$

where i_p is the peak current (A),

ν is the sweep rate (V s⁻¹).

Again a plot of i_p versus $\nu^{1/2}$ is linear and the gradient of this

plot can be used to estimate n and D provided that the reaction is reversible.

3. Controlled potential oxidation where the current transient is recorded as a function of time. The relationship between the current transient, $i(t)$ and the time, t is given by the Cottrell equation (129):

$$i(t) = nFAD^{1/2} Co^* / \pi^{1/2} t^{1/2} \quad (3.4)$$

A plot of $i(t)$ vs $t^{1/2}$ should therefore be linear and this plot should pass through origin. The diffusion coefficient of the species can then be found from the gradient of the straight line provided the value for n is known.

4. Microelectrode techniques where the diffusive flux at a spherical electrode is governed by:

$$i_d = nF D Co^* / r \quad (3.5) \quad (130)$$

where r is the radius of the electrode and commonly, $r < 100$ micron.

The relationships between the number of electrons transferred during the reaction, n , and the diffusion coefficient of the electroactive species, D , are summarised in table 3.3.

Table 3.3 Relationships for the number of electrons transferred and the diffusion coefficient of an electroactive species using different electrochemical techniques

Electrochemical Technique	$n D$
Rotating disc electrode	$n D^{3/2}$
Cyclic voltammetry	$n^{3/2} D^{1/2}$
Controlled potential oxidation	$n D^{1/2}$
Microelectrode	$n D$

From our discussions above, it is clear that the combination of any two

of the electrochemical techniques will in principle enable us to estimate the values of n and D .

We have carried out studies for the FAA modified GOx using rotating disc electrodes, cyclic voltammetry and microelectrodes. The microelectrode experiments were unsuccessful due to problems with the electrode construction. Thus, only the results from rotating disc electrode and cyclic voltammetric studies are presented and analysed.

3.2.2 *Rotating Disc Electrode Studies.*

The rotating disc and rotating ring-disc electrodes are the most popular systems for kinetic and mechanistic studies of electrochemical reactions. Both the transport of species to and from the electrode can be controlled and varied in a known way. The hydrodynamics of the rotating disc and the rotating ring-disc systems have been studied and described thoroughly in the literature (127-128,131-134). This section describes rotating disc electrode studies of the electrochemical behaviour of FAA modified GOx at platinum, gold and glassy carbon electrodes. The limiting currents for the oxidation and reduction of FAA modified GOx are analysed using the Levich equation. The current-voltage curves for FAA modified GOx are subjected to waveshape analysis and the rate constants describing electrode reactions are determined. The effects of the choice of electrode material on the shapes of the polarograms (current-voltage curves) are also discussed.

3.2.2.1 *The Current-Voltage Curves*

The sample of FAA modified GOx was prepared and purified using the method described in the literature (5-6). The iron content of the modified enzyme was determined using atomic absorption spectroscopy and an average of 20 ferrocenes per enzyme molecule was found. This result is consistent with that obtained by Bartlett et al. (122) for the FAA modified GOx in

which they reported an average of 22 ferrocenes for each enzyme molecule.

A sample of FAA modified GOx (2.5 cm^2) in phosphate buffer ($0.085 \text{ mol dm}^{-3}$, pH 7.0) was placed in a semi-macro electrochemical cell. The enzyme solution was deoxygenated for 15-20 minutes by passing oxygen-free N_2 over the solution surface while stirring. During the experiments, the enzyme solution was kept under N_2 atmosphere throughout. Current-voltage curves for the FAA modified GOx were recorded at platinum, gold and glassy carbon disc electrodes at rotation speeds between 1 and 49 Hz and over the potential range of -0.1 to +0.4 Volts (vs SCE) (figure 3.4). It is evident that firstly, the shapes of the polarograms (current-voltage curves) vary slightly with the different electrode materials indicating that there may be some surface effects on the electrode kinetics. This is discussed further in the next section. Secondly, at each rotation speed, the limiting current for oxidation is much greater than the limiting current for reduction indicating that there may be a mixture of Fe^{2+} and Fe^{3+} forms present. The possible interpretations are now presented below.

By comparing the values of limiting current for oxidation and reduction at each rotation speed the ratio between the ferro - and ferri forms of the mediators can be estimated. In table 3.4, values of the limiting current for oxidation and reduction of FAA modified GOx as well as the $\text{Fe}^{2+}/\text{Fe}^{3+}$ ratios are listed.

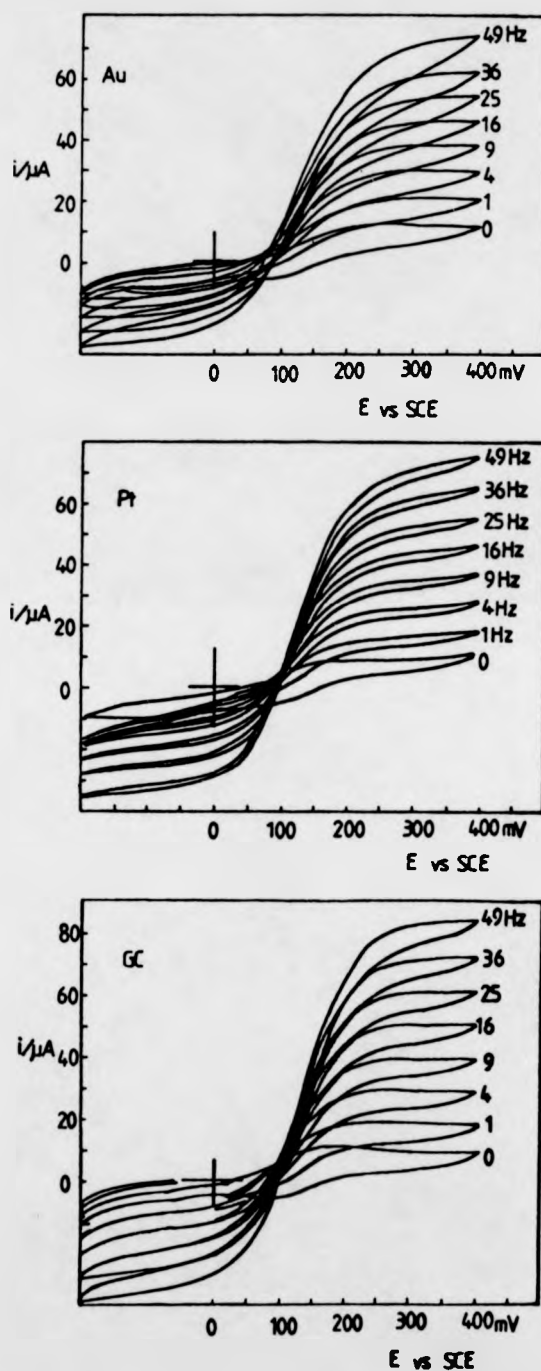


Figure 3.4 Current-voltage curves for FAA modified OQx recorded using gold, platinum and glassy carbon electrodes. $[\text{OQx}] = 8.6 \times 10^{-6} \text{ mol dm}^{-3}$ electrode areas are identical for the electrodes: 0.384 cm^2

Table 3.4 Limiting current values for oxidation and reduction of FAA modified GOx

Electrode Material	Rotation speed (Hz)	$i_L(\text{ox})$ (μA)	$i_L(\text{red})$ (μA)	$\text{Fe}^{2+}/\text{Fe}^{3+}$
Platinum	1	20	-13	1.5
	4	30	-14	2.1
	9	40	-20	2.0
	16	49	-26	1.9
	25	59	-33	1.8
	36	69	-40	1.7
	49	80	-47	1.7
	Ave. 1.8 ± 0.2			
Glassy Carbon	1	18	-10	1.8
	4	29	-12	2.4
	9	39	-14	2.8
	16	50	-19	2.6
	25	61	-25	2.4
	36	72	-32	2.3
	49	83	-39	2.1
	Ave. 2.3 ± 0.3			
Gold	1	20	-10	2.0
	4	30	-11	2.7
	9	38	-12	3.2
	16	46	-15	3.1
	25	55	-17	3.2
	36	63	-23	2.7
	49	74	-28	2.6
	Ave. 2.8 ± 0.4			

Data from table 3.4 shows that the average ratio of $\text{Fe}^{2+}/\text{Fe}^{3+}$ is between 2.0 to 3.0. That is to say, for an average of every 2-3 attached FAA molecules in modified GOx with the iron in reduced form, Fe^{2+} , there is one FAA molecule with the iron in oxidised form, Fe^{3+} .

The Levich plots of the limiting currents of reduction for FAA modified GOx (figure 3.5) show that at low rotation speed ($< 9\text{Hz}$) the limiting currents do not obey the Levich equation. At high rotation speed ($> 16\text{Hz}$) the plots are linear but they do not pass through the origin. The Levich plots of the limiting currents for oxidation are, on the contrary, much better behaved (figure 3.6). One possible explanation for the results may be that the limiting currents of reduction at low rotation speed are affected by the

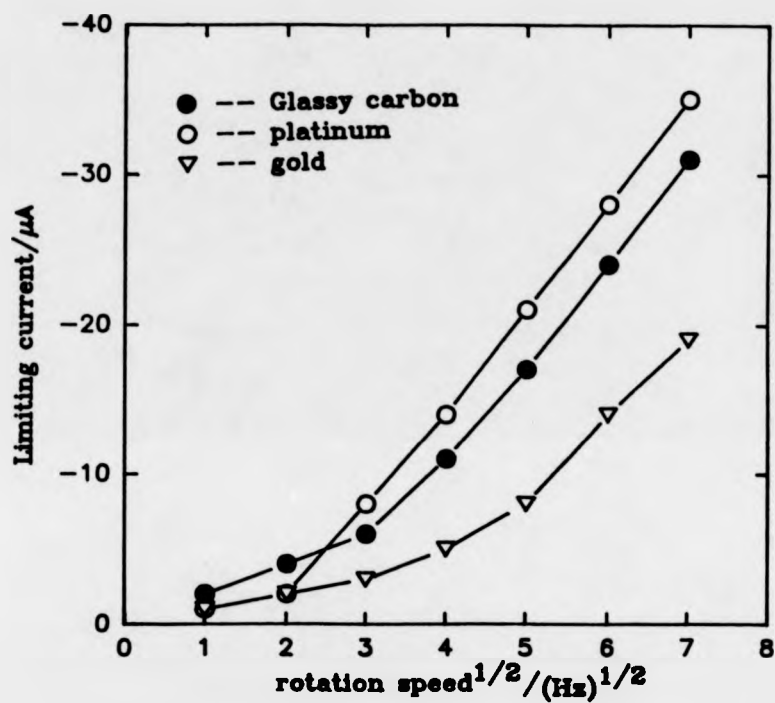


Figure 3.5 Levich plots for the reduction of FAA modified GOx at gold, platinum and glassy carbon electrodes.
 GOx concentrations are identical:
 $8.6 \times 10^{-6} \text{ mol dm}^{-3}$
 electrode areas are identical: 0.384 cm^2
 E vs SCE
 Buffer: 0.15 mol dm^{-3} sodium phosphate containing
 0.2 mol dm^{-3} NaCl, pH 7.0, oxygen-free.

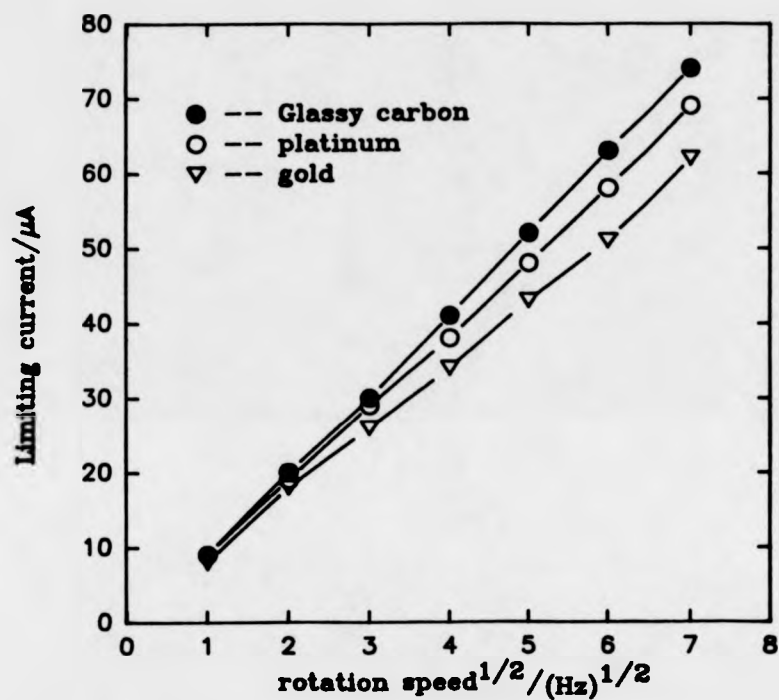
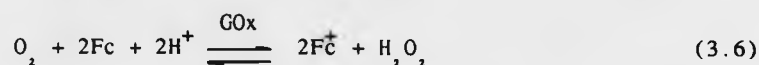
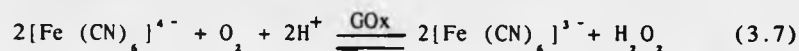


Figure 3.6 Levich plots for the oxidation currents of FAA modified GOx at gold, platinum and glassy carbon electrodes. GOx concentrations are $8.6 \times 10^{-6} \text{ mol dm}^{-3}$, electrode areas are: 0.384 cm^2 , Buffer: 0.15 mol dm^{-3} sodium phosphate containing 0.2 mol dm^{-3} NaCl, pH 7.0, oxygen-free.

existence of a catalytic reaction. Under the present circumstances, the only reaction which might be responsible is the reaction between the Fe^{2+} and oxygen catalysed by GOx,



The presence of oxygen may be due to either incomplete deoxygenation or dissolution of oxygen from the atmosphere during the experiment. In either case, the concentration of oxygen can not be determined. This kind of reaction has been observed for the system of GOx with ferrocyanide as a homogeneous mediator (135).



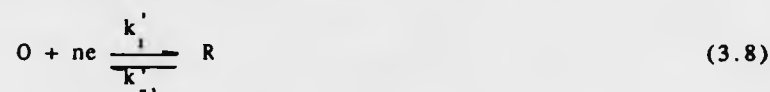
If oxygen was the cause of the presence of the mixed Fe^{2+} and Fe^{3+} forms for FAA modified GOx, the effect would be more significant at platinum electrode than glassy carbon or gold electrodes because O_2 is reduced more easily at platinum. The effect would also be more significant at high rotation speed because more oxygen should be present. Our results for the redox reaction of FAA modified GOx at these electrodes (figures 3.5) show that the effect is more significant at a platinum electrode; but at high rotation speed, we did not observe the increasing effect of oxygen. Nevertheless, we do not have a more comprehensive explanation at the present for the results above. Further studies are needed to gain a fuller understanding of the reaction mechanism.

3.2.2.2 The Waveshape Analysis

In this section, we present the analysis of the shape of the current voltage curves for FAA modified GOx at platinum, gold and glassy carbon

electrodes. The heterogeneous electrochemical rate constants for the oxidation of the enzyme bound ferrocene relays are obtained from the non-linear least square fit of the data. The effect of electrode material on the electrode kinetics is also discussed.

If we consider an electrode reaction,



We assume that the diffusion coefficient of O is equivalent to that of R,

$$D_O = D_R = D \quad (3.9)$$

and we write,

$$k_D' = D/x_D \quad (3.10)$$

where x_D is the diffusion layer thickness. For the rotating disc electrode system,

$$x_D = 0.643 \omega^{-1/2} D^{1/2} \nu^{1/4} \quad (3.11)$$

Under steady state conditions, the flux at the electrode can be expressed as:

$$j = k_1' [O]_O - k_{-1}' [R]_O \quad (\text{electrode reaction}) \quad (3.12)$$

$$= k_D' ([O]_\infty - [O]_O) \quad (\text{transport of O}) \quad (3.13)$$

$$= k_D' ([R]_O - [R]_\infty) \quad (\text{transport of R}) \quad (3.14)$$

where $[O]_O$ and $[R]_O$ are the surface concentrations of O and R respectively;

$[O]_\infty$ and $[R]_\infty$ are the bulk concentrations of O and R.

Elimination of the surface concentrations gives:

$$j = \frac{k_1' [O]_\infty - k_{-1}' [R]_\infty}{1 + k_1'/k_D' + k_{-1}'/k_D'} \quad (3.15)$$

$$\text{Now } k_1' = k_0' \exp \left(- \frac{\alpha E' F}{RT} \right) \quad \text{and} \quad (3.16)$$

$$k'_{-1} = k'_0 \exp \left(\frac{\beta E' F}{RT} \right) \quad (3.17)$$

where k'_0 is the heterogeneous rate constant for electrode reaction,

E' is the overpotential, $E' = E - E^0$ and

α, β are the transfer coefficients, $\alpha + \beta = 1$.

If we take $\alpha = \beta = 1/2$ and let $\theta = \alpha E' F / RT = \beta E' F / RT$, then eqn. (3.15) becomes:

$$j = \frac{[O]_{\infty} \exp(-\theta) - [R]_{\infty} \exp(\theta)}{1/k'_0 + \exp(-\theta)/k'_D + \exp(\theta)/k'_D} \quad (3.18)$$

Rearrange eqn. (3.18)

$$j = \frac{k'_D [O]_{\infty} \exp(-\theta) - k'_D [R]_{\infty} \exp(\theta)}{k'_D/k'_0 + \exp(-\theta) + \exp(\theta)} \quad (3.19)$$

$k'_D [O]_{\infty}$ and $k'_D [R]_{\infty}$ are the mass transport limited fluxes for reduction (j_R) and oxidation (j_O) respectively.

$$j_O = k'_D [R]_{\infty}$$

$$j_R = k'_D [O]_{\infty}$$

Substitute the expressions of j_R and j_O in eqn. (3.19) to obtain:

$$j = \frac{j_R \exp(-\theta) - j_O \exp(\theta)}{k'_D/k'_0 + \exp(-\theta) + \exp(\theta)} \quad (3.20)$$

Values of the current and voltage coordinates obtained from the polarograms can now be fitted to eqn. (3.20). From the best fit to this data, the values of k'_0 and the formal potential, E' , for FAA modified GOx can be obtained. Figure 3.7 and 3.8 show the typical results of a computer best-fit using the curve-fitting function of Sigma-plot package. Details of the programme are given in table 3.5.

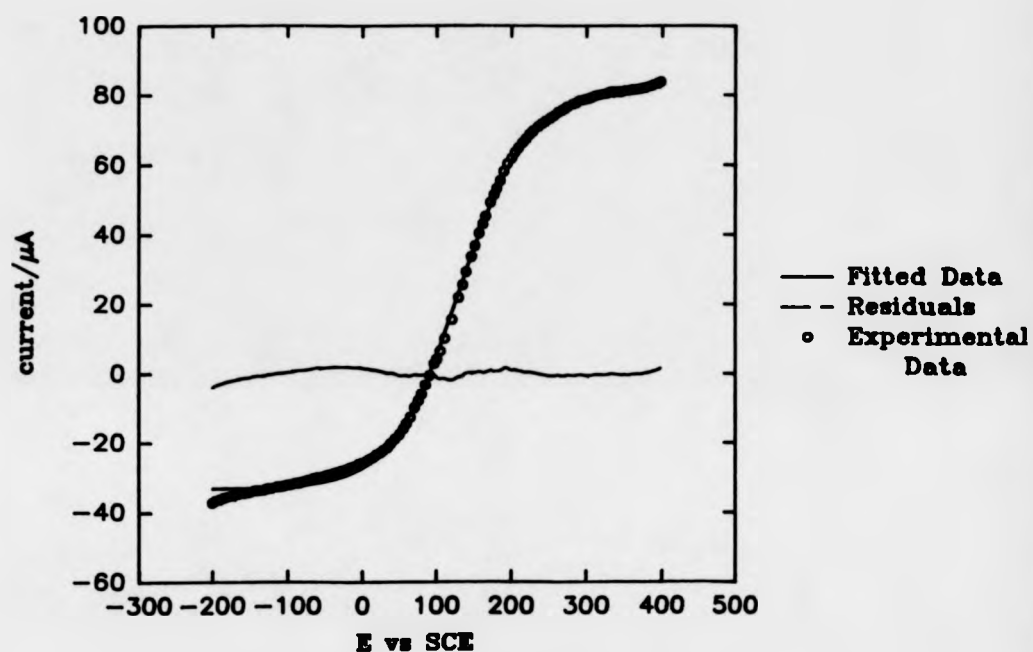


Figure 3.7 Computer generated least squares best-fit for current-voltage curve of FAA modified GOx recorded using platinum electrode
 electrode area: 0.384 cm^2
 rotation speed: 36 Hz
 $[\text{GOx}] = 8.6 \times 10^{-6} \text{ mol dm}^{-3}$

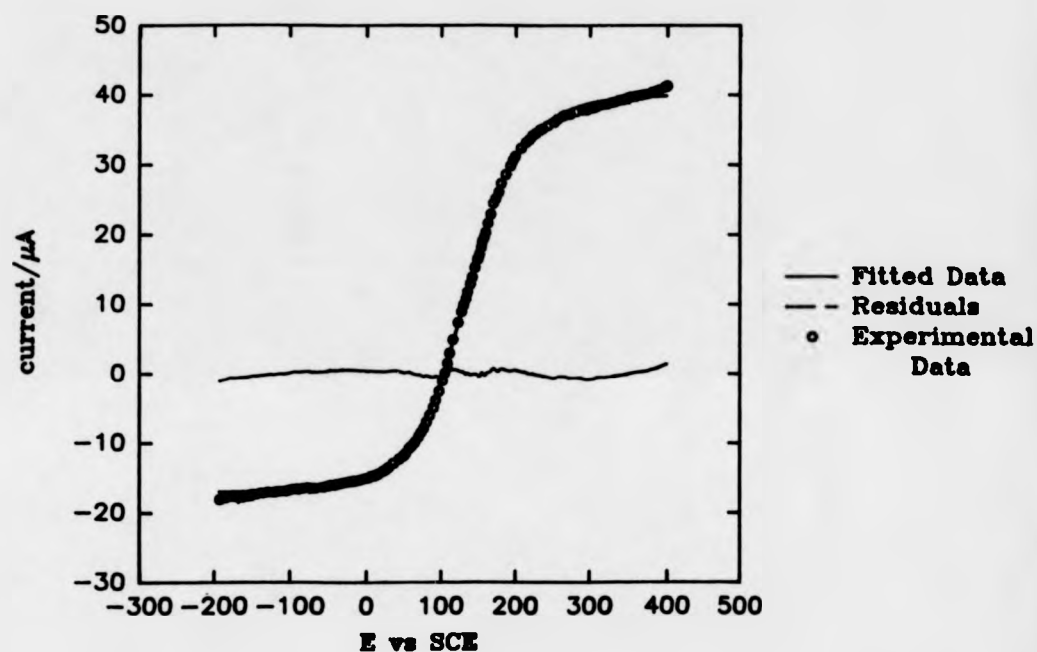


Figure 3.8 Computer generated least squares best-fit
for current-voltage curve of FAA
modified GOx recorded using glassy carbon electrode
electrode area: 0.384 cm^2
rotation speed: 49 Hz
 $[\text{GOx}] = 8.6 \times 10^{-6} \text{ mol dm}^{-3}$

Table 3.5 Computer mathematical curve fit programme
for the polarograms of FAA modified GOx

```

[parameters]
i1 = (limiting current of reduction)
i2 = (limiting current of oxidation)
κ = 1
ES = 110
[variables]
E = column number for potential data
i = column number for current data
[Equations]
T = (E-ES)/50
f = (i1*exp (-T)+i2*exp(T)/κ+2*cosh(T))
fit f to i
[constraints]
i1 < (defined value)
i1 > (defined value)
i2 > (defined value)
i2 < (defined value)
κ > 0
ES > 100

```

It was observed that the shapes of the polarograms recorded using a gold electrode deviate substantially from that predicted by eqn. (3.20) particularly at the plateau regions. These data cannot be used for non-linear least square fitting, thus only the results obtained from the polarograms recorded at platinum and glassy carbon electrodes are presented. Data from the best-fitted curves for the polarograms recorded at platinum and glassy carbon electrodes are given in table 3.6.

We now write:

$$\kappa = k_D' / k_0' \quad (3.21)$$

and substitute eqns. (3.10) and (3.11) in eqn. (3.21).

$$\kappa = \frac{1}{k_0'} \cdot 1.554 D^{2/3} \omega^{1/2} \nu^{-1/6} \quad (3.22)$$

It is clear that a plot of κ vs $\omega^{1/2}$ should be linear and pass through the origin. Thus the value of κ can be estimated from the gradient of the plot. Figure 3.9 shows these κ vs $\omega^{1/2}$ plots for the polarograms recorded at platinum and glassy carbon electrodes.

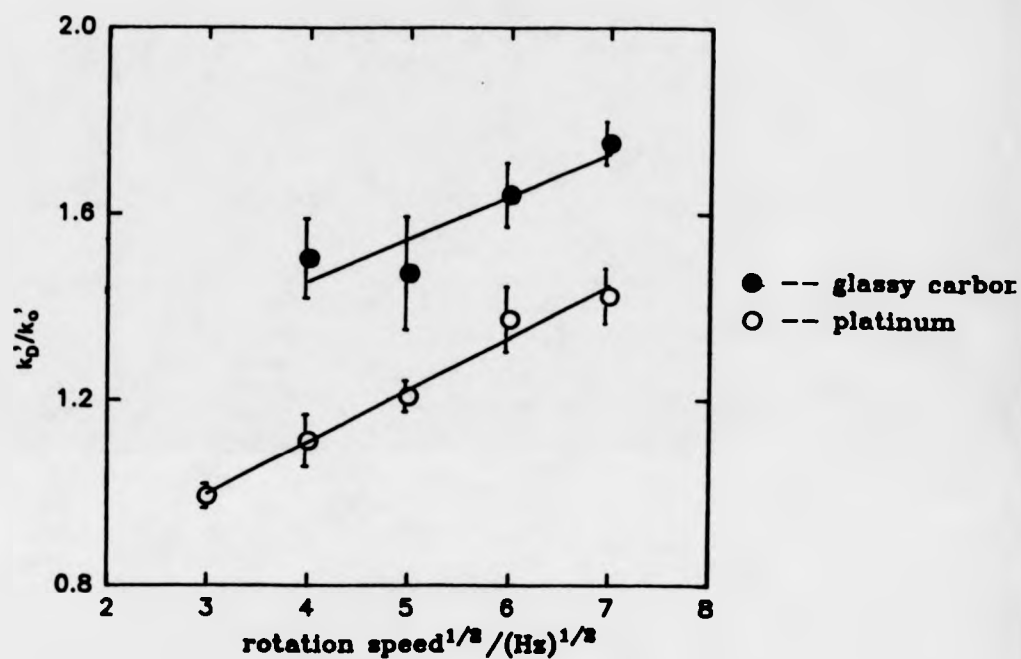


Figure 3.9 Plot of κ , from computer best-fit data, versus square root of rotation speed for current-voltage curves recorded using platinum and glassy carbon electrodes
 $\kappa = k'_D/k'_O$
 where k'_O is the standard heterogeneous electrochemical rate constant
 $k'_D = 1.554 D^{1/2} \omega^{1/2} \nu^{-1/6}$

Table 3.6 Computer best-fit data for polarograms recorded using platinum and glassy carbon electrodes

Electrode material	Rotation speed (Hz)	E' (mV vs SCE)	k'D/k'o
Gc	16	112.3±1.1	1.504±0.085
	25	114.9±1.9	1.471±0.120
	36	113.6±0.9	1.640±0.068
	49	113.2±0.6	1.751±0.046
	Ave.	112.6±1.2	
Pt	4	133.9±0.3	1.022±0.027
	9	124.5±0.4	0.991± 0.026
	16	121.2±0.8	1.112±0.056
	25	125.0±0.8	1.373±0.070
	36	124.8±0.4	1.207±0.033
	49	125.9±0.7	1.423±0.059
	Ave.	124.1±0.6	

Data from table 3.6 shows that values of the formal potential for FAA modified GOx at platinum and glassy carbon electrodes are in close agreement with that reported in the literature (6,122). They are also in good agreement with that of free FAA mediators in buffer solution (0.113 V vs SCE) (122).

The gradient values for the plots in figure 3.9 are;

$$\text{gradient} = 0.11 \text{ s}^{1/2} \quad (\text{platinum electrode})$$

$$\text{gradient} = 0.09 \text{ s}^{1/2} \quad (\text{glassy carbon electrodes})$$

If we take a value of D for glucose oxidase of $5 \times 10^{-7} \text{ cm}^2 \text{ s}^{-1}$ and a value of v of $10^{-3} \text{ cm}^3 \text{ s}^{-1}$, we can estimate the value of k_0' :

$$k_0' = 2.1 \times 10^{-3} \text{ cms}^{-1} \quad (\text{platinum electrode})$$

$$k_0' = 2.3 \times 10^{-3} \text{ cms}^{-1} \quad (\text{glassy carbon electrode})$$

It appears that the value of k_0' for the electrode reaction of FAA modified GOx at a glassy carbon electrode is slightly greater than that at a platinum electrode. However, if the value of k_0' is calculated from the individual ratios of k_D'/k_0' , then we obtain a larger k_0' for reaction at a platinum electrode than that at a glassy carbon simply because each value of κ for glassy carbon electrode lies above that for platinum (figure 3.9). These

two kinds of contradictory results may be caused by the irregular behaviour of the limiting currents for reduction for FAA modified GOx at these electrodes. In future studies, steps should be taken to ensure that the enzyme solution is fully oxygen-free. Polarograms recorded at a gold electrode do not fit the theoretical prediction (eqn. 3.19). This may be due to substantial surface adsorption of the FAA modified GOx on gold, however, we do not have sufficient experimental data at the present to be conclusive.

Next, studies of the voltammetric behaviour of FAA modified GOx are described.

3.2.3 Voltammetric Studies for FAA Modified GOx

In our previous discussions (section 3.2.1) we have shown that the diffusion coefficient and the number of electrons transferred for the modified GOx can be estimated from the $n^2 D^3$ relationship determined using four different electrochemical techniques, namely rotating disc electrodes, controlled potential oxidation, microelectrodes and cyclic voltammetry. The results from voltammetric studies for FAA modified GOx are presented in this section.

A sample of FAA modified GOx (2.5 cm^3) was placed in a semi-macro cell (section 2.2) and was deoxygenated for 15-20 minutes. D.C. cyclic voltammograms were recorded using a glassy carbon electrode over a potential range of -0.1 V to $+0.4 \text{ V}$ (vs SCE). Sweep rates were varied between 2 mV s^{-1} and 100 mV s^{-1} . Figure 3.10 shows the cyclic voltammograms of FAA modified GOx recorded at three different sweep rates.

Cathodic peak currents of the voltammograms recorded over the range from 2 mVs^{-1} to 100 mV s^{-1} were plotted against the square root of the sweep rate, figure 3.11. This plot is linear and passes through the origin. Thus we may use equation (3.3) to estimate the relationship between n and

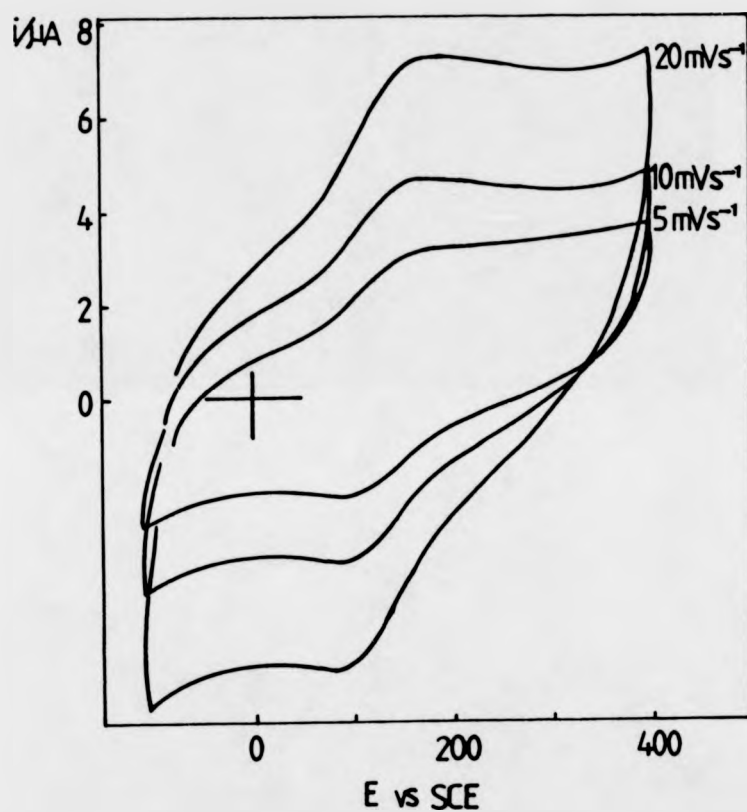


Figure 3.10 Cyclic voltammograms of FAA modified GOx recorded at three different sweep rates
 $[GOx] = 2.1 \times 10^{-5} \text{ mol dm}^{-3}$
 electrode: glassy carbon (0.384 cm^2)

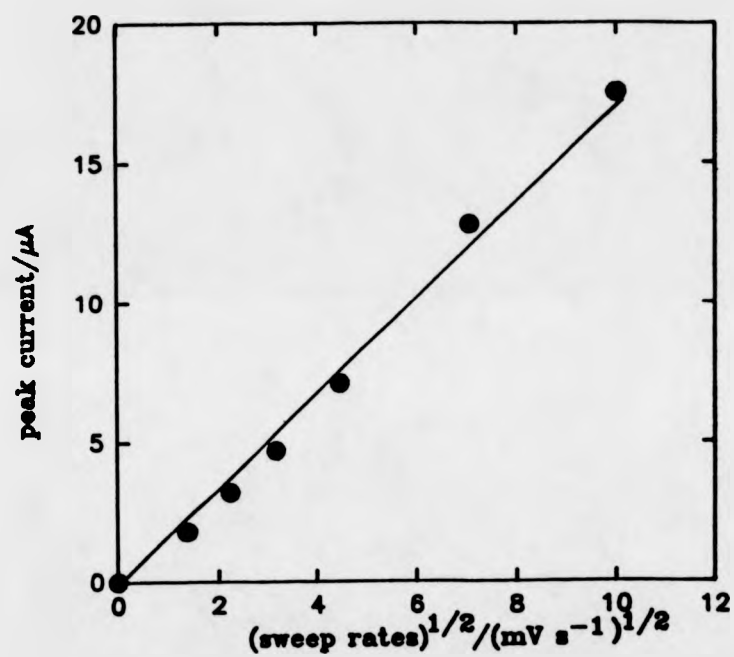


Figure 3.11 Plot of cathodic peak currents versus square root of sweep rates for FAA modified GOx.
 $[GOx] = 2.1 \times 10^{-5} \text{ mol dm}^{-3}$
 electrode: glassy carbon (0.384 cm^2)

D for FAA modified GOx assuming the reaction is reversible. At 25°C, equation (3.3) can be written as;

$$i_p = (2.69 \times 10^5) n^{1/2} A D^{1/2} v^{1/2} C_O^* \quad (3.23)$$

The slope of the i_p vs $v^{1/2}$ plot is $1.73 \mu A (mV s^{-1})^{-1/2}$. From the above expression,

$$(2.69 \times 10^5) n^{1/2} A D^{1/2} C_O^* = 1.73 \mu A (mV s^{-1})^{-1/2} \quad (3.24)$$

where $A = 0.384 \text{ cm}^2$,

$$C_O^* = 2.13 \times 10^{-3} \text{ mol dm}^{-3}$$

$$\text{so } n^{1/2} D^{1/2} = 0.0249 (cm^2 s^{-1})^{1/2} \quad (3.25).$$

Next we will present estimation for n and D by using the combined results from voltammetric and rotating disc electrodes studies.

3.2.4 Estimation of n and D for FAA Modified GOx

The same batch of FAA modified GOx was also subjected to rotating disc electrode studies. The values of limiting current for oxidation at each rotation speed were plotted against the square root of the rotation speed (Levich plot), figure 3.12. The Levich slope obtained is $1.27 \mu A (s^{-1})^{-1/2}$. Using the Levich equation (3.2), we obtain,

$$1.554 n F A D^{1/2} C_O^* v^{-1/2} = 1.27 \mu A (s^{-1})^{-1/2} \quad (3.26)$$

where $A = 0.384 \text{ cm}^2$,

$$C_O^* = 1.83 \times 10^{-3} \text{ mol dm}^{-3} = 1.83 \times 10^{-3} \text{ mol cm}^{-3}$$

Taking into consideration that the ratio between Fe^{3+} and Fe^{2+} is 2:1, thus the true concentration of Fe^{3+} is,

$$\begin{aligned} C_O^* &= 1.83 \times 10^{-3} \times 2/3 \\ &= 1.22 \times 10^{-3} \text{ mol cm}^{-3}, \end{aligned}$$

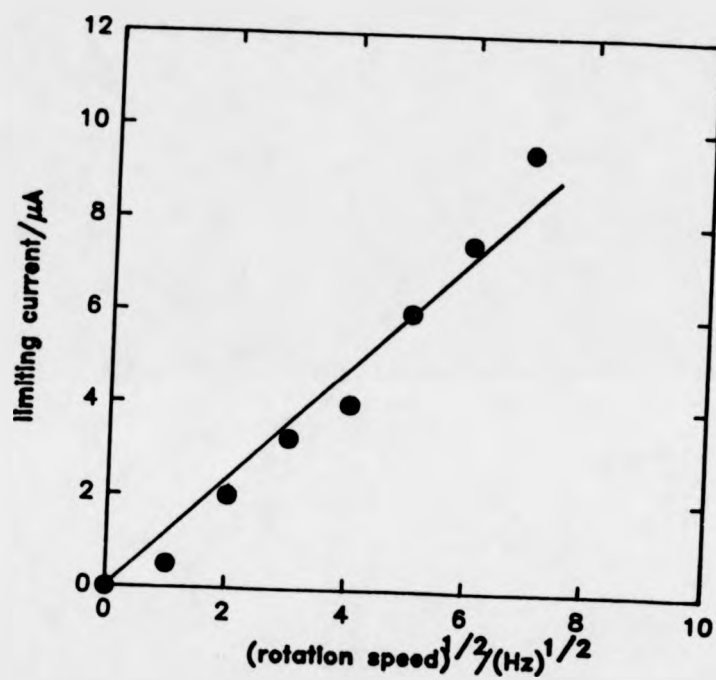


Figure 3.12 Levich plot of the limiting currents of oxidation for FAA modified GOx
 $[GO_x] = 2.1 \times 10^{-4} \text{ mol dm}^{-3}$
 electrode: glassy carbon (0.384 cm^2)

ν is the kinematic viscosity and is used as $10^{-2} \text{ cm}^2 \text{ s}^{-1}$,
 so $n D^{1/3} = 8.4 \times 10^{-4} (\text{cm}^2 \text{ s}^{-1})^{1/3}$ (3.27)

Combining equation (3.25) with (3.27), we can estimate the values for n and D .

$$D \approx 9.6 \times 10^{-7} \text{ cm}^2 \text{ s}^{-1} \quad (3.28)$$

$$n \approx 9 \quad (3.29)$$

This value for the diffusion coefficient for FAA modified GOx is in good agreement with that reported in the literature (6).

From (3.29), it is apparent that 9 electrons were transferred during the electrode reaction for FAA modified GOx. This number of electrons transferred for FAA modified GOx presumably reflects the number of accessible ferrocene groups within the enzyme structure. Thus, among the 20 ferrocene molecules attached to each enzyme molecule, 9 ferrocene groups were able to undergo direct electrochemistry at the electrode. This suggests that these 9 enzyme-bound ferrocene groups are either in a close distance to the enzyme surface or in such an orientation that direct electron transfer can be achieved. Since the three-dimensional structure of glucose oxidase is still unknown at the present, we cannot determine the exact locations of these ferrocene groups. However, the FAA binding sites in GOx are hydrophilic. For a water-soluble protein like glucose oxidase, one would expect the polypeptide chains to fold in such a manner that the hydrophobic amino acid residues are buried in the interior of the protein while the hydrophilic amino acid groups are folded close to the protein surface. Thus we might expect that, for the FAA modified GOx, the majority of the accessible ferrocene groups will be located near the enzyme surface.

We have demonstrated the use of rotating disc electrodes and cyclic voltammetry to estimate the diffusion coefficient and the number of electrons transferred for FAA modified GOx. Similar analysis can also be carried out

by combining use of any two of the electrochemical techniques listed in table 3.3.

In the next section, we will describe results obtained for FAA modified GOx in the presence of glucose.

3.3 Catalytic Activity of FAA Modified GOx

Above, we have discussed the electrochemistry of FAA modified GOx in the absence of glucose. We will now present our studies of the catalytic activities of the modified enzyme. Responses of this FAA modified GOx to additions of substrate in the absence of a homogeneous mediator are described and analysed using our model.

3.3.1 *Theory*

In this section, the theory for the kinetics of an enzyme catalysed reaction is described. Details of our model for the catalytic process with FAA modified GOx are given. First Michaelis-Menten kinetics for enzyme-substrate reactions are briefly reviewed.

3.3.1.1 *Michaelis-Menten Kinetics* (136)

Commonly, an enzyme catalysed reaction occurs in three stages: a). the formation of the appropriate enzyme-substrate complex, b). reaction in the bound enzyme-substrate complex to form the enzyme-product complex, c). dissociation of the enzyme-product complex to give free enzyme and the product of the reaction. A fundamental process is the formation of a temporary complex between the substrate and the enzyme at the enzyme active centre. The rate of an enzyme-catalysed reaction does not increase linearly with increasing substrate concentration but increases in a hyperbolic manner to reach a level of maximum activity (figure 3.13). Beyond this maximum activity, the rate of enzyme reaction is dependent only on the

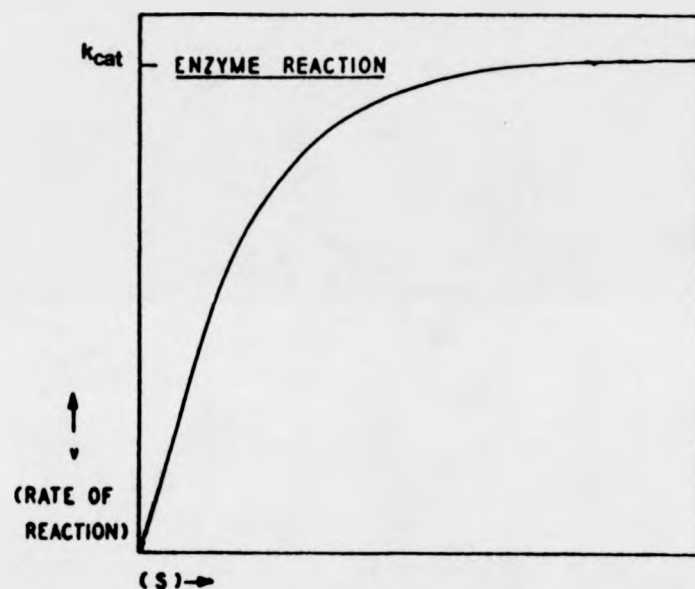


Figure 3.13 Dependence of the rate of enzyme reaction on the concentrations of substrate
 $v = k_{cat} \frac{s}{K_M + s}$
 k_{cat} is the maximum rate under specified experimental conditions,
 K_M is the Michaelis constant of the enzyme

enzyme concentration.

The rate of an enzyme-catalysed reaction can be expressed as:

$$v = \frac{k_{cat} [s]}{s + K_M} \quad (3.30)$$

where k_{cat} is the maximum rate under specified experimental conditions,

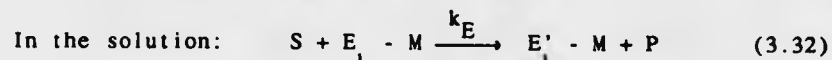
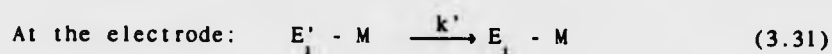
K_M is the Michaelis constant which is an inverse measure of the affinity of the enzyme for the substrate.

s is the substrate concentration.

For a particular enzyme, k_{cat} and K_M can be determined graphically by plotting $1/v$ vs $1/[s]$. This plot should be linear with a slope of K_M/k_{cat} and an intercept on y-axis of $1/k_{cat}$.

3.3.1.2 Kinetic Model for the Modified Glucose Oxidase

This section is concerned with the theoretical aspects of the reactions between the modified enzyme and substrate. The kinetic model deals with those situations where the mediator is incorporated within the enzyme either covalently (for example, the ferrocene modified GOx discussed in this chapter) or non-covalently (for example, TTF modified GOx which will be discussed in Chapter V). The reaction between the modified enzyme and the substrate may be described as follows: The enzyme (E_1) reacts with substrate resulting in the conversion of substrate (S) to product (P) and the reduction of enzyme (E_1) to reduced form (E_2). Unlike the homogeneous mediation where the enzyme (E_1) is regenerated by reaction of E_2 with a freely diffusing mediator, this reduced form of the enzyme (E_2) is assumed to be reoxidised by the mediator molecules incorporated inside the enzyme. The incorporated mediator is then oxidised at the electrode. The reaction sequence may be written as:



Assuming Michaelis-Menten kinetics for the enzyme, an expression for the limiting current can be derived for this reaction sequence:

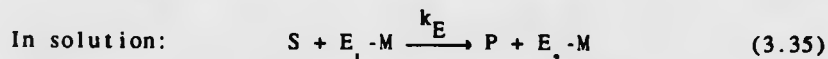
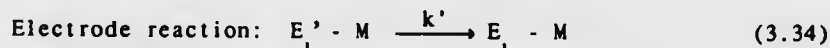
$$i_L/nFA = [\text{enzyme}] \{ Dk_{cat} [\text{glucose}]/(k_M + [\text{glucose}]) \}^{1/2} \quad (3.33)$$

where i_L is the limiting current in the presence of glucose,

D is the diffusion coefficient for the enzyme

k_{cat} and K_M describe the enzyme kinetics.

Eqn. (3.33) predicts that a plot of $(1/i_L)^2$ vs $1/[\text{glucose}]$ will be linear and values of k_{cat} and K_M can be estimated from the slope and intercept of the plot. However, our results for the same system show some deviation from this simple model. The deviation is more pronounced when GOx is modified with fewer ferrocene groups. This indicates that the regeneration of the enzyme by the incorporated mediator may be rate limiting. Thus we extend the above theoretical model to introduce an extra reaction step for the modified GOx. The reaction sequence is rewritten as:



Eqn. (3.36) describes the regeneration of enzyme by the mediator. $E_2 - M$ is assumed to be electrochemically inactive.

Under steady-state conditions and assuming that 1) the enzyme-substrate

reaction is irreversible and 2) the enzyme-mediator reaction is irreversible, we can derive the following differential equations describing the transport and kinetics of the species in solution.

For the enzyme, we write:

$$D \frac{d^2 e_1}{dx^2} - k_E e_1 s = 0 \quad (3.37)$$

$$D \frac{d^2 e_2}{dx^2} + k_E e_1 s - k_1 e_2 = 0 \quad (3.38)$$

$$D \frac{d^2 e_3}{dx^2} + k_1 e_2 = 0 \quad (3.39)$$

where D is the diffusion coefficient of the modified enzyme and it is assumed to be unchanged following oxidation or reduction.

Lower case letters represent the concentrations of species and e_1 , e_2 , e_3 are the concentrations of E_1 -M, E_2 -M and E_3 -M respectively,

x is the distance from the electrode surface and,

k_E , k_1 and k' are constants.

A complete mathematical treatment for equations (3.37) - (3.39) under certain boundary conditions is given in Appendix I.

From the solution, the following expression for e_3 is obtained.

$$e_3 = - \frac{e_s k_1 k_E s \sqrt{k_1}}{k_1 \sqrt{k_1} - k_E s \sqrt{k_E s}} \left[\frac{1}{k_E s} \exp \left(- x \sqrt{\frac{k_E s}{D}} \right) - \frac{1}{k_1} \sqrt{\frac{k_E s}{k_1}} \exp \left(- x \sqrt{\frac{k_1}{D}} \right) \right] + e_s \quad (3.40)$$

Now the flux at the electrode can be written as:

$$j = D \left. \frac{de_3}{dx} \right|_{x=0} \quad (3.41)$$

Substitution of (3.40) in (3.41) gives,

$$j = - \frac{k_1 k_E s B_1}{(k_1 - k_E s)} \left[- \sqrt{\frac{D}{k_E s}} + \sqrt{\frac{k_E s}{k_1}} \right] \quad (3.42)$$

Rearrangement of (3.42) gives,

$$j = e_{\Sigma} \sqrt{D} \cdot \frac{\sqrt{k_1 k_E s} (k_1 - k_E s)}{(k_1 \sqrt{k_1} - k_E s \sqrt{k_E s})} \quad (3.43)$$

Taking reciprocals of (3.43),

$$1/j = \frac{1}{e_{\Sigma} \sqrt{D}} \cdot \frac{(k_1 / \sqrt{k_E s} - k_E s / \sqrt{k_1})}{(k_1 - k_E s)} \quad (3.44)$$

If we again assume Michaelis-Menten kinetics for the enzyme-substrate reaction, k_E can be expressed as:

$$k_E = \frac{k_{cat}}{s + K_M} \quad (3.45)$$

We can rewrite (3.44),

$$1/j = \frac{1}{e_{\Sigma} \sqrt{D}} \cdot \frac{k_1 \sqrt{\left(\frac{s+K_M}{k_{cat}s} - \frac{k_{cat}s}{(s+K_M)} \right) \cdot \frac{1}{\sqrt{k_1}}}}{(k_1 - \frac{k_{cat}s}{s+K_M})} \quad (3.46)$$

Equation (3.46) has two limiting forms:

1. When k_1 is much greater than $k_E s$, i.e. when the mediator oxidises the flavin rapidly so that the rate limiting step is the enzyme kinetics,

$$k_1 \gg k_E s, \quad 1/j = \frac{1}{e_{\Sigma} \sqrt{D}} \cdot \sqrt{\frac{K_M + s}{k_{cat}s}} \quad (3.47)$$

$$\text{and } 1/j^2 = \frac{1}{e_{\Sigma}^2 D} \left(\frac{1}{k_{cat}} + \frac{K_M}{k_{cat}} \cdot \frac{1}{s} \right) \quad (3.48)$$

Since $i = nFAj$, therefore

$$1/i^2 = \frac{1}{(nFAe_\Sigma)^2 D} \left(\frac{1}{k_{cat}} + \frac{K_M}{k_{cat}} \cdot \frac{1}{s} \right) \quad (3.49)$$

Thus a plot of $1/i^2$ versus $1/s$ should be linear with a slope of $1/(nFAe_\Sigma)^2 D K_M/k_{cat}$ and an intercept of $1/(nFAe_\Sigma)^2 D \cdot 1/k_{cat}$. Values of K_M and k_{cat} can then be obtained.

2. When k_1 is much smaller than $k_E s$, the rate limiting step is either the reoxidation of the flavin by the mediator or the enzyme kinetics. This describes the kinetics for the plateau region of a substrate titration curve for the modified enzyme,

when $k_1 \ll k_E s$ and s is large,

$$1/j = \frac{1}{e_\Sigma \sqrt{D}} \cdot \frac{(k_1 \sqrt{k_1} - k_{cat} \sqrt{k_{cat}})}{(k_1 - k_{cat}) \sqrt{k_{cat} k_1}} \quad (3.50)$$

Equation (3.50) again has two limited forms,

$$(1). k_1 \gg k_{cat}, 1/j = \frac{1}{e_\Sigma \sqrt{D}} \cdot \frac{1}{\sqrt{k_{cat}}} \quad (3.51)$$

where the rate limiting step is the saturated enzyme kinetics, and

$$(2). k_1 \ll k_{cat}, 1/j = \frac{1}{e_\Sigma \sqrt{D}} \cdot \frac{1}{\sqrt{k_1}} \quad (3.52)$$

where the regeneration of enzyme by the mediator is rate limiting.

In figure 3.14, a set of computer calculated substrate titration curves are shown. These curves are calculated using eqn. (3.43) for a fixed value for k_{cat} . It is clear that the limiting currents for these substrate titration curves vary with the values of k_1 . Thus, practically, one may estimate the value of k_1 from the limiting current value of a substrate titration curve provided that k_{cat} is known, eqn. (3.50).

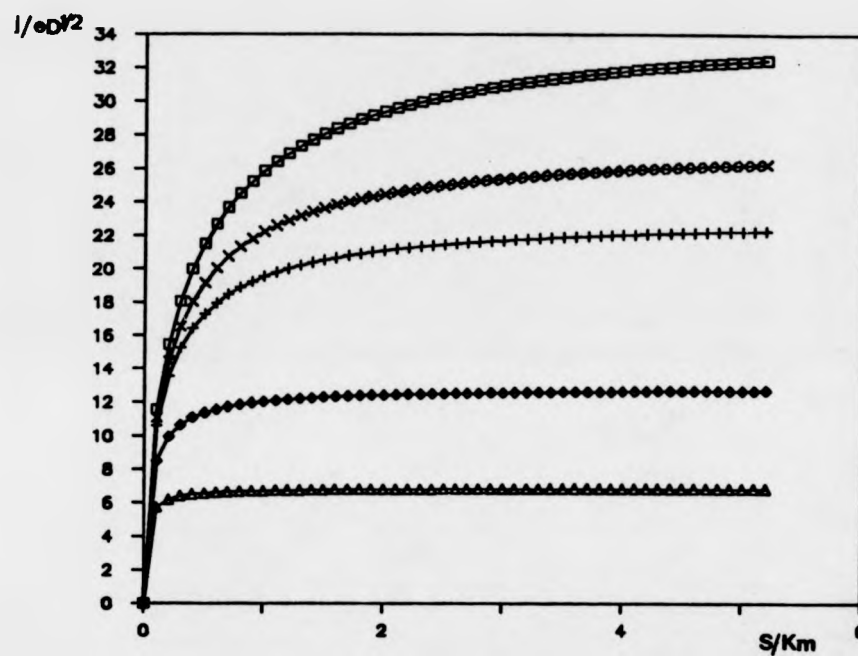


Figure 3.14 Computer calculated substrate titration curves for
 FAA modified GOx
 k_{cat} is 1500 s^{-1}
 k_i values are:
 \square - $10,000 \text{ s}^{-1}$, \times - 2000 s^{-1} , $+$ - 1000 s^{-1} , \diamond - 200 s^{-1} , \triangle - 50 s^{-1}

The theoretical plots of $\epsilon \Sigma^2 D/j$ versus K_M/s at different k_1 values give a set of lines which, at high k_1 values, appears to be linear, but for which at low k_1 values, a downward curvature is apparent, figure 3.15. Their slopes and intercepts contain the parameters k_1 , k_{cat} and K_M for the modified enzyme.

Next, we will discuss our results of the catalytic responses of FAA modified GOx and the analysis of the results using our model.

3.3.2 Electrochemistry of FAA modified GO_x

The sample of FAA modified glucose oxidase was prepared using the method reported in the literature (6). Catalytic responses of the modified enzyme to additions of substrates were studied using d.c. cyclic voltammetry.

A sample of FAA modified GOx (2.5 cm²) was placed in a semi-macro electrochemical cell (section 2.2) and was deoxygenated for 15-20 minutes by passing oxygen-free nitrogen over the solution surface while stirring. Aliquots of β -D-glucose solution (1.0 mol dm⁻³) were added and cyclic voltammograms were recorded following each addition. In the absence of substrate, the voltammogram of FAA modified GOx in buffer resembles that of the FAA itself, figure 3.16, but with an apparent shift of the oxidation and reduction potential for the FAA groups attached to GOx. In the presence of substrate, catalytic responses were observed for FAA modified GOx at platinum, gold and glassy carbon disc electrodes in neutral aqueous buffer solution, free of added mediators or molecular oxygen. Figure 3.17 shows the cyclic voltammograms of FAA modified GOx in the absence of glucose and in the presence of 50 mmol dm⁻³ glucose. A substrate titration curve was then constructed by plotting the limiting current after each substrate addition against the corresponding substrate concentration (figure 3.18).

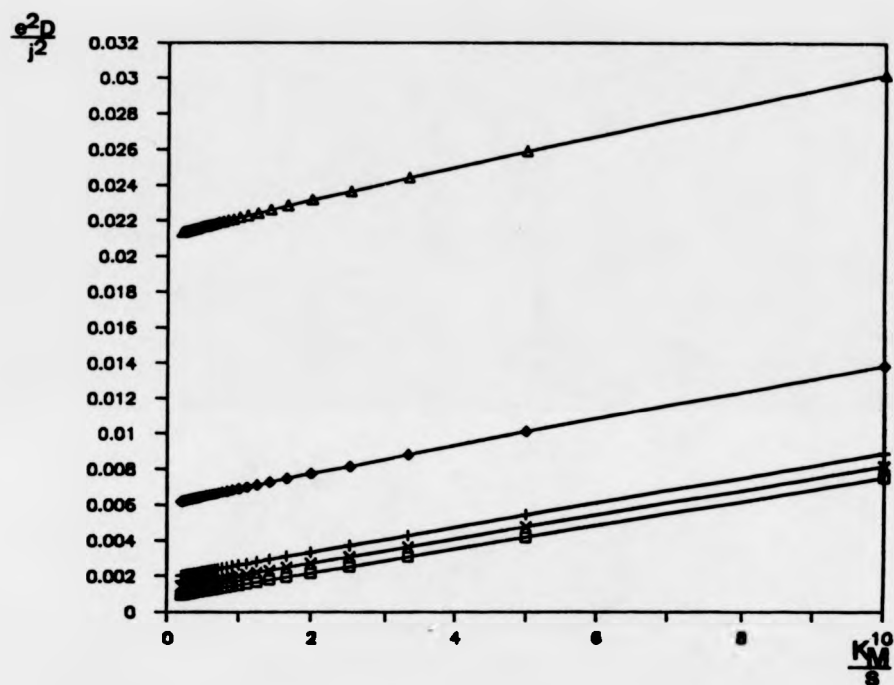


Figure 3.15 Theoretical plots of $e^2 D/j^2$ vs K_M/s for FAA modified GOx,
 $k_{cat} = 1500 \text{ s}^{-1}$
 k_i values are the same as those in figure 3.14

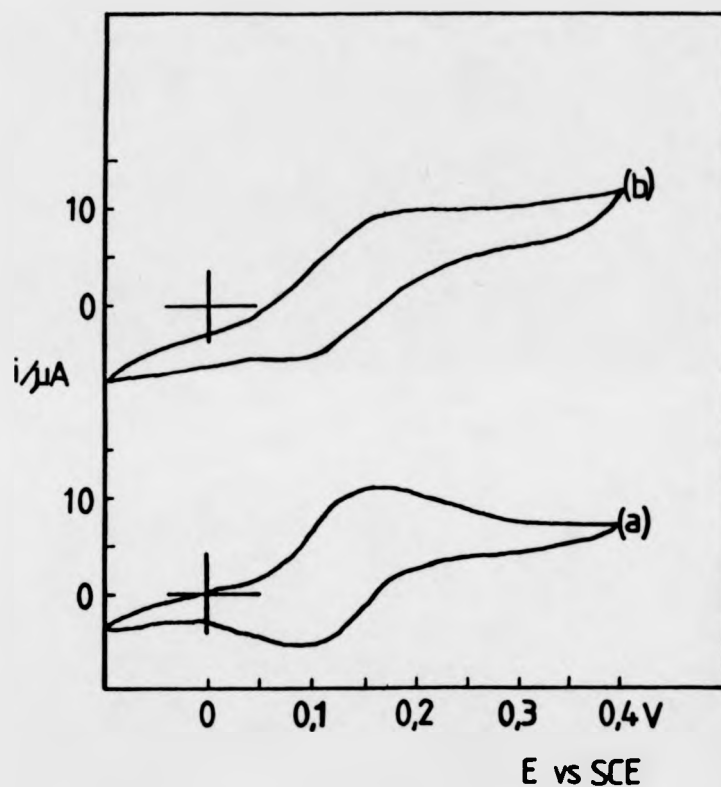


Figure 3.16 DC cyclic voltammograms of (a).
 FAA (1.0×10^{-3} mol dm $^{-3}$) in phosphate buffer
 (85 mmol dm $^{-3}$, pH 7.0), $E_{ref} = 125$ mV, and
 (b) enzyme-bound FAA in phosphate buffer
 (85 mmol dm $^{-3}$, sodium phosphate, pH 7.0),
 $E_{ref} = 135$ mV.
 $[CO_x] = 8.6 \times 10^{-4}$ mol dm $^{-3}$
 electrode: platinum (0.384 cm 2)
 sweep rate: 5 mV s $^{-1}$

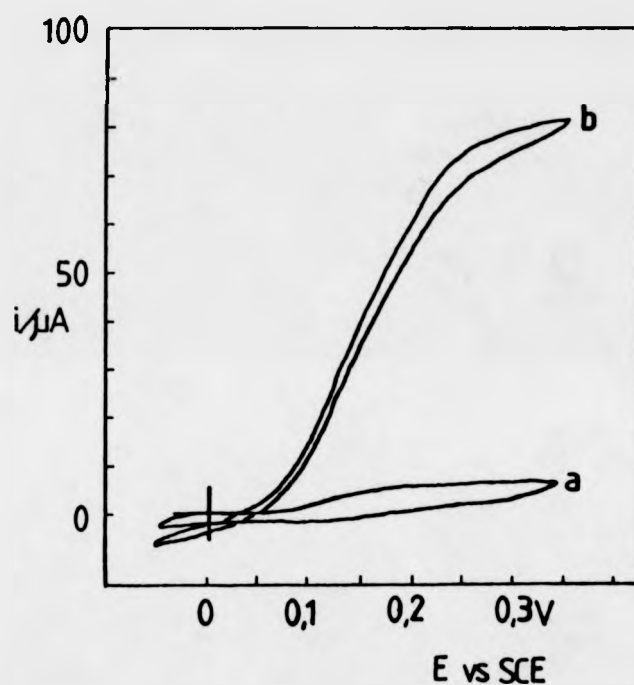


Figure 3.17 Cyclic voltammograms of FAA modified GOx ($4.0 \times 10^{-5} \text{ mol dm}^{-3}$)
 a. in the absence of glucose, and
 b. in the presence of glucose (50 mmol dm^{-3}),
 electrode: platinum (0.384 cm^2)
 sweep rate : 5 mV s^{-1}

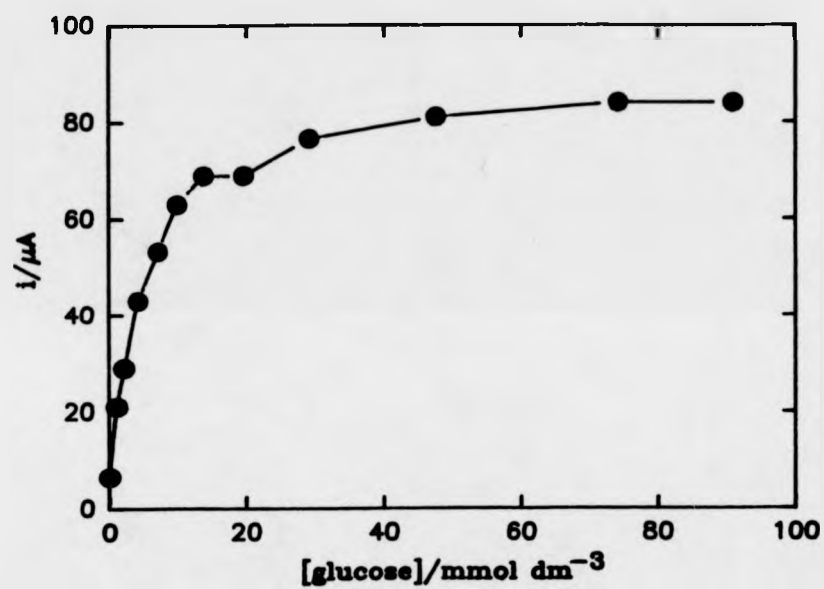


Figure 3.18 Substration titration curve for FAA modified GOx.
[GOx] = 4.0×10^{-6} mol dm $^{-3}$
electrode: platinum (0.384 cm 2)
sweep rate: 5 mV s $^{-1}$

In the next section, we will present the kinetic analysis of the above experimental data using our model.

3.3.3 Analysis for the Results of FAA Modified GOx

Equation (3.46) shows that, for modified enzyme, the relationship between the flux at the electrode and the substrate concentration is complex. One cannot derive an obvious correlation between j and s from eqn. (3.46) to construct a simple plot. Thus a few approximations have to be made. First, we assume that for FAA modified GOx, the enzyme-bound FAA molecules oxidise the flavin at a sufficient rate that the enzyme kinetics is rate limiting. Thus equation (3.49) can be used for the analysis. Second, at high substrate concentrations, the limiting current values can be used to estimate values for k_1 if value of k_{cat} is known.

We carried out the kinetic analysis for the results of several batches of FAA modified GOx and obtained values of k_{cat} and k_M in the range of 200-1500 s^{-1} and 1.0-15 $mmol\ dm^{-3}$ respectively. Parameters obtained for the batch of FAA modified enzyme with the fastest enzyme kinetics are presented below.

A plot of $1/i^2$ versus $1/s$ is shown in figure 3.19. It is an apparent linear plot with a slope of 2.2×10^{-3} ($\mu A^{-2} mmol\ dm^{-3}$) and an intercept of 1.5×10^{-4} (μA^{-2}). From eqn. (3.49). We obtain that,

$$\text{slope of the plot} = \frac{1}{(nFA e_{\Sigma})^2 D} \cdot \frac{K_M}{k_{cat}} \quad (3.53)$$

$$\text{intercept of the plot} = \frac{1}{(nFA e_{\Sigma})^2 D} \cdot \frac{1}{k_{cat}} \quad (3.54)$$

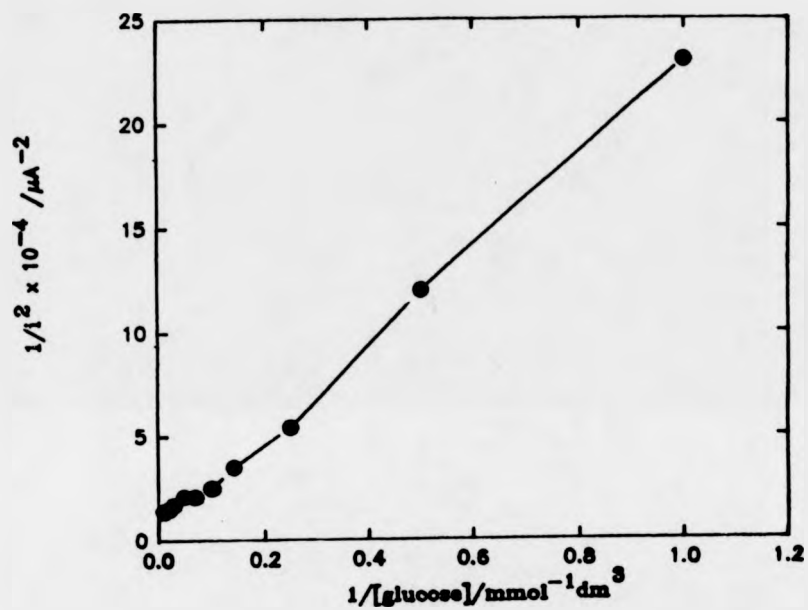


Figure 3.19 Plot of $1/i^2$ versus $1/s$ for FAA modified GOx using equation (3.46)
 $[GOx] = 4.0 \times 10^{-5} \text{ mol dm}^{-3}$
 electrode: platinum (0.384 cm^2)
 slope = $2.2 \times 10^{-3} \mu\text{A}^{-2} \text{ mmol dm}^{-3}$
 intercept = $1.5 \times 10^{-4} \mu\text{A}^{-2}$

Thus we can now derive the values for K_M and k_{cat} , using $n = 2$, $F = 96480 \text{ C mol}^{-1}$, $A = 0.384 \text{ cm}^2$, $c_\Sigma = 4.0 \times 10^{-5} \text{ mol dm}^{-3}$ and $D = 5 \times 10^{-7} \text{ cm}^2 \text{ s}^{-1}$,

$$k_{cat} = 1500 \text{ s}^{-1}$$

$$K_M = 15 \text{ mmol dm}^{-3}.$$

These values of k_{cat} and K_M are in agreement with those reported in the literature for the same system (122).

To further test the model system, results from enzyme titration experiments were also analysed. From eqn. (3.46), it is clear that, when substrate concentration is held constant, the flux at the electrode is proportional to the enzyme concentration. Thus a plot of j versus c_Σ should be linear. In figure 3.20, the plot of catalytic current versus modified enzyme concentration for FAA modified GOx is shown. This plot is linear with a slope of $4.9 \times 10^5 \text{ (}\mu\text{A mol}^{-1} \text{ dm}^3\text{)}$. Substitution of this value in eqn. (3.33) and using $n = 2$, $F = 96480 \text{ C mol}^{-1}$, $A = 0.384 \text{ cm}^2$, $D = 5 \times 10^{-7} \text{ cm}^2 \text{ s}^{-1}$, $s = 0.1 \text{ mol dm}^{-3}$ gives,

$$\frac{k_{cat} \times 0.1}{K_M + 0.1} = 88 \text{ (s}^{-1}\text{)}$$

If we take a value of K_M as 30 mmol dm^{-3} , then the value of k_{cat} calculated from this expression will be 115 s^{-1} . This value appears to be slower than that obtained for a substrate titration of modified GOx.

In the next section, we will discuss the substrate specificity of FAA modified GOx.

3.4 The Enzyme Substrate Specificity of FAA Modified GOx.

Native glucose oxidase is an enzyme generally considered as highly specific for glucose. The activity relative to glucose with many other sugars

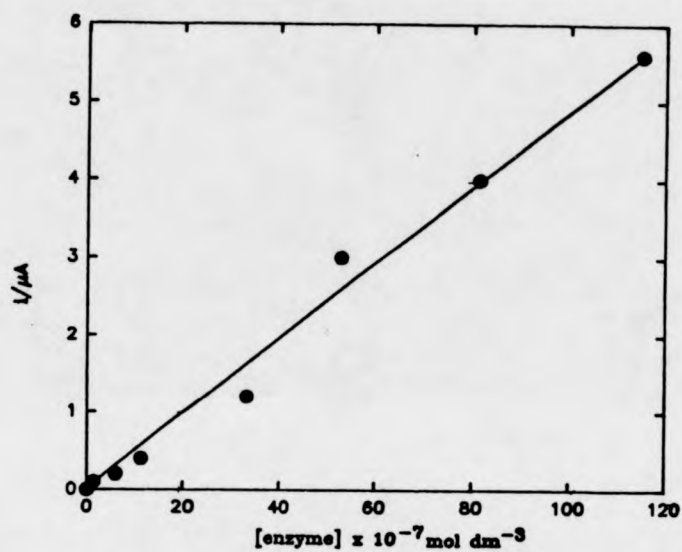


Figure 3.20 Enzyme titration for FAA modified GOx
 $E = 0.4 \text{ V vs SCE}$
 $[\text{glucose}] = 100 \text{ mmol dm}^{-3}$
 electrode: glassy carbon (0.384 cm^2)

was reported to be of the order of 1% or less, except with 2-deoxy- β -D-glucose which achieved a relative rate of 25% (26,137,141-142). This high specificity of glucose oxidase is important for its applications to the estimation of glucose in the presence of other sugars. Thus on modifications of glucose oxidase with redox mediator molecules, it is highly desirable that the enzymic specificity is retained.

The investigation of the specificity of FAA modified GOx in neutral aqueous buffer solution is described in this section. The responses of the modified enzyme to four other different sugar substrates (2-deoxy- β -D-glucose, D-mannose, D-xylose and D-galactose) were compared with that to glucose.

The enzymic specificity of native glucose oxidase to the same sugars in neutral aqueous buffer solution with FMCA (1 mmol dm⁻³) as a homogeneous mediator was also studied and the results were compared with the specificity of the FAA modified GOx. The results of substrate titration for both native and FAA modified GOx were analysed.

In figure 3.21, substrate titration curves of native and FAA modified GOx for five sugars are shown. For native GOx, results of substrate titration can be analysed using the model for homogeneous mediation (16) where

$$i = (nFA)(2D_M k_E e_\Sigma m_O)^{1/2} \quad (3.55)$$

D_M is the diffusion coefficient for the mediator
(3.9×10^{-6} cm² s⁻¹ for FMCA in neutral aqueous buffer);
 k_E describes the enzyme kinetics and

$$k_E = \frac{k_{cat} \cdot s}{K_M + s}$$

e_Σ is the enzyme concentration, and
 m_O is the mediator concentration.

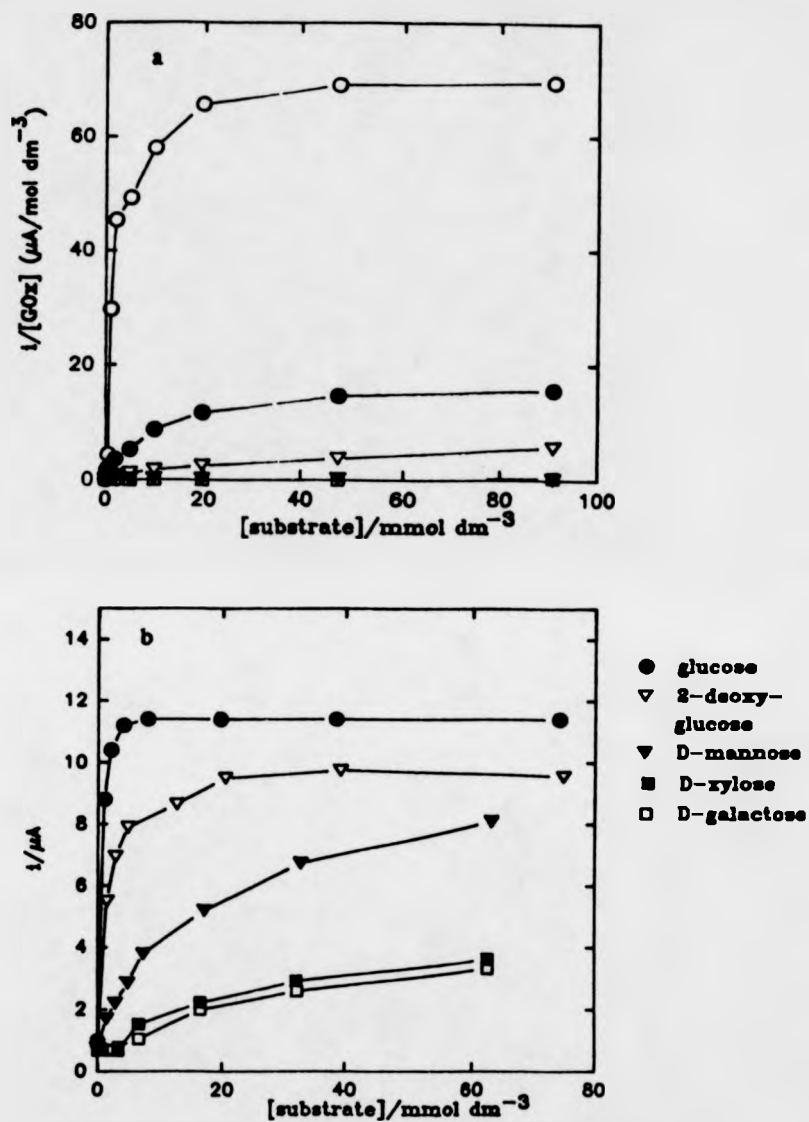


Figure 3.21 Substrates titration curves for:
a. native GOx with FMCA ($1.0 \times 10^{-3}\ mol\ dm^{-3}$)
as a homogeneous mediator
 $[GOx] = 1.8 \times 10^{-3}\ mol\ dm^{-3}$,
○ - glucose, ● - 2-deoxy-glucose,
▽ - D-mannose, ▼ - D-xylose,
□ - D-galactose
b. FAA modified GOx
 $[GOx] = 2.1 \times 10^{-3}\ mol\ dm^{-3}$
electrode: platinum ($0.384\ cm^2$)
E vs SCE

Thus a plot of $1/i^2$ vs $1/s$ should give a straight line. The values of k_{cat} and K_M can be estimated from the slope and intercept of the plot.

$$\text{slope of the plot} = \frac{1}{2(nFA)^2 D_m e_{\Sigma} m_o} \cdot \frac{K_M}{k_{cat}}$$

$$\text{intercept of the plot} = \frac{1}{2(nFA)^2 D_m e_{\Sigma} m_o} \cdot \frac{1}{k_{cat}}$$

Such a plot for 2-deoxy-glucose is shown in figure 3.22.

For the substrate titration curve of FAA modified GOx, the results can be analysed using our model. Again assumptions are made. Literature studies show that glucose oxidase is highly specific to glucose. Thus for the reactions between FAA modified GOx and other slower substrates, the rate limiting step is likely to be the enzyme kinetics. We can use eqn.(3.50) to analyse the experimental data. Figure 3.23 shows the $1/i^2$ vs $1/s$ plots for five different sugars. The values of k_{cat} and K_M are estimated from the slope and intercepts of the plots.

If we take the ratio k_{cat}/K_M as a measure of the relative rate for oxidation, the specificity of native glucose oxidase with a homogeneous mediator and GOx modified with FAA can be investigated. The k_{cat} and K_M data as well as the relative rates of oxidation for both native and FAA modified GOx are calculated and given in table 3.7.

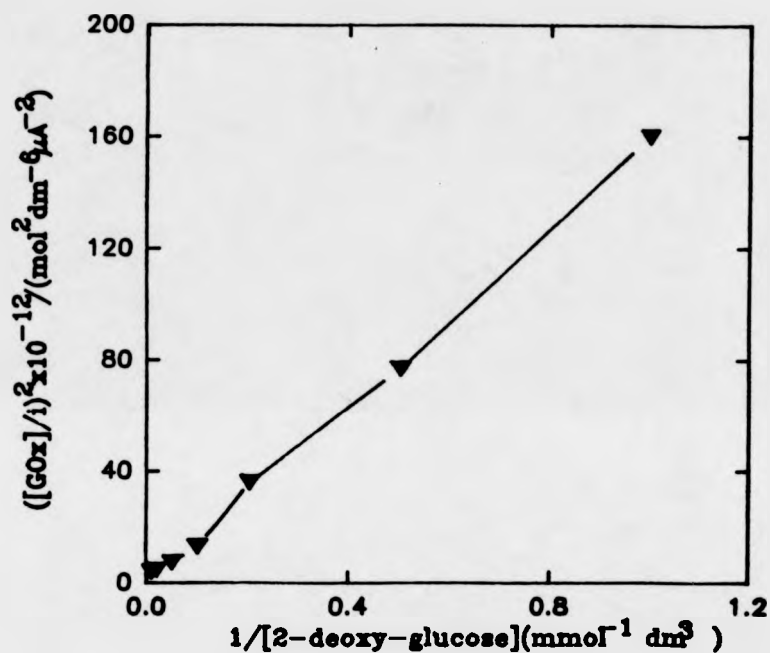


Figure 3.22 Plot of $1/i^2$ versus $1/i$ for the titration curves of 2-deoxy-glucose with native GOx using FMCA ($1.0 \times 10^{-3} \text{ mol dm}^{-3}$) as electron transfer mediators
slope = $11.8 \times 10^{-4} \mu\text{A}^{-2} \text{ mmol dm}^{-3}$
intercept = $0.42 \times 10^{-4} \mu\text{A}^{-2} \text{ mol}^2 \text{ dm}^{-6}$
 $l = nFA (2D_m e \Sigma k_E m_0)^{1/2}$, where
 $D_m = 3.9 \times 10^{-6} \text{ cm}^2 \text{ s}^{-1}$
 $e \Sigma = 1.2 \times 10^{-6} \text{ mol dm}^{-3}$
 $k_E = k_{cat} s / (s + K_M)$
 $n = 2$, $F = 96480 \text{ C mol}^{-1}$, $A = 0.384 \text{ cm}^2$

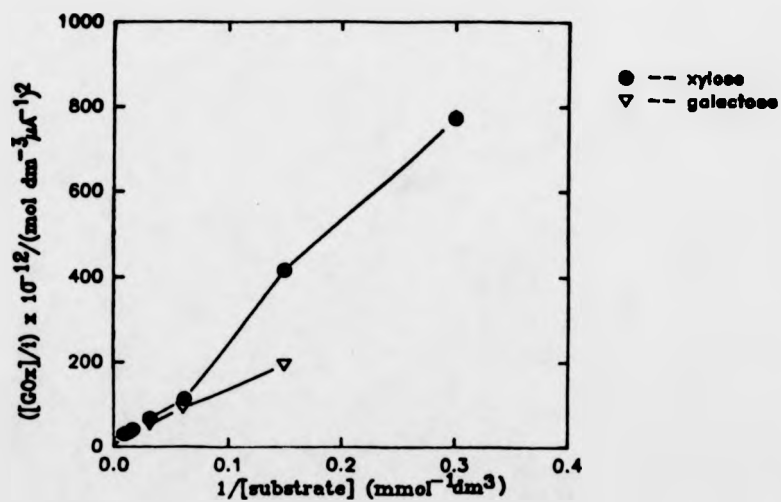
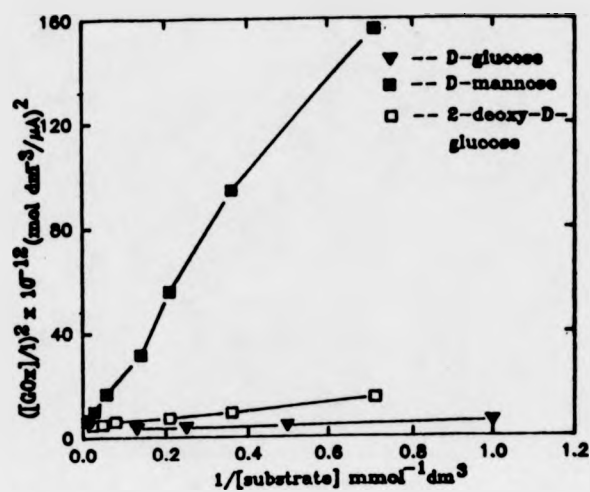


Figure 3.23 Plot of $1/i^2$ versus $1/s$ for substrate titration of FAA modified GOx with five different sugar substrates.
 $D = 5.0 \times 10^{-7} \text{ cm}^2 \text{ s}^{-1}$
 $c_{\Sigma} = 2.1 \times 10^{-5} \text{ mol dm}^{-3}$

Table 3.7 Specificity of native and FAA modified GOx

Sugars	Native GOx			FAA modified GOx		
	K_M (mmol dm ⁻³)	k_{cat} (s ⁻¹)	Relative Rate of oxidation	K_M (mmol dm ⁻³)	k_{cat} (s ⁻¹)	Relative Rate of oxidation
D-glucose	5.2	230	100	1.0	114	100
2-deoxy- glucose	28	107	9	2.5	92	26
D-mannose	110	6	0.12	123	76	0.5
D-xylose	*	*	*	113	35	0.2
D-galactase	*	*	*	100	15	0.1

* Responses are too low to analyse.

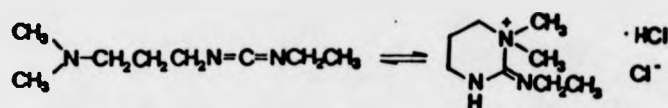
From the table, it is apparent that the specificity of FAA modified GOx has decreased slightly compared to that of the native GOx. This suggests that the modification of GOx with a number of ferrocene groups may have affected the selectivity of the enzyme to sugar substrates. However, for FAA modified GOx, the relative rates of oxidation of other sugars are still small compared to that of glucose. Thus we can still regard the FAA modified GOx as highly specific for glucose.

In the next section, we will discuss cases where the regeneration of enzyme by the mediator may be rate limiting. These cases are present when the GOx is modified with fewer FAA groups.

3.5 GOx Modified with Fewer FAA Groups

In previous sections, we have described the studies of FAA modified GOx prepared using the literature quantity of FAA (60 mg). Atomic absorption spectroscopy studies for the modified GOx sample show that an average number of 20 FAA relays have been attached to each enzyme

molecule after the modification. It was observed that using the literature method for enzyme modification, the amount of FAA used in the reaction was approximately 500 fold in excess of the amount of GOx. Taking into consideration that the coupling reagent (DEC) is hygroscopic (138), it exists in an equilibrium:



(I)

(II)

If we assume that at the most, 50% of the reagent exist as (II) isomer, the amount of FAA available for coupling is still in 250 fold excess to that of GOx. Under the present conditions, 20 ferrocene groups have been successfully coupled to enzyme molecule. If the FAA quantities used in the modification reaction were to be reduced, for example, by 50%, will the number of electron relays per enzyme also be reduced correspondingly and is there a relationship between the amount of FAA used for enzyme modification and the resulting number of electron relays attached to the modified enzyme? These questions are investigated in this section.

Four samples of FAA modified GOx were prepared using the literature method (6) but with reduced quantities of FAA and DEC, as described in section 2.5.1. The electrochemical activities of these FAA modified GOx samples were studied in the presence of β -D-glucose and the results were analysed using our theoretical model. The iron contents of the FAA modified GOx samples were determined using atomic absorption spectroscopy. Estimation of the isoelectric points for the FAA modified GOx prepared both with the literature quantity of FAA and with reduced FAA quantities using

isoelectric focusing gel electrophoresis and chromatofocusing chromatography will be described in sections 3.6 and 3.7.

3.5.1 Catalytic Activities and Iron Contents

The samples of FAA modified GOx were prepared and purified as described in sections 2.5.1 and 2.5.3. Each modified GOx sample (0.5 cm^3) was placed in a micro-cell and was deoxygenated by passing oxygen-free nitrogen over the solution surface for 15-20 minutes while stirring. Aliquots of glucose (1.0 mol dm^{-3}) were added and cyclic voltammograms were recorded at a gold electrode ($A = 0.124 \text{ cm}^2$) over the potential range of -0.1 to 0.4 Volts (vs SCE). Substrate titration curves for these FAA modified GOx samples are given in figure 3.24.

The iron contents of the FAA modified GOx samples prepared both with the literature quantity of FAA and with the reduced amounts of FAA were determined using atomic absorption spectroscopy. The average number of FAA groups per enzyme molecule for FAA modified GOx samples was calculated. The results are collected in table 3.8. The ratios between the amounts of FAA quantity and the amount of GOx used in enzyme modification are plotted against the average number of FAA groups per enzyme molecule for the resulting modified GOx, figure 3.25. This plot appears to contain two linear portions of different slopes and intercepts joining at (125, 2). One possible interpretation is that there may be two different groups of lysine residues available for amide bonding within glucose oxidase. The degree of accessibility for each lysine group may be different. Within each lysine group, the number of FAA relays bound to the enzyme is proportional to the FAA quantities used in enzyme modification.

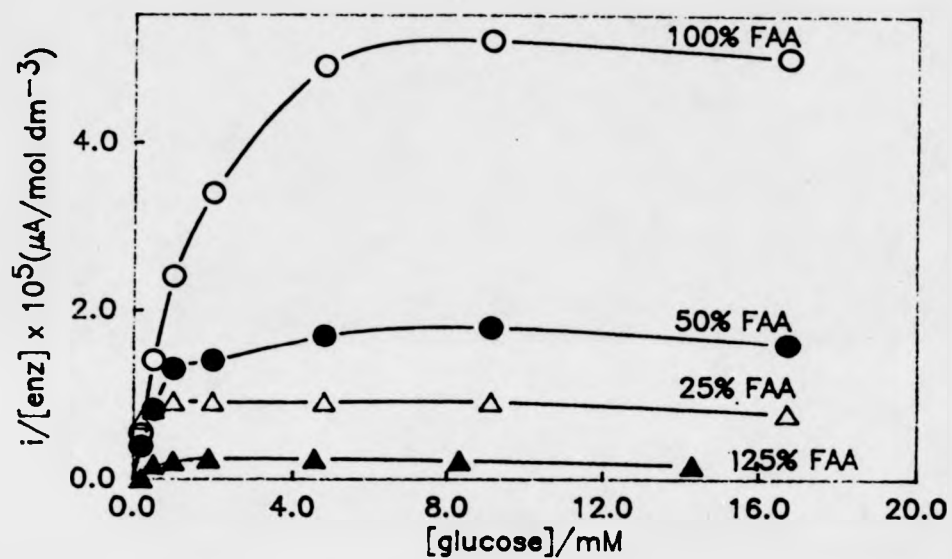


Figure 3.24 Substrate titration curves of GOx modified with different number of FAA groups.
 electrode: gold (0.125 cm²)
 sample preparations as described in section 2.5.1
 (Note: no catalytic activity was observed for 6.25% FAA modified GOx)

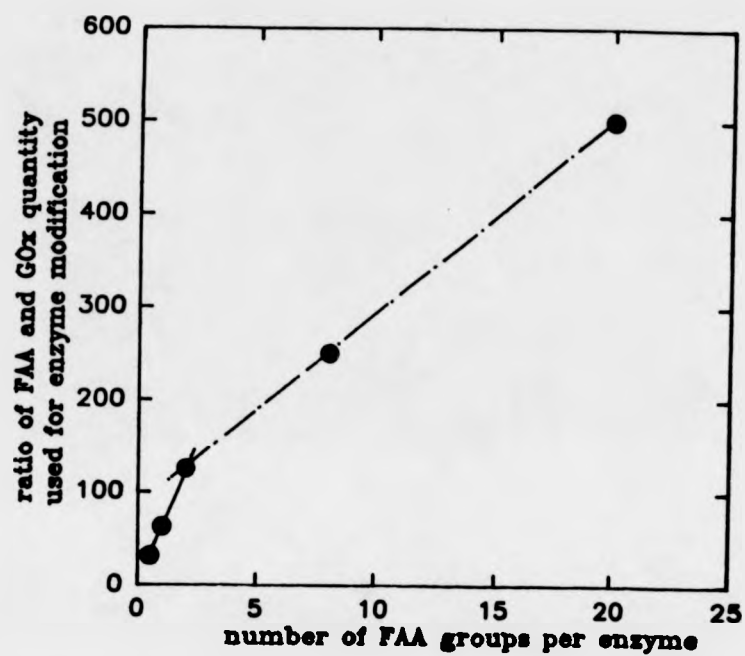


Figure 3.25 Plot of the ratio of the amounts of FAA to GOx used for enzyme modification versus the number of FAA groups per enzyme molecule in the resulting modified enzyme

Table 3.8 Iron contents for the samples of FAA modified GOx

Ratios of between the amount of FAA and the amount of GOx	Average number of FAA groups per enzyme
500	20
250	8
125	2
63	1
31	0.5

3.5.2 Kinetic Analysis

This section deals with the analysis for the results of substrate titration of GOx samples modified with different number of FAA groups. Previously, we have dealt with cases where we assumed that the enzyme kinetics was the rate limiting step for GOx modified with the literature quantity of FAA. Now we have samples of GOx modified with fewer FAA groups and experimental results show that these samples exhibit slower enzyme kinetics, we should take into consideration that the regeneration of enzyme by the attached mediators may also be rate limiting. The rate of regeneration of enzyme by the attached FAA mediator is described by the rate constant k_1 . Since the substrate titration experiments for GOx samples modified with different FAA groups were carried out under the same conditions, we assume that the value of k_{cat} is the same for all the FAA modified GOx samples. This assumption is based on the experimental evidence obtained previously in our laboratory, which an almost identical k_{cat} value was obtained for GOx modified with 20 FAA groups using oxygen electrode assay ($k_{cat} = 1100 \text{ s}^{-1}$) (124) with that obtained using electrochemical assay method ($k_{cat} = 1500 \text{ s}^{-1}$) for the same enzyme sample (section 3.3.3). If the number of FAA groups on the modified enzyme is reduced, the value of k_1 may also be reduced.

The model predicts that at different k_1 values, the plots of $e^2 \Sigma D/j^2$ vs K_M/s are a set of apparently parallel lines (figure 3.15). Figure 3.26 shows

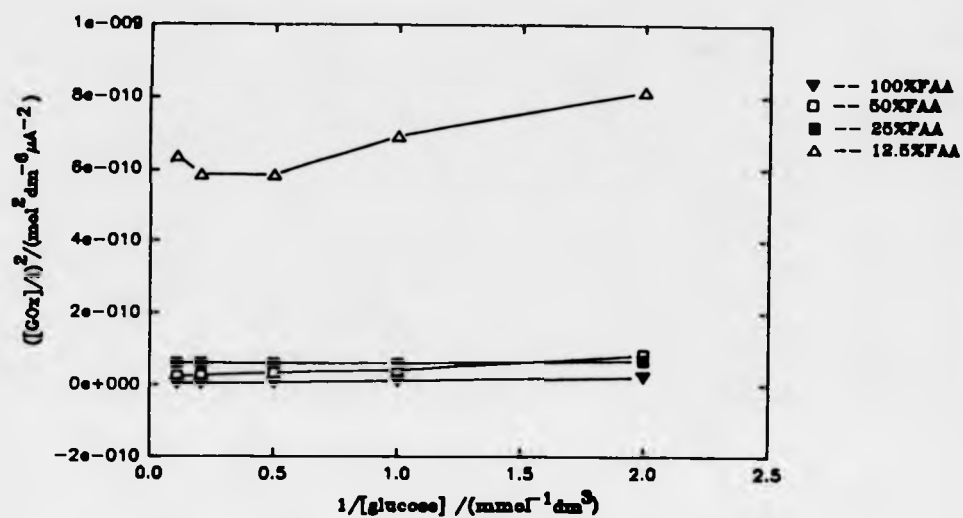


Figure 3.26 Plot of $1/i^2$ versus $1/s$ for GOx modified with different number of FAA groups
electrode: gold (0.125 cm^2)
E vs SCE

plots of $e^2 \Sigma / i^2$ versus $1/s$ for GOx samples modified with different number of FAA groups. These plots agree with our theoretical predictions. Using a value of 1500 s^{-1} for k_{cat} as obtained for 100% FAA modified GOx (section 3.3.3), thus values of k_1 for GOx samples modified with fewer ferrocene groups can be estimated from eqn. (3.51). At high substrate concentrations, the limiting currents for GOx samples modified with different number of FAA groups are obtained and the values of k_1 are calculated, table 3.9.

Table 3.9 Values of $e \Sigma / i_L$ and k_1 for GOx samples modified with different number of FAA groups

FAA modified GOx sample	$e \Sigma / i_L$ (mol dm ⁻³ μA^{-1}) $\times 10^4$	k_1 (s ⁻¹)
100% FAA	5.8	1500
50% FAA	2.1	200
25% FAA	1.3	60
12.5% FAA	0.4	6
6.25% FAA	0	-

* Note: 1. Constants used for calculation, $n = 2$, $F = 96480 \text{ C mol}^{-1}$,

$$A = 0.125 \text{ cm}^2, D = 5.0 \times 10^{-7} \text{ cm}^2 \text{ s}^{-1}.$$

Results from table 3.9 show that k_1 decreases significantly when the amount of FAA used in modification is reduced by 50%. At k_1 values lower than 200 s^{-1} , $k_1 \gg k_{ES}$ can no longer be satisfied. Instead, now the $k_1 < k_{ES}$ is valid. This clearly demonstrates that for GOx modified with fewer ferrocene groups, the rate of catalytic reaction is limited by the rate of reoxidation of the enzyme by the attached ferrocene mediators.

The enzymatic properties of these GOx samples modified with different number of FAA groups are presented in the next section where the determination of their isoelectric points (pIs) is described.

3.6 Determination of pIs for FAA Modified GOx Samples.

Isoelectric points of FAA modified GOx samples were determined

using isoelectric focusing (IEF) gel electrophoresis (139). The results are presented and discussed below.

Any charged ion or group will migrate when placed in an electric field. Since proteins carry a net charge at any pH other than their isoelectric points, they too will migrate. The rate of migration will depend on charge density (the ratio of charge to mass) of the protein; the higher the charge density, the faster the molecule will migrate (140). The application of an electric field to a protein sample in a pH gradient will therefore result in protein migrating towards one of the electrodes until it reaches the value of pH equivalent to pI of the protein. The migrating distance of the protein can be measured and a standard calibration curve can be constructed by plotting the pI values of standard proteins vs the distance they have migrated in the electric field. Figure 3.27 shows a calibration curve for a polyacrylamide gel (pH gradient 4-6.5).

Experiments were carried out using precast polyacrylamide gels (Pharmacia Phastsystem). Samples of native and FAA modified GOx (4 mg cm⁻²) were allowed to migrate in a potential of 2000 volts between the electrodes. The distance migrated towards cathode for each enzyme sample was measured and the corresponding pI values were estimated using the standard calibration curve, table 3.10.

Table 3.10 pI values of native and FAA modified GOx samples

Enzyme Sample	Distance from Cathode (cm)	pI
native	5.25	4.07
6.25% FAA	5.15 ± 0.10	4.21 ± 0.04
12.5% FAA	4.80 ± 0.10	4.36 ± 0.04
25% FAA	4.70 ± 0.10	4.46 ± 0.04
50% FAA	4.05 ± 0.15	4.93 ± 0.07
100% FAA	4.10 ± 0.15	4.86 ± 0.07

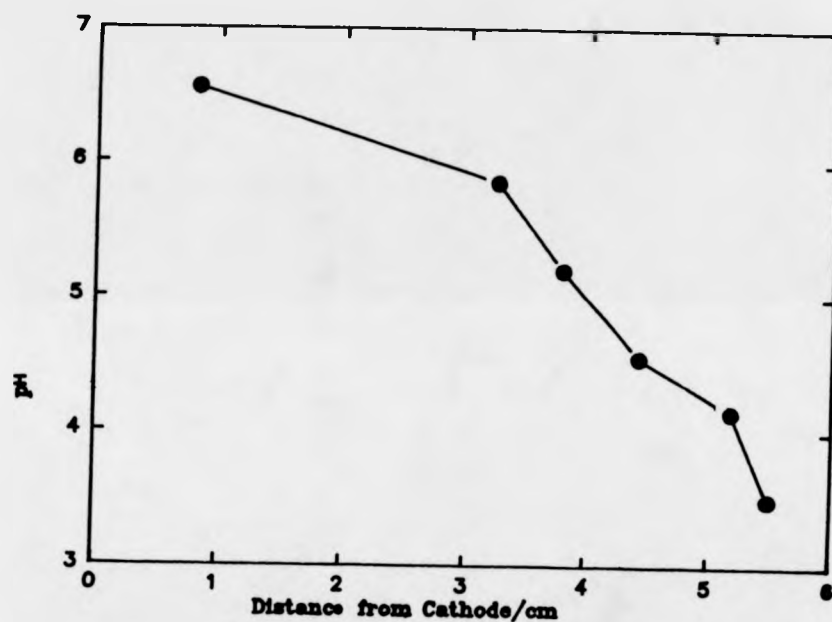
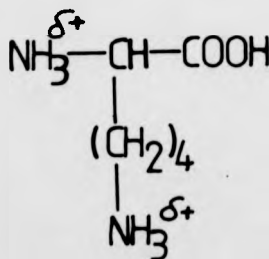


Figure 3.27 Standard calibration curve for IEF gel electrophoresis.
pH gradient 4-6.5
enzyme sample concentrations: 4 mg cm⁻¹
potential between the electrodes: 2000 volts
pI standards as listed in table 2.4

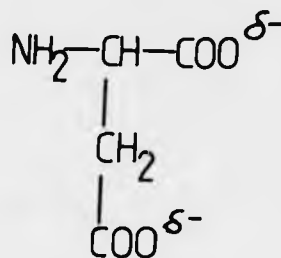
It is evident that first, the pI values of FAA modified GOx samples are higher than that of the native glucose oxidase; second, each FAA modified GOx sample exhibits 2-3 values of pI while native GOx has only one pI value. A stained and dried IEF (4-6.5) gel (figure 2.11) clearly shows that for native GOx, there is only one rather broad band present, but for the FAA modified GOx samples there are a number of bands for each modified GOx sample. This indicates that within each FAA modified GOx sample, there may be enzyme species of different pI values or enzyme species with different numbers of FAA relays attached. In other words, the number of FAA relays estimated for each sample of FAA modified GOx using atomic absorption spectroscopy, represents the average number of FAA groups for this FAA modified GOx sample but this sample is not necessarily homogeneous and may contain enzyme molecules with a different numbers of FAA groups. Enzyme species of different pI values can be isolated using chromatofocusing chromatography, the details are described in the next section.

It was observed that FAA modified GOx samples have higher pI values than that of native GOx: the more FAA groups that are attached to the GOx the higher the pIs are for the resulting modified GOx. To account for this we propose the following explanations:

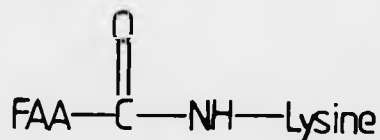
GOx consists of 583 amino acids (212), in which there are 34 lysines, 19 histidines, 29 glutamic acids, 22 arginine and 36 aspartic acids, whose side chains contain ionisable groups. At pH values lower than its pI, an amino acid is positively charged where the amino group(s) is partially protonated (141), for example, lysine (pI = 9.74);



At pH values higher than its pI, an amino acid is negatively charged where the carboxyl group(s) is partially neutralised, for example, aspartic acid (pI = 2.77).



The modification of GOx with a number of FAA groups involves the formation of peptide linkages between the carboxyl group of FAA and the amino group of lysine residue,



Thus the number of positive charges carried by the amino groups is now reduced. However, this loss of positive charges of the amino groups may be compensated by the positive charges carried by the attached FAA mediators. Our previous studies (section 3.2) have shown that at pH 7.0, FAA mediators exist in the enzyme in a mixed Fe^{2+} and Fe^{3+} forms and the ratio between the Fe^{2+} and Fe^{3+} forms is 2-3 Fe^{2+} : Fe^{3+} . Those FAA molecules with the iron in Fe^{3+} form may contribute a net increase of the positive charges to the enzyme. An increase in the number of positive charges of the enzyme will naturally result in the increase of the protein pI

value. Thus, the more FAA groups are attached to GOx the higher is the pI value for the modified enzyme.

Using the ionization constants (211) for lysines in aqueous solution, one should be able to determine the number of protonated amino groups at a given pH value, and therefore determine the total positive charges carried by the lysine groups. On the other hand, if the number of electron relays per enzyme is known for an enzyme sample, the number Fe^{3+} irons may be estimated from the $\text{Fe}^{2+}/\text{Fe}^{3+}$ ratio described above. Thus, in principle, we could calculate the net change of positive charges before and after enzyme modification. However, this is an unrealistic task since the number of FAAs per enzyme molecule is not uniform. A quantitative estimation of the net positive charges for FAA modified enzymes cannot be obtained.

In the next section, studies of native and FAA modified GOx samples using chromatofocusing chromatography are described.

3.7 Studies of FAA Modified GOx Purified by Chromatofocusing Chromatography

This section deals with the isolation of enzyme species with different pI values present within each FAA modified GOx sample. The different modified enzyme fractions for 100% FAA modified GOx isolated on the basis of their pI values were studied electrochemically to determine their catalytic activities. The iron contents of the different fractions were also determined using atomic absorption spectroscopy. The mechanism of chromatofocusing chromatography is now briefly introduced.

Chromatofocusing is a column chromatographic method for separating proteins according to their isoelectric points (143-145). If a buffer, initially adjusted to one pH, is run through an ion exchange column which is initially adjusted to a second pH, a pH gradient is formed just as if two buffers

were gradually mixed in a gradient maker (146). If such a pH gradient is used to elute proteins bound to the ion exchanger, the proteins elute in order of their isoelectric points (147).

In chromatofocusing, the pH gradient is chosen so that the isoelectric points of the proteins of interest fall roughly in the middle of the pH gradient. The appropriate Polybuffer exchanger is then equilibrated with start buffer with a pH set slightly above the upper limit of the pH gradient. The pH of the eluent, Polybuffer, is adjusted to the lower limit of the pH gradient. The sample is equilibrated in eluent and applied to the column. The column is eluted with the Polybuffer and the pH gradient forms automatically. Proteins elute in order of their isoelectric points.

A pH gradient of 5.0-4.0 was chosen for our experiments as determined using IEF electrophoresis. Native and FAA modified GOx samples were equilibrated in eluent and applied to the column. Elution for each GOx sample was recorded using a chart recorder. Figure 3.28 shows the elution charts for native and 100% FAA modified GOx.

It is clear that the elution chart for 100% FAA modified GOx is different to that of native GOx. For native GOx, three closely related peaks are apparent while four separate peaks are observed for 100% FAA modified GOx. It was observed that for 100% FAA modified GOx, fractions collected from the elution of the first peak represented 80% of the total material while for native GOx, over 60% of the total enzyme was collected from elution of the third peak. This indicates that majority of 100% FAA modified GOx has a higher pI values than that of the native GOx. Similar results were obtained for 50% FAA and 25% FAA modified GOx. This is consistent with the pI values for FAA modified GOx samples obtained from IEF gel electrophoresis.

Enzyme fractions for each elution peak in the chromatofocusing experiment for 100% FAA modified GOx was collected at their pIs and

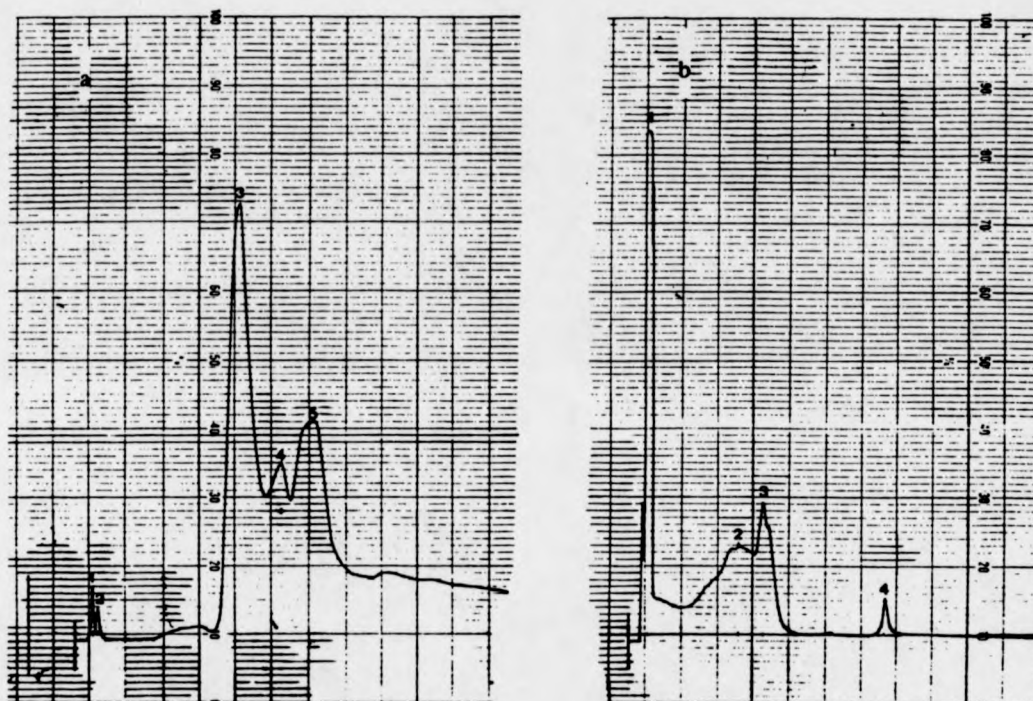


Figure 3.28 Elution charts of chromatofocusing:
 a. native GOx;
 b. 100% FAA modified GOx.
 x - axis: elution volume (5 cm^3 per cm)
 y-axis: OD at 280 nm (0-2.0)

subjected to titration with glucose. Enzyme fraction from peak 3 showed no catalytic activity. Substrate titration for enzyme fractions from peak 1, 2 and 4 are shown in figure 3.29.

Results from figure 3.29 clearly demonstrate that there are three different electroactive enzyme species within the sample of 100% FAA modified GOx. The normalised catalytic currents for enzyme concentration decrease with the reduction in pI values for the enzyme fractions. This indicates that the enzyme fractions from peak 1 of chromatofocusing experiments has highest pI and may contain the largest number of FAA groups compared to the enzyme fractions from peak 2 and peak 4. The iron contents for each enzyme fraction derived from 100% FAA, 50% FAA and 25% FAA modified GOx were determined using atomic absorption spectroscopy. Results of the AAS experiment are given in table 3.11.

Table 3.11 AAS results for enzyme fractions of 100% FAA, 50% FAA and 25% FAA modified GOx

GOx sample	Enzyme fraction from peak no.	Number of FAA groups
100% FAA	1	12*
	2	8
	3	3
	4	6
50% FAA	1	8
	2	2
	3	2
	4	3
25% FAA	1	2
	2	3
	3	2
	4	2

* This number of FAA groups for 100% FAA modified GOx is much lower than the average number of FAA groups for the same modified GOx. The reason for this is unknown at the present.

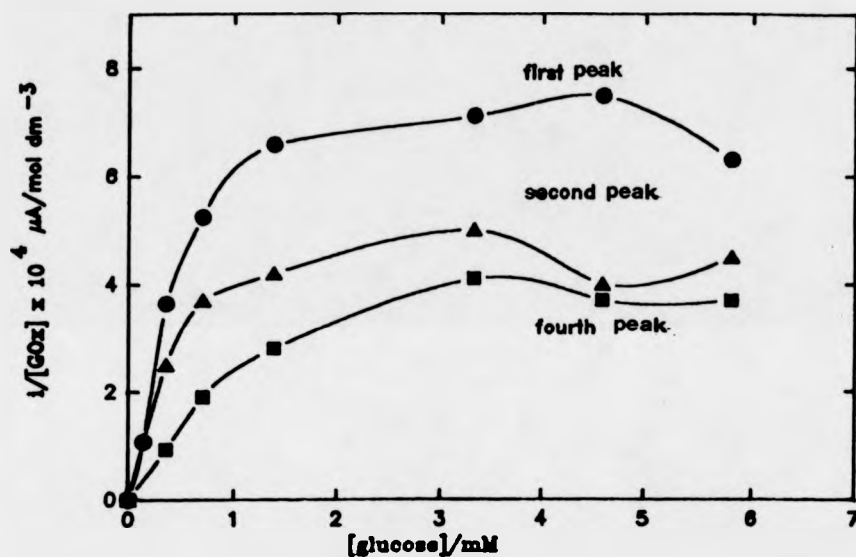


Figure 3.29 Substrate titration curves for different enzyme components of 100% FAA modified GOx isolated using chromatofocusing.
 $[GOx]_1 = 1.9 \times 10^{-5} \text{ mol dm}^{-3}$
 $[GOx]_2 = 4.0 \times 10^{-6} \text{ mol dm}^{-3}$
 $[GOx]_3 = 2.9 \times 10^{-6} \text{ mol dm}^{-3}$
 $[GOx]_4 = 5.4 \times 10^{-6} \text{ mol dm}^{-3}$
 electrode: gold (0.125 cm^2)
 E vs SCE

It is evident that the enzyme fractions from the first peaks contain more FAA groups than that from the second and third peaks. The number of FAA groups for the enzyme fractions from the first peaks are generally equivalent to the average number of FAA relays for the corresponding FAA modified GOx samples. For 100% FAA modified GOx, enzyme fraction from the first peak exhibited the largest catalytic responses in the presence of glucose.

3.8 Conclusions

In this chapter, we have described studies of the electrochemical and catalytic properties of FAA modified GOx either prepared using the literature quantity of FAA or using reduced quantities of FAA. It is clearly demonstrated that the number of FAA groups or relays attached to each GOx molecule can be reduced by decreasing the quantities of FAA used in enzyme modification. The modified GOx samples with fewer FAA groups show lower catalytic currents in the presence of glucose.

The kinetic analysis for FAA modified GOx samples using our model system reveals that: a). the rate limiting step for the catalytic reaction of 100% FAA modified GOx is the enzyme kinetics, and b). for modified GOx samples with fewer FAA groups, the regeneration of enzyme by the attached mediators becomes rate limiting.

Studies of the enzymatic properties of FAA modified GOx samples show that the isoelectric points of modified GOx are higher than that of native GOx. Results from IEF gel electrophoresis also show that each FAA modified GOx sample contains several enzyme species with different pI values. Although a literature report (148) claims that native GOx contains microheterogeneous species of different pI values due mainly to variation in the carbohydrate contents, we observed only one broad band for native GOx but multiple bands for FAA modified GOx on an IEF gel. The multiplicity

of FAA modified GOx samples was further investigated using chromatofocusing chromatography whereby the enzyme species were isolated according to their isoelectric points. Results from chromatofocusing clearly demonstrate that each FAA modified GOx sample has several enzyme species with different pI values and thus number of FAA groups. The enzyme fractions from the first elution peaks for FAA modified GOx samples are the species with the highest pI and the largest number of FAA groups.

In the next chapter, the operational or working stabilities of FAA and FMCA modified GOx are discussed.

CHAPTER IV OPERATIONAL STABILITIES OF COVALENTLY MODIFIED GLUCOSE OXIDASE

In the preceding chapter, we have discussed the enzymatic and electrocatalytic properties of glucose oxidase covalently modified with either FMCA or FAA. In sections of this chapter, our attention is devoted to the studies of the working stabilities (or operational stabilities) of the chemically modified GOx. The studies were carried out by constructing membrane enzyme electrodes with the modified enzyme. The electrochemical responses of the membrane enzyme electrodes in the presence of substrates are reported and the results are analysed using the established theoretical model (117). The stabilities of the membrane electrodes constructed with FMCA and FAA modified GOx are discussed. Results for the study of the stabilities of some oxidised ferrocene derivatives in neutral aqueous buffer solution using bulk electrolysis are presented. The correlation between the stability of the free oxidised ferrocene mediator and the stability of the membrane electrode constructed using the mediator modified GOx is described.

4.1 Introduction

4.1.1 Characteristics of Amperometric Enzyme Electrodes

Amperometric enzyme electrodes are very attractive as chemical sensors since they are selective, cheap and easy to fabricate (77,149). Commonly, an amperometric enzyme electrode is constructed by entrapping a thin layer of enzyme (10-200 μm) close to the electrode surface (24,71). An analyte, usually a substrate of the enzyme reaction, can diffuse freely in and out of the enzyme layer.

A number of amperometric enzyme electrodes of this type have been reported. In these electrodes, the enzyme may be immobilised by electrochemical deposition of a conducting (for example,

poly(pyrrole) (86-87,90) or insulating (for example poly(phenol) (90)) polymer film, by cross-linking the enzyme in a protein matrix (151-152), by gel entrapment (79), or by covalent attachment to a pre-existing polymer film (150) or in our case, by physical entrapment behind a membrane. Electrodes of this type can operate in a number of ways: i) the electrode may be used to detect a product of an enzymatic reaction (34,45), ii) a homogeneous mediator may be used to shuttle charge between the electrode surface and the active sites of the enzyme (61,71), iii) the enzyme may react directly at the electrode surface (102-103,106). The direct reaction of the enzyme at the electrode surface can also be brought about in different ways: i) the enzyme may undergo direct electron transfer at an appropriate electrode surface (such as the conducting organic salt electrodes) (1-4), ii) the electrode surface may be modified by an electron transfer promoter (153), iii) the enzyme itself may be modified by an electron transfer mediator (5-6, 114, 122).

The use of modified enzymes in amperometric electrodes is interesting for a number of reasons. Firstly, it offers the prospect of reagentless biosensors (the term "reagentless" is used as there is no requirement for the presence of molecular oxygen or mediators in the system); secondly, it is well suited for *in vivo* applications since the enzymatic reaction is independent of the presence of a homogeneous mediator; thirdly, since the mediators are covalently attached to the enzyme, problems of toxicity in living systems may be reduced; fourthly, it enables one to study the electron transfer process between the enzyme and the electrode.

In order to produce a viable enzyme electrode the modified enzyme must be stable. The stabilities of the modified enzymes were assessed by studying the rate of decay of the limiting currents of the membrane enzyme electrodes. The entrapment of the modified enzyme behind a membrane is a good method for the stability studies as only a small quantity of the

modified enzyme is used, thus high sensitivity may be obtained and the enzyme is prevented from being lost to the bulk solution. However, before discussing the working stabilities of the modified enzyme, it is appropriate to summarize its stabilities under various storage conditions.

4.1.2 Storage Stabilities of Covalently Modified GOx

Degani and Heller (5-6) reported measurements of the enzymatic and electrochemical activity of the chemically modified enzyme as a function of time by incubating these in 30 mmol dm⁻³ glucose. Their results have already been reviewed in section 3.1.2. The storage stabilities of glucose oxidase modified with ferrocenemonocarboxylic acid, ferroceneacetic acid and ferrocenebutanoic acid, were investigated in detail by R.G. Whitaker (120). His results are described below.

The modified enzyme samples were prepared using the literature method (5-6). Cold stored (2-4 °C) samples were assayed for their enzymic activity over a six day period using the dye-linked spectrophotometric assay method (section 2.4). It was found that, at 4 °C, the FAA modified GOx retained 88% of its original activity after a six day period as opposed to 50% retention for the FMCA modified GOx. There was an initial loss of activity of 30 to 40% over the first two hours for the FMCA modified GOx stored either in buffer solution (85 mmol dm⁻³ phosphate, pH 7.0) at either 4 °C or at room temperature in either the presence or absence of catalase. GOx modified with ferrocenebutanoic was found to be very unstable to storage. It retained less than 10% of its original activity after a six day period at 4 °C. Figure 4.1 shows the comparison of storage stability of FMCA and FAA modified GOx at 4°C and the effect of different storage conditions on the activity of FMCA modified GOx. The stability data are given in Table 4.1.

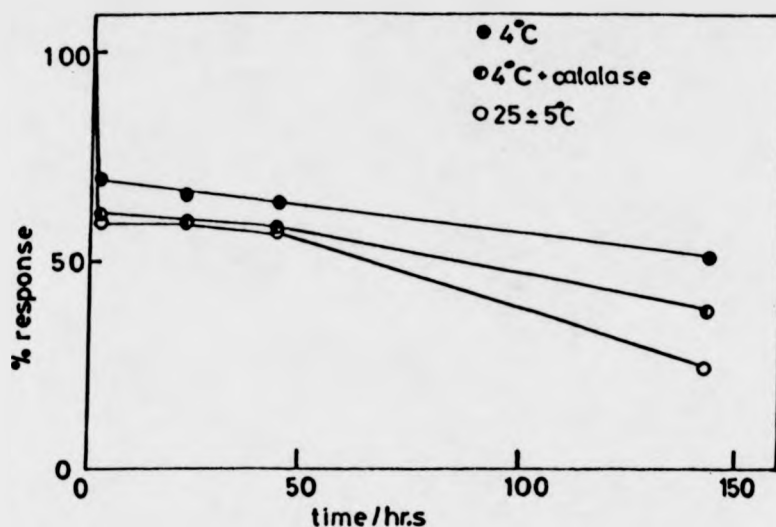


Figure 4.1a The effect of different storage conditions on the activity of the FMCA modified GOx
(Reproduced from PhD thesis, R.G. Whittaker, 1989, University of Warwick)

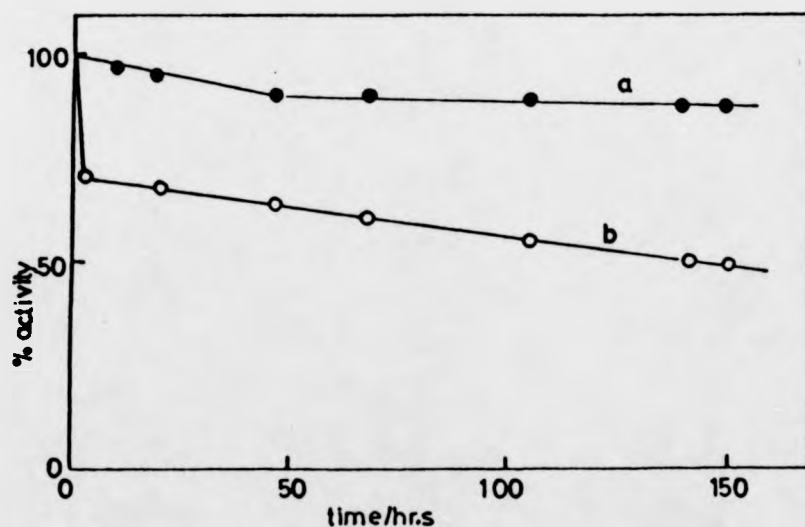


Figure 4.1b Comparison of the storage stability of: a) FAA modified GOx, b) FMCA modified GOx, at 4°C, pH 7.0 under N₂.
(Reproduced from PhD thesis, R.G. Whitaker, 1989 University of Warwick).

Table 4.1 Stability data for ferrocenes modified GOx (at 4 °C, pH 7.0 under N₂).

Enzyme Modifier	% initial activity remaining (10 hrs storage)	% initial activity remaining (150 hrs storage)
Ferrocenemono carboxylic acid	69	49
Ferrocene acetic acid	97	88
Ferrocene butanoic acid	20	< 10

4.1.3 Operational Stability

Whitaker (120) also investigated the stability of the modified enzyme to continuous potential cycling in aqueous solution at saturating substrate concentration, in which the electrochemical responses were measured by d.c. cyclic voltammetry at a glassy carbon electrode and current responses were measured after a period of time. It was found that there appeared to be little difference between the operational stabilities of the FMCA and FAA modified GOx. It was also found that over the first four hours, little activity was lost for either FMCA or FAA modified GOx but around 70% of the responses were lost over the next 25 hours (figure 4.2). This loss of electrochemical response to continuous potential cycling was further investigated in terms of loss of enzyme activity, loss of attached ferrocenes and loss of enzyme FAD co-factors. For the FAA modified GOx, 55% of its initial catalytic activity was retained after 312 hours. The possible loss of FAD was determined by purifying an "aged" sample using gel filtration on sephadex G-25; any free FAD present in solution was measured by recording A₄₅₀ of the column fractions. No detectable loss of FAD was recorded. Atomic adsorption spectroscopic determination of iron contents for the FAA

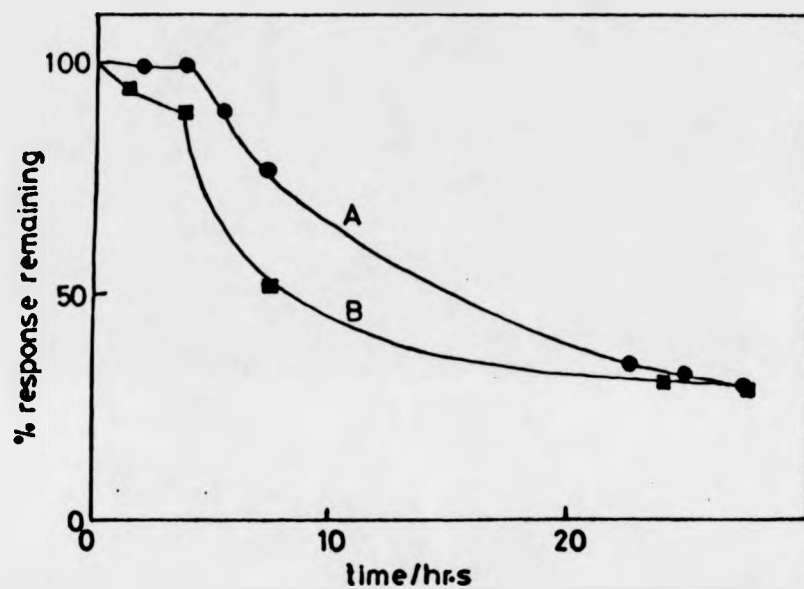


Figure 4.2 Stability of A) FAA modified GOx and B) FMCA modified GOx to continuous potential cycling (5 mV s^{-1} , 20°C) (Reproduced from PhD thesis, R.G. Whitaker, 1989 University of Warwick).

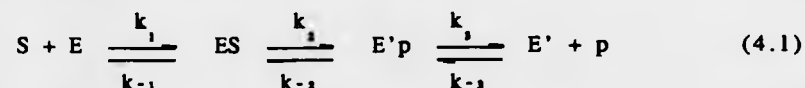
modified GOx sample after a second column purification revealed that the number of FAA molecules per enzyme had decreased from 22 (± 2) (freshly prepared sample) to 6.5 (± 1) (after 312 hrs). These studies indicate that the loss of electrochemical responses of the chemically modified GOx may be due to a combination of the loss of enzymic activity and the loss of ferrocene mediators.

In the remaining parts of this chapter, our results of the stability studies of FMCA and FAA modified GOx using membrane electrodes will be described together with the analysis using the theoretical model (117). The theory is discussed next.

4.2 Theory

A theoretical treatment for amperometric enzyme electrodes has been well established by Albery *et al.* (117). The model is described below.

The model assumes that an enzyme, E, converts one substrate to one product and in the course of the reaction itself is converted to E'. The reaction may be written as:



where S is substrate

P is product.

For each step, the equilibrium constant K_n can be expressed as

$$K_n = k_n/k_{-n} \quad (4.2)$$

where k_n and k_{-n} are rate constants for the forward and backward reaction and $n = 1, 2$ or 3 .

The overall equilibrium constant K_{TD} is written as:

$$K_{TD} = K_1 \cdot K_2 \cdot K_3 \quad (4.3)$$

Diffusion of substrate S and product P through the membrane is described by the mass transfer rate constants k_s' and k_p' .

$$k_s' = D_s K_s / L_m \quad \text{and} \quad (4.4)$$

$$K_p' = D_p K_p / L_m$$

where D_s and D_p are the diffusion coefficients for the substrate and product, K_s and K_p are the partition coefficients of the substrate and product in the membrane, and L_m is the thickness of the membrane.

The electrode reaction has a rate constant k' and is assumed to be irreversible.

Under steady state conditions, the flux j ($\text{mol cm}^{-2} \text{ s}^{-1}$) can be written as:

$$j = k_s' (s_\infty - s_0) \quad (\text{diffusion of substrate}) \quad (4.5)$$

$$= L [k_1 s_0 e - k_{-1} es] \quad (\text{enzyme kinetics}) \quad (4.6)$$

$$= L [k_2 es - k_{-2} e'p] \quad (\text{enzyme kinetics}) \quad (4.7)$$

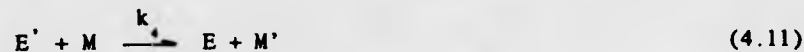
$$= L [k_3 e'p - k_{-3} e'p_0] \quad (\text{enzyme kinetics}) \quad (4.8)$$

$$= k_p' (p_0 - p_\infty) \quad (\text{diffusion of product}) \quad (4.9)$$

$$= k'e' \quad (\text{electrode reaction}) \quad (4.10)$$

The kinetic scheme is given in figure 4.3.

Equation (4.10) is true for the situation where an enzyme is regenerated by direct reaction at the electrode. However, for cases where a mediator is used for enzyme electrodes the enzyme is regenerated by reaction with the mediator. When the mediator is immobilised on the electrode surface then k' in the reaction scheme describes the heterogeneous reaction of the enzyme with the immobilised mediator, thus the same mathematical treatment applies. When a mediator is present throughout the enzyme layer, the enzyme is regenerated by homogeneous reaction with the mediator:



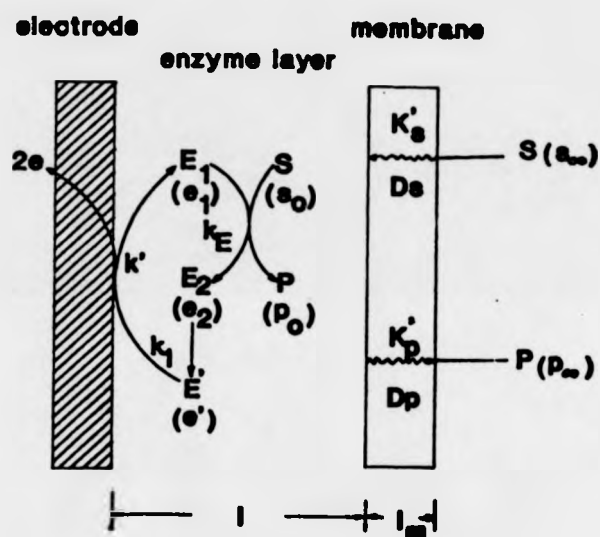


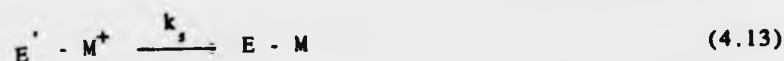
Figure 4.3 Reaction mechanism for an enzyme electrode.



Thus k' is now replaced by $Lk_s m$ and eqn. (4.10) becomes,

$$j = Lk_s m e' \quad (4.12)$$

In the case of modified enzyme, the enzyme is regenerated by the attached mediators:



So k' now describes the reaction between the enzyme E' and the attached mediators, $k' = Lk_s$ and eqn. (4.10) is rewritten as:

$$j = Lk_s e' \quad (4.14)$$

First, we solve the equations (4.5) - (4.10) for the cases where the enzyme is directly converted at the electrode surface then we shall extend the solution to the homogeneous mediation and the modified enzyme cases.

We know the total enzyme concentration, e_Σ , is given by

$$e_\Sigma = e + es + e'p + e' \quad (4.15)$$

Elimination of the enzyme concentrations, e_0 and p_0 from eqns. (4.5)-(4.10), the following expression is obtained.

$$\begin{aligned} \frac{e_\Sigma}{j} = & \left[1 + \frac{j}{k'_s s_\infty} \right] \left[\frac{1}{Lk_{cat}} + \frac{1}{k'} + \frac{K_1^{-1}(1+K_2^{-1})}{k'} \left[p_\infty + \frac{j}{k'_p} \right] \right] \\ & + \frac{1}{s_\infty} \left[\frac{K_M}{Lk_{cat}} + \frac{K_1^{-1} K_2^{-1} K_3^{-1}}{k'} \left[p_\infty + \frac{j}{k'_p} \right] \right] \\ & + \frac{e_\Sigma}{k'_s s_\infty} \end{aligned} \quad (4.16)$$

where $1/k_{cat} = 1/k_s + 1/K_1 k_s + 1/k_2$, and

$$K_M/k_{cat} = 1/k_1 + 1/K_1 k_s + 1/K_1 K_2 k_s$$

In special cases where there is no product inhibition, equation (4.16) can be simplified to give:

$$\frac{s_{\infty}}{j} = \frac{1}{k'_{ME}} \left[1 + \frac{s_{\infty}}{K_{ME}} \left(1 + \frac{j}{k'_s s_{\infty}} \right) \right] \quad (4.17)$$

In this equation, k'_{ME} is the effective electrochemical rate constant for the enzyme electrode at low substrate concentrations,

$$1/k'_{ME} = K_M/(e_{\Sigma} L k_{cat}) + 1/k'_s \quad (4.18)$$

and K_{ME} is the equivalent of the Michaelis constant for the enzyme electrode,

$$K_{ME} = \frac{K_M(Lk_{cat})^{-1} + e_{\Sigma}(k'_s)^{-1}}{(Lk_{cat})^{-1} + (k')^{-1}} \quad (4.19)$$

Thus for the analysis of membrane enzyme electrode data, a plot of s_{∞}/j vs s_{∞} may be constructed. The intercept of this plot, $(s_{\infty}/j)_0$ is the inverse of k'_{ME} . We then introduce new parameters,

$$\rho = [j/s_{\infty}]/[j/s_{\infty}]_0 \leq 1 \quad (4.20)$$

for values of s_{∞}/j significantly greater than $[s_{\infty}/j]_0$, and

$$y = \frac{\rho^{-1} - 1}{s_{\infty}} = \frac{1}{K_{ME}} \left[1 - \frac{\rho k'_{ME}}{k'_s} \right] \quad (4.21)$$

Therefore a plot of y versus ρ can then be used to determine the value of K_{ME} . At $y = 0$, the intercept on ρ axis gives the value of the ratio k'_s/k'_{ME} and at $\rho = 0$, the intercept on y axis gives the value of $1/K_{ME}$. This ratio k'_s/k'_{ME} is important because it indicates which is the rate limiting step in the overall reaction. If the ratio is unity, then the transport of

substrate through the membrane is rate limiting; if the ratio is much less than unity, then the rate limiting step is the unsaturated enzyme kinetics. The stages of the analysis are summarised in table 4.2.

Now we will consider extensions of eqn. (4.16) to cases of homogeneous mediation and modified enzymes.

In most cases of homogeneous mediation, the concentration of M will be sufficiently large so as to remain uniform during the reaction. Thus k' of eqn (4.16) can be replaced by the equivalent rate constant, Lk_m :

$$\frac{e_{\Sigma}}{j} = \left[1 - \frac{j}{k'_s s_{\infty}} \right] \left[\frac{1}{Lk_{cat}} + \frac{1}{Lk_m} + \frac{K_s^{-1}(1+K_s^{-1})}{Lk_m} \left[P_{\infty} + \frac{j}{k'_p} \right] \right] + \frac{1}{s_{\infty}} \left[\frac{K_M}{Lk_{cat}} + \frac{K_s^{-1} K_s^{-1} K_s^{-1}}{Lk_m} \left[P_{\infty} + \frac{j}{k'_p} \right] \right] + \frac{e_{\Sigma}}{k'_s s_{\infty}} \quad (4.22)$$

A similar solution may be applied to the case of modified enzyme where k' becomes equivalent to the rate constant, Lk_s , describing the enzyme mediator reaction:

$$\frac{e_{\Sigma}}{j} = \left[1 - \frac{j}{k'_s s_{\infty}} \right] \left[\frac{1}{Lk_{cat}} + \frac{1}{Lk_s} + \frac{K_s^{-1}(1+K_s^{-1})}{Lk_s} \left[P_{\infty} + \frac{j}{k'_p} \right] \right] + \frac{1}{s_{\infty}} \left[\frac{K_M}{Lk_{cat}} + \frac{K_s^{-1} K_s^{-1} K_s^{-1}}{Lk_s} \left[P_{\infty} + \frac{j}{k'_p} \right] \right] + \frac{e_{\Sigma}}{k'_s s_{\infty}} \quad (4.23)$$

Discussions of eqn. (4.16) above may also apply to equations (4.22) and (4.23).

Table 4.2 Summary of the analysis of data for membrane enzyme electrodes.

-
1. Plot of s_{∞}/i vs s_{∞} ; where s_{∞} is the bulk substrate concentration and i is the current (corrected for any background current).
 2. Extrapolate the curve to estimate the intercept on the s_{∞}/i axis at $s_{\infty} = 0$. $[s_{\infty}/i]_0 = 1/nFAk_{ME}'$
 3. Use the data for the values of s_{∞}/i significantly greater than $[s_{\infty}/i]_0$ to calculate values of the dimensionless ratio: $\rho = [i/s_{\infty}]/[i/s_{\infty}]_0$.
 4. Calculate values of y where $y = (\rho^{-1} - 1)/s_{\infty}$.
 5. Plot y against ρ . This should give a straight line with a slope of $-k'_{ME}/(k'_s K_{ME})$, an intercept on the y -axis of $1/K_{ME}$, and an intercept on the ρ -axis of k'_s/k'_{ME} .
 6. From the plots calculate the values of K_{ME} , k'_{ME} and k'_s .
-

In the remaining sections of this chapter, this theoretical treatment will be employed to analyse our experimental results.

4.3 Membrane Enzyme Electrodes Based on Native Glucose Oxidase

In this section, the determination of the rate of transport of substrate through the membrane, expressed by the rate constant k'_s (cm s^{-1}) will be described. Since the diffusion of substrate through the membrane will remain constant for the same type of membrane, under the same experimental conditions, the rate constant k'_s can be used in our later analysis of the enzyme membrane electrodes based on the modified enzymes.

Typically, a membrane enzyme electrode was constructed using native GOx (0.12 mg) with FMCA (1 mmol dm^{-3}) present in the bulk solution as the homogeneous mediator. The response of the membrane enzyme electrodes to the additions of aliquots glucose were recorded. Typical results are shown in figure 4.4.

Following the theoretical model, a plot of s_∞/i versus s_∞ (figure 4.5) was constructed. From the intercept, we obtain,

$$[s_\infty/i]_0 = 1/nFAk'_{ME} = 0.72 \text{ mmol dm}^{-3}/\mu\text{A}$$

where n is the number of electrons transferred and $n=2$ for this reaction,

F is the Faraday,

A is the electrode area and, $A = 0.125 \text{ cm}^2$.

Thus a value of k'_{ME} is obtained as:

$$k'_{ME} = 5.8. \times 10^{-4} \text{ cm s}^{-1}$$

the parameters p and y were then calculated according to equations (4.20) and (4.21), and y was plotted against p , figure 4.6.

Again the intercept on p -axis and the intercept on y -axis were estimated.

Intercept on p -axis = 0.78 and

Intercept on y -axis = $0.0134 \text{ mmol}^{-1} \text{ dm}^3$

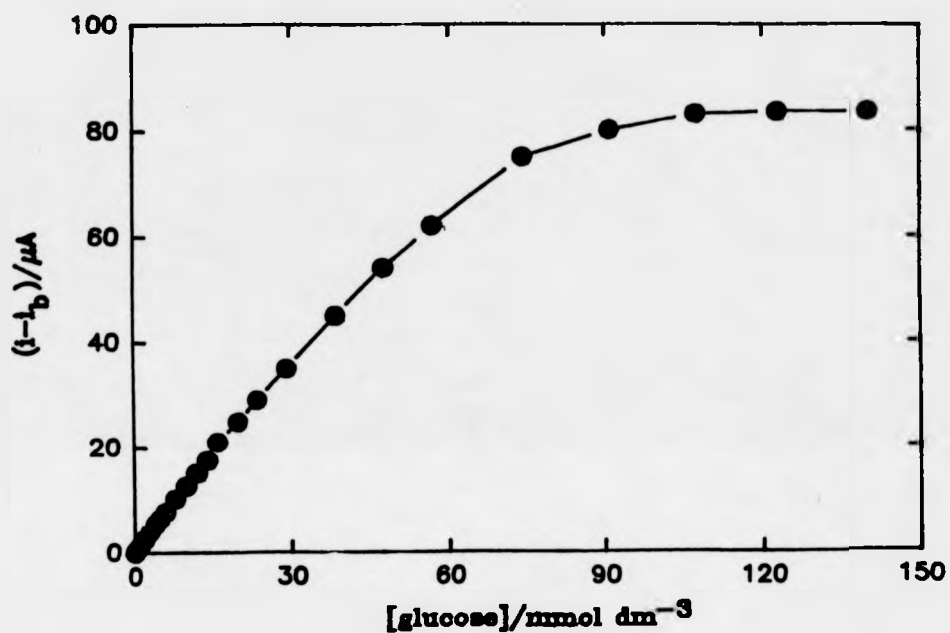


Figure 4.4 Substrate titration curve for the membrane enzyme electrode based on native GOx(0.12 mg) with $1\ mmol\ dm^{-3}$ FMCA present in the bulk solution.
 E 0.508 Volts vs SCE
 A $0.125\ cm^2$

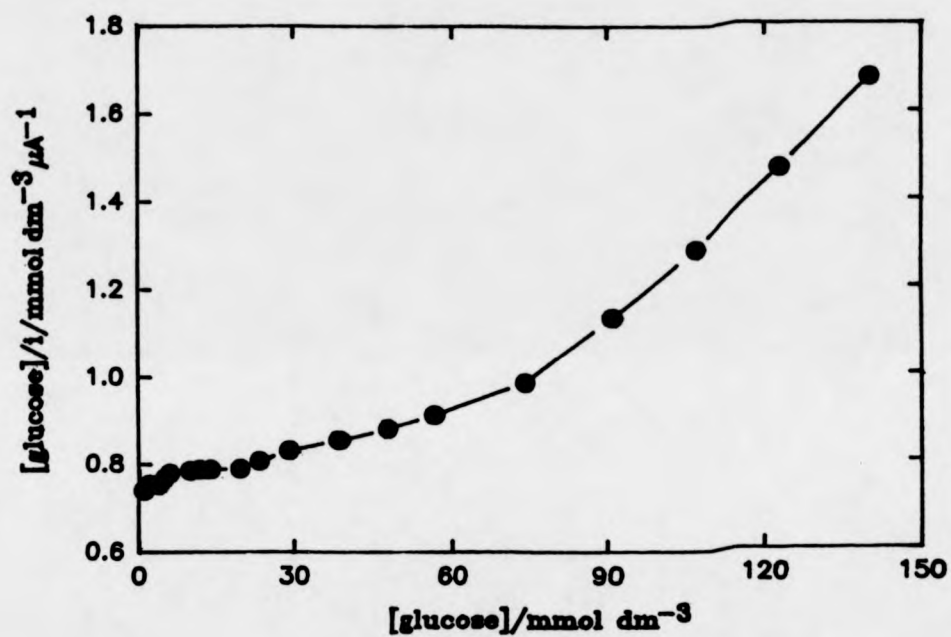


Figure 4.5 Plot of s_{∞}/i (mmol dm⁻³/μA) vs s_{∞} (mmol dm⁻³)
for the membrane enzyme electrode based on
native GOx(0.12 mg)
A 0.125 cm²
E 0.508 Volts vs SCE

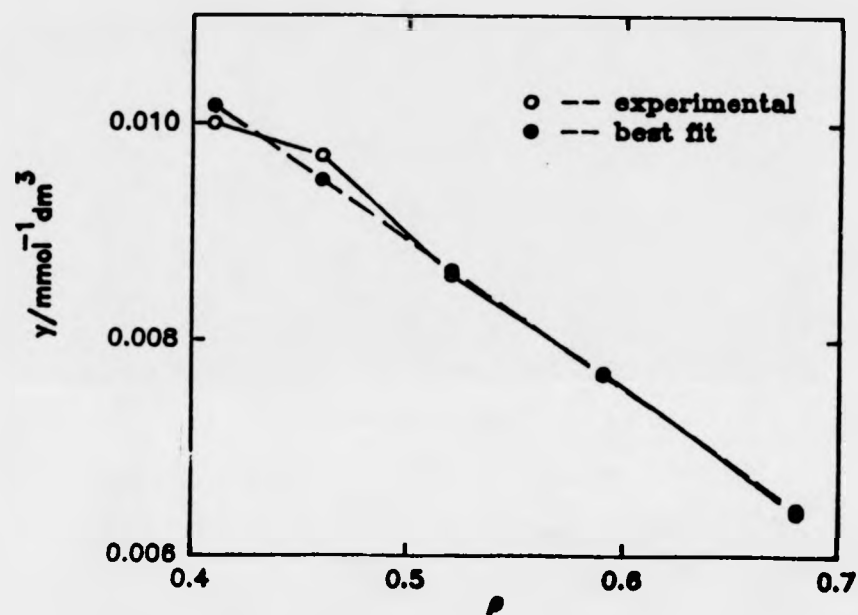


Figure 4.6 Plot of y ($\text{mmol}^{-1} \text{dm}^3$) vs p for the membrane enzyme electrode based on native GOx (0.12 mg).

Thus $K_{ME} = 1/\text{intercept on y-axis} = 75 \text{ mmol dm}^{-3}$

The intercept on p-axis is the ratio between the effective electrochemical rate constant k'_{ME} , for the enzyme electrode at low substrate concentrations and the mass transport rate constant k'_s , for the substrate diffusion through the membrane.

Thus $k'_{ME}/k'_s = 0.78$

Using the value of k'_{ME} obtained above,

$k'_s = 7.4 \times 10^{-5} \text{ cm s}^{-1}$, which is in good agreement with the value reported in the literature (117).

From the analysis, it is found that at low glucose concentrations, the response is determined by the diffusion of glucose through the membrane. At high glucose concentrations, the response reaches a plateau, limited either by the rate of reaction between enzyme and mediator or by the enzyme kinetics. In figure 4.7, the responses of this membrane enzyme electrode based on native GOx are plotted against the FMCA concentrations in the bulk solution at a saturated glucose concentration. It is apparent that, at low FMCA concentration ($< 0.5 \text{ mmol dm}^{-3}$) the current depends on the mediator concentration and thus reaction of the mediator with the enzyme is the rate limiting factor. At high FMCA concentrations ($> 0.5 \text{ mmol dm}^{-3}$), the current is limited by the saturated enzyme kinetics. Since substrate titrations for membrane enzyme electrode were carried out at high FMCA concentration (1 mmol dm^{-3}) we conclude that, at high glucose concentrations, the enzyme kinetics is the rate limiting step.

4.4 Membrane Enzyme Electrodes Based on FMCA Modified GOx

Studies from the membrane enzyme electrodes using native GOx showed encouraging results for this type of amperometric enzyme electrode. In particular, it is pleasing that the results are reproducible and the response time is fast, usually less than 10 seconds upon addition of substrate.

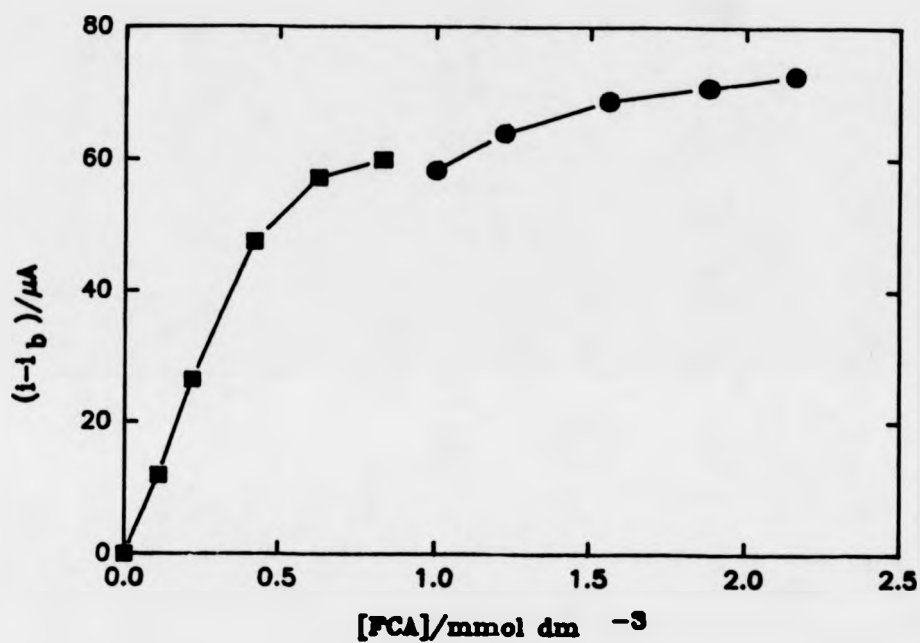


Figure 4.7 Plot of the current, corrected for background (0.16μA) as a function of the concentration of ferrocenemonocarboxylic acid added to the bulk solution for a membrane enzyme electrode based on native GOx (0.15 mg) placed in 0.11 mol dm⁻³ glucose.

Following the success of the covalent modification of the enzyme with ferrocenemonocarboxylic acid (FMCA), we have now employed this FMCA modified GOx to construct membrane enzyme electrodes. As stated in the previous chapter, the covalently modified GOx undergoes direct oxidation at simple, or bare metallic electrode surfaces, and the membrane enzyme electrode constructed with this FMCA modified GOx offers a real prospect of producing reagentless biosensors. Studies of the membrane enzyme electrodes with different modified enzyme loadings are presented together with the kinetic analysis using the theoretical model. The stabilities of these enzyme electrodes are discussed.

4.4.1 Electrochemical Responses

Samples of FMCA modified GOx were prepared and purified using the method reported by Degani and Heller (5-6). Membrane enzyme electrodes were constructed with the FMCA modified GOx sample following the method described previously in section 2.7. Five different enzyme loadings were used for these membrane electrodes. Table 4.3 gives the values of enzyme loadings for two batches of membrane enzyme electrodes prepared from two batches of FMCA modified enzymes.

Table 4.3 Values of enzyme loadings for FMCA modified GOx membrane enzyme electrodes.

Electrode	Surface Area (cm ²)	Enzyme loading (mg)
Batch I		
E--1	0.125	0.08
E--2	0.124	0.12
E--3	0.122	0.16
E--4	0.126	0.20
E--6	0.125	0.24
Batch II		
E--2	0.124	0.06
E--3	0.122	0.08
E--4	0.126	0.11
E--5	0.127	0.14
E--6	0.125	0.17

The prepared membrane enzyme electrodes were pretreated by equilibrating in a neutral aqueous buffer solution (0.085 mol dm⁻³ sodium phosphate, pH 7.0) at room temperature for 30 minutes followed by equilibrating in the same buffer solution (deoxygenated) while holding the electrode at FMCA oxidising potential (0.50 Volts vs SCE) until a stable background current was obtained for each electrode. The electrochemical equilibrium process took approximately 20 minutes. The catalytic responses of these FMCA modified GOx membrane enzyme electrodes to additions of substrate were recorded using chronoamperometry with the potential held at 0.50 Volts vs SCE throughout. Typical results of substrate titration for the two batches of the membrane enzyme electrodes based on FMCA modified GOx are shown in figures 4.8 and 4.9.

We again carried out analysis using the theoretical model by first constructing s_{∞}/i versus s_{∞} plots (figures 4.10 and 4.11) for each membrane enzyme electrode. From the intercepts of these s_{∞}/i versus s_{∞} plots, the values of k'_{ME} , the effective rate constants for the enzyme electrodes, were obtained. In table 4.4, values of the intercepts and the k'_{ME} values for the two batches of the membrane enzyme electrodes based on FMCA modified GOx are collected together.

Table 4.4 Values of $[s_{\infty}/i]_0$ and k'_{ME} for the FMCA modified GOx membrane enzyme electrodes.

Electrode	$[s_{\infty}/i]_0$ (mmol dm ⁻³ μ A ⁻¹)	k'_{ME} (cm s ⁻¹)
Batch I		
E--1	40.0	1.0×10^{-6}
E--2	10.8	3.9×10^{-6}
E--3	60.8	0.7×10^{-6}
E--4	9.0	4.6×10^{-6}
Batch II		
E--2	27.8	1.5×10^{-6}
E--3	8.1	5.2×10^{-6}
E--4	55.6	0.7×10^{-6}
E--5	26.9	1.5×10^{-6}

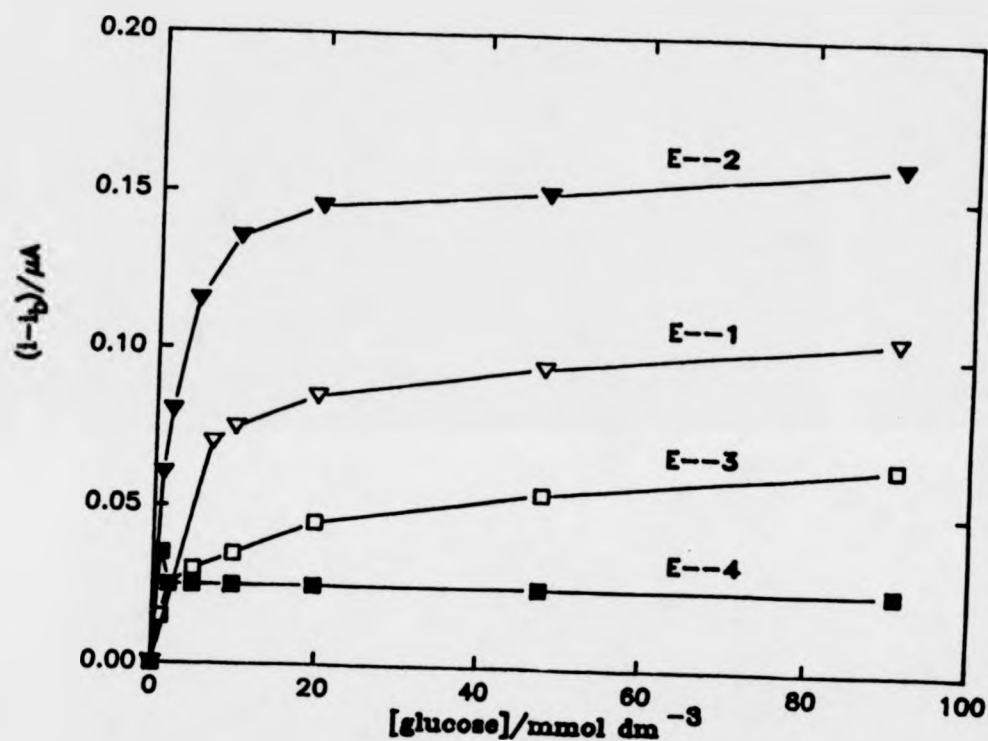


Figure 4.8 Substrate titration curves for Batch I of the FMCA modified GOx membrane enzyme electrodes.
 E 0.50 volts vs SCE
 Enzyme loadings and electrode surface areas are given in table 4.3
 Background currents for the electrodes:
 $i_{b1} = 1.25 \times 10^{-3} \mu A$, $i_{b2} = 0.02 \mu A$,
 $i_{b3} = 0.035 \mu A$, $i_{b4} = 0.085 \mu A$.

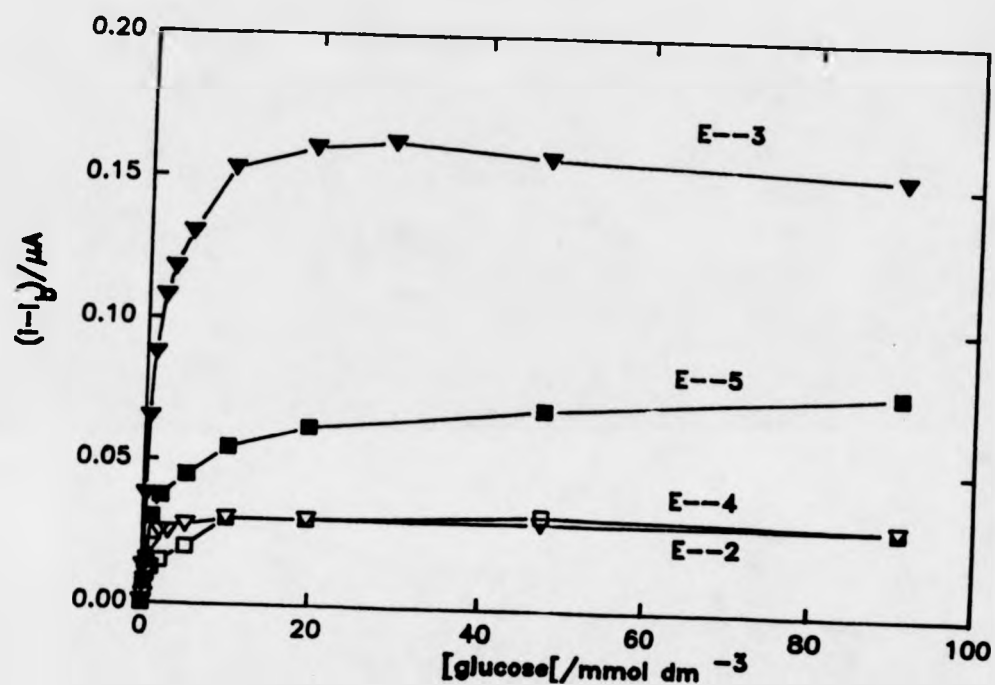


Figure 4.9 Substrate titration curves for Batch II of the FMCA modified GOx membrane enzyme electrodes.
 E 0.50 Volts vs SCE
 Enzyme loadings and electrode surface areas are given in table 4.3
 Background currents for the electrodes:
 $i_{b_1} = 7.25 \times 10^{-3} \mu A$, $i_{b_2} = 0.0225 \mu A$,
 $i_{b_3} = 0.085 \mu A$, $i_{b_4} = 0.015 \mu A$.

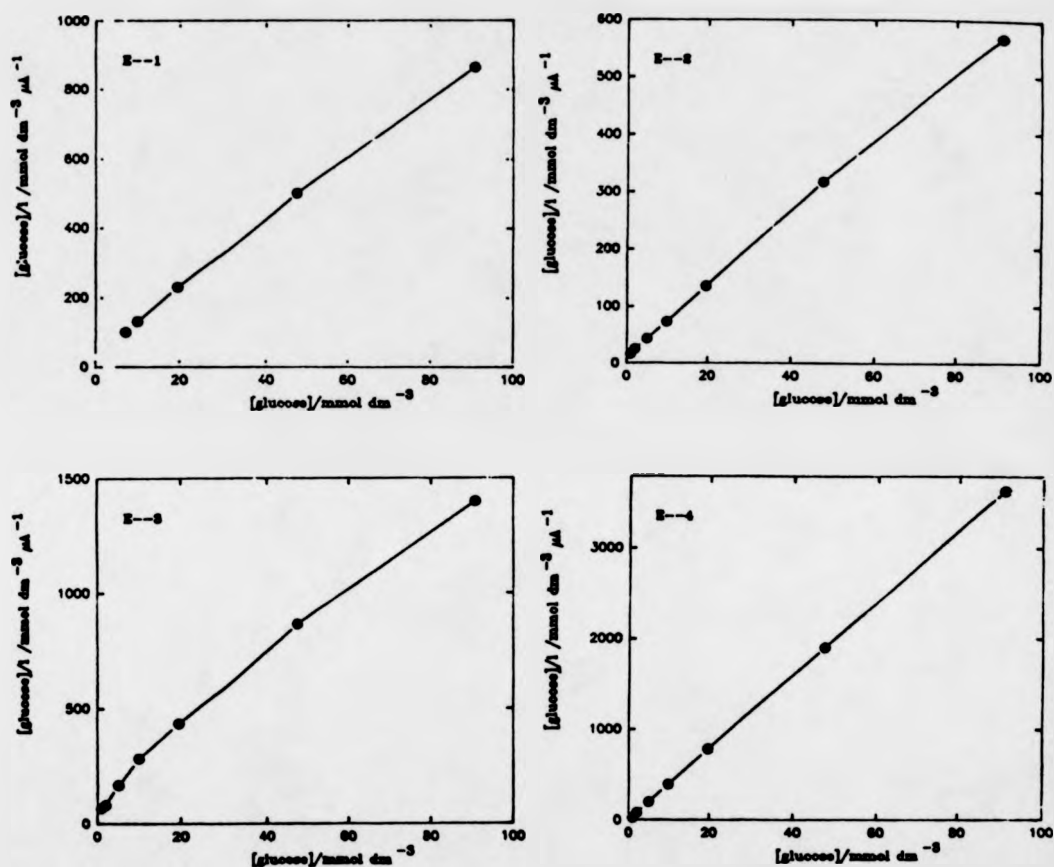


Figure 4.10 s_{∞}/i vs s_{∞} plots for Batch I of the FMCA modified GOx membrane enzyme electrodes. Enzyme loadings and electrode surface areas are listed in table 4.3

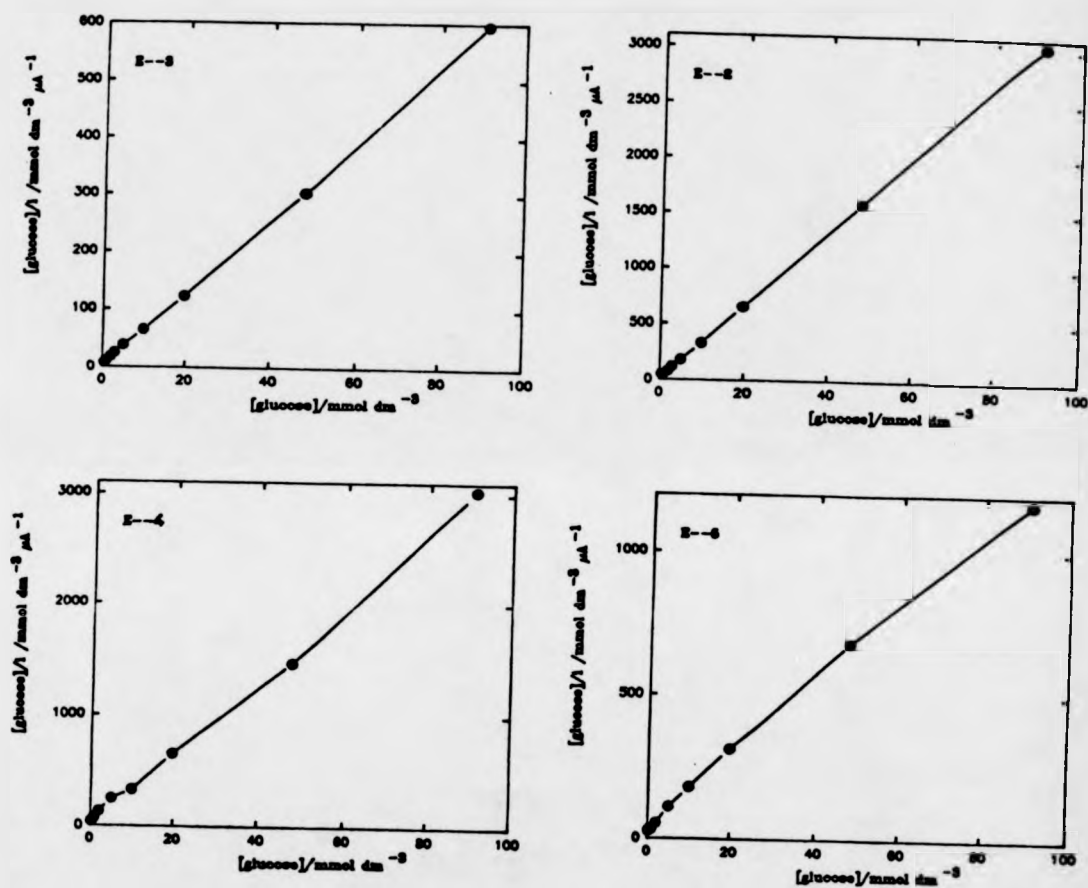


Figure 4.11 s_{∞}/i vs s_{∞} plots for Batch II of the FMCA modified GOx membrane enzyme electrodes
Enzyme loadings and electrode surface areas are listed in table 4.3

Following the steps of analysis described by the model, we now calculated values of y and p using the values of $[S_\infty/i]_0$ obtained above. A series of y versus p diagnostic plots were then constructed (figures 4.12 and 4.13). These y/p plots for both batches of the FMCA modified GOx membrane enzyme electrodes are horizontal lines, corresponding to infinite intercepts on the p -axis. From the model, it is obvious that the unsaturated enzyme kinetics are rate limiting. Values of K_{ME} , the constant similar to the Michaelis constant in homogeneous enzyme kinetics, were then derived from the intercepts on the y -axis.

The true Michaelis constant K_M and the enzyme turn-over number k_{cat} for the FMCA modified GOx may be obtained from the expressions for K_{ME} (eqn. 4.19) and k'_{ME} (eqn. 4.18); where

$$K_{ME} = \frac{K_M(Lk_{cat})^{-1} + e_\Sigma(k'_s)^{-1}}{(Lk_{cat})^{-1} + (k')^{-1}} \quad \text{and}$$

$$1/k'_{ME} = K_M(Lk_{cat})^{-1} + (k'_s)^{-1}$$

The function of K_{ME} is similar to that of the Michaelis constant in homogeneous enzyme kinetics. Thus, for concentrations smaller than K_{ME} the system is unsaturated, the current is proportional to the substrate concentration and the reaction is ruled by the rate constant k'_{ME} . For concentrations greater than K_{ME} , the system becomes saturated. The maximum flux may be characterised by the equivalent of k_{cat} :

$$(k'_{cat,E})^{-1} = (Lk_{cat})^{-1} + (k')^{-1} = e_\Sigma/j_{max} \quad (4.24)$$

where $k'_{cat,E}$ has the dimensions of cm s^{-1} .

This observed $k'_{cat,E}$ is either determined by the enzyme kinetics or by the electrochemical rate constant k' , describing the regeneration of the mediators.

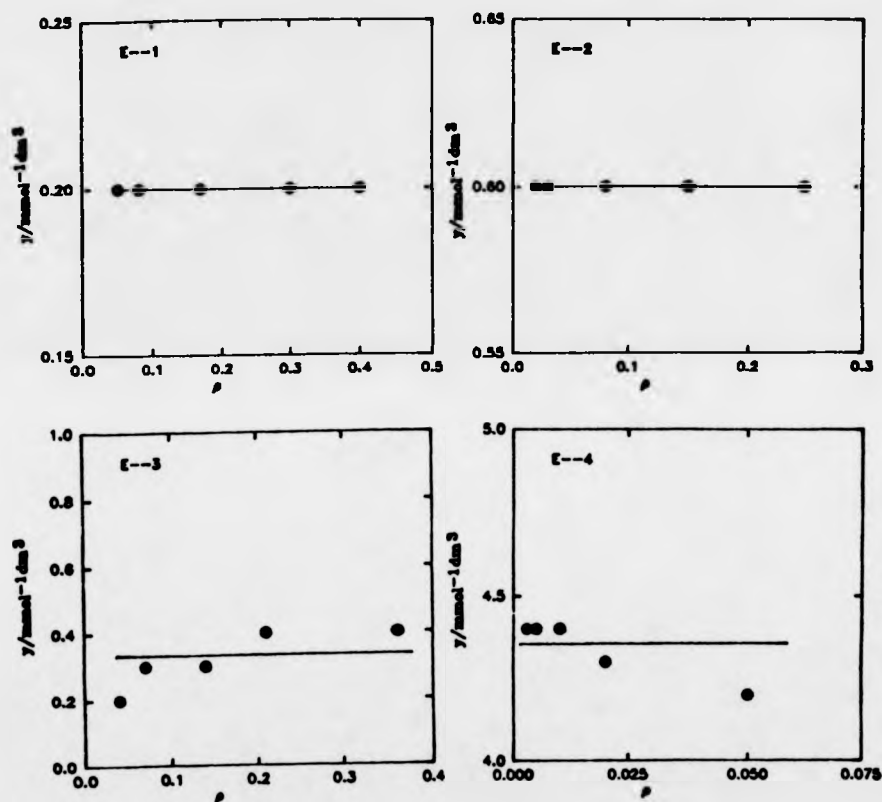


Figure 4.12 Plots of y (mmol⁻¹ dm³) vs p for Batch I of the FMCA modified membrane enzyme electrodes

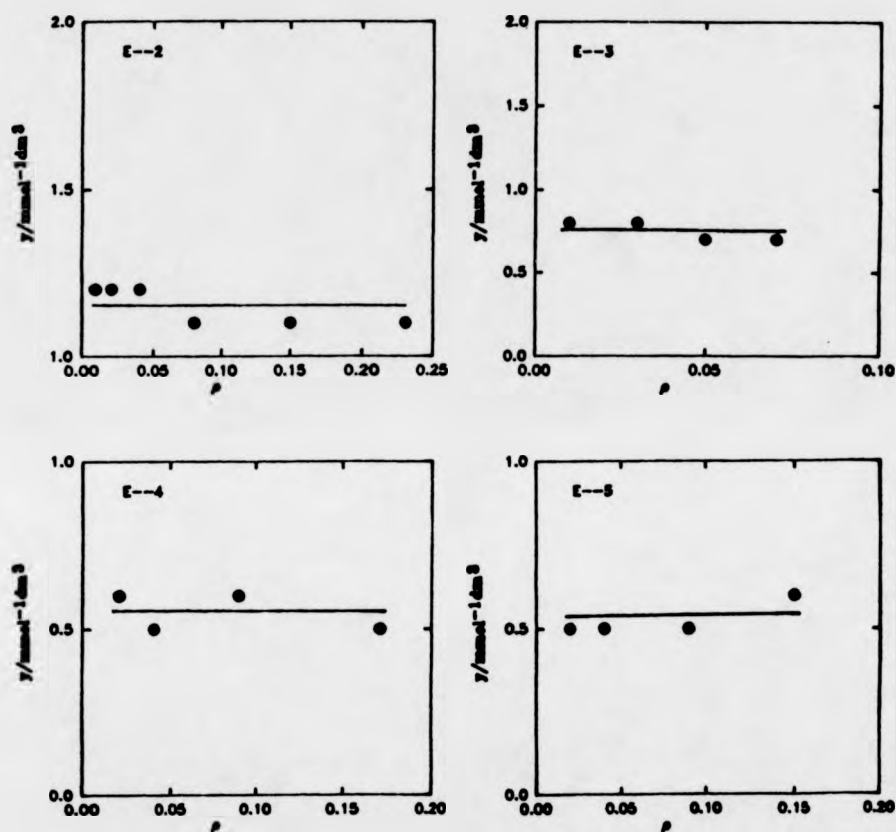


Figure 4.13 Plots of y (nmol⁻¹ dm³) vs p for Batch II of the FMCA modified membrane enzyme electrodes

From our discussions of the results for the membrane enzyme electrodes based on FMCA modified GOx, we can conclude that the enzyme kinetics are rate limiting. Thus, if we assume that all the enzymes entrapped behind the membrane are enzymically active, an approximation of $(Lk_{cat})^{-1} \gg (k')^{-1}$ may be made. We can now rearrange the expression for K_{ME} ,

$$K_{ME} = \frac{K_M(Lk_{cat})^{-1} + e_{\Sigma}k'_s)^{-1}}{(Lk_{cat})^{-1}} \quad (4.25)$$

and

$$K_{ME} = K_M + e_{\Sigma}(Lk_{cat}/k'_s) \quad (4.26)$$

Since e_{Σ} is the total enzyme concentration within the enzyme layer, $e_{\Sigma} \cdot L$ may be expressed by the total quantity of enzyme within the enzyme layer:

$$e_{\Sigma} \cdot L = e_{\Sigma} \cdot \frac{V}{A} \quad (4.27)$$

where V is the total volume of the enzyme layer,

A is the total surface area of the electrode (electrode and the surrounding mantle, 0.785 cm^2)

Eqn. (4.27) can be further written as:

$$e_{\Sigma} \cdot L = E/A \quad (4.28)$$

where E is the total enzyme quantity within the enzyme layer and E is equivalent to the values of enzyme loadings for each membrane enzyme electrode.

Thus the expressions for K_M and k_{cat} are derived:

$$K_M = K_{ME} \left(1 - \frac{k'_{ME}}{k'_s} \right) \quad (4.29)$$

$$k_{cat} = K_{ME} \cdot k'_{ME} \cdot A/E \quad (4.30)$$

The values of K_M and k_{cat} for the two batches of membrane enzyme electrodes using FMCA modified GOx are calculated and the results are given in table 4.5.

Table 4.5 Values of K_{ME} , K_M and k_{cat} for two batches of membrane enzyme electrodes using FMCA modified GOx

Electrode	K_{ME} (mmol dm ⁻³)	K_M (mmol dm ⁻³)	k_{cat} (s ⁻¹)
Batch I			
E--1	5.0	4.9	0.009
E--2	1.7	1.6	0.008
E--3	3.0	3.0	0.002
E--4	0.2	0.2	0.001
Batch II			
E--2	0.9	0.9	0.002
E--3	1.3	1.2	0.002
E--4	1.8	1.8	0.002
E--5	2.0	2.0	0.002

Values of K_M are in the same order of magnitude as that measured in homogeneous solution (1 mmol dm⁻³) (122) but the values of k_{cat} are much smaller than the value of 5 s⁻¹ for homogeneous mediation (122). The reason for obtaining these incredibly low k_{cat} values could be due to

- over estimation of the active enzyme loading, it is possible that much of the FMCA modified GOx becomes inactive during the preparation of the electrode;
- loss of the covalently attached mediators. We shall discuss these points in the next section where the operational stabilities of these FMCA modified GOx membrane enzyme electrodes are described

4.4.2 Operational Stabilities of the Membrane Enzyme Electrodes Based on FMCA Modified GOx

In order to assess the suitability of the chemically modified GOx for

use in sensor devices we investigated their stability in operation. The studies were carried out by comparing the catalytic responses of a freshly prepared membrane electrode with that of the same electrode 20 minutes after the initial measurements. The results show that 98% of the catalytic activity was lost from the membrane electrode (figure 4.14, curve a, b). However, when 1 mmol dm^{-3} of FMCA was added to the bulk solution and the same membrane enzyme electrode was employed for substrate titration, large catalytic responses were observed (figure 4.14, curve c). These large responses are comparable to the responses observed for the membrane enzyme electrodes based on native GOx. This large catalytic response for the membrane enzyme electrode in the presence of a homogeneous mediator indicates that the poor electrode stability is not due to the loss of enzymic activity of the entrapped modified enzyme but possibly due to the loss of the covalently bound mediators.

In figure 4.15, the catalytic responses for a batch of freshly prepared FMCA modified GOx membrane enzyme electrodes (group plots A) are shown to increase significantly when 1 mmol dm^{-3} FMCA was present in the bulk solution (group plots B). These results further demonstrate that the catalytic responses of these membrane enzyme electrodes constructed with FMCA modified GOx were limited by the rate of reoxidation of the reduced enzyme by the covalently attached mediator molecules.

Again the theory for amperometric enzyme electrodes was applied to analyse the results and the values of k'_{ME} and K_{ME} for these electrodes were obtained (table 4.6).

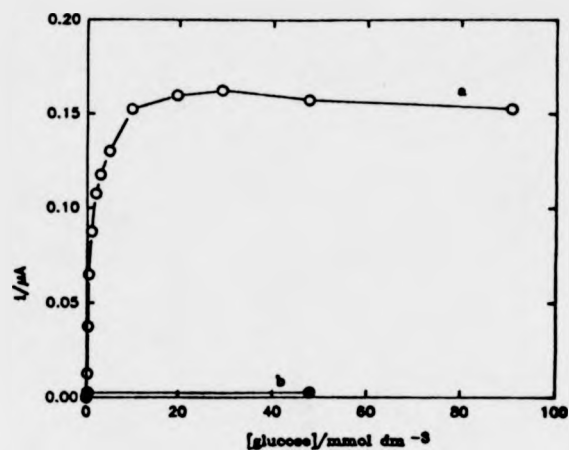


Figure 4.14A Calibration curves of membrane enzyme electrode based on FMCA modified GOx(0.08 mg).
 Curve a -- freshly prepared,
 Curve b -- 20 minutes after the initial measurements.
 E: 0.50 Volts vs SCE

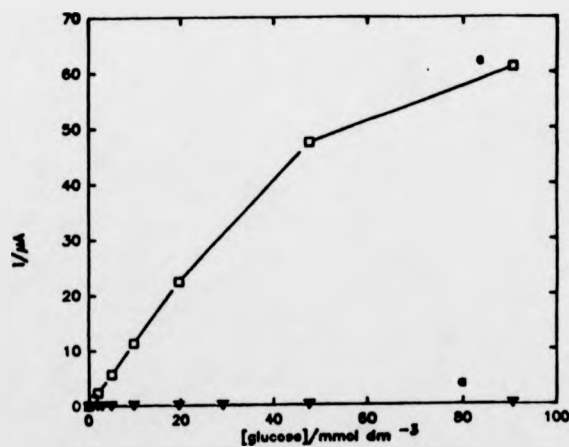


Figure 4.14B Calibration curves of membrane enzyme electrode based on FMCA modified GOx (0.08 mg).
 Curve a -- freshly prepared, curve c -- the same electrode but with 1 mmol dm⁻³ FMCA present in the bulk.
 E: 0.50 Volts vs SCE

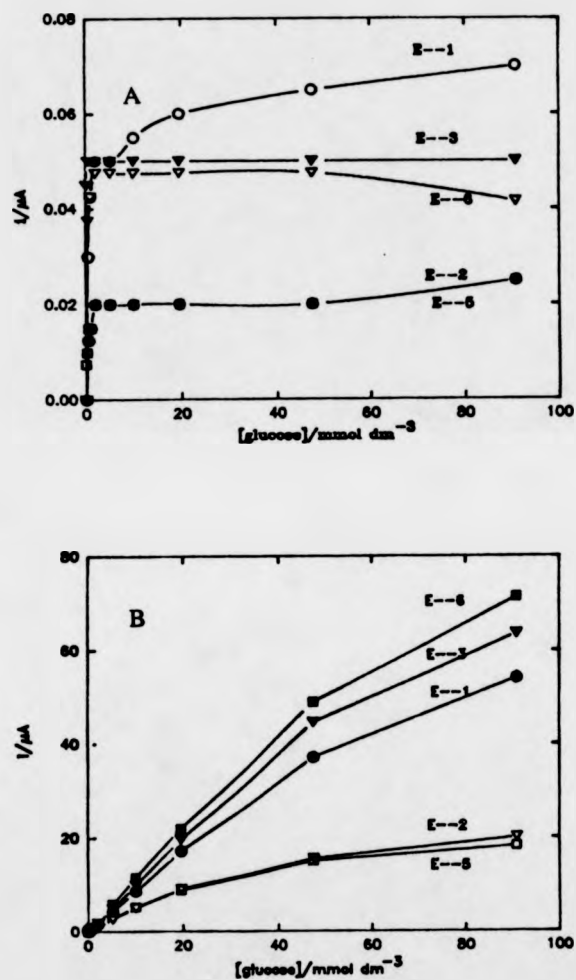


Figure 4.15 Calibration curves for Batch III of the membrane enzyme electrodes based on FMCA modified GOx
 Group plots A -- in the absence of 1.0 mmol dm⁻³ FMCA, Group plots B -- in the presence of 1.0 mmol dm⁻³ FMCA
 E: 0.50 Volts vsSCE
 Enzyme loadings: E--1, 0.04 mg; E--2, 0.06 mg;
 E--3, 0.08 mg; E--5, 0.10 mg;
 E--6, 0.12 mg.

Table 4.6 Results of batch III of the FMCA modified GOx membrane enzyme electrodes in the presence and absence of 1 mmol dm⁻³ FMCA.

Enzyme loading (mg)		k'_{ME} (cm s ⁻¹)	K_{ME} (mmol dm ⁻³)
with no FMCA in the bulk			
E--1	0.04	2.8×10^{-6}	1.1
E--2	0.06	2.8×10^{-6}	0.3
E--3	0.08	4.3×10^{-6}	0.5
E--4	0.10	4.1×10^{-6}	0.2
with 1 mmol dm ⁻³ FMCA present in bulk			
E--1	0.04	3.7×10^{-5}	87.0
E--2	0.06	2.5×10^{-5}	14.3
E--3	0.08	4.3×10^{-5}	83.3
E--4	0.10	2.3×10^{-5}	52.1
E--6	0.12	4.9×10^{-5}	105.0

From the table, it is obvious that values of k'_{ME} and K_{ME} both increased significantly for the same membrane enzyme electrodes once free mediator had been added to the bulk solution. Results for these membrane enzyme electrodes in the presence FMCA (1 mmol dm⁻³) are found to be comparable to the parameters obtained for native GOx membrane enzyme electrodes ($k'_s = 7.4 \times 10^{-5}$ cm s⁻¹ and $K_{ME} = 75$ mmol dm⁻³). Results from table 4.6 clearly show that firstly, the FMCA modified enzymes in the membrane enzyme electrodes retained most of the enzymic activity under the experimental conditions; secondly, the limiting currents of these membrane enzyme electrodes using FMCA modified GOx were governed by the rate of mediator-enzyme reaction.

It was observed that the instability of these FMCA modified GOx membrane enzyme electrodes was more marked when the electrode was held at a potential where the FMCA was oxidised. This observation indicates that the oxidised form of FMCA, the ferricinium form, may be the more unstable species. The decay of the current as a function of time for a FMCA modified GOx membrane electrode was recorded in the presence of 91 mmol dm⁻³ glucose (figure 4.16). The results show that the current

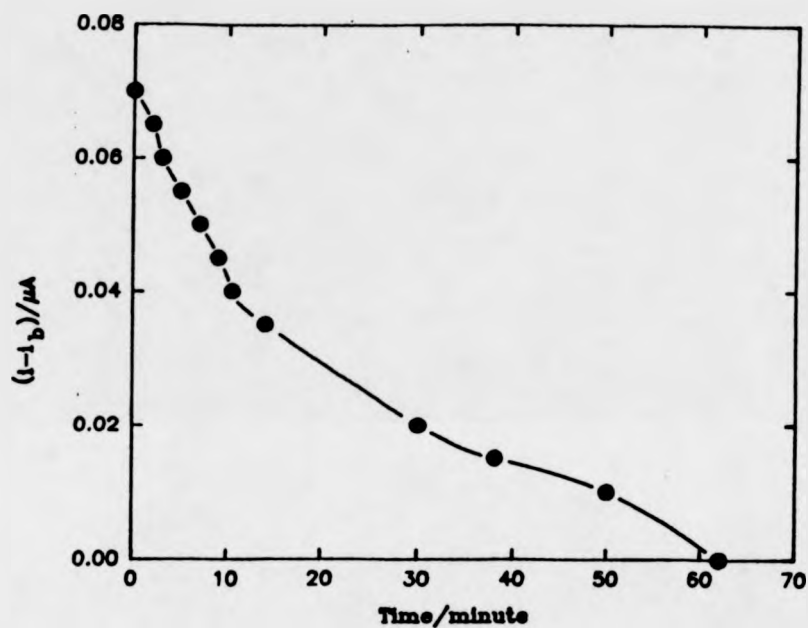


Figure 4.16 Decrease of catalytic current as a function of time for a membrane enzyme electrode based on FMCA modified GOx (0.06 mg) in $90.9 \text{ mmol dm}^{-3}$ glucose.
 Electrode surface area: 0.125 cm^2
 E: 0.50 Volts vs SCE
 Background current: $0.19 \mu A$

decreases in an approximately exponential manner. The half life of the FMCA modified GOx membrane enzyme electrode was estimated from the data and found to be of the order of 20 minutes. This value for half life of the FMCA modified GOx membrane enzyme electrode is in good agreement with the reported value of half life for oxidised FMCA in neutral aqueous buffer solution determined by bulk electrolysis (115). This strongly supports our previous statement that the instability of the FMCA modified GOx membrane enzyme electrodes may be due mainly to the instability of the oxidised FMCA, the ferricinium species.

In the next section, results for membrane enzyme electrodes using FAA modified GOx are presented.

4.5 Membrane Enzyme Electrodes Based on FAA Modified GOx

Above we discussed the stability of the membrane enzyme electrodes constructed with samples of FMCA modified GOx. The results indicate that the instability of these electrodes is not due to the loss of enzymic activity but rather to the loss of the covalently bound mediators. Since FAA is a more stable mediator (115) and the modification of GOx with FAA has been successfully carried out (6), we investigated the use of FAA modified GOx to prepare membrane enzyme electrodes.

4.5.1 *Electrochemical Responses*

The FAA modified GOx samples were prepared and purified using the method reported in the literature (6). Membrane enzyme electrodes based on this modified enzyme were constructed as described in section 2.7. The membrane electrodes were again firstly equilibrated in buffer (0.085 mol dm⁻³ sodium phosphate, pH 7.0) for 30 minutes at room temperature, then secondly equilibrated electrochemically in the same buffer (deoxygenated) at a

potential of 0.4 Volts vs SCE until a steady background current was obtained.

Two batches of membrane enzyme electrodes were made with samples of the FAA modified GOx. For the first batch, identical enzyme loadings were used. For the second batch, the enzyme loadings were varied. The catalytic responses of these two batches of membrane enzyme electrodes based on FAA modified GOx to glucose were recorded at a fixed potential of 0.4 Volts vs SCE (figures 4.17 and 4.18). These membrane electrodes showed greater limiting currents and faster kinetics compared to the membrane enzyme electrodes based on FMCA modified GOx. Results of kinetic analysis for the two batches of membrane enzyme electrodes based on FAA modified GOx are given in table 4.7.

Table 4.7 Kinetic analysis of the results for the membrane enzyme electrodes based on FAA modified GOx

	Enzyme loading (mg)	k'_{ME} (cm s^{-1})	K_{ME} (mmol dm^{-3})
Batch I, identical loadings			
E--1	0.21	1.4×10^{-3}	3.6
E--3	0.21	2.8×10^{-3}	1.2
E--5	0.21	1.4×10^{-3}	1.7
E--6	0.21	2.1×10^{-3}	1.9
Batch IIa, freshly prepared			
E--1	0.14	2.6×10^{-3}	1.0
E--3	0.21	1.1×10^{-3}	1.2
E--5	0.28	2.6×10^{-3}	2.2
E--6	0.42	6.9×10^{-3}	1.6
Batch IIb, 20 hours after initial measurements			
E--1	0.14	4.2×10^{-4}	3.6
E--3	0.21	1.0×10^{-4}	1.2
E--5	0.28	4.1×10^{-4}	1.7
E--6	0.42	1.1×10^{-4}	1.1

Figure 4.19 and 4.20 are the i_{lim}/i_0 versus i_0 plots for the Batch I and Batch II of the FAA modified GOx membrane enzyme electrodes respectively. Compared to the results obtained for membrane enzyme

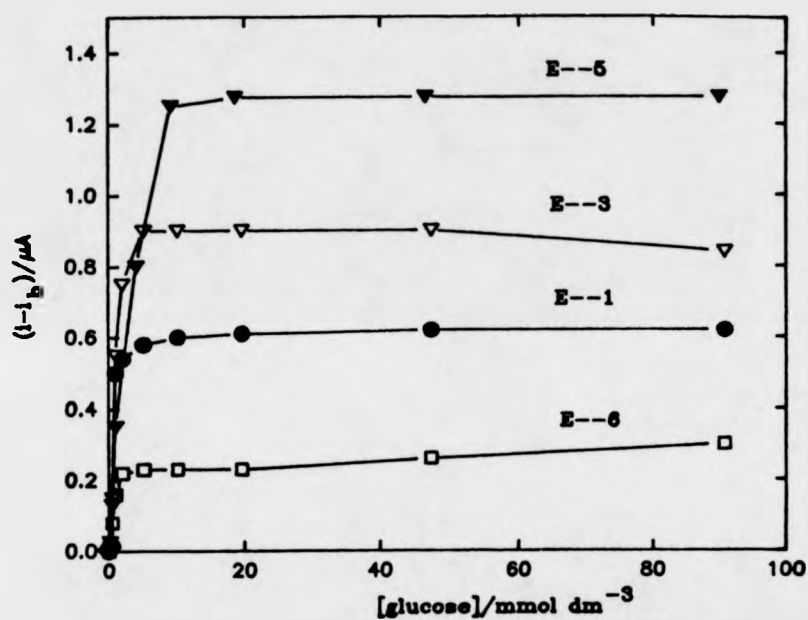


Figure 4.17 Substrate titration curves for a batch of freshly prepared membrane enzyme electrodes based on FAA modified GOx
 E: 0.40 Volts vs SCE
 Enzyme loadings E--1, 0.14 mg; E--3, 0.21 mg;
 E--5, 0.28 mg; E--6, 0.42 mg.
 Background currents for electrodes:
 $i_{b1} = 0.28 \mu\text{A}$, $i_{b3} = 0.12 \mu\text{A}$,
 $i_{b5} = 0.55 \mu\text{A}$, $i_{b6} = 0.18 \mu\text{A}$

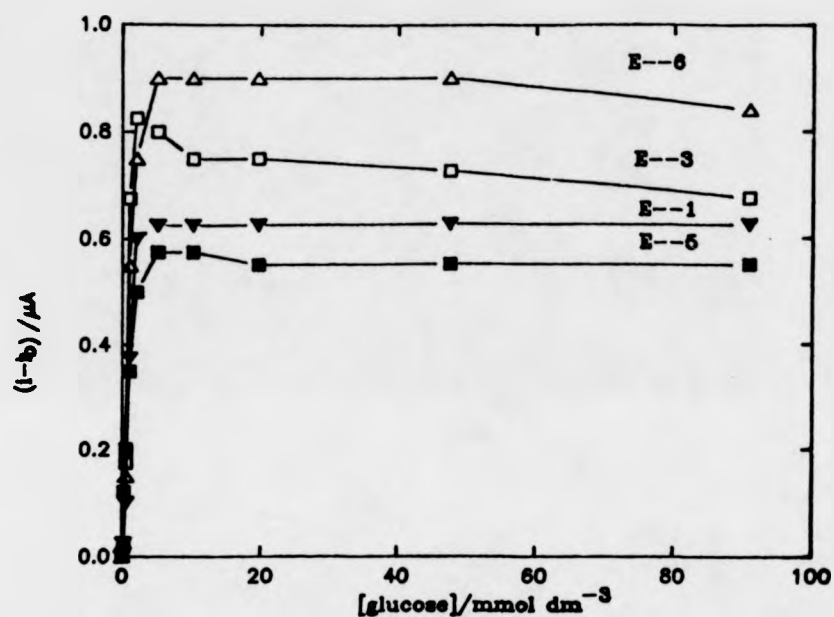


Figure 4.18 Substrate titration curves for a batch of freshly prepared membrane enzyme electrodes based on FAA modified GOx with identical loadings (0.21 mg).
 E: 0.40 Volts vs SCE
 Background currents for electrodes:
 $i_{b1} = 0.275 \mu A$, $i_{b2} = 0.325 \mu A$,
 $i_{b3} = 0.30 \mu A$, $i_{b4} = 0.4 \mu A$

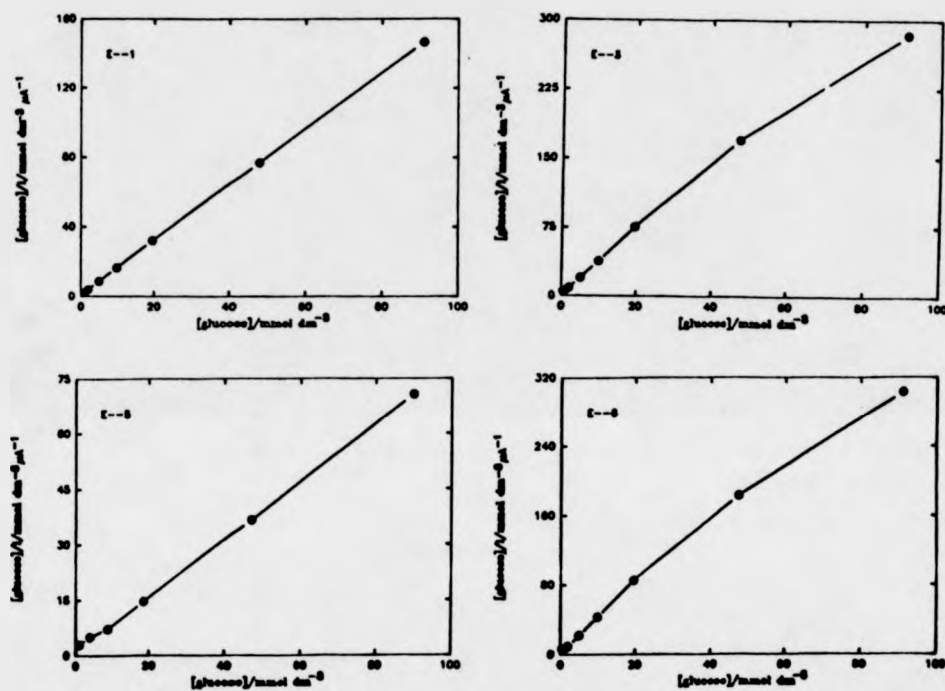


Figure 4.19 s_m/i vs s_m plots for the membrane enzyme electrodes based on FAA modified GOx with different enzyme loadings.
Enzyme loadings: E--1, 0.14 mg; E--3, 0.21 mg;
E--5, 0.28 mg; E--6, 0.42 mg

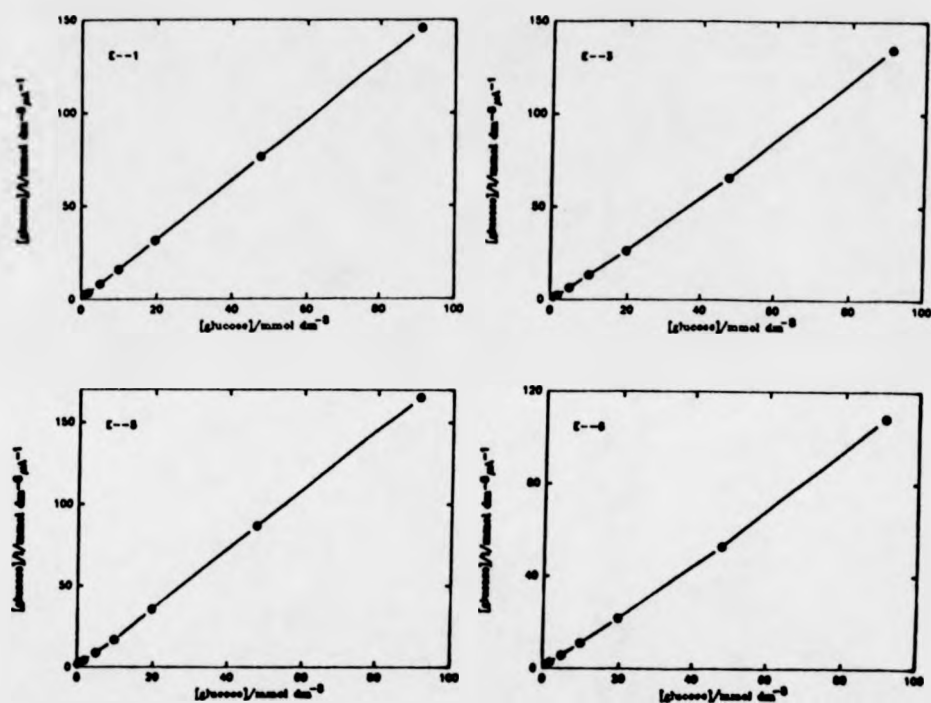


Figure 4.20 s_m/i vs s_∞ plots for the membrane enzyme electrodes based on FAA modified GOx with identical loadings (0.21 mg).

electrodes based on FMCA modified GOx, these FAA modified GOx membrane enzyme electrodes show far better stability and reproducibility. Membrane enzyme electrodes based on FAA modified GOx with identical enzyme loadings gave similar responses to substrate additions (vary within $\pm 23\%$ of the average limiting current values) and the responses of those electrodes with individual enzyme loadings still retained 10% of their original value after being stored in buffer ($0.085 \text{ mol dm}^{-3}$ sodium phosphate, pH 7.0) at room temperature for 20 hours (figure 4.21). Data for these "stored" membrane enzyme electrodes based on FAA modified GOx were also analysed (figure 4.22, table 4.7). From table 4.7, it is apparent that the values of k'_{ME} for the freshly prepared membrane electrodes based on FAA modified GOx are approximately 10 times greater than the corresponding k'_{ME} values for the electrodes based on FMCA modified GOx (table 4.4), indicating comparatively faster kinetics. These values of k'_{ME} for FAA modified GOx membrane enzyme electrodes are also of the same magnitude as k'_s , the rate constant describing the diffusion of substrate through the membrane. Thus, for the FAA modified GOx membrane enzyme electrodes, the rate limiting step of the catalytic reaction is the diffusion of substrate through the membrane. Values of k_{cat} , the rate constant for enzyme kinetics, cannot be derived.

The half lives of the FAA modified GOx membrane enzyme electrodes were estimated and found to be of the order of a few hours, compared to 20 minutes for the FMCA modified GOx membrane enzyme electrodes. Since the membrane enzyme electrodes were held at oxidising potential during the experiment and therefore the mediators would be in the oxidised form, the ferricinium form, the results for the half lives of both FMCA and FAA modified membrane enzyme electrodes suggest that the oxidised form of FAA is more stable than the corresponding oxidised form of FMCA. Thus a

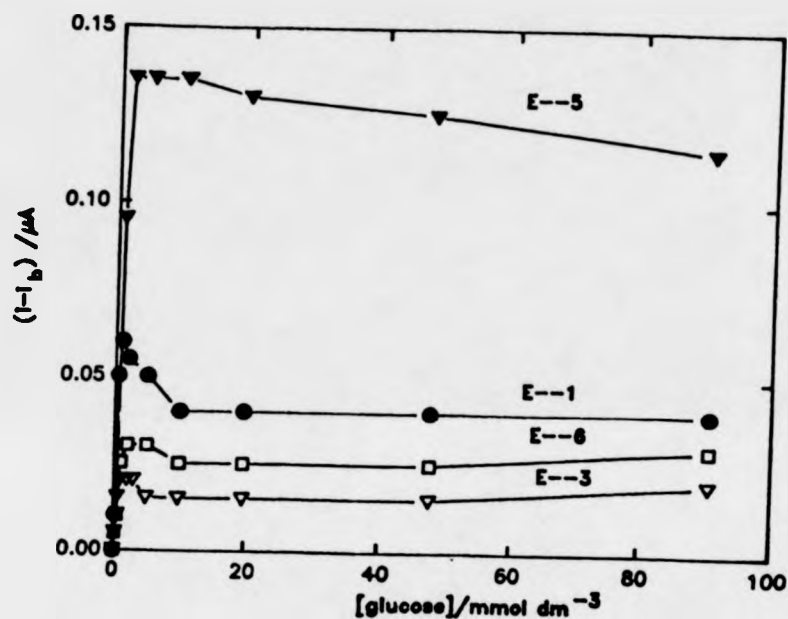


Figure 4.21 Substrate titration curves for the batch of membrane enzyme electrodes based on FAA modified GOx with different enzyme loadings, after being stored in buffer (0.15 mol dm⁻³ sodium phosphate containing 0.20 mol dm⁻³ NaCl, pH 7.0) for 20 hrs at room temperature. E: 0.40 Volts vs SCE.

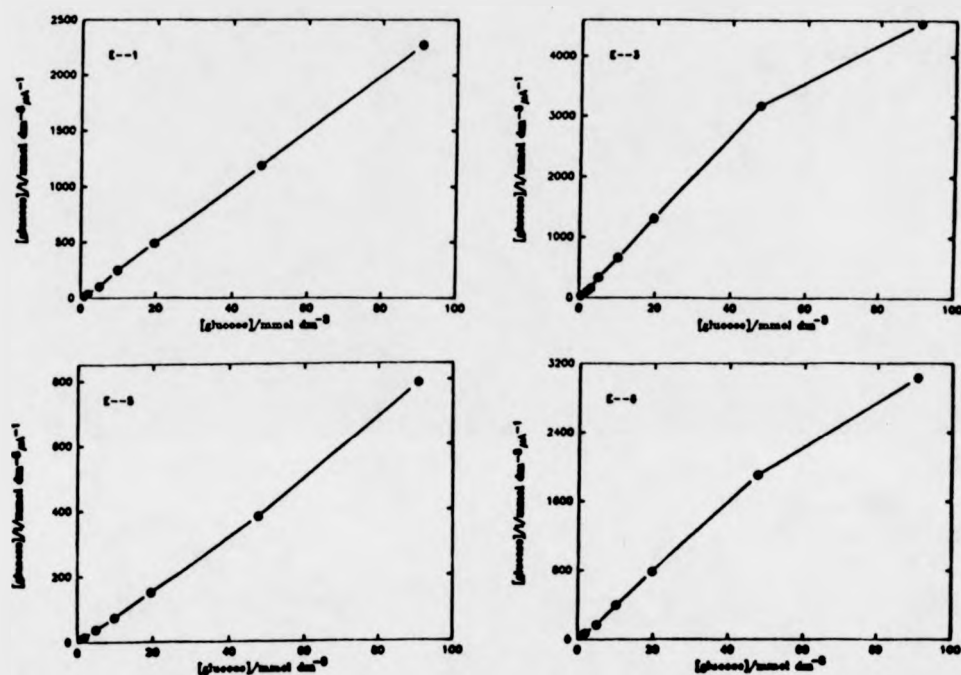


Figure 4.22 $s_{m/i}$ for the batch of membrane enzyme electrodes based on FAA modified GOx with different enzyme loadings, after being stored in buffer ($0.15\ mol\ dm^{-3}$ sodium phosphate containing $0.20\ mol\ dm^{-3}$ NaCl, pH 7.0) for 20 hrs at room temperature.

more stable membrane enzyme electrode may be made by using an enzyme modified with a more stable redox mediator.

4.5.2 The Selectivity of the FAA Modified GOx

In Chapter III, we investigated the specificity of the FAA modified GOx in homogeneous solution by studying the catalytic reaction of the modified GOx with four other sugar substrates, 2-deoxy-D-glucose, D-mannose, D-xylose and D-galactose. The results showed that the modified enzyme responded in the same order of preference to sugar substrates as the native GOx (figure 3.2). We now extend our investigation to the studies of the selectivity of the FAA modified GOx membrane enzyme electrodes.

The above sugar substrates were again employed for the study. The electrochemical responses of the FAA modified GOx membrane enzyme electrodes to additions of sugar were recorded in deoxygenated neutral aqueous buffer solution (0.085 mol dm⁻³ sodium phosphate) at a fixed potential of 0.4 Volts vs SCE (figure 4.23). The responses are consistent with our results obtained for native enzyme substrate titration: β -D-glucose > 2-deoxy-D-glucose > D-mannose > D-xylose = D-galactose.

The results of substrate titration for FAA modified GOx membrane enzyme electrodes were also analysed using the model. Kinetic parameters obtained for 2-deoxy-D-glucose and D-mannose are given in table 4.8.

Table 4.8 Analysis of the results for the substrate specificity studies using FAA modified GOx membrane enzyme electrodes

Substrate	k'_{ME} (cm s ⁻¹)	K_{ME} (mmol dm ⁻³)	K_M (mmol dm ⁻³)	k_{cat} (s ⁻¹)
2-deoxy-D-glucose	2.8×10^{-6}	1.82	1.75	3.5×10^{-3}
D-mannose	4.2×10^{-7}	1.05	1.04	6.4×10^{-3}
D-glucose	2.8×10^{-5}	1.47	-	-

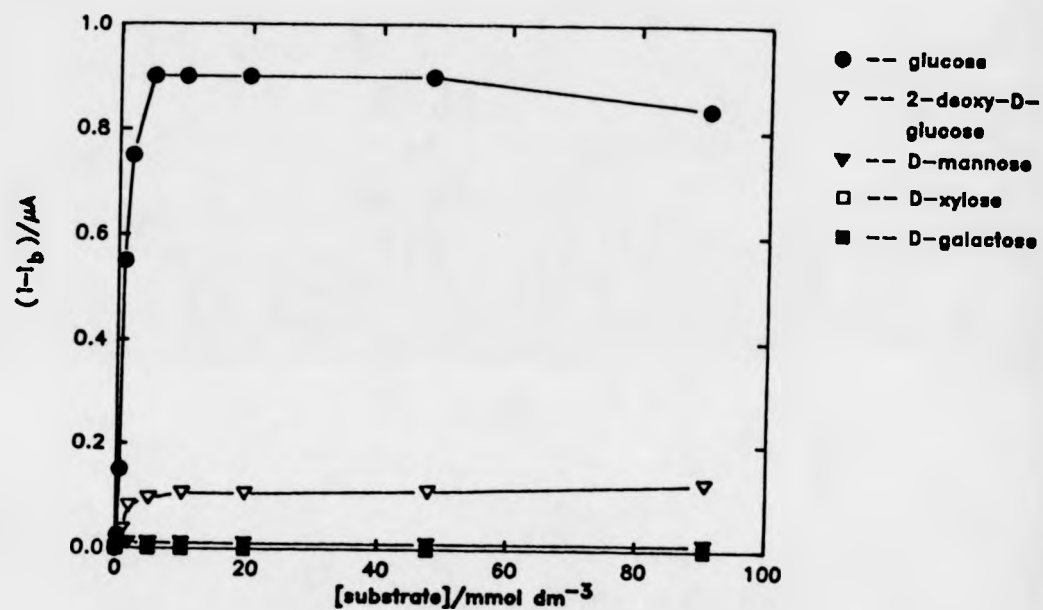


Figure 4.23 Responses of a membrane enzyme electrode based on FAA modified GOx to five different sugar substrates.
Enzyme loading: 0.21 mg
E: 0.40 Volts vs SCE

It is apparent that, from the data shown in table 4.8, the rate of oxidation of 2-deoxy-D-glucose and D-mannose at the FAA modified GOx membrane enzyme electrode is much slower than that of the D-glucose at the enzyme electrode: D-glucose: 2-deoxy-D-glucose: D-mannose = 100: 15 : 1.5. This result shows that the membrane enzyme electrode based on FAA modified GOx retains the specificity of the native GOx. The selectivity of an enzyme electrode is crucial for practical applications.

Next, we will present the studies of the stabilities of some ferrocene derivatives.

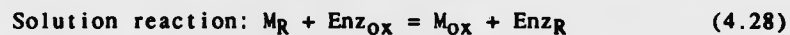
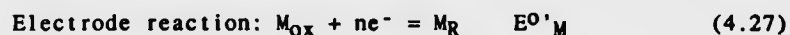
4.6 Stabilities of Some Ferrocene Derivatives

We have shown above that the stabilities of the covalently attached ferrocene mediator molecules in their oxidised form are directly relevant to the stabilities of the membrane enzyme electrodes based on FMCA or FAA modified GOx. Thus, in order to produce a membrane enzyme electrode of longer working life, a more stable modified enzyme, i.e. an enzyme modified with a more stable redox mediator must be employed. In this section, the half lives of the oxidised forms of some ferrocene derivatives in neutral aqueous buffer solution are reported.

4.6.1 *Ferrocene Derivatives as Mediator-Titrants* (115)

Szentrimay *et al.* introduced mediator-titrants for the indirect coulometric titration (ICT) of biocomponents. Their work is reviewed in this section. The indirect coulometric titration method was initially developed for the accurate assessment of stoichiometry (n value) and formal potential ($E^{0'}$) of bioredox components. The fundamental problem in the accurate assessment of n and ($E^{0'}$) values of biocomponents is the slow heterogeneous electron transfer rate between the biocomponent and the electrode. This is significant particularly with large macromolecules such as proteins and enzymes, where

the redox sites may be "buried" deeply inside the molecular structure. Thus, mediators are usually added to the bulk solution to facilitate the charge transfer between the biocomponents and the electrode. In ICT method, a titrant (either a reductant or an oxidant) is generated electrochemically to transfer charge to the biocomponent. For a reduction, the reaction sequence is written as:



where M_{OX} and M_{R} are the oxidised and reduced forms of the mediator respectively,

Enz_{OX} and Enz_{R} represent the oxidised and reduced forms of the biocomponent.

The equilibrium of (4.28) is given by:

$$\Delta E^{\circ'} = E^{\circ'}_{\text{ENZ}} - E^{\circ'}_{\text{M}} = RT \ln K_{\text{eq}} \quad (4.29)$$

Thus, the n and $E^{\circ'}_{\text{ENZ}}$ values are determined from the best fit between the experimental and computer simulated plots of the electrochemical charge, q , and the change in the optical absorbance, ΔA , of the biocomponents. A typical plot of ΔA vs q for the generation and removal of 1,1'-bis(hydroxymethyl) ferricinium ion is shown in figure 4.24 (115). Values of n may be estimated from the slope of the ΔA vs q plot.

The "ideal" properties of mediator-titrants are summarised by the authors as:

1. well-defined n value ($n = 1$ preferable for most cases),
2. known $E^{\circ'}$ value under experimental conditions,
3. fast heterogeneous and homogeneous electron transfer,
4. soluble in aqueous media at or near pH 7.0,
5. stable redox species,

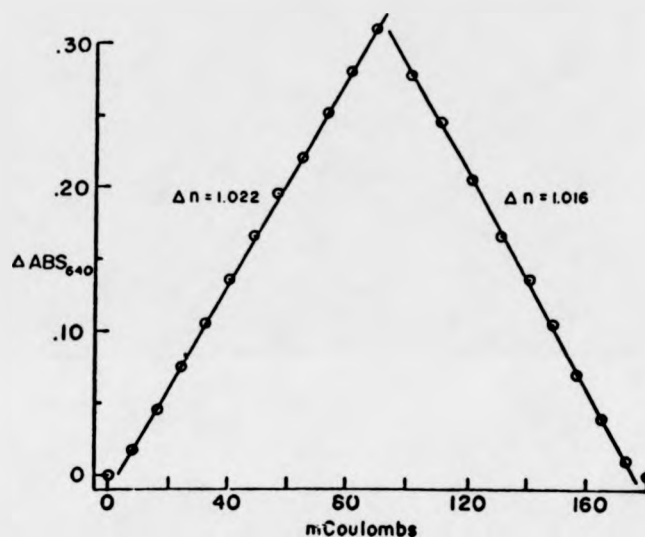


Figure 4.24 (115) Change in optical absorbance vs charge plots for the generation and removal of 1,1'-bis(hydroxymethyl) ferricinium ion. Concentration of 1,1'-bis(hydroxymethyl) ferrocene $1.03 \text{ mmol dm}^{-3}$, and $1.22 \text{ mmol dm}^{-3}$ benzylviologen chloride in phosphate buffer, pH 7.0; Wavelength: 640 nm, Optical cell path: 1.25 cm.

6. good optical window,
7. does not inhibit or interact with biocomponents.

The unique structure and properties of ferrocene and its many derivatives have resulted in a great deal of theoretical and experimental studies. The aspects of particular interest are the wide range of positive potentials⁽¹⁵⁴⁻¹⁵⁷⁾ accessible through the variety of substituents of ferrocene, the fast electron transfer rates, the clear optical window in the visible region and the well defined n value of unity. The main problems of using ferrocenes as mediator-titrants are firstly, the low solubility of some ferrocenes in their reduced form and secondly, the instability of the oxidised form, in aqueous solutions.

The limited solubility of some ferrocenes may be overcome by solubilization in micelles as formed by non-ionic detergents such as Tween-20 (158). The stability of the ferricinium ions was determined by monitoring their optical absorbance after they were generated by coulometry. Figure 4.25 shows the plots of absorbance, A , versus time for three ferricinium ions, $FMCA^+$ (ferrocenemonocarboxylic acid), FAA^+ (ferroceneacetic acid) and $BHMF^+$ (1,1'-bis-(hydroxymethyl)ferrocene) in aqueous solution at pH 7.0. These plots are characteristic of first order kinetics and the half lives are estimated to be 0.50, 4.3 and > 24 hours for $FMCA^+$, FAA^+ and $BHMF^+$ respectively (115). It was observed by Szeutrimay *et al.* that, when all of the ferricinium ions have been lost completely, 50-75% of the initial concentration can be regenerated again by oxidative electrolysis. The results seem to suggest that the ferricinium ion undergoes a hydrolysis reaction involving a disproportionation reaction mechanism (115,159). This disproportionation produces one-third ferric hydroxide and the remainder, the parent ferrocene. The data for the half lives of some ferrocenes and the E^0 values obtained from voltammetric

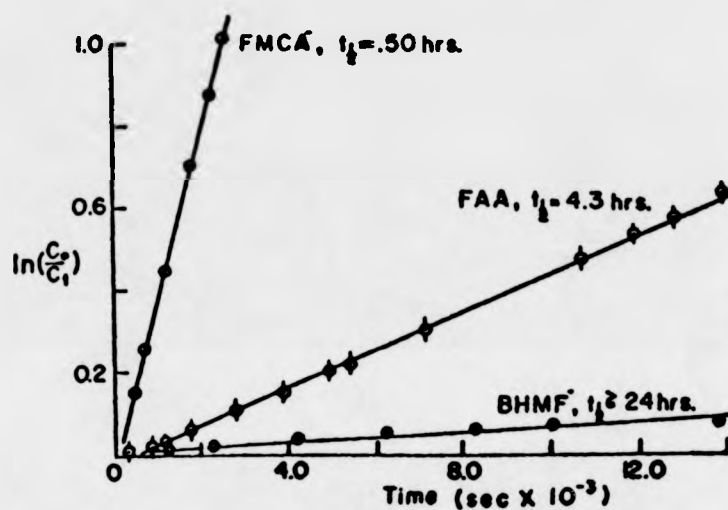


Figure 4.25 Plots of absorbance vs time for $\text{FMCA}^+ = \circ$; $\text{FAA}^+ = \phi$; and $\text{BHMF} = \bullet$. Concentrations are 1-2 mmol cm^{-3} in phosphate buffer at pH 7.0 (Reproduced from reference (115))

studies as well as spectra and potentiometric data obtained by the authors are collected in table 4.9.

Table 4.9(115) Electrochemical and optical properties of ferrocene

Ferrocene derivatives	$E^{0'}$ (mV vs SCE)	ΔE_p (mV)	λ_{max} (nm)	t_1/s (hr)
1,1'-dimethyl	100 ± 9	51	655	32
acetic acid	124 ± 10	57	630	4.3
hydroxy ethyl	161 ± 10	58	625	>25
ferrocene (parent)	181 ± 10	62	615	14
1,1'-bis (hydroxymethyl)	224 ± 5	57	638	>24
hydroxy-2- phenylethyl	239 ± 5	61		
monocarboxylic acid	289 ± 10	64	630	0.5
chloro ferrocenyl	357 ± 8	57		
methyl	386 ± 11	57	625	1
tri-methyl ammonium salt				
1,1'-dicarb- oxylic acid	403 ± 12	40		

4.6.2 Stability of Some Ferrocene Derivatives

We adapted the method described by Szentrimay *et al.* to study the stability of some ferricinium ions which are of interest to us by monitoring their optical absorbance after they were generated by coulometry. The experiments were carried out in phosphate buffer (0.15 mol dm^{-3} , pH 7.0, containing 0.20 mol dm^{-3} sodium chloride). Saturated solutions of the ferrocene derivatives in the phosphate buffer were prepared at room temperature. The ferricinium ions were generated qualitatively by coulometry using a large platinum gauze (surface area = 1.8 cm^2). The absorbance change, ΔA , of the ferricinium ions at their λ_{max} as a function of time

was recorded. Figure 4.26 shows a typical plot of ΔA vs t for ferrocenemonocarboxylic acid. The plots of $\ln A$ against time are linear and characteristic for first order kinetics. Such a plot for ferrocenemonocarboxylic acid is shown in figure 4.27. The half lives of the ferrocene derivatives were estimated and their E^0 values were obtained using cyclic voltammetry at a platinum electrode (0.348 cm^2). The values of E^0 and the half lives for the ferrocene derivatives are given in table 4.10.

Table 4.10 Values of E^0 and the half lives of some ferrocene derivatives

Ferrocene derivative	λ_{\max}^* (nm)	E^0 (mV vs SCE)	$t_{1/2}$ (hours)
butanoic acid	630	90	> 24
1,1'-dimethyl	649	95	> 24
acetic acid	630	120	2.1
1-(3-hydroxy) propanyl	630	125	> 24
boronic acid	622	140	17.4
ethanolamine	667	145	44
ferrocene (parent)	620	175	14(+)
t-butyl	625	225	2.7
monocarboxylic acid	630	290	0.5
dimethyl amino methyl	630	330	1.6

* λ_{\max} values of the ferricinium ions
(+) taken from the literature (--)

1,1'-dicarboxylic acid was found to be extremely unstable. It decomposes practically instantly upon electrolysis. Among the ferrocene derivatives studied, ferrocene-ethanolamine is the most stable compound. Although ferrocene butanoic acid has a longer half live than ferroceneacetic acid, the glucose oxidase modified with the former ferrocene was reported to have slower kinetics than the ferrocene acetic acid modified enzyme (122).

4.7 Conclusions

In this chapter, we have presented the studies of the working stabilities of the FMCA and FAA modified glucose oxidase via the construction of

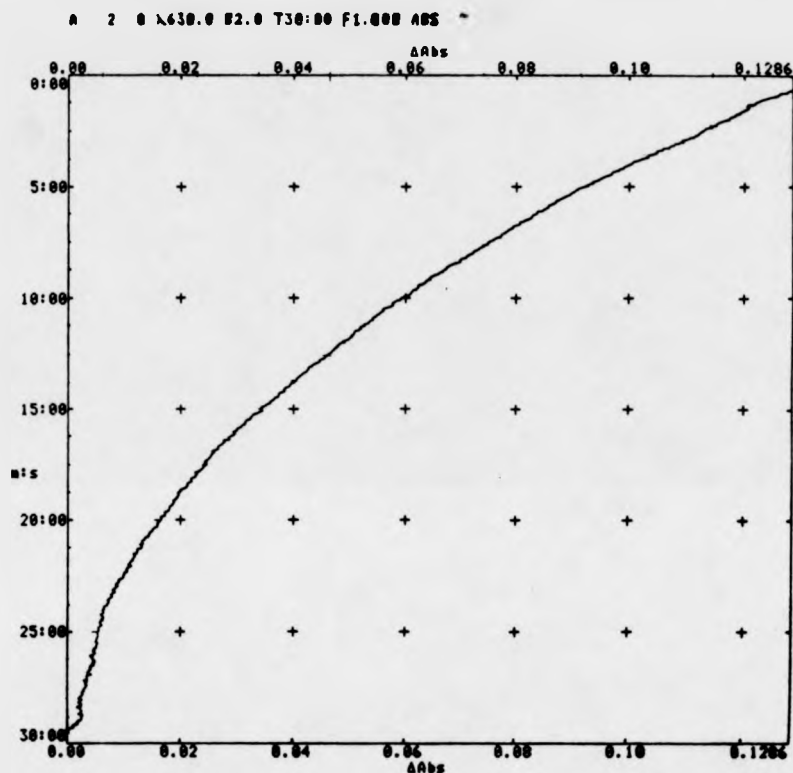


Figure 4.26 A typical plot of the decrease of absorbance as a function of time for ferrocenemonocarboxylic acid. Concentration of FMCA: $1.02 \text{ mmol dm}^{-3}$, in sodium phosphate buffer, 0.15 mol dm^{-3} containing 0.20 mol dm^{-3} NaCl, pH 7.0. Optical wave length: 630 nm Cell path: 1 cm

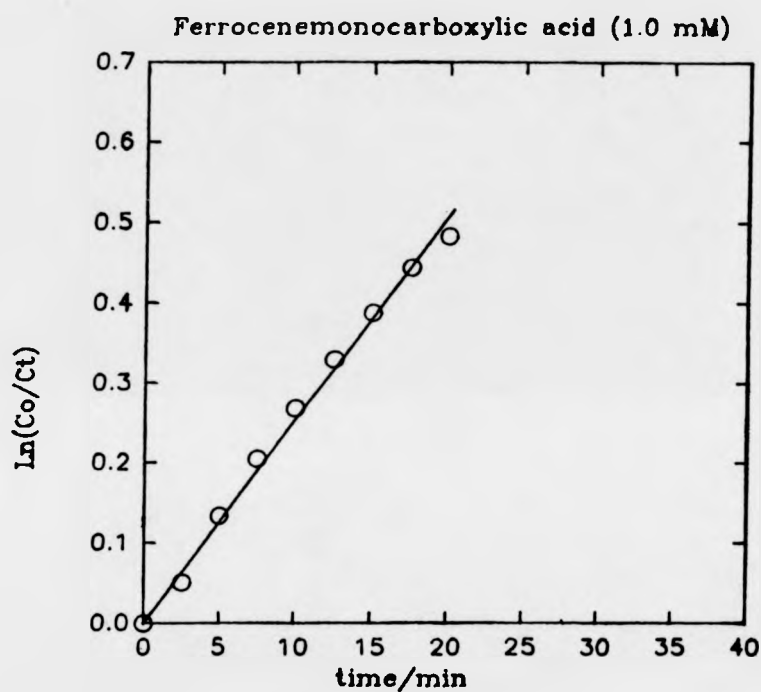


Figure 4.27 A typical plot of $\ln(c_0/c_t)$ vs t for the ferricinium ions of ferrocenemonocarboxylic acid (1.02 mmol dm⁻³ in 0.15 mol dm⁻³ sodium phosphate buffer containing 0.20 mol dm⁻³ NaCl, pH 7.0 at room temperature)

membrane enzyme electrodes. Membrane enzyme electrodes are an effective means to study the stability in operation for the chemically modified enzyme since there are only small quantities of the enzyme entrapped behind the dialysis membrane and the enzyme is prevented from being lost to the bulk solution.

Our studies show that the loss of catalytic responses of the FMCA and FAA modified GOx membrane enzyme electrodes is not caused by the loss of enzymic activity of the modified enzyme but is mostly caused by the instability of the oxidised forms of the covalently attached ferrocene mediators; large responses were obtained when free mediators were added to the bulk solution. Our studies also show that membrane enzyme electrodes based on FAA modified GOx are much more stable than those based on FMCA modified GOx. The half lives of FMCA modified GOx membrane enzyme electrodes are around 20 minutes while the half lives of the FAA modified GOx membrane enzyme electrodes are a few hours. These results for the half lives of the membrane enzyme electrodes are in agreement with the values of half lives of the ferricinium ions suggesting that the stabilities of the membrane enzyme electrodes are closely related to the stabilities of the oxidised forms of the mediators. The ferricinium ions are known to undergo a hydrolysis reaction involving a disproportionation mechanism which produces a third of ferric hydroxide and the remainder, the parent ferrocene (115). Thus, one possible option for improving the stability of the membrane enzyme electrodes is to modify the GOx with more stable mediators.

Our results for the half lives of some ferrocene derivatives show no apparent relationship between the structures of the substituents of the ferrocenes and the stabilities of the ferricinium ions. Thus, a systematic recommendation of the stabilities of potential ferrocene derivatives cannot be established at the present time.

In the next chapter, a novel modification method for glucose oxidase will be described.

CHAPTER V NON-COVALENT MODIFICATION OF GLUCOSE OXIDASE

In this chapter, a novel enzyme modification method is described. Modification of glucose oxidase has been achieved by incorporating hydrophobic electron transfer mediators (e.g. tetrathiafulvalene, iron(II)phthalocyanine and some ferrocene derivatives) with GOx in aqueous media. The non-covalently modified GOx undergoes direct electron transfer at simple metallic electrode surfaces.

Studies of the electrochemical catalytic activity for TTF modified GOx samples prepared at different pH values are presented. Results for iron (II)phthalocyanine and ferrocene derivative modified GOx are also discussed. Attempts to quantify the incorporated of mediators are described.

5.1 Introduction

We will begin this section by first briefly describing the characteristics of conducting organic salts and their use as electrode materials. Second, the use of conducting organic salt electrodes in enzyme catalysis and the existing theoretical models for the mechanism of biocatalysis at these electrodes are reviewed. Finally, the non-covalent modification of glucose oxidase with organic salts and its contribution to the mechanism of conducting organic salt electrodes in enzyme catalysis are detailed.

5.1.1 *Conducting Organic Salts and Conducting Organic Salt Electrodes*

Conducting organic materials have attracted much attention because of their unique properties. Much of the early reports were concerned with electrical and magnetic properties, crystal structures and degree of charge transfer in the material (161-170). Around 1979, Jaeger and Bard (110) first studied conducting organic salts as electrode materials and Kulys and

co-workers first applied these materials as electrodes for biocatalysis (1).

Commonly, conducting organic salts consist of an electron donor (D) and an electron acceptor (A). These compounds are typically planar molecules with a π -electron density both above and below the molecular plane (160). The most widely studied conducting organic salt is probably the tetrathiafulvalene-tetracyanoquinodimethane (TTF, TCNQ) charge transfer complex. Figure 5.1 shows the structures of TTF, TCNQ and several other common electron donors and acceptors.

The high electrical conductivities displayed by organic charge transfer complexes arise from a special feature of their crystal structures: electrons and holes are delocalised along segregated stacks of the cation donor and anion acceptor molecules (160). It is essential that the donor and acceptor molecules form such segregated stacks. Systems in which the donors and acceptors are mixed in the stacks are insulators rather than conductors (171). It is also necessary that the donor (or acceptor) form a new sextet by the loss (or gain) of an electron, (160) figure 5.2. This ensures the mobility of charge carriers within the stacks. Finally, it is important that there is partial charge transfer between the stacks (160). If charge transfer is complete, the charge carriers are not mobile up and down the stacks, hence the material is an insulator. When the above requirements are fulfilled, a donor and acceptor will form a conducting organic salt. At room temperature the electrical conductivity of the TTF:TCNQ charge transfer complex is comparable with that of graphite (109,172).

Working electrodes of conducting organic salts can be constructed in a number of ways. A detailed preparation procedure can be found in reference (160) by P. N. Bartlett. The different kinds of conducting organic salt electrodes reported in the literature (160) are now described.

1. Drop coated electrodes. This method was described by Bartlett as the simplest for the preparation of a conducting organic salt electrode. A

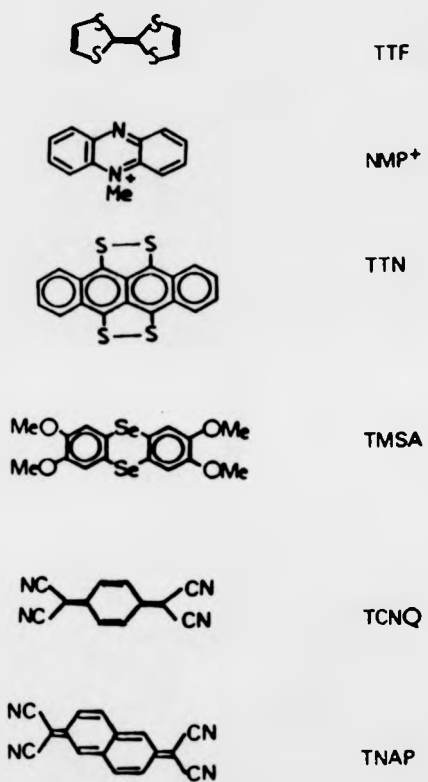


Figure 5.1 The structures of some common donor and acceptor molecules

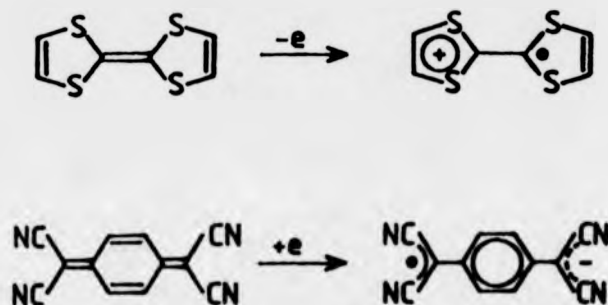


Figure 5.2 Structure of the oxidised and reduced forms of TTF and TCNQ respectively (Reproduced from ref. (160))

drop coated electrode was made by placing a drop of the organic salt dissolved in a volatile organic solvent (e.g. acetonitrile) on the surface of a glassy carbon or platinum disc electrode (home-made or commercial type). The drop coating technique was found to work best on glassy carbon electrodes. The coating can be made more adherent if small quantity of PVC is used. The drop coating solution should be freshly prepared prior to construction of an electrode since the conducting salts are often unstable in organic solvents. This method has the advantage of being simple, quick and requires only small quantities of material. The disadvantage is that the electrode surface is poorly defined and very rough.

2. Packed cavity electrode. The packed cavity electrode was constructed by press fitting a platinum disc attached to a brass rod into a Teflon sheath. Typical dimensions of the cavity are 5 mm diameter and 1-2 mm depth. The packing mixture was made by dissolving some conducting salts in a solution of PVC and purified THF. THF was found to be the best solvent since it is a good solvent for the PVC binder. The mixture was then applied into the cavity and the cavity was allowed to dry.

This electrode has the advantage of being long lasting and it can be re-used as required. The most common problem with the cavity electrode appears to be poor electrical contact between the platinum and the packing material.

3. Paste electrode. These electrodes were prepared by mixing the conducting salts with an inert oil to form a stiff paste and then packing the paste into an electrode cavity as described above. Paste electrodes are easy to fabricate and give low background currents.
4. Pressed pellets electrodes. In this method, conducting organic salt pellets were prepared using a conventional infrared pellet press. A pressed

pellet electrode was constructed by placing the pellet at the end of a glassy tube of the same diameter and fixing in place with Araldite. Electrical contact was made either with silver-loaded conducting paint or with a drop of mercury in contact with a piece of copper wire.

The pressed pellet electrodes is a good method for making conducting organic salt electrodes. Although a large amount of material is required, the electrodes can be re-used by polishing the pellet surface each time.

5. Single crystal electrodes. These electrodes are difficult to make and very fragile, however, single crystal conducting salt electrodes give much lower background currents and have well defined surfaces. They are suited to fundamental studies of the electrochemistry of the conducting salts.

The use of conducting organic salt electrodes in enzyme catalysis and the mechanism of electrode reactions will now be described.

5.1.2 Enzyme Electrocatalysis at Conducting Organic Salt Electrodes

Direct oxidation of redox enzymes and proteins at conducting organic salt electrodes has been reported by a few research groups (1-4). Kulys and co-workers showed that reduced GOx could be oxidised at certain conducting salt electrodes at low potentials in the absence of added mediator (1,112). Albery et al. studied the direct oxidation of GOx on seven different one-dimensional conducting donor acceptor salts, (7) and they suggested TTF. TCNQ was the best choice due to its low background currents (7). Electrode of this material might be extremely useful for an *in vivo* glucose sensor, but the mechanism of electron transfer is still a subject of controversy. The possible mechanisms for electron transfer at conducting organic salt electrodes, in particular NMP^+ , TCNQ^- and TTF.TCNQ electrodes, are described below.

Kulys et al. suggested that the oxidation of flavin oxidases (e.g. GOx and xanthine oxidase) proceeds in a mediated manner (102,112). The homogeneous mediators were formed in solution near the electrode surface due to a slight dissolution of the organic metal (e.g. NMP^+ , TCNQ^-). This electron exchange mechanism is supported by first, the potential values of substrate oxidation that proceeds at the mediator redox conversion potentials, second, by the inhibition of the substrate oxidation process by oxygen at low substrate concentrations. Thirdly, the current at an enzyme electrode with a constant generating mediator concentration can be expressed as:

$$I = 0.33 nFA k d[\text{Enz}] [\text{M}] \quad (5.1)$$

where n , F , and A are the number of electrons transferred, the Faraday, and the electrode area; d is the catalytic layer thickness; k is the rate constant of the enzyme active centre reaction with the mediator; $[\text{Enz}]$ and $[\text{M}]$ are the concentrations of enzyme and mediator respectively. Consequently, the direct dependence of the current on the enzyme concentration in the catalytic layer is in agreement with the theory. Fourthly, the calculated mediator surface concentration using the above equation is agreeable to that measured fluorimetrically ($9\text{--}18 \mu\text{mol dm}^{-3}$). Using this mechanism for electron transfer at organic metal electrodes, Kulys et al. measured the homogeneous second order rate constant for the reaction of NMP^+ and TCNQ^- with reduced GOx and obtained rate constants in the order of $10^4 \text{ dm}^3 \text{ mol}^{-1} \text{ s}^{-1}$.

However, experiments carried out by Albery et al. show that this homogeneous mediation mechanism is improbable. They propose that the oxidation of flavin oxidases takes place by direct electron exchange at the conducting organic salt electrode surfaces. Albery et al. carried out rotating ring-disc electrode studies with a disc electrode made of NMP^+ TCNQ^- and

measured at the ring electrode the flux of NMP^+ and TCNQ^- leaving the disc surface. At potentials where $\text{NMP}^+ \text{TCNQ}^-$ dissolves producing $\text{NMP} + \text{TCNQ}^-$ ($E < 100 \text{ mV vs SCE}$) or $\text{NMP}^+ + \text{TCNQ}$ ($E > 300 \text{ mV vs SCE}$), the current at the ring electrode is less than 10^{-7} A . This value of ring current corresponds to a surface concentration of NMP^+ or TCNQ^- which is significantly less than $10^{-6} \text{ mol dm}^{-2}$. Using this value of surface concentration, the homogeneous second order rate constant obtained by Kulys et al. ($\sim 10^4 \text{ dm}^3 \text{ mol}^{-1} \text{ s}^{-1}$) and the thickness of the electrolyte layer ($\sim 10^{-4} \text{ cm}$), they found that the heterogeneous electrochemical rate constant (k') is smaller than $10^{-4} \text{ cm s}^{-1}$. This was much smaller than that observed experimentally ($10^{-1} \text{ cm s}^{-1}$). Thus they concluded that the conducting organic salt materials are too insoluble and their homogeneous rate constants are too slow to explain the observed electrode kinetics by the homogeneous mediated transfer mechanism.

Wilson et al. (4) also studied the oxidation of GOx at TTF.TCNQ electrodes and they suggested a different electron transfer mechanism. Their data show that firstly, direct electron transfer between enzymatically active GOx and the TTF.TCNQ electrode is extremely unlikely. It is believed to be biologically implausible that an enzyme which has evolved to interact with a specific small molecule could interact with the electrode surface efficiently. Secondly, electron transfer by a soluble component of the organic salt electrode is also dubious. The data indicate that the solubility of the organic salt electrodes in aqueous solutions is too low to be useful. The currents observed at the organic salt electrodes would require a large mediator flux. Although their studies did not provide a conclusive mechanism of electron transfer, it was suggested that the electron transfer may take place through two types of adsorbed enzymes. One type is adsorbed irreversibly at the electrode surface and is inactive. Another type is weakly or reversibly adsorbed. The latter type of adsorbed enzyme is directly responsible for

catalysis. It appears, from their results, that the strongly absorbed enzyme modifies the surface in some way to facilitate the mediated electron transfer of soluble or weakly absorbed enzyme.

5.1.3 *Hydrophobic Interaction between Neutral Components of Organic Salts and Glucose Oxidase.*

The various types of electron transfer mechanism for enzyme catalysis at conducting organic salt electrodes described above fail either to fit the experimental data or to have sufficient experimental support. It is suggested that the organic salt TTF.TCNQ is in equilibrium with its neutral components and can dissociate to water-insoluble TTF^0 and TCNQ^0 (3). The extent of this dissociation depends on the polarity of the medium, a non-polar medium favouring this reaction. It is also well known that the interior of GOx is hydrophobic (173). Thus we supposed that for the catalysis of GOx at TTF.TCNQ electrode, the neutral TTF^0 and TCNQ^0 species might be incorporated into hydrophobic sites with GOx through intermolecular interaction between the TTF^0 , TCNQ^0 species and the aromatic amino acid residues of the enzyme. This incorporation of TTF^0 and TCNQ^0 with GOx would lead to the modification of GOx with an electroactive species. Direct oxidation of GOx at conducting organic salt electrodes could then occur through the incorporated electron transfer mediator.

Studies by Jaeger and Bard (110-111) show that the redox potentials of the $\text{TTF}^0/\text{TTF}^+$ (0.33 V vs SCE, $\text{CH}_3\text{CN}/0.1\text{M TEAP}$) and $\text{TCNQ}^0/\text{TCNQ}^-$ (0.115V vs SCE, $\text{CH}_3\text{CN}/0.1\text{M TEAP}$) couples are in the potential range of interest for GOx oxidation. This clearly confirms that the reduced GOx can be reoxidised by TTF^+ or TCNQ^0 .

We have successfully carried out non-covalent modifications of GOx with neutral organic salt components TTF,(116) TCNQ and the TTF. TCNQ. This method is described as non-covalent modification as opposed to covalent

modification in the literature (5-6), because in our method, the enzyme is modified through the intermolecular interaction of the mediators with the enzyme, not by chemical bonding. Although TTF.TCNQ, TTF and TCNQ modified GOx all undergoes direct oxidation at metal electrode surfaces, the TTF modified GOx was found to give the best catalytic responses and the most reproducible results. Thus we will focus our attention on the studies of TTF modified GOx hereafter this chapter. The electro-catalytic responses of TTF modified GOx samples prepared at different pH values are presented and studies of the stability of TTF modified GOx using membrane enzyme electrodes are described.

We have extended this modification method to use other water-insoluble materials, for example, iron(II)phthalocyanine, and some ferrocene derivatives, to modified GOx. These results are also presented.

5.2 Electrochemistry of TTF Modified GOx.

This section describes the catalytic responses of TTF modified GOx in the absence and presence of glucose.

The modification of GOx with TTF was carried out at room temperature. Some experiments were carried out in the dark as TTF is light sensitive, but no significant difference was observed in the results. Three different kinds of modified enzyme samples were prepared.

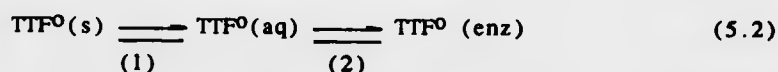
First, the buffer solution was saturated with TTF by stirring with excess TTF in the buffer solution for 2-3 hours. The solution was then filtered using a cotton wool plug and a known concentration of enzyme was added. This procedure is used to prepare a control to eliminate the possibility that the electrochemical responses might arise because of the mediator dissolved in the homogeneous solution.

Second, a mixture of excess TTF solid and a known concentration of enzyme were added to the buffer and stirred for 2-3 hours.

Third, a mixture of excess TTF, a known concentration of enzyme and urea (3 mol dm^{-3}) were stirred together for 2-3 hours.

The second and third TTF modified GOx samples were purified by filtration through a cotton wool plug and the third was further purified using gel filtration on Sephadex G-15. Electrochemical measurements were carried out using a semi-macro cell with a platinum disc electrode (0.384 cm^2). The responses of each modified GOx sample towards additions of aliquots glucose (1.0 mol dm^{-3}) were recorded at a fixed potential (0.35 Volts vs SCE). Figure 5.3 shows the substrate titration curves for the above TTF modified GOx samples.

It is clear from figure 5.3 that the catalytic current of the first modified GOx sample is negligible compared to that from the second and third TTF GOx samples. This demonstrates that the contribution to the current from the homogeneous TTF species is minimal. When purified by gel filtration, the TTF modified GOx (the third sample) appears to give less catalytic current. This may be due to a shift of the equilibrium,



Since $\text{TTF}^0(\text{aq})$ will be removed by gel filtration, some $\text{TTF}^0(\text{enz})$ will become $\text{TTF}^0(\text{aq})$ in order to establish a new equilibrium. Thus the amount of TTF incorporated in the enzyme will be reduced and this may account for the reduction in catalytic current for the modified GOx.

Voltammetric studies show that, in the absence of glucose, two poorly resolved waves are observed at 0.10 and 0.40 V, figure 5.4a. (These two waves correspond to the reactions of



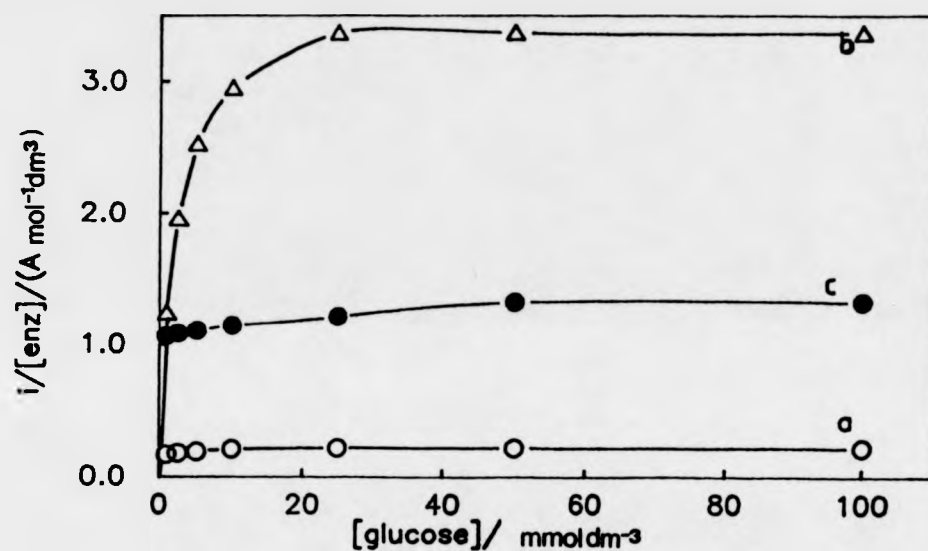


Figure 5.3 Calibration curves of TTF modified glucose oxidase. Curves a, b and c correspond to the responses of the three different kinds of samples (first, second and third) described in section 5.2. Electrode material, Pt (0.384 cm²). Recorded at a fixed potential of 0.35 V vs SCE.

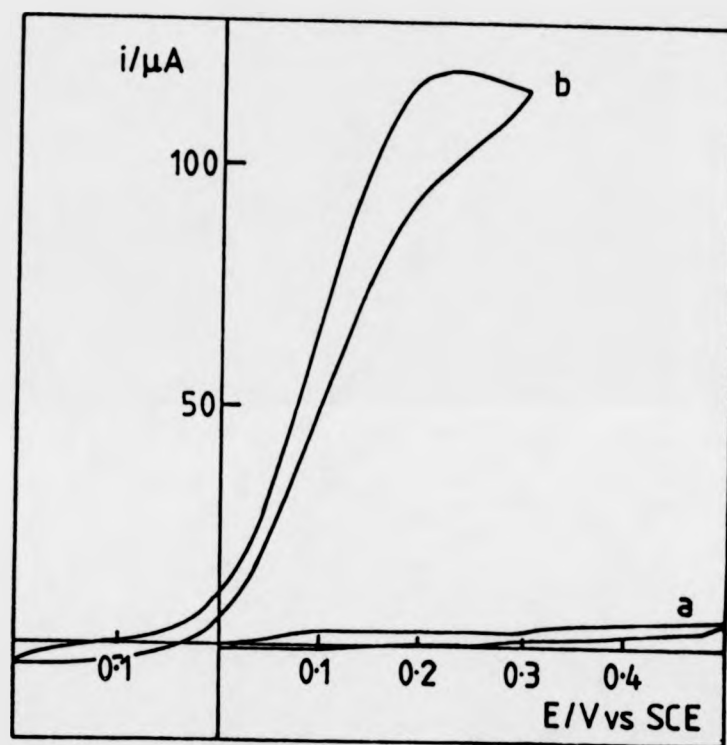


Figure 5.4 Cyclic voltammograms of TTF modified glucose oxidase:
 (a) in the absence of glucose; (b) in the presence of
 glucose (90 mmol dm^{-3}).
 Sweep rate: 5 mV s^{-1} , $[\text{GOx}] = 1.02 \times 10^{-5} \text{ mol dm}^{-3}$
 Electrode: GC (0.384 cm^2)
 Buffer: 85 mmol dm^{-3} phosphate, pH 7.0

On addition of glucose, a characteristic catalytic response is observed, figure 5.4b. This is consistent with the enzyme catalysed electrooxidation of the added glucose mediated by the hydrophobic TTF molecules incorporated within the enzyme. Note that no catalytic response is observed for unmodified enzyme in the absence of TTF.

It is apparent that, from our discussions in section 3.8, GOx carried a net charge at pH values other than its isoelectric point. When the pH of the enzyme solution is equivalent to the protein pI, GOx molecules are neutral. Thus, at this particular pH value, the protein pI, GOx will be at its most hydrophobic and the interaction of hydrophobic mediators with the enzyme will be expected to be the strongest. It is therefore logical to investigate the incorporation of TTF with GOx at different pH values. The results are described next.

5.3 Electrochemistry of TTF Modified GOx Samples Prepared at Different pH Values

In the preparations of these TTF modified GOx samples, small quantities of surfactant (0.2% Triton X-100) were employed. The surfactant forms micelles in aqueous medium; this solubilises the TTF solids efficiently. This solubilisation of TTF may facilitate step (1) of the equilibrium in eqn. (5.2) and step (2) of the equilibrium may be consequently made easier. The surfactant can be removed effectively by gel filtration on Sephadex G-15.

Samples of TTF modified GOx were prepared at five different pH values (3.0, 4.0, 5.0, 6.0 and 7.0). At each pH, the sample preparation was carried out in the presence and absence of surfactant (Triton X-100, 0.2%). The modified enzyme samples were purified using gel filtration. Electrocatalytic activities of the TTF modified GOx samples were studied using cyclic voltammetry at a gold electrode (0.125 cm²). Enzymatic activities

of the TTF modified GOx samples were determined using the spectroscopic assay method described in section 2.4.

Figure 5.5 shows the substrate titration curves of TTF modified GOx samples prepared at pH values, 4.0, 5.0, 6.0 and 7.0, in the presence and absence of surfactant. No catalytic responses were observed for the TTF modified GOx sample prepared at pH 3.0.

It is evident that at pH values 4.0, 5.0 and 6.0, modified GOx samples prepared in the presence of surfactant show greater catalytic current than that prepared without surfactant. This confirms that the surfactant promotes the incorporation process of TTF with GOx. At pH 7.0, surfactant appears to have no significant effect on the modification of GOx with TTF.

Since the hydrophobic incorporation of TTF with GOx is a thermodynamic reaction process, the absence of surfactant may be compensated by incubating the TTF with GOx for a greater period. Figure 5.6 shows the substrate titration curves of TTF modified GOx prepared at pH 7.0, with surfactant or without surfactant for 1 hour and without surfactants for 3 hours. It is apparent that the TTF modified GOx sample prepared for 3 hours show relatively lower catalytic current than the samples prepared for 1 hour. This may be due to the loss of enzymatic activity, for the modified GOx sample prepared for 3 hours, caused by longer stirring at room temperature. The enzymatic activities for the samples of TTF modified GOx were determined using spectroscopic enzyme assay method. The results are described below.

Purified samples of TTF modified GOx from gel filtration were assayed for their enzymatic activity immediately after the samples were collected. The results are summarised in table 5.1.

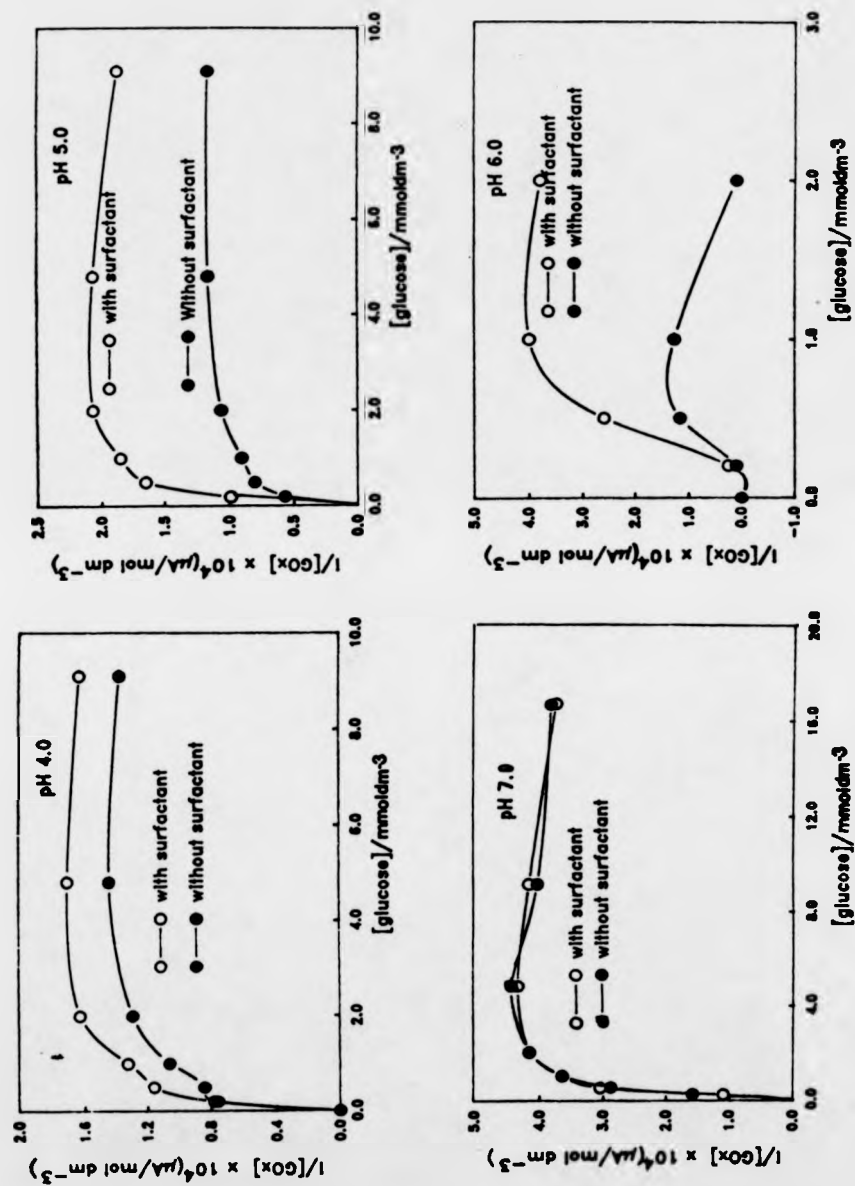


Figure 5.5 Substrate titration curves for the samples of GOx modified with TTF at pH values 4.0, 5.0, 6.0 and 7.0 in the absence and presence of surfactant (Titron X-100).
E: 0.35 V vs SCE
Electrode: Au ($0.125\ cm^2$)

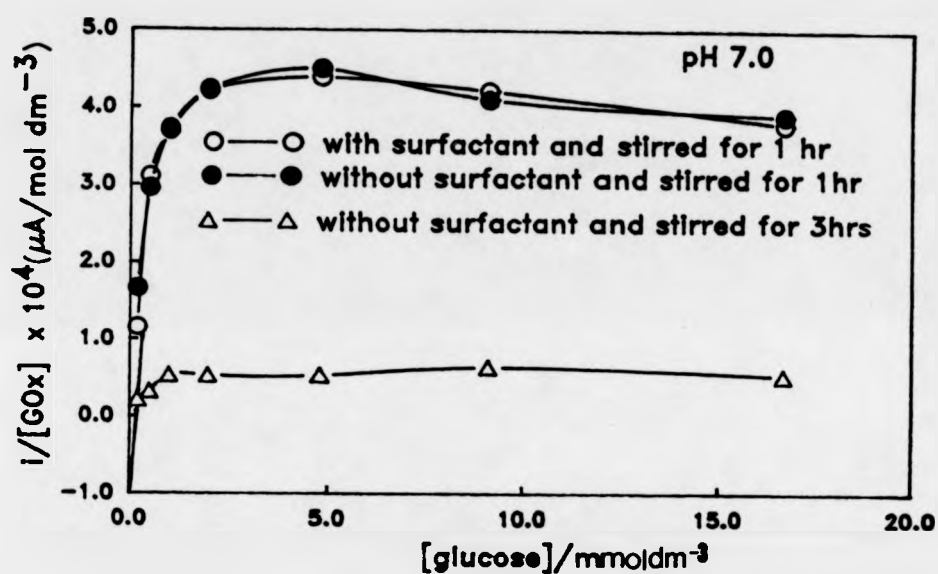


Figure 5.6 Calibration curve for TTF modified GOx prepared at pH 7.0, in the presence of surfactant (Titron X-100) for 1 hour and in the absence of surfactant for 1 hour or 3 hours.
E: 0.35 V vs SCE
Electrode: Au (0.125 cm²)

Table 5.1. Activities of GOx samples modified with TTF at different pH values

pH	Enzyme activity (U mg ⁻¹)	
	without surfactant	with surfactant
4.0	132.2	68.0
5.0	154.9	126.0
6.0	123.0	70.8
7.0	194.2	125.0
7.0	136.9 (without surfactant, 3 hours)	
	82.9 (stored at 4°C overnight)	
	182.0 (native GOx)	

The data in the table clearly demonstrate that modified GOx samples prepared with surfactant are enzymatically less active than those prepared without the surfactant. This seems to contradict the earlier results that samples of TTF modified GOx prepared in the presence of surfactant showed greater catalytic responses than those prepared in the absence of surfactant. This could be due to the fact that although less active enzymatically, modified GOx sample prepared with surfactant may incorporate greater quantities of TTF than those prepared without surfactant. The comparatively greater quantities of TTF for the modified GOx prepared with surfactant may be sufficient to compensate the loss of enzyme activity during the enzyme modification. At pH values 5.0 and 7.0, GOx modified with TTF show greater activity than those prepared at 4.0 and 6.0. Modified GOx sample prepared at pH 7.0 for 3 hours show a decrease of 30% in activity compared to that prepared for 1 hour. This is consistent with our earlier results of the catalytic responses for the same sample (figure 5.6). The modification of GOx with TTF appears to have destabilised the enzyme. At pH 7.0, the TTF modified GOx show a loss of 60% in activity when being stored at 4°C overnight.

Next, our attempts to determine the amount of TTF quantity incorporated in the enzyme are presented.

5.4 Determination of TTF Quantities for the Modified GOx

Unlike the ferrocenes modified GOx samples where the amount of mediator attached to the modified enzyme can be determined using atomic absorption spectroscopy for iron, determination of the amounts of TTF incorporated in the TTF modified GOx has proved to be difficult. First, the amount of TTF incorporated in GOx is very low so high sensitivity is required for the method of determination. Second, TTF contains elements which are also found in the amino acid residues of the enzyme thus TTF molecules cannot be distinguished from GOx using microanalysis or atomic absorption spectroscopy. We have attempted to quantify TTF mediators in GOx using fluorescence spectroscopy, UV-Visible spectroscopy and by a conventional chemical method whereby the TTF modified GOx is denatured and the incorporated TTF molecules are recovered using an organic solvent. The results of these experiments are presented below. Two other potential analytical methods are mass spectrometry of TTF modified GOx or the use of radio labelled TTF. These possibilities are also discussed.

5.4.1 *Fluorescence Spectroscopic Studies*

In biological systems, there are two types of fluorescence quenching processes which are frequently studied (174). The first type is collisional quenching which causes a decrease in the lifetime of the excited state (175-176). The second type is a result of a long-range non-radiative process called resonance energy transfer from one chromophore to another (174-176). Analysis of the latter quenching allows the distance between the chromophores to be measured.

The most common type of energy transfer is from the excited singlet of a donor to the excited singlet state of an acceptor (174). In this transfer of energy, the donor returns from the excited state to the ground state and the acceptor is simultaneously excited from its ground to its excited state. The

energy separations in each case must be in resonance. If the acceptor fluoresces, the original excitation energy reappears as acceptor emission. If the acceptor molecule is nonfluorescent, the transferred energy is dissipated by non-radiative processes.

Förster (177) has explained this resonance energy-transfer in terms of a dipole-dipole interaction between the donor and acceptor pair and obtained the following equations:

$$\text{first, } E_T = \frac{R_0^6}{R^6 + R_0^6} \quad (5.3)$$

where E_T is the efficiency for the depopulation of the excited state by resonance energy transfer,

R is the intermolecular distance, and

R_0 is the distance at which the energy transfer is 50% efficient second,

$$\frac{\Phi_T}{\Phi_D} = 1 - E_T \quad (5.4)$$

where Φ_T and Φ_D represent the quantum yields of the donor in the presence and absence of resonance-energy transfer.

Thus, from a measurement of the quenching of the fluorescence (Φ_T and Φ_D) in the presence and absence of the acceptor, R can be calculated if R_0 is known.

It is known that free flavins in the oxidised form shown an intense fluorescence with $\lambda_{\text{max}} = 530 \text{ nm}$ (209). Figure 5.7a shows an emission spectrum of FAD. However, this fluorescence is completely quenched when FAD is bound to proteins in GOx (178-180). For native GOx, only the fluorescence of tryptophan is observed, figure 5.7b.

Since the tryptophan residues are likely to be located within the hydrophobic region of GOx, their fluorescence may be quenched in the

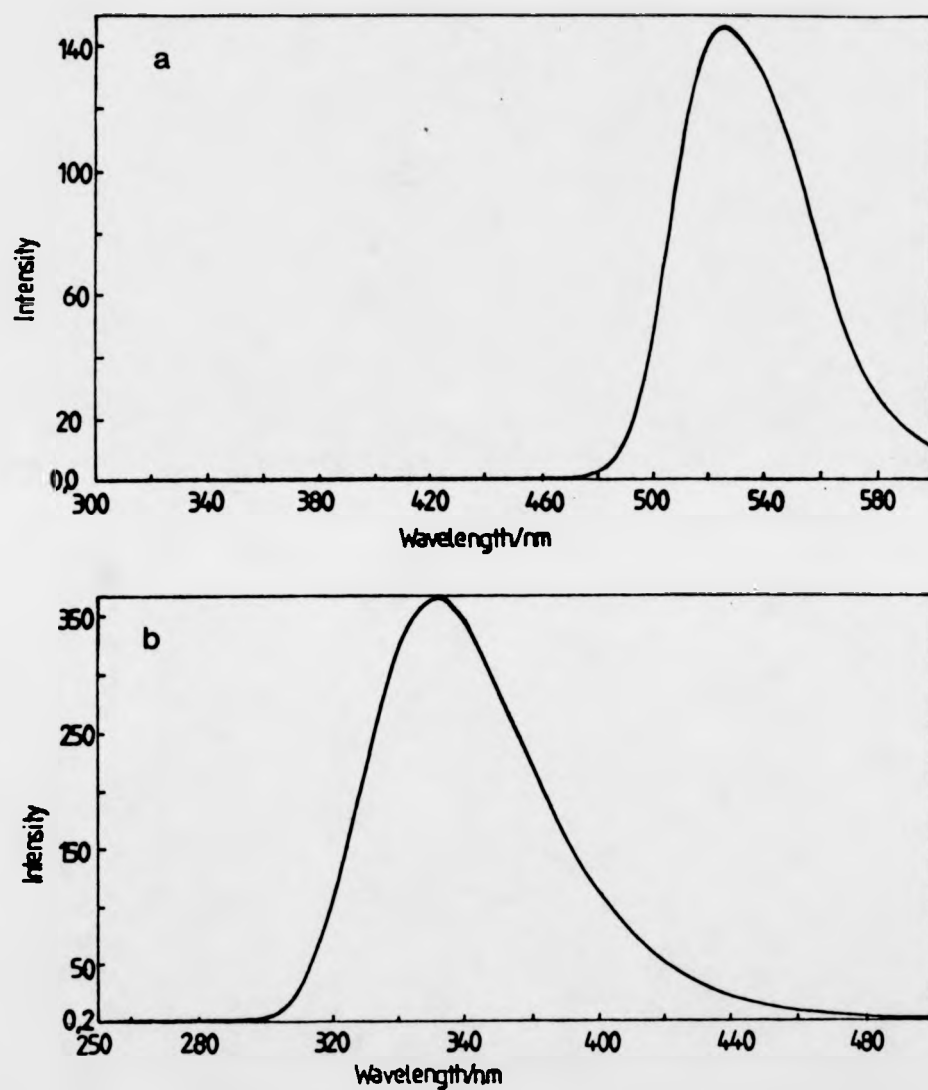


Figure 5.7 Emission spectra of FAD: (a) in H_2O , $[FAD] = 1.3 \times 10^{-4} \text{ mol dm}^{-3}$; (b) in native GOx, $[GOx] = 7.8 \times 10^{-5} \text{ mol dm}^{-3}$
 $\lambda_{EX} = 280 \text{ nm}$
 Cell path: 1 cm

presence of TTF molecules by resonance-energy transfer. Experimental results show that for TTF modified GOx, the tryptophan fluorescence intensity has decreased by a small amount compared to that of native GOx, figure 2.8. It is clear that, from figure 2.8, $I_T = 136.3$, $I_D = 143.2$ where I_T and I_D are the fluorescence intensities in the presence and absence of energy transfer respectively.

Using equation (5.4) and considering correction for concentration,

$$E_T = 1 - \frac{I_T}{I_D} \cdot \frac{[GOx]_{nat}}{[GOx]_{mod}} = 1 - \frac{136.3}{3.2 \times 10^{-6}} \cdot \frac{2.8 \times 10^{-6}}{143.2} \quad (5.5)$$

$$= 1 - 0.83 = 0.17$$

Thus from eqn. (5.3), $\frac{R}{R_0} = 1.31 \quad (5.6)$

This demonstrates that TTF molecules have been incorporated into GOx. The fluorescence of tryptophan residues are quenched in the presence of TTF molecules and the distance between the TTF molecules and the tryptophan residues may be obtained if R_0 is known.

R_0 is a constant for each donor-acceptor pair. The value of R_0 (in nanometers) can be obtained from the expression,

$$R_0 = 9.79 \times 10^3 (J \bar{n}^4 k^2 \Phi_D)^{1/4} \quad (5.7)$$

where n is the refractive index of the medium, Φ_D is the quantum yield of the energy donor (in the absence of acceptor), k^2 is the orientation factor between the donor and acceptor electric transition dipole moments and it is often assumed to be $2/3$, J is the integral of the spectral overlap of the absorption spectrum of the acceptor and the emission spectrum of the donor. The value of J is usually calculated graphically. A detailed discussion on the calculation of R_0 can be found in reference (174).

5.4.2 UV-Visible Spectroscopic Studies

We have attempted to detect TTF molecules incorporated in GOx using UV-Visible spectroscopy. When dissolved in an organic solvent or in aqueous solution with surfactant (e.g. Triton X-100), TTF shows an adsorption peak at around 300 nm, figure 5.8 (3). Although the UV-Visible spectrum of TTF modified GOx closely resembled that of native GOx, a slight increase in absorption at 270 nm is apparent due to the presence of TTF, figure 5.8 (1, 2). This result also confirms that TTF molecules have been incorporated into GOx.

The UV spectrum for a solution of TTF saturated buffer shows no absorption in the visible region. This is consistent with the observation (7) that TTF is insoluble in aqueous solution.

Quantitative determination for the amounts of TTF in GOx cannot be carried out at the present since we do not have any estimation of the extinction coefficient for the TTF incorporated in the enzyme. More detailed UV-Visible spectroscopic studies are needed.

5.4.3 Attempts for Determination of the Amount of TTF Using a Conventional Chemical Method.

Attempts were made for the determination of TTF taking advantage of the high solubility of TTF in most organic solvents. The proteins in the TTF modified GOx were precipitated using 5% trichloroacetic acid (TCA). The supernatant and precipitate were washed repeatedly with cyclohexane to retrieve the incorporated TTF molecules. In this experiment, a significantly greater amount of modified GOx sample was used (20 times greater than that used previously). Although it seems that some TTF have been transferred to cyclohexene, the amount is too low to pursue any further analysis. It is possible that the experiment may succeed when even a greater amount of modified GOx is employed.

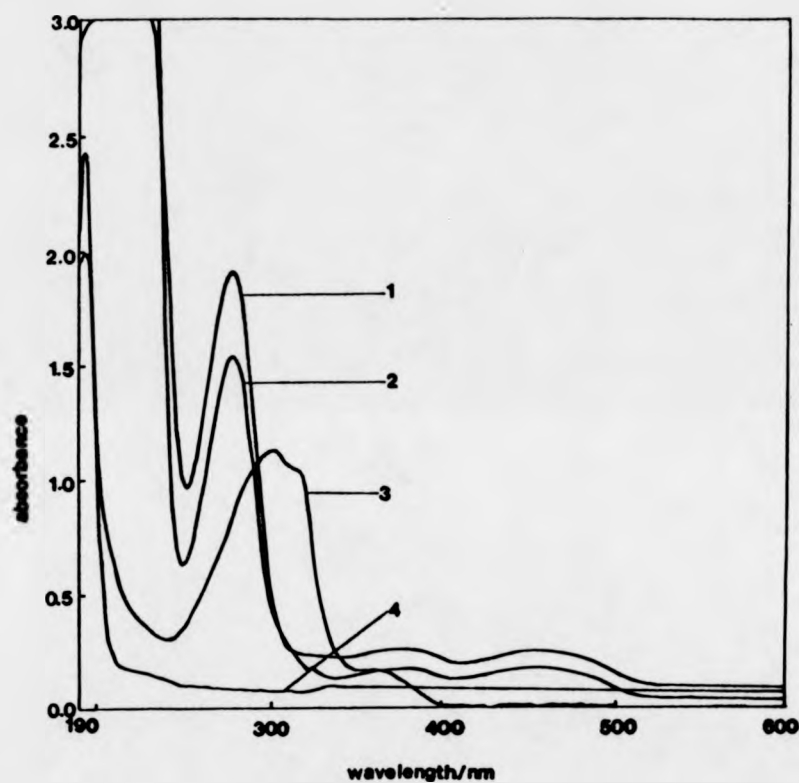


Figure 5.8

UV - Visible spectra of: 1. purified sample of TTF modified GOx, $A_{280} = 0.17$; 2. native GOx, $A_{280} = 0.18$; 3. TTF in EtOH, $[TTF] = 7 \times 10^{-4} \text{ mol dm}^{-3}$; 4. TTF saturated in buffer (0.15 mol dm^{-3} sodium phosphate containing 0.2 mol dm^{-3} NaCl, pH 7.0). Cell path: 1 mm

This method requires large quantities of modified enzyme sample and its many operation procedures will unavoidably bring in experimental errors. It is the least accurate method among the three discussed so far.

Mass spectrometry may be used to detect TTF molecules in the modified enzyme. It is highly recommended since this is a method of high precision and it requires a small amount of sample. However, mass spectrometry for large proteins such as GOx with a MW of 186,000 Dalton is difficult to carry out in reality.

Using radiolabelled TTF to modify GOx seems to be a simple method to practice. TTF may be tritiated or synthesized with radio active carbon or sulphur isotopes. The traces of radiation from radio-labelled TTF molecules in GOx can then be easily followed. This is also a method worthy of pursuing in the future.

The working stabilities of TTF modified GOx were also studied using membrane enzyme electrodes. The results are presented in the next section.

5.5 Stability Studies of TTF Modified GOx

In Chapter IV, we have demonstrated that membrane enzyme electrodes are an effective means to study the working stabilities of GOx covalently modified with FMCA or FAA. We now construct membrane enzyme electrodes with TTF modified GOx and to investigate the stabilities of this modified enzyme.

The membrane enzyme electrodes were prepared as described in section 2.7. Each freshly prepared membrane electrode was equilibrated firstly by soaking in buffer (0.15 mol dm^{-3} sodium phosphate containing 0.2 mol dm^{-3} NaCl, pH 7.0) at room temperature for 30 minutes and secondly in the same buffer but with the electrode held at a fixed potential of 0.20 Volts (vs SCE) for a few minutes until a steady background current was obtained.

Aliquots of glucose (1.0 mol dm^{-3}) were then added and the responses were recorded at this fixed potential.

For the five membrane enzyme electrodes prepared with TTF modified GOx (enzyme loading ranging from 0.04 mg to 0.24 mg), two electrodes (enzyme loadings are: 0.08 and 0.16 mg) showed no catalytic responses and only very small catalytic currents were observed for the remaining three electrodes (enzyme loadings are: 0.04 mg, 0.12 mg and 0.24 mg respectively). However, when free FAA mediator ($1.0 \times 10^{-3} \text{ mol dm}^{-3}$) was added to the solution and the same membrane enzyme electrodes were again employed for substrate titration studies, large catalytic currents (a few thousand times greater than those obtained in the absence of free mediators) were observed. This suggests that the TTF modified GOx in the membrane electrodes was still enzymically active. The apparent low catalytic responses for the membrane enzyme electrodes may be due to the low quantities of the TTF incorporated or the loss of the TTF incorporated in GOx. The loss of TTF molecules is likely to be the cause since during substrate titration studies, the membrane electrodes were held at oxidising potentials so that the TTF molecules would be oxidised to TTF^+ . TTF^+ is water-soluble (181), therefore the TTF^+ ions can diffuse out of the enzyme and through the membrane to be lost to the bulk solution. When incubated at a constant potential of 0.2V (vs SCE) in saturated glucose (0.1 mol dm^{-3}), the half life of a membrane enzyme electrode (0.24 mg TTF modified GOx) was found to be around 2 to 3 minutes.

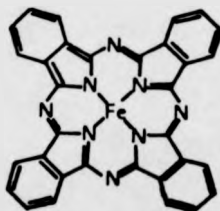
It is evident from the above studies that, the membrane enzyme electrodes constructed with TTF modified GOx have very poor stability. The low catalytic responses observed for these electrodes are likely to be caused by the loss of oxidised form of TTF.

5.6 Non-covalent Modification of GOx with Iron(II)phthalocyanine and Some Ferrocene Derivatives.

Above, we have described non-covalent modification of GOx with TTF and the studies of this TTF modified enzyme. We will now extend this non-covalent modification method to use other hydrophobic electroactive species to modify GOx. The non-covalent modifications of GOx with iron (II) phthalocyanine (FePc) and some water-insoluble ferrocene derivatives are described in this section. Results for the catalytic activities of modified enzymes are presented. The quantities of mediator incorporated in GOx were determined using atomic absorption spectroscopy for iron.

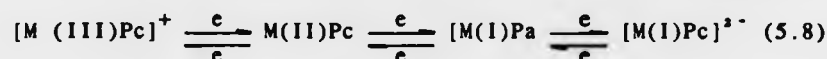
5.6.1 *Electrochemistry of FePc*

Metallo-phthalocyanines (MPcs) catalyze a wide variety of oxidations and reductions (182-191). These macrocyclic complexes have been used as both homogeneous and heterogeneous catalysts (192); in some cases deposited on electrode surface as films with semiconductor and electrochromic properties (185). Our interest in MPc's is as electron mediators for the non-covalent modifications of enzymes. Iron(II) and cobalt(II) phthalocyanines are of particular interest since electrons can be transferred to and from the central metal atoms. These compounds are considered to be models for porphyrin and corrin complexes which play a central role in biological redox reactions (182-184). The structure of FePc is shown below.



Iron(II)phthalocyanine

In non-aqueous solvents, FePc and CoPc undergo the following reactions (193-197):



It is well established that the first one-electron reductions of Fe(II)Pc and Co(II)Pc occur at the metal centre (192). Reduction of the $[M(I)Pc]^{\cdot-}$ species involves the phthalocyanine ring and leads to a $[M(I)Pc]^{\cdot-}$ radical anion (192).

We have studied the electrochemical behaviour of Fe(II)Pc using cyclic voltammetry with a variety of electrode materials. Figure 5.9 shows CVs of FePc recorded at edge plane graphite (EPG), basal plane graphite (BPG), glassy carbon, platinum and gold electrodes.

It is evident that the CVs of FePc recorded using different electrodes vary with the electrode materials. On EPG and BPG electrodes, three pairs of oxidation and reduction peaks are clearly visible (figure 5.9, a and b). On glassy carbon electrode these peaks are slightly distorted (figure 5.9, c). On platinum and gold electrodes, CV of FePc are completely distorted (figure 5.9, d and e). The cause of this CV distortion at Pt, Au and glassy carbon electrodes is unknown at the present but these differences probably reflect adsorption of FePc at the electrode surfaces.

The first step of reduction in eqn. (5.8) is the one that interests us since it is the reduction of the metal ion, for FePc, the half wave potential for this process is 65-70 mV (vs SCE). This potential is sufficient to reoxidise reduced GOx ($E_{1/2}$ for FAD - 0.250 Volts vs SCE) and thus in principle, FePc can be used as an electron transfer mediator for the reoxidation of GOx.

Next, electrocatalytic activities of FePc modified GOx are presented.

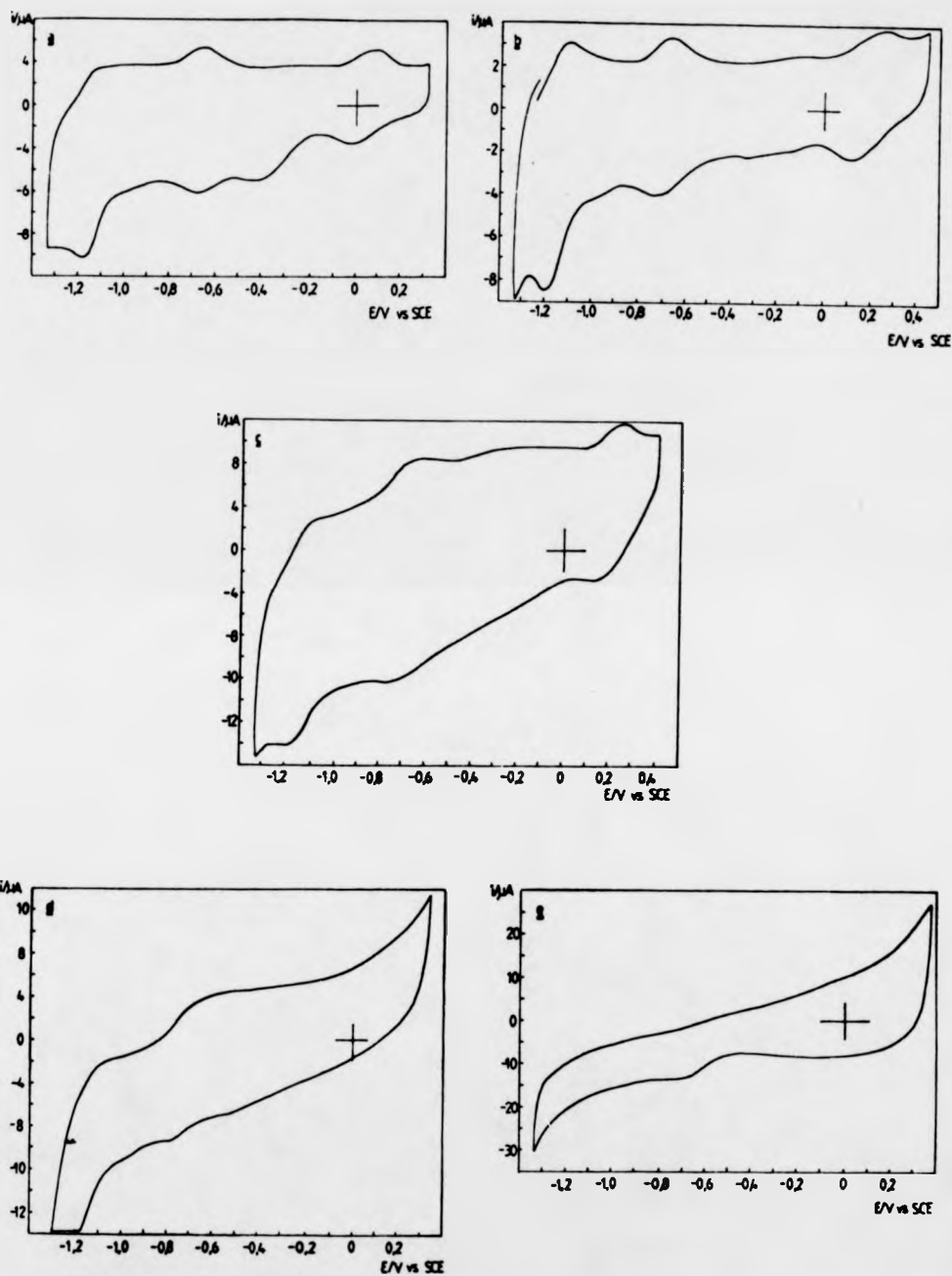


Figure 5.9 Electrochemistry of iron(II)phthalocyanine at different electrode surfaces: a. edge plane graphite (GP/E), b. basal plane graphite (GP/B), c. glassy carbon (GC/K), d. platinum (PLT/KT), E. gold electrode (Au/T).
Solvent: DMSO
Electrolyte: $0.1 \text{ mol dm}^{-3} \text{ LiCl}$
Sweep rate: 100 mV s^{-1}

5.6.2 Catalytic Activity of FePc Modified GOx

GOx was modified with FePc using hydrophobic incorporation. In 2 cm³ buffer (0.15 mol dm⁻³ sodium phosphate containing 0.20 mol dm⁻³ NaCl, pH 7.0), urea (360 mg), stock GOx (25.9 mg) and excess FePc solid were added together with surfactant Triton X-100 (0.2% v/v). The mixture was stirred at room temperature for 2 hours.

The undissolved FePc was filtered off using a 0.22 μ m membrane filter and the clear enzyme solution was further purified using gel filtration on Sephadex G-15.

The FePc modified GOx has a very distinct lime green colour. Figure 5.10 shows UV spectra of native and FePc modified GOx. This green colour of FePc modified GOx may be due to the combination of the yellow colour of FAD and the dark blue colour of FePc incorporated in GOx.

A sample of FePc modified GOx (0.5 cm³) was placed in a micro-cell and deoxygenated for 15-20 minutes. Aliquots of glucose were then added and the catalytic responses were recorded using cyclic voltammetry over potential range of -0.1 to 0.4V (vs SCE) at a gold electrode (0.125 cm²). A substrate titration curve for the sample of FePc modified GOx is shown in figure 5.11.

The results clearly demonstrate that FePc modified GOx can undergo direct oxidation in the absence of an homogeneous mediator suggesting that the modification is successful. AAS experiments show that an average of three FePc molecules have been incorporated into each GOx molecule.

Ferrocene derivatives are the most commonly used mediators for GOx oxidation. Since many ferrocene compounds can also be very hydrophobic, it may be possible to use these compounds to non-covalently modify GOx. This is the subject of study for the following section.

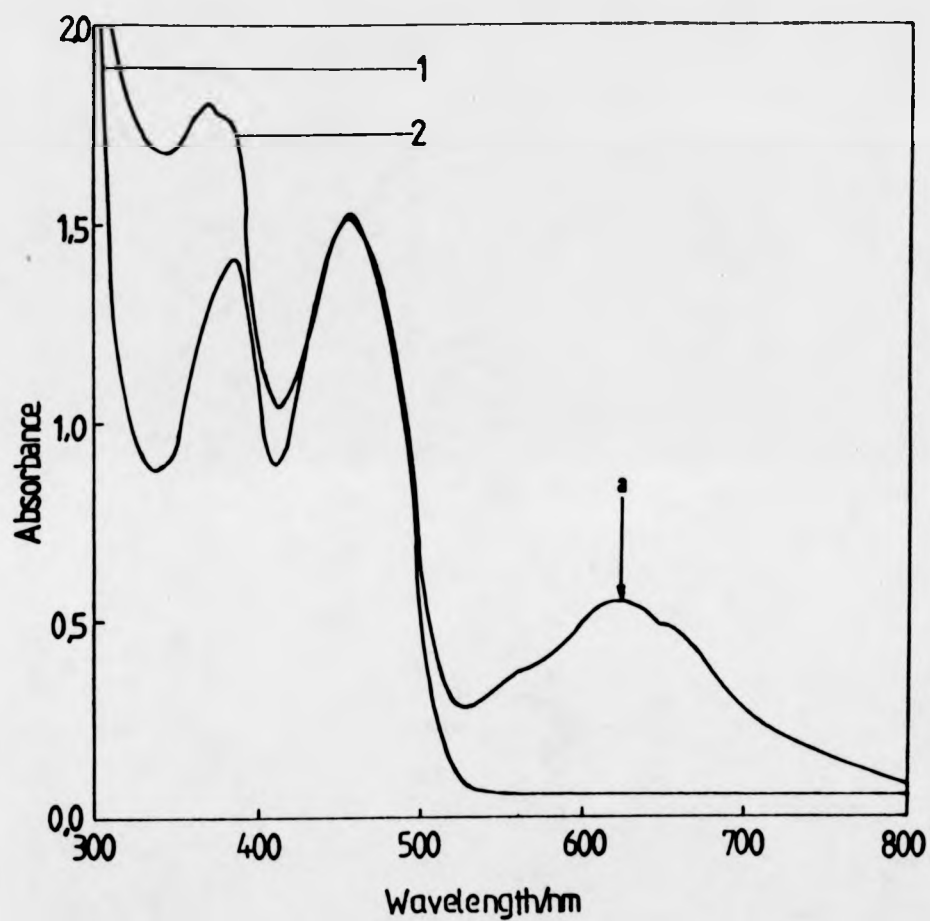


Figure 5.10 UV-visible spectra of GOx: 1. native, $[GOx] = 5.3 \times 10^{-5} \text{ mol dm}^{-3}$
 2. modified with FePc, $[GOx] = 5.3 \times 10^{-5} \text{ mol dm}^{-3}$. peak a: characteristic absorption for the FePc modified GOx
 Cell path: 1 cm
 Buffer: 85 mmol dm^{-3} phosphate, pH 7.0

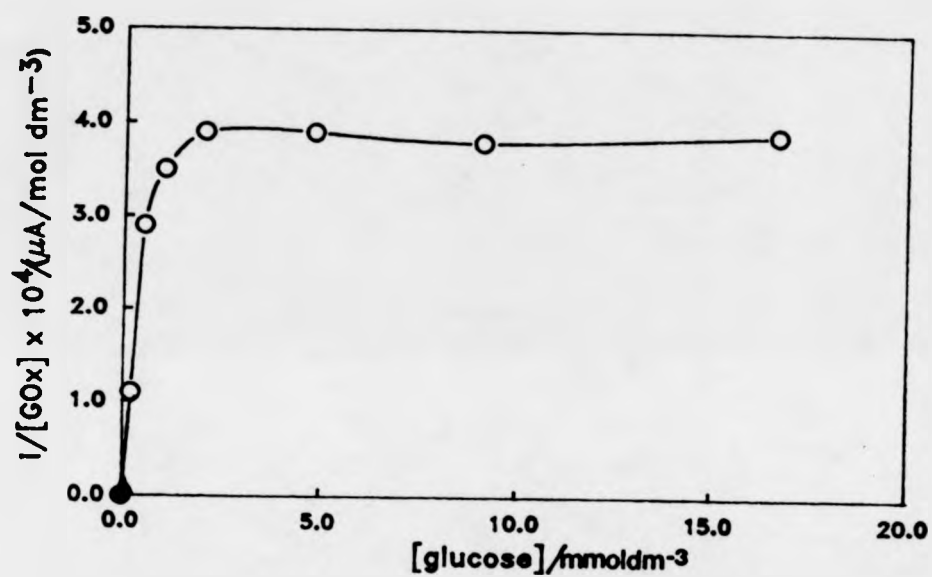


Figure 5.11 Substrate titration curve of FePc modified GOx
E: 0.35 V vs SCE
Electrode: Au (0.125 cm²)

5.6.3 Non-Covalent Modification of GOx with Water-Insoluble Ferrocenes.

Seven water-insoluble ferrocenes were used to modify GOx non-covalently. Their structures are given in figure 5.12.

The non-covalent modification and purification of GOx with ferrocene derivatives were carried out using the method described above. Catalytic responses for each modified GOx in the presence of glucose were investigated using cyclic voltammetry at a platinum electrode over the potential range 0-0.5 V (vs SCE).

Of all the samples of GOx non-covalently modified with ferrocene derivatives, only ferrocene derivative (I), FD (I) modified GOx sample showed catalytic activity when glucose is present, figure 5.13, 5.14. Results from AAS show that an average three FD (I) molecules per enzyme are present for this modified GOx.

The successful modification of GOx with FD (I) is consistent with the fact that FD (I) is the most insoluble compound among the ferrocenes studied, thus it is most likely to be incorporated into the hydrophobic environment of GOx.

5.6.4 A Comparison of the Catalytic Activities for GOx Modified with Different Mediators

So far we have described two types of modified glucose oxidases: first, the covalently modified GOx with either FMCA or FAA (Chapters III and IV); second, the non-covalently modified GOx with TTF, FePc or a ferrocene derivative, FD (I). The efficiency of different enzyme modification is now compared and discussed.

In table 5.2, the values of limiting currents for GOx modified with different mediators are given.

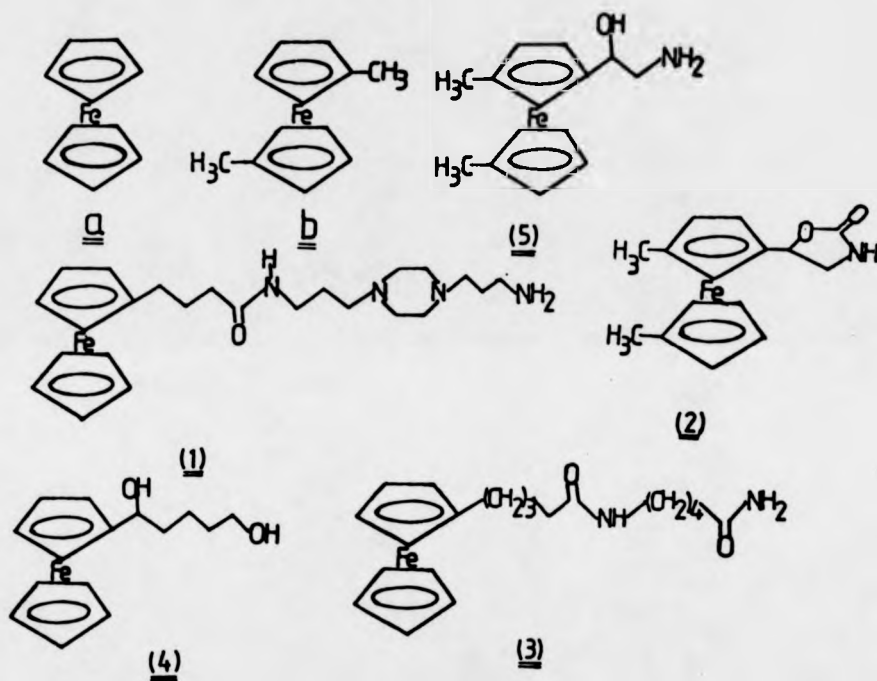


Figure 5.12 The structures of some ferrocene derivatives used for enzyme modification.
 a. ferrocene (parent), b. 1,1'-dimethyl ferrocene.
 The other ferrocene derivatives listed are nominated as FD(1), FD(2), FD(3), FD(4) and FD(5) respectively.

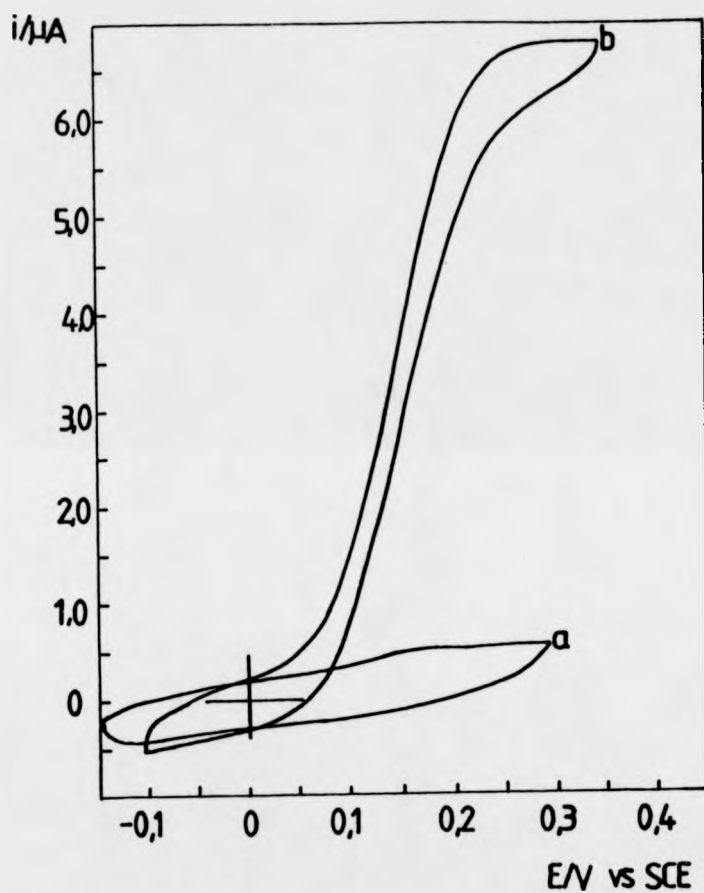


Figure 5.13 Cyclic voltammograms of GOx modified with a ferrocene derivative, FD(1): a. in the absence of glucose, b. in the presence of glucose (8 mmol dm^{-3}). $[\text{GOx}] = 4.0 \times 10^{-5} \text{ mol dm}^{-3}$
Electrode: platinum (0.35 cm^2)
sweep rate: 5 mV s^{-1}

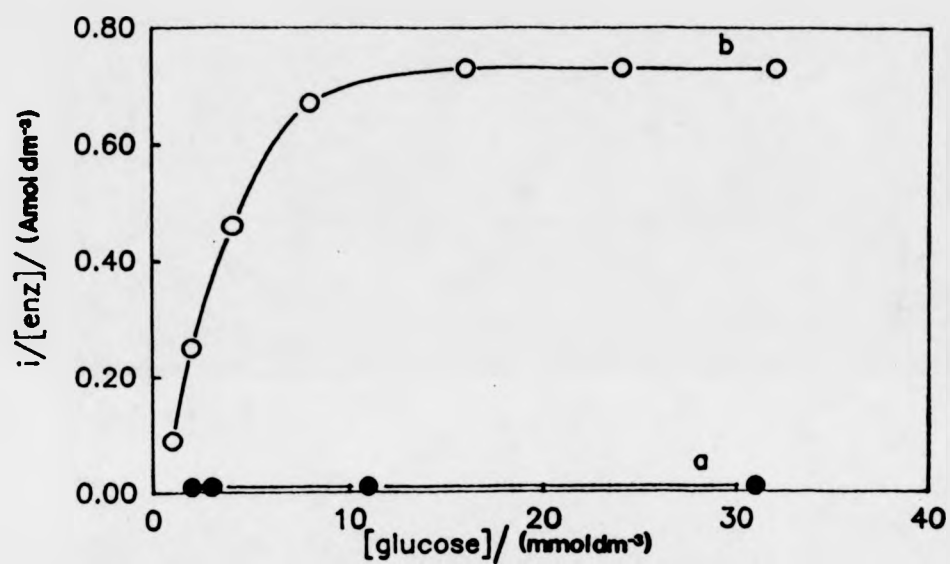


Figure 5.14 Glucose calibration curves for the samples of GOx modified with a ferrocene derivative, FD(1):
 a. solution of saturated FD(1) in buffer (85 mmol dm⁻³ phosphate, pH 7.0), with a known concentration of enzyme, [GOx] = 1.0 x 10⁻⁶ mol dm⁻³; b. FD (1) modified GOx, purified by gel filtration, [GOx] = 4.02 x 10⁻⁶ mol dm⁻³

Table 5.2 The values of limiting currents for GOx modified with different mediators

Mediator modified GOx (pH7.0)	Electrode area (cm ²)	$i_{Lim}/[GOx]$ ($\mu\text{A mol}^{-1} \text{dm}^2$)	k_{cat} (s ⁻¹)
FMCA	0.384	8.4×10^4	5 ⁽¹²²⁾
FAA	0.384	2.1×10^5	1100 ⁽¹²²⁾
TTF	0.125	4.4×10^4	
FePc	0.125	4.0×10^4	
FD (1)	0.384	7.2×10^4	

The data clearly shows that, at saturated substrate concentrations, GOx modified with either FMCA or FAA exhibit larger catalytic currents than that of GOx modified with TTF, FePc or FD (1). The values of limiting currents are comparable for TTF, FePc or FD (1) modified GOxs taking into consideration of the differences in electrode areas. Our earlier studies have shown that GOx modified with FMCA has relatively poorer working stability than FAA modified GOx due to the poorer instability of the Fe³⁺ in FMCA. Our results also show that GOx modified with TTF is very unstable owing to the exit of TTF⁺ from the enzyme. Thus, it is clear that FAA modified GOx gives the largest catalytic currents and is the most stable amongst the different mediators modified GOxs.

5.7 Conclusions

In this chapter, we have described a novel enzyme modification method, the non-covalent modification of glucose oxidase with hydrophobic mediators. It is evident that, in this method, the enzyme is modified via inter-molecular interaction and not by chemical bonding. The principal of this modification method is that GOx has a hydrophobic interior (173) thus water-insoluble

mediator molecules are likely to be incorporated into the enzyme and act as electron transfer relays. We have demonstrated that GOx modified with hydrophobic materials, TTF, FePc and FD (1) undergo direct electrochemistry at metallic electrode surfaces and exhibit catalytic activity in the presence of glucose.

The successful modification of GOx with TTF has provided us with vital information to explain the mechanism of enzyme catalysis at conducting organic salt electrodes. It seems that as TTF.TCNQ is in equilibrium with its neutral components TTF⁰ and TCNQ⁰, and TTF⁰, TCNQ⁰ are both water-insoluble, thus direct electron transfer of enzymes at these electrode surfaces may be through the TTF⁰ or TCNQ⁰ molecules incorporated inside the enzyme. Although complete theoretical support for this model has not yet been published at present, experimental results clearly show that modification of GOx with TTF⁰ or TCNQ⁰ at the conducting organic salt electrode surface is likely to take place.

This non-covalent enzyme modification method is simple to carry out and can be used with many hydrophobic mediators. The modification of GOx with FePc clearly demonstrates that GOx can be modified with non toxic hydrophobic mediators. This kind of modified enzyme could well be used to develop *in vivo* biosensors if their stability can be improved.

The hydrophobic interactions between proteins and mediators are further investigated in the next chapter where the incorporation of TTF in aqueous/BSA media is presented.

CHAPTER VI ELECTROCHEMICAL STUDIES OF TTF OXIDATION IN AQUEOUS/BSA MEDIA

This chapter describes the studies for the oxidation of TTF, solubilized in a solution of bovine serum albumin (BSA). For this system we found behaviour similar to that observed by Eddowes and Grätzel for the oxidation of TTF solubilized in cetyl trimethylammonium chloride (CTAC) micellar media (198-199). Our results show that the hydrophobic region in BSA presents a similar environment to that found in the surfactant micelles. The oxidation of TTF solubilized in BSA was studied using stationary electrode and rotating disc voltammetry. The results are presented and an analysis of the results, following the method of Eddowes and Grätzel is also given.

6.1. Introduction

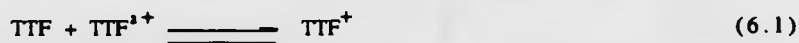
Electrochemical studies of redox species solubilized in micellar media have been carried out by a number of research groups (158, 200-202). Surfactant micelles incorporating solubilized redox species are of interest both as models for the distinct microenvironments present in biological membranes and enzymes (203) and as a means of kinetic control of light induced electron transfer events in proposed artificial photosynthetic systems (204). The mechanistic studies of such model systems using electrochemical methods may provide information for example, on the solubilization equilibria of the electroactive species between hydrophilic and hydrophobic environments.

Eddowes and Grätzel (198-199) reported detailed studies of the oxidation of TTF in aqueous/CTAC solution, using cyclic voltammetry and rotating disc voltammetry. Using these techniques they derived a variety of both thermodynamic and kinetic information about the system. Their results indicate that, in aqueous/CTAC micellar solution, TTF may be electrochemically oxidized in two consecutive one-electron steps, first to the

radical monocation TTF^+ , and then to the dication TTF^{2+} . The first oxidation step is electrochemically reversible and diffusion controlled, which provides a value of the diffusion coefficient for TTF in CTAC of $D = 7.3 \times 10^{-11} \text{ m}^2 \text{ s}^{-1}$.

They determined the half wave potential for the first oxidation step from cyclic voltammograms and rotating disc voltammograms and obtained $E_{1/2} = 170$ and 160 mV vs SCE respectively. The authors concluded that the difference in half-wave potentials determined by the two techniques is consistent with a difference in diffusion coefficients between the reduced and oxidised species, $D_O/D_R = 13 (\pm 6)$. This difference in diffusion coefficient indicates that the neutral, reduced TTF species is predominantly solubilized in the micellar phase while the oxidised mono- and di- cations of TTF are solubilized predominantly in the aqueous phase. They obtained a micelle/solubilize association equilibrium constant, $K_M = 8 \times 10^4 \text{ mol}^{-1} \text{ dm}^3$ for the solubilisation of TTF in CTAC.

The authors found that oxidation of the micellar TTF species to its aqueous cation radical proceeds via the species in the aqueous phase and is proceeded by the exit of TTF species in a reaction layer close to the electrode surface. They observed no direct electron transfer between the electrode and the micellar species itself. They studied the homogeneous solution reaction of TTF with its electrochemically generated dication to form the monocation,



and found that this reaction also proceeded predominately via species in the aqueous phase. Reaction (6.1) may be directly accountable for the large current observed for the second oxidation step as compared with that due to the first oxidation in their experiments.

The studies of TTF in aqueous/micellar solution described above clearly demonstrate the potential of electrochemical methods as a means to gain an understanding of basic properties of such systems, including solubilization equilibrium and the kinetics of the exchanges of species between aqueous and micellar phases.

The existence of hydrophobic amino acid side chains in protein molecules suggests the possibility of interaction between proteins and small water-insoluble species. In this chapter, we present kinetic studies for the oxidation of TTF solubilized in BSA. This work is aimed at providing an understanding of the heterogeneous and homogeneous electron transfer reactions of TTF to its mono- and dications in aqueous/BSA solutions. The TTF/BSA system serves as an intermediate model system for the interaction between TTF and GOx (Chapter V) because BSA is inexpensive and well studied. An understanding of the kinetic processes of TTF oxidation in BSA solution should enable us to gain further knowledge of the mechanism of the incorporation of TTF in GOx and the role of TTF as electron transfer mediators in the modified GOx.

Since the analysis of our results for TTF/BSA system was carried out following the method by Eddowes and Grätzel for TTF oxidation in aqueous/CTAC micellar solutions, we will now briefly describe their work.

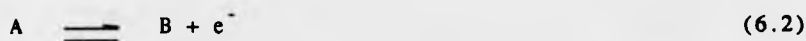
6.2. Theory

Eddowes and Grätzel established a detailed theoretical model for the oxidation of TTF in aqueous/CTAC media (198-199). The theory describes, first, the relationships between the micelle solubilization constant, the formal potential, E° , and the observed reversible half-wave potential, $E_{1/2}^r$, for a micelle solubilized redox species. Second, a proposed reaction scheme and the corresponding steady-state rotating disc electrode (RDE) response for a one-electron process are described. Third, the kinetics of the two-electron-

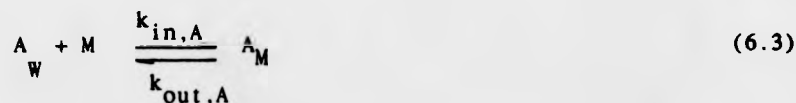
transfer process in micellar media are outlined. The first two aspects of the theory are used in the analysis of our data thus their details are described below.

6.2.1 *Relationships between the Micelle Solubilization Equilibrium Constant, the Formal Potential ($E^{\circ'}$) and the Observed Reversible Half-Wave Potential ($E^{\circ'}_{1/2}$).*

Consider the one-electron transfer process,



for the couple A/B in micellar media, where the oxidized form B, is completely solubilized in the aqueous phase and the reduced form A, is predominately solubilized in the micelles and undergoes phase exchange, where



In equation (6.3), M represents the micelle, k_{in} and k_{out} are the rate constants for micelle entry and exit, subscripts W and M refer to aqueous and micellar species respectively. Thus the equilibrium constant, K_A , for the solubilization can be defined as:

$$K_A = k_{in,A} [M] / k_{out,A} = [A_M]_{eq} / [A_W]_{eq} \quad (6.4)$$

Similarly, the solubilization equilibrium for species B can be defined by the corresponding constant K_B . The equilibrium potentials (E_W , E_M) and formal potentials ($E_W^{\circ'}$, $E_M^{\circ'}$) of the redox species in aqueous and micellar

phases can be expressed by:

$$E_W = E_W^{*'} + (RT/nF) \ln ([B_W]/[A_W]) \quad (6.5)$$

$$E_M = E_M^{*'} + (RT/nF) \ln ([B_M]/[A_M]) \quad (6.6)$$

At equilibrium, the potentials of the aqueous and the micellar phases must be equal, thus by equating eqn. (6.5) and (6.6), and substituting the equilibrium concentrations with the solubilization constants K_A and K_B , the following expression is obtained:

$$\exp (\psi_{M/W}^0) = \frac{(1 + K_A) K_B}{(1 + K_B) K_A} \exp (\psi_M^0) = \frac{(1 + K_A)}{(1 + K_B)} \exp (\psi_W^0) \quad (6.7)$$

where $\psi^0 = (nF/RT)E^0$ and the subscripts M/W refer to the mixed aqueous/micellar systems. Since species B is assumed to be predominantly dissolved in the aqueous phase, $K_B \ll 1$, and (6.7) can be rewritten as:

$$\exp (\psi_{M/W}^0) \approx (1 + K_A) \exp (\psi_W^0) \quad (6.8)$$

Equation (6.8) demonstrates that the observed shift in the formal potential between aqueous/micellar media is related to the solubilization equilibrium constant, K_A .

Commonly, the potential of a system measured in voltammetry is the half-wave potential, $E_{1/2}$. The reversible half-wave potential, $E_{1/2}^r$ and the formal potential, $E^{*'}$, are related by:

$$E_{1/2, CV}^r = E^{*'} - (RT/nF) \ln (D_B/D_A)^{1/2} \quad (6.9)$$

for cyclic voltammetry and

$$E_{1/2, RDE}^r = E^{0'} - (RT/nF) \ln (D_B/D_A)^{1/2} \quad (6.10)$$

for the rotating disc electrode.

6.2.2 Reaction Scheme for the One-Electron Transfer Process.

As described earlier, the electrochemical oxidation or reduction of a micelle solubilized species is assumed to involve the exit of the species from the micelle prior to electron transfer. The reaction sequence is:

$$A_{M\infty} \xrightarrow{k_{DA}} A_{Ms} \text{ (mass transport to the electrode surface)} \quad (6.11)$$

$$A_{Ms} \xrightarrow[k_{in}]{k_{out}} A_{Ws} \text{ (exit from micelle at the electrode surface)} \quad (6.12)$$

$$A_{Ws} \xrightarrow[k_{-e}]{k_e} B_{Ws} \text{ (electron transfer at the electrode surface)} \quad (6.13)$$

$$B_{Ws} \xrightarrow{k_{DB}} B_{W\infty} \text{ (mass transport of product to the bulk of solution)} \quad (6.14)$$

Where k_{DA} (ms^{-1}) and k_{DB} (ms^{-1}) are rate constants describing mass transport rates of the reduced species A and the oxidised species B respectively. For the mass transport of A from bulk to the RDE surface, k_{DA} is given by the Levich equation:

$$k_{DA} = 1.554 D_A^{1/2} \nu^{-1/6} \omega^{1/2} \quad (6.15)$$

(parameters of Levich equation have been defined in section 3.2). k_{out} and k_{in} are the micelle-exit (s^{-1}) and entry ($\text{mol}^{-1} \text{ dm}^3 \text{ s}^{-1}$) rate constants for the micellar and the aqueous species, k_e and k_{-e} are the potential-dependent electron-transfer rate constants for oxidation and reduction. They are given by:

$$k_e = k_e^0 \exp [\alpha(nF/RT) (E - E_w^{0'})] \quad (6.16)$$

and

$$k_{-e} = k_e^0 \exp [-\beta(nF/RT)(E - E_w^{0'})] \quad (6.17)$$

k_e^0 is the standard electrochemical rate constant, $E^{0'}$ is the formal potential for A_w/B_w couple and α, β are transfer coefficients.

Under steady-state conditions, the flux at the RDE can be written as:

$$j = k_{DA} ([A_M]_{\infty} - [A_M]_s) \quad (6.18)$$

$$= (D_w/x_R) ([A_M]_s / K_A - [A_w]_s) \quad (6.19)$$

$$= k_e [A_w]_s - k_{-e} [B_w]_s \quad (6.20)$$

$$= k_{DB} ([B_w]_s - [B_w]_{\infty}) \quad (6.21)$$

In equation (6.19), x_R is the reaction layer thickness, given by

$$x_R = \sqrt{D_w/k_{in}[M]} \quad (6.22)$$

Elimination of the surface concentrations in eqns. (6.18) - (6.21), and for the oxidation of A to B, B is initially absent from the bulk of solution ($[B_w]_{\infty} = 0$), gives an equation similar to the Koutecky-Levich equation:

$$1/j = 1/[A]_{\infty} (1/k_{DA} + K_A \exp(-\psi)/k_{DB} + K_A/k_e + 1/k_R) \quad (6.23)$$

where $\psi = (nF/RT) (E - E_w^{0'})$.

The first two terms in the bracket in eqn. (6.23) describe the dependence of flux on mass transport, the third term represents the electron-transfer step and the fourth term describes that of the micelle-exit step. The rate constant, k_R (ms^{-1}), describing micelle-exit, is given by:

$$k_R = D_w/K_A x_R = \sqrt{D_w k_{out}^2/k_{in}[M]} \quad (6.24)$$

In the following sections, our studies for the oxidation of TTF, solubilized in BSA solution and a kinetic analysis using above theoretical model, are presented.

6.3 Determination of TTF Concentrations in BSA

This section describes the determination of TTF concentration using UV-Visible spectroscopy. When dissolved in a BSA solution, TTF shows an absorption maximum at 320 nm (figure 2.13). This absorption maximum was used to determine, first, the extinction coefficient of TTF in BSA at this wavelength, and subsequently, the relative concentrations of saturated TTF in BSA solutions.

6.3.1 *The Extinction Coefficient of TTF in BSA at 320 nm.*

Different quantities of TTF were dissolved in BSA solutions of identical concentrations (195 mg cm^{-3}). UV adsorption at 320 nm for these TTF/BSA solutions were recorded and plotted against the corresponding calculated TTF concentrations (figure 2.14). The slope of this plot was used to estimate the extinction coefficient and a value of $5.9 \times 10^5 \text{ mol}^{-1} \text{ dm}^3 \text{ cm}^{-1}$ was found. This value for the extinction coefficient of TTF in BSA at 320 nm is lower than that of TTF in aqueous/CTAC micellar solution, for which Eddowes and Grätzel gives a value of $1.2 \times 10^6 \text{ mol}^{-1} \text{ dm}^3 \text{ cm}^{-1}$ at the absorption maximum of 308 nm (198).

6.3.2. *Saturated TTF Concentrations in BSA*

Throughout our kinetic studies for the model system of TTF, solubilized in BSA solutions, saturating TTF concentrations were used. For a series of BSA solutions saturated with TTF, the absorption at 320 nm was recorded and the concentrations of TTF were derived using our value for the extinction coefficient obtained above. The TTF concentrations were plotted against the

corresponding BSA concentrations and a linear relationship was obtained (figure 6.1).

The intercept of this plot is 1×10^{-6} mol dm⁻³ and this presumably corresponds to the solubility of TTF in aqueous solution.

This value of TTF solubility in aqueous buffer solution is much greater than that of TTF in water estimated in the literature (4), in which the authors placed an upper bound of 5×10^{-8} mol dm⁻³.

From slope we can estimate the number of TTF molecules solubilized/incorporated in each BSA molecule at saturation. From the graph, we find 6.0 TTF per BSA molecule.

6.4 Half-wave Potentials and Electron Transfer Processes

In this section, studies of the electron transfer processes and the half-wave potentials for both the first and second oxidation steps of TTF in aqueous/BSA solution are reported. The studies were carried out using cyclic voltammetry and rotating disc voltammetry.

6.4.1 *Half-Wave Potentials*

A solution of TTF (saturated) in aqueous buffer (0.15 mol dm⁻³ Na phosphate containing 0.20 mol dm⁻³ NaCl, pH 7.0)/BSA solution (19.8 mg cm⁻³) was investigated by cyclic voltammetry at platinum and glassy carbon electrodes in the potential region 0 to 0.5 V (vs SCE). The cyclic voltammograms (figure 6.2) exhibit two oxidation waves which we attribute to the oxidation of TTF, first to its radical mono-cation (TTF^{•+}) and second to its di-cation (TTF²⁺), and on the reverse sweep exhibit two reduction waves which we attribute to the reduction of these oxidation products. The half-wave potentials estimated from the cyclic voltammograms are 160 mV and 390 mV (vs SCE) respectively for the first and second oxidation step.

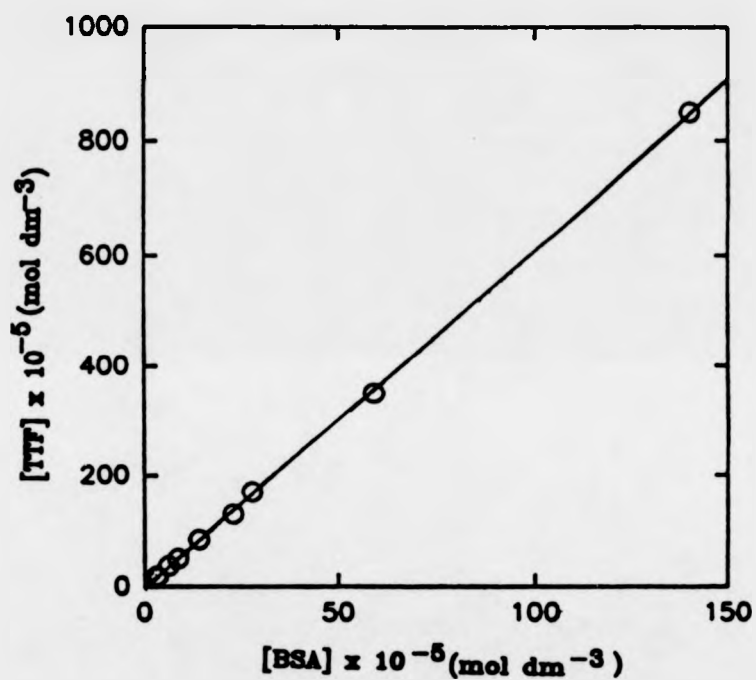


Figure 6.1 A plot of TTF concentrations versus the corresponding BSA concentrations. The molar extinction coefficient used is $5.9 \times 10^3 \text{ dm}^3 \text{ mol}^{-1} \text{ cm}^{-1}$

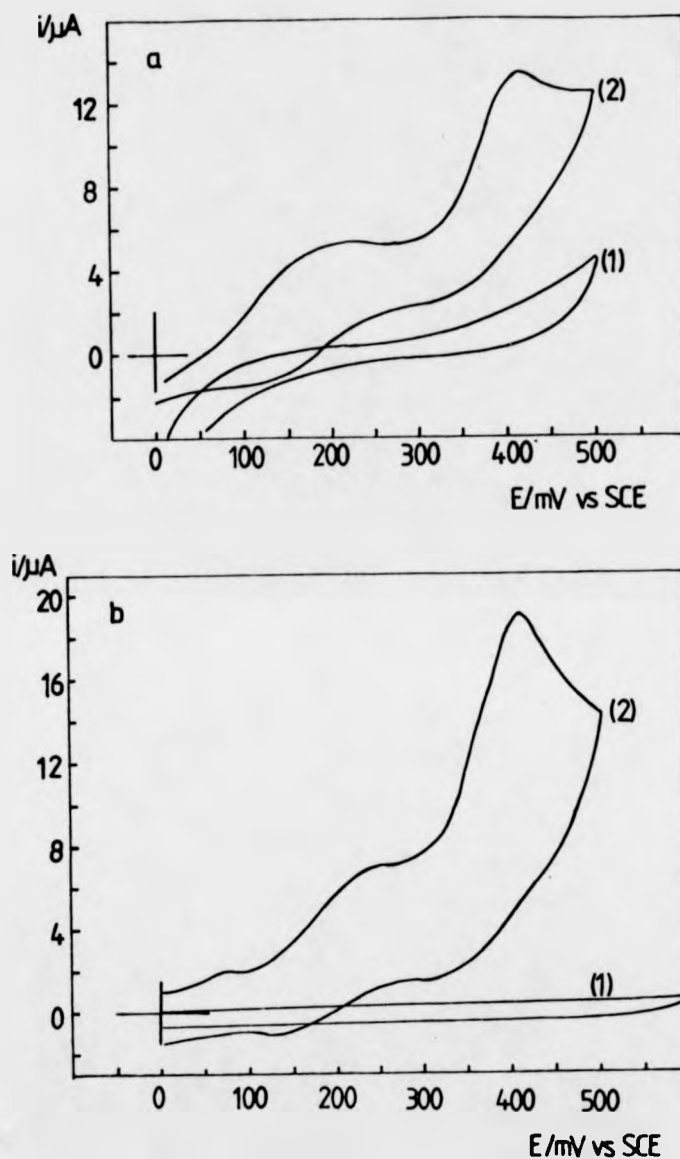


Figure 6.2 Cyclic voltammograms of (1) TTF saturated in buffer (0.15 mol dm^{-3} sodium phosphate containing 0.2 mol dm^{-3} NaCl, pH 7.0) and (2) TTF saturated in a BSA solution ($[\text{BSA}] = 19.8 \text{ mg cm}^{-3}$) at (a) platinum and (b) glassy carbon electrode. Sweep rates: 5 mV s^{-1} . Electrode areas: $A_{\text{Pt}} = A_{\text{GC}} = 0.384 \text{ cm}^2$.

Voltammetry of a TTF saturated aqueous/BSA solution (94 mg cm^{-3}) at a rotating platinum disc electrode shows two distinct oxidation waves (figure 6.3) which again correspond to the oxidation of TTF to the mono- and dication. The results of rotating disc voltammetry were analysed using the corrected Tafel equation: $(\ln (i_L/i - 1)) = RT\eta/nF$. Tafel plots for the two oxidation waves are presented in figure 6.4. From these plots we obtain values of the half-wave potentials for the two oxidation steps, $E_{1/2,1} = 160 \text{ mV}$ and $E_{1/2,2} = 400 \text{ mV}$ (vs SCE).

The half wave potentials obtained above for the first oxidation step of TTF in aqueous/BSA solution are in close agreement with that of TTF in aqueous/CTAC micelle ($E_{1/2,1} = 170 \text{ mV}$, CV; $E_{1/2,1} = 160 \text{ mV}$, RDE; E vs SCE) (199) while the half-wave potentials for the second oxidation step of TTF in BSA are lower than that of TTF in CTAC micelle ($E_{1/2,2} = 500 \text{ mV}$ vs SCE CV or RDE) (199). It is apparent that the difference in half-wave potentials between the first and second oxidation step for TTF in BSA is lower than those of TTF in CTAC micelle and TTF in acetonitrile. The half wave potentials of TTF in BSA, in CTAC micelle and in acetonitrile are summarised in table 6.1.

Table 6.1 Summary of the half-wave potentials (vs SCE) for TTF oxidation in BSA,CTAC and acetonitrile

$E_{1/2}^{\circ} (\text{mV})$	TTF/BSA		TTF/micelle		TTF/ CH_3CN
$E_{1/2} (\text{mV})$	CV	RDE	CV	RDE	CV
$E_{1/2,1}$	160	160	170	160	365
$E_{1/2,2}$	390	400	500	500	750

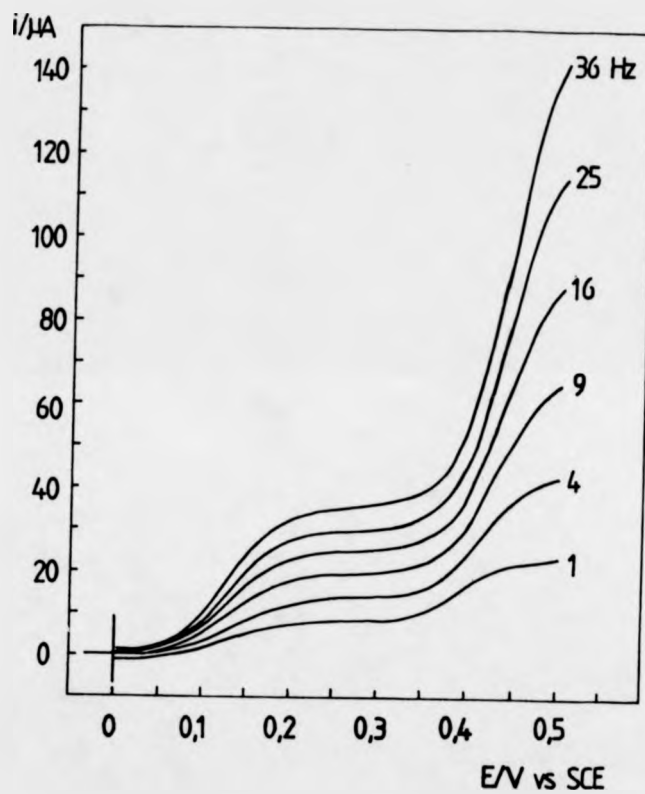


Figure 6.3 Polarograms of TTF saturated in a BSA solution ($[\text{BSA}] = 94 \text{ mg cm}^{-3}$) recorded at a platinum electrode (0.384 cm^2). Sweep rate: 5 mV s^{-1}

6.4.2 Electron Transfer Processes

The number of electrons transferred in each oxidation step of TTF solubilised in a BSA solution were estimated from the stationary and rotating disc voltammetric studies. Tafel slopes (figure 6.4) for both oxidation waves are 31 V^{-1} and 28 V^{-1} per e, suggesting that each step corresponds to a one-electron process for the oxidation of TTF and TTF^+ in aqueous/BSA solution. The peak current separation in the voltammograms for TTF oxidation in BSA solution (figure 6.2) was used to estimate the number of electrons transferred in the following way:

$$\Delta E_{p_1} \text{ (for the first oxidation step)} = 0.075 \text{ V} \quad (6.25)$$

$$\Delta E_{p_2} \text{ (for the second oxidation step)} = 0.065 \text{ V} \quad (6.26)$$

As ΔE_p is always close to 2.3 RT/nF (129), for a reversible process, so

$$\Delta E_{p_1} = 2.3 \text{ RT/n}_1\text{F} \quad (6.27)$$

$$\Delta E_{p_2} = 2.3 \text{ RT/n}_2\text{F} \quad (6.28)$$

we obtain

$$n_1 = 0.8 \approx 1$$

$$n_2 = 0.9 \approx 1$$

These results are also consistent with two separate one-electron transfer processes for the oxidation of TTF in the aqueous/BSA solution.

Our findings of the electron transfer processes of TTF oxidation in BSA are similar to those of TTF in CTAC micellar media, in which the oxidation of TTF^{\bullet} also proceeds via two one-electron transfer steps (198-199).

The determination of the diffusion coefficients for the neutral TTF species and for the electrochemically generated cation radical TTF^+ was carried out using the results from cyclic voltammetry and rotating disc voltammetry studies. This is detailed in the next section.

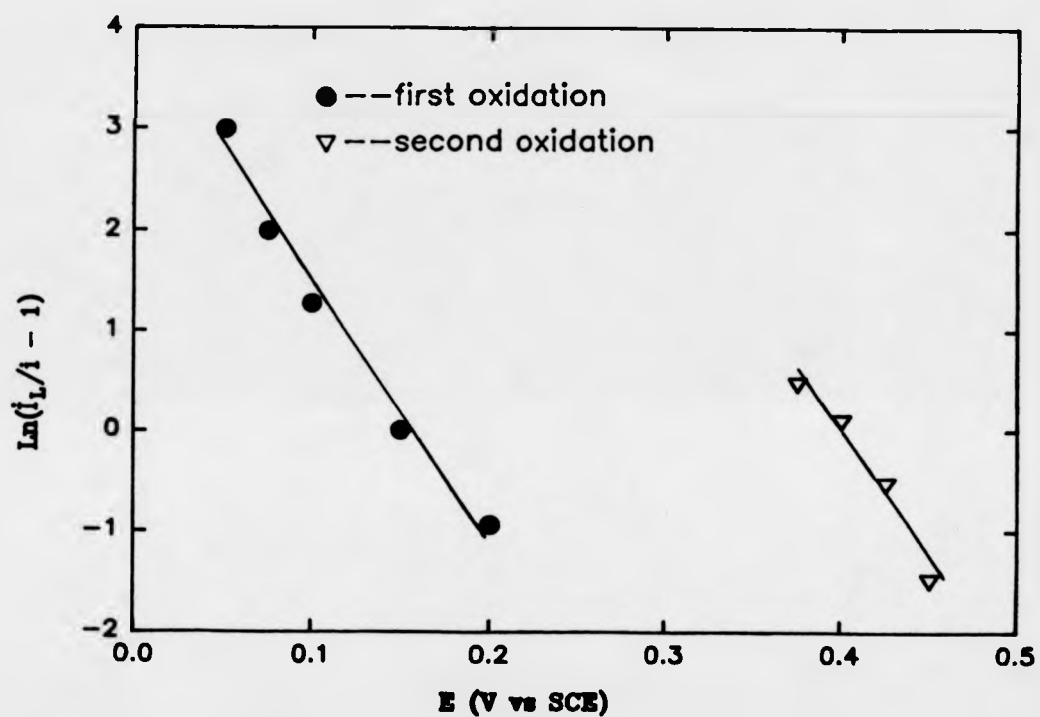


Figure 6.4 Corrected Tafel plots for the first and second oxidation steps of TIF saturated in a BSA solution ([BSA] = 94 mg cm⁻³)

6.5 Determination of the Diffusion Coefficients

From rotating disc voltammetric studies, the limiting current was found to obey the Koutecky-Levich equation (209) where a plot of $1/i$ vs $1/\omega^{1/2}$ is linear. These plots for the first TTF and second steps of TTF oxidation are shown in figure 6.5. The slopes of these plots are now used to estimate the values of diffusion coefficients for TTF and TTF⁺

$$\text{slope for the first oxidation step} = 0.112 \mu\text{A}^{-1}(\text{Hz})^{1/2} \quad (6.29)$$

and

$$\text{slope for the second oxidation step} = 0.04 \mu\text{A}^{-1}(\text{Hz})^{1/2} \quad (6.30)$$

Assuming that the kinematic viscosity is close to the value of $10^{-2} \text{ cm}^2 \text{ s}^{-1}$ and taking the value of $2.08 \times 10^{-3} \text{ mol dm}^{-3}$ for the concentration of TTF (6.0 times the corresponding BSA concentration) solubilised in BSA, $n = 1$ for both oxidation steps and $A = 0.38 \text{ cm}^2$, we obtain values for D .

$$D_{1,\text{RDE}} = 8.1 \times 10^{-7} \text{ cm}^2 \text{ s}^{-1}$$

$$D_{2,\text{RDE}} = 3.8 \times 10^{-6} \text{ cm}^2 \text{ s}^{-1}$$

Cyclic voltammograms of TTF solubilised in a BSA solution were recorded using different sweep rates (1 mV s^{-1} - 200 mV s^{-1}). The cathodic peak currents for both the first and the second oxidation waves vary linearly with the square root of scan rates, $v^{1/2}$, at a platinum electrode (figure 6.6). The values for the diffusion coefficients are also estimated from this plot. Assuming that both the oxidation processes are reversible, then the following equation can be applied:

$$i_p = (2.69 \times 10^5) n^{3/2} A D^{1/2} v^{1/2} C_o^* \quad (6.31)$$

where i_p is the peak current in ampere, A is the electrode area, in cm^2 , D in $\text{cm}^2 \text{ s}^{-1}$, C_o^* in mol cm^{-3} and v in Vs^{-1} .

The slope for the first oxidation wave is $1.8 \mu\text{A} (\text{mV s}^{-1})^{-1/2}$ and it is $4.83 \mu\text{A} (\text{mV s}^{-1})^{-1/2}$ for the second oxidation. Again taking $n = 1$ for both oxidation waves, and $C_o^* = 8.74 \times 10^{-4} \text{ mol dm}^{-3}$ for TTF in BSA, the values for D are derived,

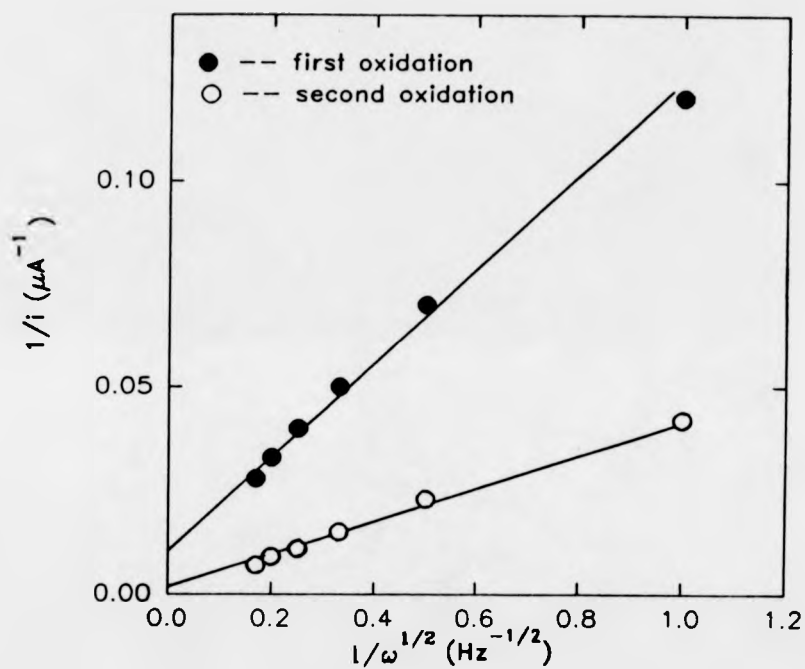


Figure 6.5 Koutecky-Levich plots for the first and second oxidation steps of TTF saturated in a BSA solution ([BSA] = 94 mg cm⁻³) at E_1 = 300 mV and E_2 = 500 mV.

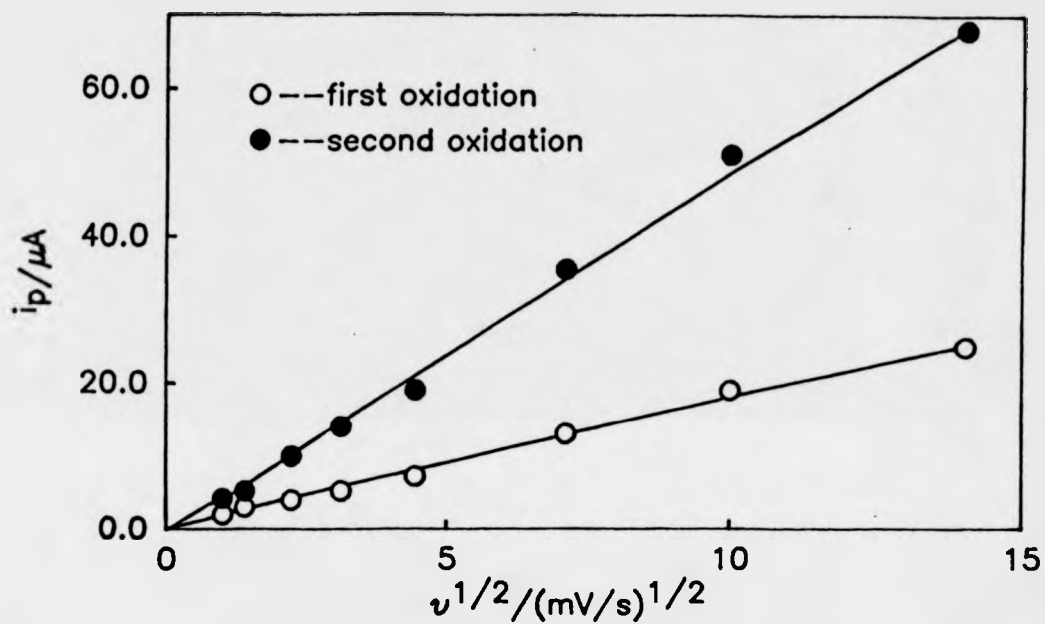


Figure 6.6 Plots of cathodic peak currents versus the square root of sweep rates for both the first and second oxidation steps of TTF saturated in a BSA solution ($[\text{BSA}] = 19 \text{ mg cm}^{-3}$).
Potential range: 0-500 mV vs SCE.
Electrode: platinum (0.384 cm^2)

$$D_1, cv = 4.0 \times 10^{-7} \text{ cm}^2 \text{ s}^{-1}$$

$$D_2, cv = 2.9 \times 10^{-6} \text{ cm}^2 \text{ s}^{-1}$$

The diffusion coefficients of TTF and TTF⁺ in aqueous/BSA media obtained using cyclic voltammetry are in good agreement with those obtained using rotating disc voltammetry. Our results for the diffusion coefficients of TTF and TTF⁺ in BSA solution are also in fair agreement with that of TTF, TTF⁺ in CTAC micellar media where a value of $7.3 \times 10^{-7} \text{ cm}^2 \text{ s}^{-1}$ for D_1 and $3.4 \times 10^{-6} \text{ cm}^2 \text{ s}^{-1}$ for D_2 were found by Eddowes and Grätzel.

The difference in diffusion coefficients between the reduced, neutral TTF species (D_1) and the electrochemically generated cation radical TTF⁺ (D_2) are consistent with the proposal that TTF species is predominately BSA solubilised hence more slowly diffusing than its oxidation product which is predominately solubilized in the aqueous phase. It is evident that the diffusion coefficients of the neutral TTF species solubilised in a BSA solution is also comparable to that of BSA itself, for which values ranging from $3.3 \times 10^{-7} \text{ cm}^2 \text{ s}^{-1}$ to $9.1 \times 10^{-7} \text{ cm}^2 \text{ s}^{-1}$ (205-207) have been reported for BSA in aqueous solution at pH 7.0. This again confirms that the neutral TTF species are essentially solubilised in BSA phase.

The studies for the electrochemical oxidation of aqueous/BSA solubilised TTF indicates that there is a difference in the partitioning of the electrochemically generated mono-cation (TTF⁺) and di-cation (TTF²⁺) and their parent molecule between the aqueous and BSA environment. The rate of phase exchange for the BSA solubilised TTF can be described by a rate constant k_R , which represents the exit of TTF from the BSA phase. Determination of this rate constant is outlined in the next section.

6.6 RDE Kinetics of TTF Oxidation to Its Monocation, TTF^+ , in BSA

In this section, we describe the kinetic studies of TTF oxidation to its monocation radical, TTF^+ , using rotating disc electrode voltammetry. The kinetic analysis based on the theory by Eddowes and Grätzel are presented and the proposal for a reaction mechanism which is unique for our model system of TTF/BSA is also discussed.

RDE studies were carried out on solutions of TTF saturating in BSA, with BSA concentrations ranging from 2.2 mg cm^{-3} to 98 mg cm^{-3} . For each solution, the polarograms were recorded at rotation speed from 1 to 36 Hz over a potential range of 0 to 500 mV (vs SCE). The data thus derived from the polarograms were then subjected to the double reciprocal Koutecky-Levich treatment (198, 208). Figure 6.7 shows typical Koutecky-Levich plots for a BSA solution saturated with TTF at a range of potentials.

It is apparent that the Koutecky-Levich intercept decreases progressively with increasing potential and approaches a limiting intercept at large overpotential. For the model system of TTF/CTAC, Eddowes and Grätzel reported that the oxidation of TTF proceeded via the TTF species in the aqueous phase thus step involving TTF exit from the micellar phase took place prior to the oxidation reaction. The exit of TTF from the micelles is described by an apparent heterogeneous rate constant, k_R . The value of k_R can be estimated from the Koutecky-Levich limiting intercept at large, overpotential, for which k_e , the potential-dependent electron-transfer rate constant is sufficiently large that its reciprocal becomes negligible, eqn. (6.23). Eddowes and Grätzel found, for TTF/CTAC system, that k_R was proportional to the inverse of the square root of micelle concentrations as predicted by the theory (eqn. 6.24).

However, the values of k_R derived for our system of TTF/BSA remain constant for a series of BSA concentrations, table 6.2.

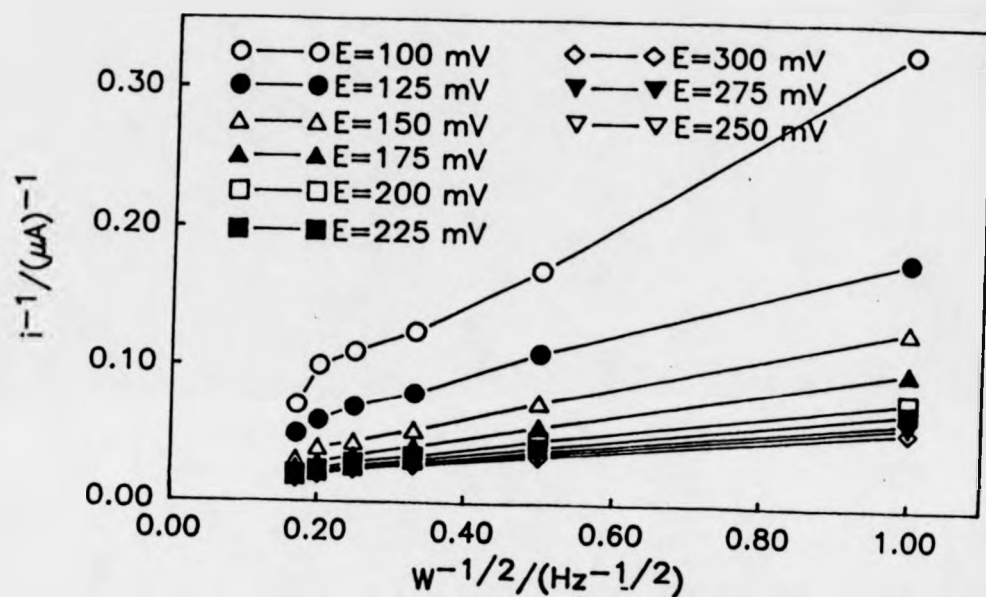
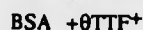
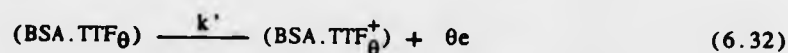


Figure 6.7 Koutecky-Levich plots for the first oxidation step of TTF saturated in a BSA solution
 ([BSA] = 98.0 mg cm⁻³)
 Electrode: platinum (0.384 cm²)
 Potential range : 0-350 mV vs SCE

Table 6.2 Analysis of the rate constant (k_R) for TTF solubilised in BSA solution

[BSA] (mol dm ⁻³)	[TTF] (mol dm ⁻³)	Lim. intercept (μA^{-1})	k_R (m s ⁻¹)
3.2×10^{-5}	1.9×10^{-4}	0.29	4.9×10^{-4}
6.2×10^{-5}	3.7×10^{-4}	0.18	4.0×10^{-4}
8.6×10^{-5}	5.0×10^{-4}	0.10	5.4×10^{-4}
1.4×10^{-4}	8.4×10^{-4}	0.14	2.3×10^{-4}
2.3×10^{-4}	1.3×10^{-3}	0.06	3.5×10^{-4}
2.8×10^{-4}	1.7×10^{-3}	0.03	5.3×10^{-4}
5.9×10^{-4}	3.5×10^{-3}	0.02	3.9×10^{-4}
1.4×10^{-3}	8.5×10^{-3}	0.01	3.2×10^{-4}

This indicates that the mechanism of TTF exit from the micelles prior to oxidation does not apply to the TTF oxidation reaction in BSA. Perhaps this is not surprising since the interaction between TTF and BSA is much stronger than that of TTF and CTAC. The ratio between the concentration of BSA solubilised TTF and TTF in aqueous is approximately 8000 for 1 mmol dm⁻³ BSA while this ratio is 720 for the equivalent concentration of micelles. Thus, for our model system of TTF solubilised in a BSA solution, we propose that the oxidation of TTF species takes place via the direct oxidation of TTF.BSA conjugates at the electrode and the monocations exit from the BSA phase after the reaction;



where θ is the number of TTF molecules in each BSA.

The Koutecky-Leych limiting intercept is now given by,

$$\text{intercept} = \frac{1}{k_7 [\text{BSA.TTF}_\theta] nFA\theta} \quad (6.33)$$

k_7 is the rate constant.

Thus a plot of $1/\text{intercept}$ vs $[\text{BSA}]_{\text{total}}$ (assuming that $[\text{BSA} \cdot \text{TTF}_\theta] = [\text{BSA}]_{\text{total}}$ because saturated TTF concentrations were used throughout) should be linear and k_7 can be derived from the slope. This plot is shown in figure 6.8

Slope of the plot = $0.90 \times 10^4 \text{ A mol}^{-1} \text{ dm}^3$

So $k_7 = \text{slope}/nFA\theta$, using $n=1$, $F = 96480 \text{ C mol}^{-1}$,

$A = 0.384 \text{ cm}^2$ and $\theta = 6.0$,

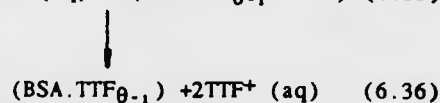
$k_7 = (4.06 \pm 1.1) \times 10^{-4} \text{ cm s}^{-1}$

This rate constant k_7 is not fully understood at the present, it presumably corresponds to some type of absorption process.

We observed increased size of the second oxidation peak for TTF in BSA. Similar behaviour has been reported by Eddowes and Grätzel for TTF in CTAC (198). For the oxidation of TTF in CTAC, this increased size for the second oxidation peak is due to the reaction,



For the oxidation of TTF in BSA, this can be explained in terms of,



6.7 Conclusions

The oxidation of TTF solubilised in a BSA solution has been studied. Our studies show that this oxidation reaction takes place via two one-electron transfer steps similar to that reported by Eddowes and Grätzel for the oxidation of TTF in CTAC micellar media. The diffusion coefficients obtained from the first and the second oxidation steps clearly demonstrate

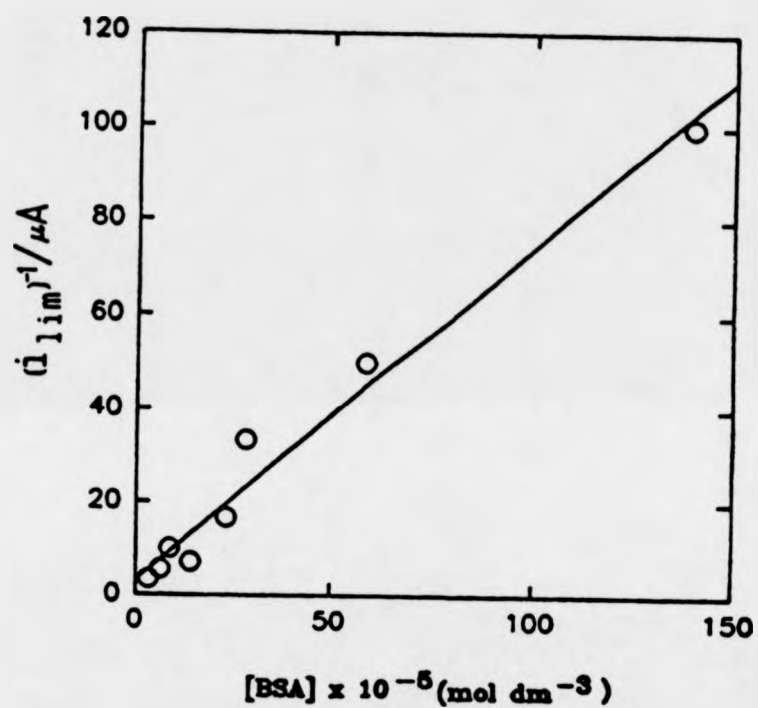


Figure 6.8 A plot of the reciprocal of the Koutecky-Levich limiting intercept versus the concentrations of BSA. (Data from table 6.2)

oxidation of TTF in CTAC micellar media. The diffusion coefficients obtained from the first and the second oxidation steps clearly demonstrate that the neutral, parent TTF species is predominately solubilised in BSA phase while the mono- and di-cations are essentially solubilised in the aqueous phase. The diffusion coefficient of BSA solubilised TTF is comparable with that of BSA itself.

Studies carried out by Eddowes and Grätzel for the oxidation of TTF in CTAC micellar media evidently affirm that the micellar solubilised TTF species undergoes rapid phase exchange with rate constant for micelle-exit and entry, $k_{\text{out}} \sim 7 \times 10^3 \text{ s}^{-1}$ and $k_{\text{in}} \sim 5 \times 10^3 \text{ mol}^{-1} \text{ dm}^3 \text{ s}^{-1}$ respectively. They also found that only the TTF species in the aqueous phase was electro-active. For our systems of TTF solubilised in BSA, we propose that the TTF.BSA conjugate is oxidised directly at the electrode and the oxidation product, TTF^+ , exits from BSA phase after the reaction. This mechanism is suggested on the basis of the much stronger interaction between TTF and BSA molecules than that between TTF and CTAC micelles. A rate constant is derived, which presumably corresponds to some type of absorption process of the TTF.BSA conjugates at the electrode.

The overall conclusions of work presented in this thesis and suggestions for future directions of this project are outlined in the next chapter.

CHAPTER VII CONCLUSIONS AND FUTURE DIRECTIONS

7.1 Conclusions

The work presented in this thesis is concerned with the modifications of redox enzymes and the studies of the electrochemistry of the modified enzymes. Two types of modified enzyme are described. Firstly, the covalently modified enzyme based on ferrocenes are studied and data obtained for the systems analysed using our theoretical model. The working stabilities of the covalently modified enzymes have been investigated by assessing the stability of an enzyme electrode with the modified enzyme entrapped behind a dialysis membrane. Our studies show that this type of modified enzymes is not suitable for sensor applications at the present due to their instabilities. This instability of the modified enzyme is mostly caused by the instability of the ferricinium ions of the attached ferrocenes. Secondly, a novel method for enzyme modification, the non-covalent modification is presented. The successful modifications of glucose oxidase with hydrophobic mediators are described. Studies of the hydrophobic interaction between mediators and proteins are also reported.

7.2 Future Directions

This work has opened up many interesting areas in both the theoretical and practical aspects of bioelectrochemistry. In particular, it is worth pursuing further the area of non-covalent modification for redox enzymes. Several successful examples have been given in the thesis. The modification of glucose oxidase by the incorporation of hydrophobic mediators through molecular interaction has proven the effectiveness and ease of this method. It could be of use particularly with those enzymes which are not as well behaved and characterised as glucose oxidase. It appears that large, planar

hydrophobic redox mediators are most suitable for incorporation with enzymes.

This is a very new area. Much more work needs to be undertaken in the future to understand the kinetics and mechanism of the enzyme reaction.

REFERENCES

1. J.J. Kulys, *Biosensors*, 2 (1986) 3.
2. W.J. Albery, P.N. Bartlett, M. Bycroft, D.H. Craston and B.J. Driscoll, *J. Electroanal. Chem.*, 218 (1987) 119.
3. W.J. Albery, P.N. Bartlett and A.E.G. Cass, *Phil. Trans. R. Soc. Lond.*, B316 (1987) 107.
4. B.S. Hill, C.A. Scolari and G.S. Wilson, *J. Electroanal. Chem.*, 252 (1988) 125.
5. Y. Degani and A. Heller, *J. Phys. Chem.*, 91 (1987) 1285.
6. Y. Degani and A. Heller, *J. Amer. Chem. Soc.*, 110 (1988) 2615.
7. W.J. Albery, P.N. Bartlett and D.H. Craston, *J. Electroanal. Chem.*, 194 (1985) 223.
8. A.L. Lehinger, *Biochemistry*, 2nd Ed., (1981), Worth, New York, 477-508.
9. M. Dixon and E.C. Webb, *Enzymes*, (1979), Longman, London, 277-290.
10. L.C. Clark, *Biotechnol. Symp.*, 3 (1972) 377.
11. S.A. Salisbury, H.S. Forrest, W.B.T. Cruse and O. Kennard, *Nature*, 280 (1979) 843.
12. J.A. Duine and J.J. Frank, *Trends in Biological Sciences*, 6 (1981) 278.
13. G. Davis, H.A.O. Hill, W.J. Aston, I.J. Higgins and A.P.F. Tumer, *Enzyme Microb. Technol.*, 5 (1983) 383.
14. E.J. D'Costa, I.J. Higgins and A.P.F. Tumer, *Biosensors*, 2 (1986) 71.
15. B.J. Van Schie, K.J. Hellingwerf, J.P. Van Dijken, M.G.L. Elferink, J.M. Van Diji, J.G. Kuenen and W.N. Konings, *J. Bacteriol.*, 163 (1985) 493.
16. P.N. Bartlett, P. Tebbutt and R.G. Whitaker, *Kinetic Aspects of the Use of Modified Electrodes and Mediators in Bioelectrochemistry*, in press.
17. M. Dixon and E.C. Webb, *Enzymes*, (1979), Longman, London, p479.
18. C. Walsh, *Acc. Chem. Res.*, 13 (1980) 148.

19. P. Hemmerich, C. Veeger and H.C.S. Wood, *Angew. Chem., Int. Ed. Engl.*, 4 (1965) 671.
20. S. Ghisla and V. Massey, *Euro. J. Biochem.*, 181 (1989) 1.
21. P. Hemmerich, V. Massey, H. Michel and C. Schug, *Advances in Biochem. Eng.* (1982) 119.
22. M. Dixon and E.C. Webb, *Enzymes*, Longman, London, (1979) p483.
23. G. Dryhurst, K.M. Kadish, F. Scheller and R. Rennebery, *Biological Electrochemistry*, Vol. 1, Academic Press, New York, (1982) p459.
24. J. Frew and H.A.O. Hill, *Anal. Chem.*, 59 (1987) 933A.
25. B.E.P. Swoboda and V. Massey, *J. Biol. Chem.*, 240 (1965) 2209.
26. D. Kellin and E.F. Hartree, *J. Biochem.* 42 (1948) 221.
27. L.M. Schoper, V. Massey and A. Claiborne, *Flavins and Flavoproteins*, Eds. V. Massey and C.H. Williams, Elsevier, New York, (1982) 102.
28. G.E. Schultz, R.H. Schirmer and E.F. Pai., *J. Mol. Biol.*, 160 (1982) 287.
29. R.A. Marcus and N. Sutin, *Biochim. Biophys. Acta*, 811 (1985) 265.
30. B. Janik and P.J. Elving, *Chem. Rev.*, 68 (1968) 295.
31. G. Dryhurst, *Electrochemistry of Biological Molecules*, Academic Press, London, (1977) 365.
32. D.E. Metzler, *Biochemistry*, Academic Press, New York, Int. Edn., (1977) 478.
33. Sueko Hayashi and Satoshi Nakamura, *Biochim. Biophys. Acta*, 438 (1976) 37.
34. L.T. Clark and C. Lyons, *Ann. NY Acad. Sci.*, 102 (1962) 29.
35. A.P.F. Turner and J.C. Pickup, *Biosensors*, 1 (1985) 85.
36. M. Schichiri, R.M. Kawamori and Y. Yamasaki, *Lancet*, 2(1982) 1129.
37. C. van Dijk, C. Laane and V. Veeger, *Recl. Trav. Chim. Pays-Bas*, 104 (1985) 245.
38. M. Cardosi and A.P.F. Turner, *The Diabetes Annual*, 3 (1987) 560.
39. S. Borman, *Anal. Chem.* 59 (1987) 1091A.

40. S.L. Brooks and A.P.F. Turner, *Measurement and Control*, 20 (1987) 37.
41. M.L. Hitchman and H.A.O. Hill, *Chemistry in Britain*, December (1987) 117.
42. G. Nagy and E. Pungor, *Bioelectrochem. and Bioenerg.* 20 (1988)1.
43. W. Tretrnak and O.S. Wolfbeis, *Anal. Chim. Acta*, 221 (1989) 195.
44. H. Durliat and M. Comtat, *Anal. Chem.*, 56 (1984) 148.
45. G.G. Guilbault and G.J. Lubrano, *Anal. Chim. Acta*, 64 (1973) 439.
46. J.L. Romette, B. Froment and D. Thomas, *Clin. Chim. Acta*, 95 (1979) 249.
47. P.N. Bartlett, V.Q. Bradford and R.G. Whitaker, *Talanta* 38(1991)57.
48. H.M. Free and A.H. Free, *Anal. Chem.*, 56 (1984) 664A.
49. H.M. Kalisz, H.J. Hecht, D. Schomburg and R.D. Schmid, *J. Mol. Biol.* 213 (1990) 207.
50. S. Nakamura, S. Hayami and K. Koga, *Biochim. Biophys. Acta.*, 445 (1976) 294.
51. M.T. Stankovic, L.M. Schopfer and V. Massey, *J. Biol. Chem.*, 253 (1978) 4971.
52. J.L. Vermilion and M.J. Coon, *J. Biol. Chem.*, 253 (1978) 2694.
53. F. Scheller, G. Strand, B. Neumann, M. Kuhn and W. Ostrowski, *Bioelectrochem, Bioenerg.*, 6 (1979) 117.
54. B. Kuznetsov, N. Mestechkina and G. Schumakovich, *Bioelectrochem, Bioenerg.* 4(1977)1,
55. C. Tanford, *J. Amer. Chem. Soc.* 74 (1952) 6036.
56. F. Scheller, M. Jänchen, J. Lampe, H-J Prümke, J. Blanck and E. Palacek, *Biochim. Biophys. Acta*, 412 (1975) 157.
57. T. Kakutani, K. Toriyama, I. Ideka and M. Senda, *Bull. Chem. Soc. Jpn.* 53 (1980) 947.
58. K.S.V. Santhranam, N. Jespersen and A.J. Bard., *J. Amer. Chem. Soc.*, 99 (1977) 274.

59. G. Dryhurst, K.M. Kasdich, F. Scheller and R. Renneberg, *Biological Electrochemistry*, Vol. 1, Academic Press, New York (1982) p436.
60. A. Szucs, G.D. Hitchins and J. O'M. Bockris, *Bioelectrochem. Bioenerg.* 21 (1989) 133.
61. R.M. Ianniello, T.J. Lindsay and A.M. Yacynych, *Anal. Chem.* 54 (1982) 1980.
62. R.A. Kamin and G.S. Wilson, *Anal. Chem.*, 52 (1980) 1198.
63. G.G. Guibault and G.J. Lubrano, *Anal. Chim. Acta*, 64 (1973) 439.
64. R.M. Ianniello and A.M. Yacynych, *Anal. Chim. Acta*, 131 (1981) 123.
65. C. Bourdillon, J.P. Bourgeois and D. Thomas, *J. Amer. Chem. Soc.*, 102 (1980) 4231.
66. Y.A. Aleksandrovskii, L.V. Bezhikina and Y.V. Rodionov., *Biokhimiya (trans.)*, 46 (1981) 708.
67. J. Mahenc and H. Aussaresses, *C.R. Acad. Sci. Paris*, 289 (1979) 357.
68. A.E.G. Cass, G. Davis, M.J. Green and H.A.O. Hill, *J. Electroanal. Chem.*, 190 (1985) 117.
69. A.J. Deeming in G. Wilkinson F.L. Stone and E. Abel (Eds.), *Comprehensive Organometallic Chemistry*, Vol. 4, Pergamon Press, Oxford, (1982) 377.
70. G. Marr and B.W. Rockett, *J. Organomet. Chem.*, 227 (1982) 373.
71. A. Szucs, G.D. Hitchins and J. O'M. Bockris, *J. Electrochem. Soc.*, 136 (1989) 3748.
72. G. Davis, H.A.O. Hill, W.J. Aston, A.P.F. Turner, I.J. Higgins and J. Colby in R.K. Poole and D.S. Dow (Eds.), *Soc. Gen. Microbiol. Symp.*, Academic Press, London, (1985) 161.
73. G. Davis, *Biosensors*, 1 (1985) 161.
74. G. Davis, in *Biosensors: Fundamentals and Applications*, Eds. A.P.F. Turner, I. Karube and G.S. Wilson, OUP, Oxford, (1987) p247.
75. R.S. Nicholson and I. Shain, *Anal. Chem.*, 37 (1965) 178.

76. C.W. Conroy, P. Tyma, P.H. Daum and J.E. Erman, *Biochim. Biophys. Acta*, 537 (1978) 62.
77. W.J. Albery and D.H. Craston, in *Biosensors: Fundamentals and Applications*, Eds. A.P.F. Turner, I. Karube and G.S. Wilson, OUP, Oxford (1987) p180.
78. W.J. Albery, P.N. Bartlett, M. Bycroft, D.H. Craston and B.L. Driscoll, *J. Electroanal. Chem.*, 218 (1987) 119.
79. D.L. Williams, A.R. Doig and A. Korosi, *Anal. Chem.*, 42 (1970) 118.
80. G. Davis, H.A.O. Hill, I.J. Higgins and A.P.F. Turner, *Implantable Sensors for Closed Loop Prosthetic Systems*, Ed. W.H. Ko, Futura, New York (1985) 189.
81. A.E.G. Cass, G. Davis, G.D. Francis, H.A.O. Hill, W.J. Aston, I.J. Higgins, E.V. Plotkin, L.D.L. Scott and A.P.F. Turner, *Anal. Chem.*, 56 (1984) 667.
82. A.E.G. Cass, G. Davis, H.A.O. Hill, I.J. Higgins, E.V. Plotkin, A.P.F. Turner and W.J. Aston, *Charge and Field Effects in Biosystems*. Eds. M.J. Allen and P.N.R. Usherwood, Abacus, (1984) 475.
83. E.J. D'Costa, I.J. Higgins and A.P.F. Turner, *Biosensors*, 2 (1986) 71.
84. A.P.F. Turner, W.J. Aston, I.J. Higgins, J.M. Bell, J. Colby, G. Davis and H.A.O. Hill, *Anal. Chim. Acta*, 163 (1984) 161.
85. J.M. Dicks, W.J. Aston, G. Davis and A.P.F. Turner, *Anal. Chim. Acta*, 182 (1986) 103.
86. N.C. Foulds and C.R. Lowe, *J. Chem. Soc., Faraday Trans. 1*, 82 (1986) 1259.
87. M. Umana and J. Waller, *Anal. Chem.*, 58 (1986) 2979.
88. S-I. Yakuki, H. Shinohara and M. Aizawa, *J. Chem. Soc., Chem. Commun.*, (1989) 945.
89. D. Belander, J. Nadreau and G. Fortier, *J. Electroanal. Chem.*, 274 (1989) 143.

90. P.N. Bartlett and R.G. Whitaker, *J. Electroanal. Chem.*, 224 (1987) 37.
91. P.N. Bartlett and R.G. Whitaker, *Biosensors* 3(1987/88) 359.
92. P.C. Pandey, *J. Chem. Soc., Faraday Trans. 1*, 84 (1988) 2259.
93. H. Shinohara, T. Chiba and M. Aizawa, *Sensors and Actuators*, 13 (1988) 79.
94. D. Belanger, E. Brassard and G. Fortier, *Anal. Chim. Acta*, 228 (1990) 311.
95. J.M. Dicks, S. Hattori, I. Karube, A.P.F. Tumer and T. Yokozawa, *Ann. Biol. Clin.*, 47 (1989) 607.
96. T. Schalkhammer, E. Mann-Buxbaum, G. Urban and F. Pittner, Abstract number P. 3.1.b., *Euroensors IV*, Karlsruhe, Oct. 1-3 1990.
97. G. Johansson and L. Gorton, *Biosensors*, 1 (1985) 355.
98. J.J. Kulys and G-J. Svirmickas, *Anal. Chim. Acta*, 117 (1980) 115.
99. J.J. Kulys, A.S. Samalius and G-J. S. Svirmickas, *FEBS lett.*, 114 (1980) 7.
100. J.J. Kulys, *Enzyme Microb. Technol.*, 3 (1981) 344.
101. J.J. Kulys, M.W. Pesliakienė and A.S. Samalius, *Bioelectrochem. Bioenerg.*, 8 (1981) 81.
102. J.J. Kulys, N.K. Cenas, G-J. Svirmickas and V.P. Svirmickienė, *Anal. Chim. Acta.*, 138 (1982) 19.
103. W.J. Albery, P.N. Bartlett, D.H. Craston, M. Bycroft and C.P. Jones, *Eur. Pat. Appl. EPI94,909* (CL. C12Q1/100), 18 June 1986. GB Appl. 84/28, 599, 13 Nov. 1984; 47 pp.
104. P.D. Hale and R.M. Wightman, *Mol. Cryst. Liq. Cryst.*, 160 (1988) 269.
105. K. McKenna and A. Brajter-Toth, *Anal. Chem.*, 59 (1987) 954.
106. W.J. Albery, P.N. Bartlett, A.E.G. Cass, D.H. Craston and B.G.D. Hagget, *J. Chem. Soc., Faraday Trans. 1*, 82 (1986) 1033.
107. W.J. Albery, P.N. Bartlett, A.E.G. Cass and K.W. Sim, *J. Electroanal. Chem.*, 218 (1987) 127.

108. R.C. Wheland and J.L. Gilson, *J. Amer. Chem. Soc.*, 98 (1976) 3916.
109. J. Ferraris, D.O. Cowan, V. Walatka, Jr., and J.H. Perlstein, *J. Amer. Chem. Soc.*, 95 (1973) 948.
110. C.D. Jaeger and A.J. Bard, *J. Amer. Chem. Soc.*, 101 (1979) 1690.
111. C.D. Jaeger and A.J. Bard, *J. Amer. Chem. Soc.*, 102 (1980) 5435.
112. N.K. Cenas and J.J. Kulys, *Bioelectrochem. Bioenerg.*, 8(1981) 103.
113. M.G. Boutelle, C. Stanford, M. Fillenz, W.J. Albery and P.N. Bartlett, *Neurosci. lett.*, 72 (1987) 283.
114. H.A.O. Hill, *Eur. Pat. Appl.* EP 0, 125, 139 A2 (C 12Q1/68), 14 November 1984, p 45.
115. R. Szentrimay, P. Yeh and T. Kuwana, *Electrochemical Studies of Biological Systems*, Ed. D. Sawyer, ACS, Washington DC, (1977) 143.
116. P.N. Bartlett and V.Q. Bradford, *J. Chem. Soc., Chem. Commun.*, 16 (1990) 1135.
117. W.J. Albery and P.N. Bartlett, *J. Electroanal. Chem.*, 194 (1985) 211.
118. D. Barham and P. Trinder, *Analyst*, 97 (1972) 142.
119. P. Trinder, *Ann. Clin. Biochem.*, 6 (1969) 24.
120. R.G. Whitaker, *The Electrochemistry of Redox Enzymes, PhD Thesis*, University of Warwick (1989) 213.
121. K. Yagi, Y. Ozawa and T. Ooi, *Biochim. Biophys. Acta*, 54 (1961) 199.
122. P.N. Bartlett, R.G. Whitaker, M.J. Green and J. Frew, *J. Chem. Soc. Chem. Commun.*, 20 (1987) 1603.
123. N. Sugiura, H. Ohama, A. Kotaki and K. Yagi, *J. Biochem.*, 73 (1973) 901.
124. D. Carauna, *3rd Year Project Report*, University of Warwick, (1990) 49.
125. P. Wiltzius, *Phys. Rev. lett.*, 58 (1987) 710.
126. P.W. Atkins, *Physical Chemistry*, Oxford University Press, (1978) 835.
127. W.J. Albery and M.L. Hitchman, *Ring-Disc Electrodes*, Clarendon Press, Oxford, (1971) Chapter 4.

128. A.J. Bard and L.R. Faulkner, *Electrochemical Methods: Fundamentals and Applications*, John Wiley and Sons (1980) 218.
129. Southampton Electrochemistry Group, *Instrumental Methods in Electrochemistry*, Ellis Horwood Limited, (1985) 50.
130. Southampton Electrochemistry Group, *Instrumental Methods in Electrochemistry*, Ellis Horwood Limited, (1985) 48.
131. V.G. Levich, *Physicochemical Hydrodynamics*, Prince-Hall, Englewood Cliffs, N.J. 1962.
132. J.S. Newman, *J. Phys. Chem.*, 70 (1966) 1327.
133. R.N. Adams, *Electrochemistry at Solid Electrodes*, Marcel Dekker, New York, (1969) 67-114.
134. B. Miller and S. Bruckenstein, *Anal. Chem.*, 46 (1974) 2026.
135. P.N. Bartlett, Z. Ali and V. Eastwick-Field, "Electrochemical Immobilisation of Enzymes Part IV: Co-immobilisation of Glucose Oxidase and Ferro Ferricyanide in Poly(-N-Methylpyrrole) Films", (1991) in press.
136. J.L. Webb, *Enzyme and Metabolic Inhibitors*, Vol. 1, Academic Press, New York and London, (1963) Chapter 2.
137. M. Dixon and E.C. Webb, *Enzymes*, 3rd Edition, Longman, London (1979) 243.
138. J.C. Sheeman, P.A. Cruickshank and G.L. Boshart, *J. Org. Chem.*, 26 (1961) 2525.
139. B.D. Hames and D. Rickwood, Eds., *Gel Electrophoresis of Proteins: A Practical Approach*, IRL Press, Oxford, Washington DC, (1980) Chapter 1.
140. J.P. Greenstein and M. Winitz, *Chemistry of the Amino Acids*, Vol. 1, John Wiley and Sons, New York, London, (1961) Chapter 4.
141. D. Kelen and E.F. Hartree, *Biochem. J.* 50 (1952) 331.
142. A. Sols, *Biochim. Biophys. Acta.* 24 (1957) 207.

143. L.A.E. Sluyterman and J. Wijdenes, *Proc. Int. Symp. Electrofocusing and Isotachopheresis*, B.J. Radola and D. Graesslin, Eds., de Gruyter, Berlin, (1977) 463.
144. L.A.E. Sluyterman and O. Elgersma, *J. Chromatogr.*, 150 (1978) 17.
145. L.A.E. Sluyterman and J. Wijdenes, *J. Chromatogr.*, 150 (1978) 31.
146. *Ion Exchange Chromatography - Principles and Methods*, Pharmacia.
147. *Chromatofocusing with Polybuffer and PBE*, Pharmacia.
148. Sueko Hayashi and Satoshi Nakamura, *Biochim. et Biophys. Acta*, 657 (1981) 40.
149. W.J. Albery and P.N. Bartlett, *J. Chem. Soc. Chem. Commun.*, (1984) 234.
150. D.R. Trevenot and R. Sternberg, *Anal. Chem.*, 51 (1979) 96.
151. L.D. Bowers and P.W. Carr, *Immobilised Enzymes in Analytical and Clinical Chemistry*, Wiley; New York, (1980) 197.
152. *Immobilised Cells and Enzymes: A Practical Approach*, Ed. J. Woodward, IRL Press, Oxford (1985).
153. A. Merz, *Topics in Current Chemistry*, 152 (1990) 51.
154. H. Hennig and O. Gurtler, *J. Organometal. Chem.*, 11 (1968) 307.
155. J.G. Mason and M. Rosenblum, *J. Amer. Chem. Soc.* 82 (1960) 4206.
156. S.P. Gubin and E.G. Perevalova, *Dokl. Akad. Nauk SSSR*, 143 (1962) 1351.
157. E.G. Perevalova, S.P. Gubin, S.A. Smimova and A.N. Nesmeyanov, *Dokl. Akad. Nauk SSSR*, 155 (1964) 857.
158. P. Yeh and T. Kuwana, *J. Electrochem. Soc.*, 123 (1976) 1334.
159. A.A. Penden, M.S. Zakharevskii and P.K. Leont'evskaya, *Kinetika: Kalaliz*, 7 (1966) 1074.
160. P.N. Bartlett, in *Biosensors: A Practical approach*, A.E.G. Cass, Ed., Oxford University Press, (1990) Chapter 3.
161. R.C. Wheland, *J. Amer. Chem. Soc.* 98 (1976) 3926.

162. F. Wudl, G.M. Smith and E.J. Hufnagel, *J. Chem. Soc. Chem. Commun.*, (1970) 1453.
163. B.A. Scott, S.J. La Place, J.B. Torrance, B.D. Silverman and B. Welber, *J. Amer. Chem. Soc.*, 99 (1977) 6631.
164. R.V. Gemmer, D.O. Cowan, T.O. Poehler, A.N. Bloch, R.E. Pyle and R.H. Banks, *J. Org. Chem.*, 40 (1975) 3544.
165. R.C. Wheland and J.L. Gillson, *J. Amer. Chem. Soc.*, 98 (1976) 3916.
166. W.F. Cooper, N.C. Kenny, J.W. Edmonds, A. Nagel, F. Wudl and P. Coppens *J. Chem. Soc. Chem. Commun.*, (1971) 889.
167. E. Engler, B. Scott, S. Etemad, T. Penny and V. Patel, *J. Amer. Chem. Soc.*, 99 (1977) 5909.
168. P. Nielsen, A. Epstein and D. Sandman, *Solid State Commun.*, 15 (1974) 53.
169. J. Torrence and B. Silverman, *Phys. Rev. B*, 15, (1977) 788.
170. R. Metzger, *J. Chem. Phys.*, 63 (1975) 5090.
171. J.H. Perlstein, *Angew. Chem. Int. Ed. Engl.*, 16 (1977) 519.
172. L.B. Coleman, M.J. Cohen, D.J. Sandman, F.G. Yamagishi, A.F. Garito and A.J. Heegar, *Solid State Commun.*, 12 (1973) 1125.
173. C. Tanford, *The hydrophobic effect: formation of micelles and biological membranes*, 2nd. Ed., John Wiley and Sons Inc., (1980) Chapter 14.
174. I.D. Campell and R.A. Dwek, *Biological Spectroscopy*, The Benjamin/Cummings Publishing Company Inc., (1984) Chapter 5.
175. Barltrop and Coyle, *Excited States in Organic Chemistry*, John Wiley and Sons, (1975) Chapter 4.
176. M.T. Montero, J. Hernandez and J. Estelrich, *Biochemical Education*, 18 (1990) 99.
177. L. Stryer, *Ann. Rev. Biochem.*, 47 (1978) 819.
178. B.E.P. Swoboda, *Biochim. Biophys. Acta*, 175 (1969) 365.
179. B.E.P. Swoboda, *Biochim. Biophys. Acta*, 175 (1969) 380.

180. J.A. D'Anna, Jr., and G. Tollin, *Biochemistry*, 11 (1972) 1073.
181. F.B. Kaufman, E.N. Engler, D.C. Green and J.Q. Chambers, *J. Amer. Chem. Soc.*, 98 (1976) 1596.
182. F.H. Moster and A.L. Thomas, *The Phthalocyanines*, Vol. 1, CRC Press, Boca Raton, (1983) 79.
183. S. Zecevic, B. Simic-Glavaski, E. Yeager, A.B.P. Lever and P.C. Minor, *J. Electroanal. Chem.*, 196 (1985) 339.
184. R. Scheffold, G. Rytz and L. Walder, in *Modern Synthetic Methods*, R. Scheffold, Ed., Vol. 3, Wiley, New York, (1983) 355.
185. J.H. Kalh, L.R. Faulkner, K. Dwarakanath and T. Tachikawa, *J. Amer. Chem. Soc.*, 108 (1986) 5434.
186. H. Eckert and I. Ugi, *Angew. Chem. (Int. Ed.)*, 14 (1975) 825.
187. H. Eckert and Y. Kiesel, *Angew. Chem. (Int. Ed.)*, 20 (1981) 473.
188. R. Jasinski, *Nature (London)* 201 (1964) 1212.
189. J. Zagal, P. Bindra and E. Yeager, *J. Electrochem. Soc.*, 127 (1980) 1506.
190. C.M. Lieber and N.S. Lewis, *J. Amer. Chem. Soc.*, 106 (1984) 5033.
191. S. Kapusta and N. Hackerman, *J. Electrochem. Soc.*, 131 (1984) 1511.
192. A. Owlia and J. Rusling, *J. Electroanal. Chem.*, 234 (1987) 297.
193. D.W. Clack, N.S. Hush and I.S. Woosey, *Inorg. Chim. Acta*, 19 (1976) 129.
194. A.B.P. Lever and J.P. Wilshire, *Can. J. Chem.*, 54 (1976) 2514.
195. K.M. Kadish, L.A. Bottomley and J.S. Cheng, *J. Amer. Chem. Soc.*, 100. (1978) 2731.
196. A.B.P. Lever and J.P. Wilshire, *Inorg. Chem.*, 17 (1978) 1145.
197. A.B.P. Lever, S. Licoccia, K. Magnell, P.C. Minor and B.S. Ramaswamy, *Acs. Symp. Ser.* 201 (1982) 237.
198. M.J. Eddowes and M. Grätzel, *J. Electroanal. Chem.*, 163 (1984) 31.
199. M.J. Eddowes and M. Grätzel, *J. Electroanal. Chem.*, 152 (1983) 143.

200. G.L. McIntire and H.N. Blount, *J. Amer. Chem. Soc.*, 101 (1979) 7720.
201. Y. Ohsawa, Y. Shimazaki and S. Aoyagui, *J. Electroanal. Chem.*, 114 (1980) 235.
202. Y. Ohsawa and S. Aoyagui, *J. Electroanal. Chem.*, 136 (1982) 353.
203. J.H. Fendler and E.J. Fendler, *Catalysis in Micellar and Macromolecular Systems*, Academic Press, New York, 1975.
204. P.-A. Brugger and M. Gratzel, *J. Amer. Chem. Soc.*, 102 (1980) 2461.
205. I. Tinoco, Jr., and P.A. Lyons, *J. Phys. Chem.*, 60 (1956) 1342.
206. W. Stricks and I.M. Kolthoff, *J. Amer. Chem. Soc.*, 61 (1949) 1519.
207. M.L. Wagner and H.A. Scheraga, *J. Phys. Chem.*, 60 (1956) 1066.
208. J. Koutecky and V.G. Levich, *Zh. Fiz. Khim.*, 32 (1956) 1565.
209. G.K. Radda and G.H. Dodd, *Luminescence in Chemistry*, E.J. Bowen, Ed., D. Van Nostrand Company Limited., London, (1968) Chapter 10.
210. A.J. Bard and L.R. Faulkner, *Electrochemical Methods: Fundamentals and Applications*, John Wiley and Sons, (1980) 291.
211. *Hand Book of Chemistry and Physics*, 69th Edition, CRC Press, 1988-1989, C-704.
212. K.R. Frederick, J. Tung, R.S. Emerick, F.R. Masiarz, S.H. Chamberlain, A. Vasavada, S. Rosenberg, S. Chakraborty, L.W. Schopfer and V. Massey, *J. Biol. Chem.*, 265 (1990) 3793.

Appendix I A Mathematical Treatment for the Kinetics of Modified Enzymes

The equations describing the enzyme kinetics are (Chapter III):

$$Dd^2e_1/dx^2 - k_E e_1 s = 0 \quad (\text{A.1})$$

$$Dd^2e_2/dx^2 + k_E e_1 s - k_1 e_2 = 0 \quad (\text{A.2})$$

$$Dd^2e_3/dx^2 + k_1 e_2 = 0 \quad (\text{A.3})$$

The appropriate boundary conditions are:

1. At the electrode surface, all E_1-M' is converted to E_1-M thus at $x=0$, $e_3=0$; since E_2-M is electrochemically inactive, therefore at $x=0$, $de_2/dx=0$; also at the electrode, from the mass balance, $de_1/dx = -de_3/dx$.
2. In the solution, all the enzyme exist as E_1-M' since both the enzyme-substrate and enzyme-mediator reactions are irreversible. Thus as $x \rightarrow \infty$, $e_1=0$, $e_2=0$, $e_3=e_T$ where e_T is the total enzyme concentration, $e_T = e_1 + e_2 + e_3$. we also assume that there is no concentration polarisation for the substrate S so $[s]$ is independent of x .

With these boundary conditions, we can now solve equations (A.1--A.3) above. A general solution for (A.1) has the form,

$$e_1 = A_1 \exp(x\sqrt{k_E s/D}) + B_1 \exp(-x\sqrt{k_E s/D}) \quad (\text{A.4})$$

Using the boundary conditions above, as $x \rightarrow \infty$, $e_1=0$, we can write,

$$0 = A_1 \exp(x\sqrt{k_E s/D}) + B_1 \cdot 0 \quad (\text{A.5})$$

$$\therefore A_1 = 0 \quad (\text{A.6})$$

Thus the expression for e_1 is,

$$e_1 = B_1 \exp(-x\sqrt{k_E s/D}) \quad (\text{A.7})$$

$$\text{and } de_1/dx = -B_1 \sqrt{k_E s/D} \exp(-x\sqrt{k_E s/D}) \quad (\text{A.8})$$

Substitution of (A.7) in (A.2) gives,

$$Dd^2e_2/dx^2 + k_E s B_1 \exp(-x\sqrt{k_E s/D}) - k_1 e_2 = 0 \quad (A.9)$$

A general solution for eqn. (A.9) has the form,

$$e_2 = A_2 \exp(x\sqrt{k_1/D}) + B_2 \exp(-x\sqrt{k_1/D}) + C \exp(-x\sqrt{k_E s/D}) \quad (A.10)$$

Again using the boundary conditions as $x \rightarrow \infty$, $e_2 = 0$, eqn. (A.10) becomes,

$$0 = A_2 \exp(x\sqrt{k_1/D}) + B_2 \cdot 0 + C \cdot 0 \quad (A.11)$$

$$\therefore A_2 = 0 \quad (A.12)$$

Expression for e_2 is ,

$$e_2 = B_2 \exp(-x\sqrt{k_1/D}) + C \exp(-x\sqrt{k_E s/D}) \quad (A.13)$$

$$\text{so } de_2/dx = -B_2 \sqrt{k_1/D} \exp(-x\sqrt{k_1/D}) - C \sqrt{k_E s/D} \exp(-x\sqrt{k_E s/D}) \quad (A.14)$$

$$\text{and } d^2e_2/dx^2 = B_2 k_1/D \exp(-x\sqrt{k_1/D}) + C k_E s/D \exp(-x\sqrt{k_E s/D}) \quad (A.15)$$

$$\therefore Dd^2e_2/dx^2 = B_2 k_1 \exp(-x\sqrt{k_1/D}) + C k_E s \exp(-x\sqrt{k_E s/D}) \quad (A.16)$$

Rearrangement of (A.13) and substitution from (A.16) gives,

$$Dd^2e_2/dx^2 = k_1 e_2 - k_1 C \exp(-x\sqrt{k_E s/D}) + C k_E s \exp(-x\sqrt{k_E s/D}) \quad (A.17)$$

$$\text{and } Dd^2e_2/dx^2 = k_1 e_2 - (k_1 C - C k_E s) \exp(-x\sqrt{k_E s/D}) \quad (A.18)$$

Comparing eqn. (A.18) and (A.9) we obtain,

$$k_1 C - k_E s C = k_E B_1 s \quad (A.19)$$

$$\therefore C = k_E B_1 s / (k_1 - k_E s) \quad (A.20)$$

Substitution of (A.20) in (A.13) gives,

$$c_2 = B_2 \exp(-x\sqrt{k_1/D}) + k_E s B_1 / (k_1 - k_E s) \exp(-x\sqrt{k_E s/D}) \quad (\text{A.21})$$

$$\text{so } de^2/dx = -B_2 \sqrt{k_1/D} \exp(-x\sqrt{k_1/D}) - k_E s B_1 / (k_1 - k_E s) \sqrt{k_E s/D} \exp(-x\sqrt{k_E s/D}) \quad (\text{A.22})$$

Refer to the boundary condition $x=0$, $de_2/dx=0$,

$$\therefore 0 = -B_2 \sqrt{k_1/D} - k_E s B_1 / (k_1 - k_E s) \sqrt{k_E s/D} \quad (\text{A.23})$$

$$\text{Thus } B_2 = -\sqrt{k_E s/k_1} \cdot k_E s / (k_1 - k_E s) \cdot B_1 \quad (\text{A.24})$$

Substitution of (A.24) in (A.21) gives,

$$c_2 = k_E s B_1 / (k_1 - k_E s) [\exp(-x\sqrt{k_E s/D}) - \sqrt{k_E s/k_1} \exp(-x\sqrt{k_1/D})] \quad (\text{A.25})$$

Substitution of (A.25) in (A.13) gives,

$$D d^2 c_3 / dx^2 + k_1 k_E s B_1 / (k_1 - k_E s) [\exp(-x\sqrt{k_E s/D}) - \sqrt{k_E s/k_1} \exp(-x\sqrt{k_1/D})] = 0 \quad (\text{A.26})$$

Equation (A.26) is a second-order differential equation and its solution can be obtained by normal intergration.

First Intergral of (A.26),

$$de_3/dx = -k_1 k_E s B_1 / D (k_1 - k_E s) [-\sqrt{D/k_E s} \exp(-x\sqrt{k_E s/D}) + \sqrt{k_E s/k_1} \sqrt{D/k_1} \exp(-x\sqrt{k_1/D})] + A_3 \quad (\text{A.27})$$

Second intergral of (A.26),

$$c_3 = -k_1 k_E s B_1 / D (k_1 - k_E s) [D/k_E s \exp(-x\sqrt{k_E s/D}) - D/k_1 \sqrt{k_E s/k_1} \exp(-x\sqrt{k_1/D})] + A_3 x + B_3 \quad (\text{A.28})$$

Rewrite (A.28),

$$e_3 = -k_1 k_E s B_1 / (k_1 - k_E s) [1/k_E s \exp(-x \sqrt{k_E s/D}) - 1/k_1 \sqrt{k_E s/k_1} \exp(-x \sqrt{k_1/D})] + A_3 x + B_3 \quad (\text{A.29})$$

Application of the boundary condition $x \rightarrow \infty$, $e_3 = e_\Sigma$ gives,

$$e_\Sigma = -k_1 k_E s B_1 / (k_1 - k_E s) [1/k_E s \cdot 0 - 1/k_1 \sqrt{k_E s/k_1} \cdot 0] + A_3 x + B_3 \quad (\text{A.30})$$

$$\text{so } A_3 = 0 \quad (\text{A.31})$$

$$B_3 = e_\Sigma \quad (\text{A.32})$$

$$\therefore e_3 = -k_1 k_E s B_1 / (k_1 - k_E s) [1/k_E s \exp(-x \sqrt{k_E s/D}) - 1/k_1 \sqrt{k_E s/k_1} \exp(-x \sqrt{k_1/D})] + e_\Sigma \quad (\text{A.33})$$

At $x=0$, $e_3=0$, thus

$$0 = -k_1 k_E s B_1 / (k_1 - k_E s) [1/k_E s - 1/k_1 \sqrt{k_E s}] + e_\Sigma \quad (\text{A.34})$$

$$\therefore B_1 = e_\Sigma (k_1 - k_E s) / k_1 k_E s \cdot k_E s k_1 \sqrt{k_1} / (k_1 \sqrt{k_1} - k_E s \sqrt{k_E s}) \quad (\text{A.35})$$

Rewrite (A.33) we obtain,

$$e_3 = -e_\Sigma k_E s k_1 \sqrt{k_1} / (k_1 \sqrt{k_1} - k_E s \sqrt{k_E s}) [1/k_E s \exp(-x \sqrt{k_E s/D}) - 1/k_1 \sqrt{k_E s/k_1} \exp(-x \sqrt{k_1/D})] + e_\Sigma \quad (\text{A.36})$$

PUBLISHED
PAPERS
NOT
FILMED
FOR
COPYRIGHT
REASONS

APPENDIX II
P 269 - END

THE BRITISH LIBRARY
BRITISH THESIS SERVICE

TITLE ELECTROCHEMICAL STUDIES OF MODIFIED REDOX ENZYMES

AUTHOR VERONICA QING BRADFORD

DEGREE

AWARDING BODY

DATE University of Warwick OCTOBER 1991

THESIS
NUMBER

THIS THESIS HAS BEEN MICROFILMED EXACTLY AS RECEIVED

The quality of this reproduction is dependent upon the quality of the original thesis submitted for microfilming. Every effort has been made to ensure the highest quality of reproduction.

Some pages may have indistinct print, especially if the original papers were poorly produced or if the awarding body sent an inferior copy.

If pages are missing, please contact the awarding body which granted the degree.

Previously copyrighted materials (journal articles, published texts, etc.) are not filmed.

This copy of the thesis has been supplied on condition that anyone who consults it is understood to recognise that its copyright rests with its author and that no information derived from it may be published without the author's prior written consent.

Reproduction of this thesis, other than as permitted under the United Kingdom Copyright Designs and Patents Act 1988, or under specific agreement with the copyright holder, is prohibited.

cms	1	2	3	4	5	6	REDUCTION X	12
							CAMERA	3
							No. of pages	